REDUCTION OF RADIOLOGICAL ACCIDENT CONSEQUENCES

Action	Research and Innovation Action NFRP-2018-1
Grant Agreement #	847656
Project name	**R**eduction of **R**adiological **C**onsequences of design basis and design extension **A**ccidents
Project Acronym	R2CA
Project start date	01.09.2019
Deliverable #	D2.3
Title	Report on SGTR and LOCA available experimental data
Author(s)	Zoltán Hózer (EK), Adam Kecek (NRI Rez), Katia Dieschbourg (IRSN), Tatiana Taurines (IRSN), Martina Adorni (Bel V), Nikolaus Müllner (BOKU), Mattia Massone (ENEA), Matthias Jobst (HZDR), Asko Arkoma (VTT), Péter Szabó (EK), Ruslan Lishchuk (ARB), Stanislav Sholomitsky (ARB), Michael Schöppner (BOKU), Cedric Leclere (IRSN), Luis E. Herranz (CIEMAT), Rafael Iglesias (CIEMAT), Vincent Busser (IRSN)
Version	01
Related WP	WP2 METHO - Methodologies
Related Task	T2.1.3. Review of experimental database (MTA-EK)
Lead organization	MTA-EK
Submission date	24.08.2020
Dissemination level	PU

History

Date	Submitted by	Reviewed by	Version (Notes)
24.08.2020	Z. Hózer (EK) and al.	P. Bradt (TE) N. Girault (IRSN)	01

Contents

Abbreviations

AEKI	Atomic Energy Research Institute
ANL	Argonne National Laboratory
ARTIST	Aerosol Trapping In Steam GeneraTor
CODEX	Core Degradation Experiment
EdF	Electricité de France
FZK	Forschungszentrum Karlsruhe
FSCB	Full Scale Containment Blowdown experiments
IAEA	International Atomic Energy Agency
IFPE	International Fuel Performance Experiments
IGR	
IKE	Institut für Kernenergetik und Energiesysteme, University of Stuttgart
ITS	Integral Thermal Shock
JAEA	Japan Atomic Energy Agency
JAERI	Japan Atomic Energy Research Institute
KfK	Kernforschungszentrum Karlsruhe
LOCA	Loss Of Coolant Accident
MRBT	Multi-Rod Burst Tests
MTA EK	Hungarian Academy of Sciences Centre for Energy Research
NPP	Nuclear Power Plant
OECD NEA	Organisation for Economic Co-operation and Development, Nuclear Energy Agency
ORNL	Oak Ridge National Laboratory
PIE	Post-Irradiation Examination
PBF	Power Burst Facility
RCS	Reactor Coolant System
REBEKA	Reactor typical Bundle Experiment Karlsruhe
SGTR	Steam Generator Tube Ruprure
SRP	Standard Review Plan
STEM	Source Term Evaluation and Mitigation

Introduction

The experimental data on reactor incidents and accidents provide the basis for code validation and development activities and serve as the background of current knowledge on related phenomena. In the framework of the Task 2.1.3 of R2CA project the available experimental databases were reviewed focusing on fuel failure, on fission products release from the fuel rods and on activity transport up to the environment during LOCA and SGTR events.

This review also included available information obtained from the monitoring of normal operation and transients in NPPs and from some accidental situations.

It was expected that this review will cover all important LOCA and SGTR phenomena by experimental data and will support code validation activities in the R2CA project.

Content and structure of the report

The present report includes the description of each test series in individual chapters. Short summaries were produced to identify the test objectives, introduce the tested materials, test facility, measured parameters and PIE data, and present the general conclusions drawn after the completion of the tests.

The main characteristics of each test series are summarised in form of matrices, which are shown in the attachment of this report.

The users of the database can find more information on the given test series in the references, which are grouped into special directories. In some cases, the data available for the test series inside of R2CA project are also given in these directories. The data files are available in their original format as provided by the data owner. It was intended to include all available information on the related experiments and NPP measurements, even if the data are not available for the project.

Experimental matrices

Three large matrices have been compiled to support detailed discussions on
- phenomena,
- test characterization and
- data availability.

In the *phenomena* matrices (Appendix I.) the fuel failure, the activity release and the transport phenomena were characterised by several processes and conditions:

Fuel failure during LOCA:
- cladding oxidation
- ballooning and burst
- brittle failure after heavy oxidation
- water quench
- fuel fragmentation and dispersal

Fuel failure during SGTR:
- secondary defect
- brittle failure
- hydrogen uptake by Zr
- local hydriding of Zr clad
- water logged fuel rod

Activity release from fuel during LOCA:
- noble gas release from the fuel rod - steady state
- noble gas release from the fuel rod - transient
- volatile fission product release from the fuel rod - transient
- semi-volatile fission product release from the fuel rod - transient
- fission product release from high burnup structure

Activity release from fuel during SGTR:
- noble gas release from the fuel rod - steady state
- noble gas release from the fuel rod - transient
- volatile fission product release from the fuel rod - transient
- semi-volatile fission product release from the fuel rod - transient
- leaching of fuel pellets by water
- fission product release from high burnup structure

Activity transport during LOCA:
- transport in the primary circuit (from core to break)
- deposition in the primary circuit, retention by primary circuit components
- transport in the containment
- deposition on the containment wall
- deposition in the containment sump water
- transport to the environment outside of containment
- noble gas transport
- volatile fission product (I, Cs) transport
- semi-volatile fission product transport

Activity transport during SGTR:
- transport in the primary circuit (from core to break)
- deposition in the primary circuit, retention by primary circuit components
- deposition in the steam generator, retention by steam generator
- transport to the environment outside of containment
- noble gas transport
- volatile fission product (I, Cs) transport
- semi-volatile fission product transport

The *test characterisation* matrices (Appendix II.) identified the
- test types (separate effect tests, integral tests and NPP measurements)
- scale (scaled down or full size)
- atmosphere (steam, inert gas, hydrogen, oxidising, reducing)
- tested sample (small cladding sample, small pellet sample, single rod, bundle, non-core material, irradiated, non-irradiated)
- cladding type (Zircaloy-4, Zirlo, M5, E110, pre-charged with H, pre-oxidised)
- fuel type (UO_2, MOX, high burnup)
- heating method (nuclear, electric, internal, furnace, induction) and
- fission product transport (pH, dose rate, temperature, transport by natural circulation/gravity, transport by forced flow, transport in gas atmosphere, transport in liquids , interfacial mass transfer).

The *data* matrices (Appendix III.) identified the

- availability of data (available for the R2CA project, included into the Appendix of the database report, or accessible for some R2CA partners, but cannot be shared within the project)
- On-line data (temperature history, pressure history, fission product release monitoring from fuel, fission product release monitoring from primary circuit, fission product release monitoring from steam generator, FPs concentration in containment atmosphere, FPs concentration in containment sump FPs deposition on surface, pH, dose rate)
- PIE data (clad deformation, clad corrosion state (oxidation, H content), fission product inventory in the gap, cumulative fission product release from fuel rod, cumulative fission product release from primary circuit, cumulative fission product release from steam generator, cumulative fission product release from containment, FPs deposition on surface) and
- Validation (the measured data were used by R2CA partners before the project for code validation purposes or the measured data will be used by R2CA partners in the project for code/new/updated model validation purposes and model re-assessments within DBA and DEC-A conditions).

Considered test series

The R2CA project partners reviewed the experimental database taking into account the following sources:
- tests and measurements in national or institutional projects,
- OECD State-of-the-art Report on Nuclear Fuel Behaviour in Loss-of-coolant Accident (LOCA) Conditions,
- OECD and EU projects,
- publications in scientific journals, conference materials and other open libraries (IAEA and NUREG reports).

In most of the cases some experts were involved in these tests series or participated in the evaluation of the data.

The current list of tests, which was agreed during the Task 2.1.3. meeting in January 2020, includes 42 items, which are described in the following chapters. During the screening process several severe accident type experiments were removed from the list, as the R2CA project will deal with DBC and DEC-A conditions only.

.

1. Edgar tests

Edgar tests have been performed for several decades at CEA (France) in order to study and model zirconium based alloys creep and burst in LOCA conditions. Extensive description of some series of EDGAR tests can be found in reference [1] and in its update from 2018 (to be published) [2].

1.1 Objectives

The main objective of EDGAR tests was to be able to model creep and burst of zirconium alloys pressurized tubes in LOCA conditions for large and intermediate breaks.

1.2 Tested materials, test facility

Several materials were tested in the EDGAR facilities but mainly Zircaloy-4 and M5 alloys with as-received and pre-hydrided samples. Tested tubes are 300 mm long, directly heated by Joule effect in steam atmosphere. EDGAR tests were performed on different facilities over decades. The EDGAR-2 facility is described in [1] as follows it "operates in the temperature range from 350 to 1 400 °C in steady-state (creep tests) or transient conditions. The heating rates can be controlled between 0.1 and 250 K/s. The maximum internal pressure is limited to 200 bars. Pressure rates can be controlled between -10 to +10 bar/s in transient conditions". For pressure steady-state test, the pressure is maintained constant thanks to buffer volumes.

1.3 Measured parameters, PIE data

From [1], the measured parameters are mainly temperature, internal pressure and diametral deformation. "The temperatures and the diametral deformation are measured at the same axial location of the specimen, around the middle of the useful part of the specimen. The temperature gradient in the useful part is less than 5 K. The external clad temperature is measured by optical pyrometers or by spot-welded Pt-PtRh type thermocouples. The internal gas temperature is measured by an internal K type thermocouple. The change in the cladding diameter during the test is continuously measured by a laser device that operates, like the pyrometers, through a quartz window fitted in the vessel."

Post-test measurements are made with thin paper ribbons at three cladding elevations, one at the largest diameter in the ballooned section and 20 mm above and below the edges of the burst opening. The total elongation is defined as the circumferential strain at the largest diameter. The largest of the other two diameters defines the uniform elongation. This approach is illustrated on Fig. 1.
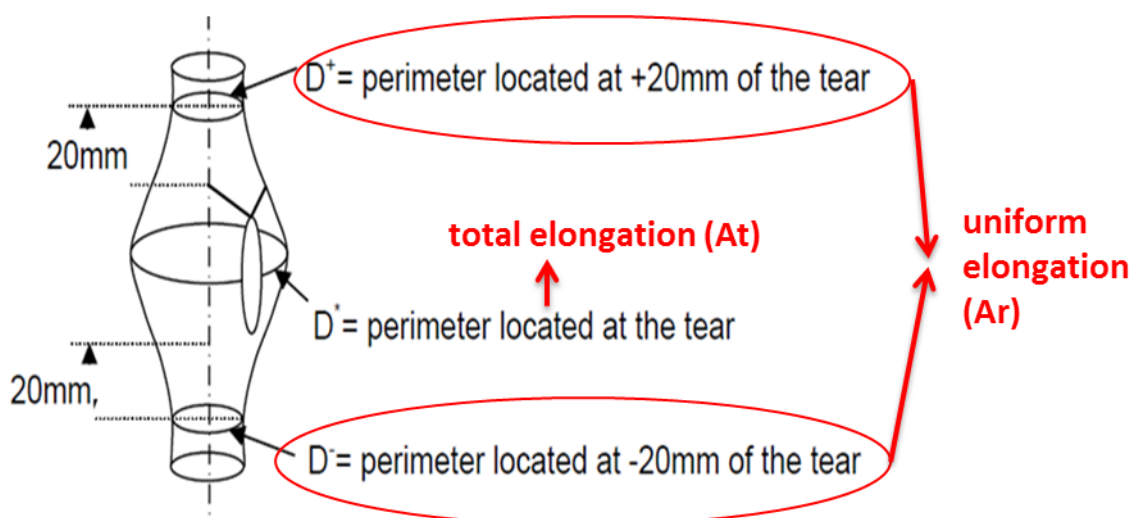

Fig. 1. Schematic overview of total and uniform elongation defined in EDGAR programs.

1.4 General conclusions

Only a few data are available in the open literature; the results are not complete for each test but only partial data such as the total elongation versus burst temperature (as illustrated on Fig. 2) or time to burst versus initial hoop stress. Some R2CA partners (IRSN, EDF) own detailed data for some tests but these data cannot be shared with other R2CA partners.
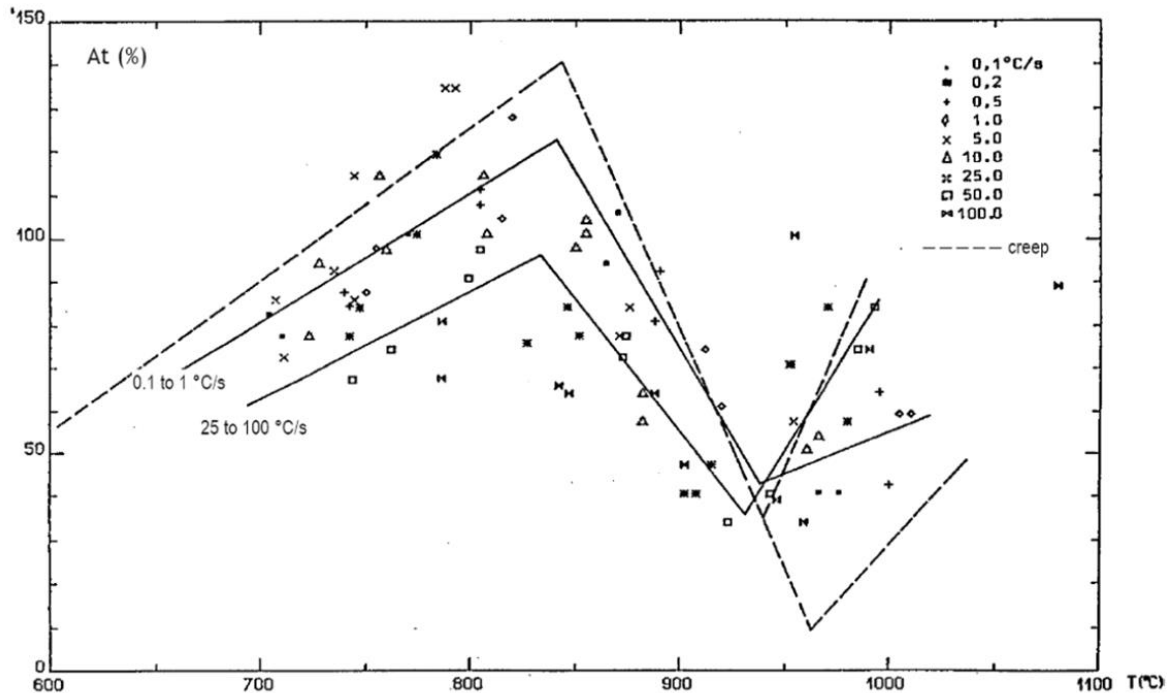
Fig. 2. Total elongation (%) versus burst temperature (°C) in EDGAR tests (Zy-4) [1].

Main conclusions from EDGAR tests and taken from [1] are listed hereafter:
- Very large maximum circumferential strain were observed (higher than 50 % for burst under 900°C),
- Transient tests lead to lower burst strain than creep tests if burst temperature is considered,
- M5 (RXA) seems to lead to lower burst strain than Zy-4 (SRA),
- Hydrogen seems to lower creep resistance and ductility.

These conclusions have to be taken carefully since phase transition from alpha to beta has a significant impact on creep properties and burst characteristics. It is therefore complicated to compare the influence of temperature transients, alloys composition, hydrogen impact and so on.

1.5 References

[1] *Nuclear Fuel Behaviour in Loss-of-Coolant Accident (LOCA) Conditions, NEA No. 6846, 2009, NEA.
[2] ALSO update of Nuclear Fuel Behaviour in Loss-of-Coolant Accident (LOCA) Conditions. NEA, To be published
*available in the R2CA database

2. COCAGNE tests

COCAGNE tests are being performed at IRSN since 2017 in the frame of the PERFROI project [3].

2.1 Objectives

COCAGNE tests aim to "investigate the thermal mechanical swelling of cladding tubes simulating multi-rods configuration. This configuration (COCAGNE tests), never studied experimentally up to now, will provide new insights regarding balloons formation before and after contact between adjacent rods. It will also quantify the effect of azimuthal temperature gradients" [4]. This experimental program will lead to updated models in codes like DRACCAR (IRSN code used to model multi rods under LOCA conditions) [5][6].

2.2 Tested materials, test facility

COCAGNE facility (see Fig. 3) allows to heat directly by Joule effect a pressurized 600 mm long cladding tube (external diameter 9.5 mm, 570 µm thick) up to 1200°C with an internal pressure up to 100-150 bars under vacuum. Alumina pellets simulate fuel pellets and were designed in order to localize ballooning (by using hollow pellets around mid-height). The temperatures of the neighbouring structures are controlled independently, thus it is possible to induce an azimuthal temperature gradient around the tested rod.
Zy-4 cladding with a thin external oxide layer (to allow pyrometry measurements) and two-sided pre-oxidized and pre-hydrided samples are being investigated. A first campaign was performed in a single rod configuration and a second one with four neighbouring rods. Tests are under progress to better understand burst behaviour in a five-rods like configuration.
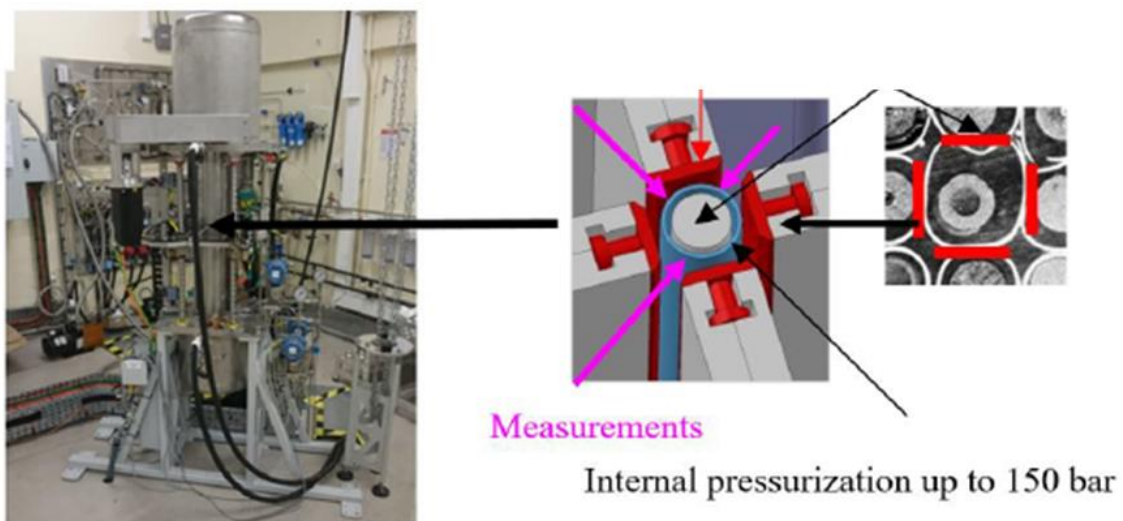
Fig. 3. COCAGNE facility and test section

.

2.3 Measured parameters, PIE data

One of COCAGNE facility great interest is the advanced on-line mobile measurements. Three UV pyrometers and laser telemeters are embedded on a mobile platform moving at high velocity (up to 900 mm/s) (see Fig. 4.).
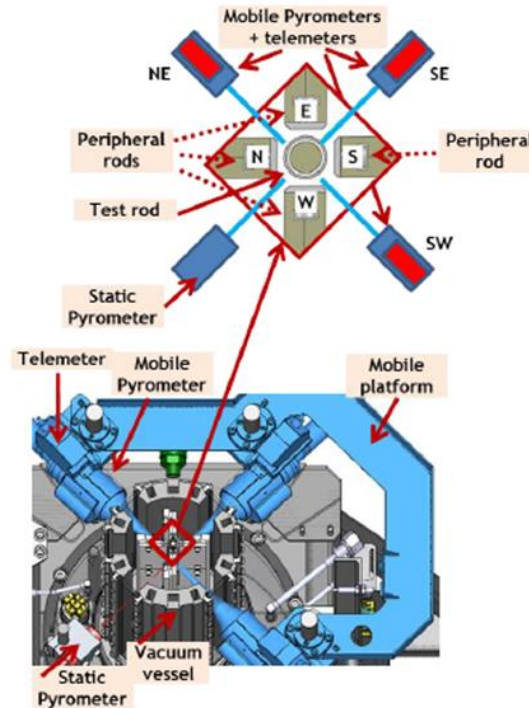
Fig. 4. Position of pyrometers and telemeters in COCAGNE facility [5].

Static measurements are also available (cladding temperature by a fix pyrometer, thermocouples, rod internal pressure and axial displacement). All these innovative measurements allow to know burst temperature precisely at burst location. Post-mortem, samples are scanned with a 3D-scanner to determine strain profile.

2.4 General conclusions

For the moment, data related to burst from the COCAGNE program is not sharable with R2CA partners but will be included in the burst database used by IRSN to review models in WP3.

2.5 References

[3] *Repetto, G., et al., The R&D PERFROI project on thermal mechanical and thermal hydraulics behaviors of a fuel rod assembly during a Loss Of Coolant Accident, in NURETH, International Topical Meeting on Nuclear Reactor Thermal Hydraulics 2016: Chicago.

[4] ALSO update of Nuclear Fuel Behaviour in Loss-of-Coolant Accident (LOCA) Conditions. NEA, To be published.

[5] Dominguez, C., COCAGNE Program: Preliminary experimental report: Single-rod tests, RT IRSN PSN 2019-00184, 2019.

[6] Glantz, T., et al., DRACCAR: a multi-physics code for computational analysis of multi-rod ballooning and fuel relocation during LOCA transients. Part one: General modeling description. Nuclear Engineering and Design, 2017.

*available in the R2CA database

3. REBEKA tests

3.1 Objectives

The REBEKA tests (Reactor typical Bundle Experiment Karlsruhe) at Kernforschungszentrum Karlsruhe (nowadays KIT) was a long-term research program for investigation of the interaction between thermal-hydraulics and cladding tube deformation performed from late 1970s to 1990s [7]. The test program was performed in several consecutive test series from single-rod tests conducted in steam atmosphere to bundle tests with several bundle sizes (5x5 and 7x7 bundles) [8]. The test rigs were designed in order to simulate typical reflooding conditions common to German PWR of the Siemens-KWU design (water injection in both the hot and cold leg). Later, the single-rod test facility was used to investigate creep burst of ZrNb1- cladding tubes of Russian VVER [9].

3.2 Tested materials, test facility

An important step of the research program was the development of an electrically heated fuel rod simulator. Excellent agreement between the fuel rod simulator and nuclear fuel has been shown in an extensive experimental work. The fuel rod simulator consisted of an Inconel thermal heater, isolated from the Zircaloy-4 cladding tube by annular alumina pellets. The cladding outer diameter of 10.75 mm and 0.725 mm thickness corresponds to the cladding of fuel assemblies used in German PWR (16x16-fuel assembly, KWU design prior to Konvoi). A cosine-shaped power distribution has been implemented by special design of the Inconel heater and its MgO core (applied for 7x7 bundle tests, see Fig. 5, for 5x5 bundle tests a profile with 7 axial steps was applied).
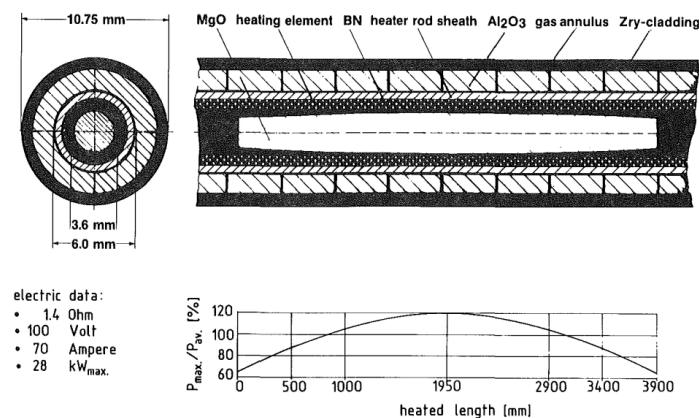
Fig. 5. REBEKA fuel rod simulator [7].

Single-rod Test Rig
For the single-rod test rig, fuel rod simulators of 325 mm heated length with constant axial power were used. The tubes were pressurized during the tests by applying helium. Test parameters covered 10 to 140 bar inner tube pressure, 1 to 30 K/s heat-up rate. The surrounding atmosphere in these tests was almost stagnant steam at atmospheric pressure and 200 °C [7].

Bundle Test Loop
Bundle configurations in a 5x5 and 7x7 square array with original Siemens-KWU fuel assembly design parameters were used (pitch to diameter ratio of 1.33, heated length of 3900 mm, axial power profile factor of 1.19). With the applied test facility design, it was possible to investigate temperature and pressure transients of the cladding tubes without controlling the power supply [7]. Table 1 gives an overview of the bundle tests with references to detailed reports [10].

3.3 Measured parameters, PIE data

Single-rod Test Rig
- Cladding temperatures (outer surface of the cladding)
- Internal rod pressure
- Time dependent ballooning (strain ε, $\dot{\varepsilon}$) (by X-ray system/camera)

Bundle Test Loop
- Outer cladding temperatures and heater rod temperatures (in total 150 thermocouples in the 7x7 bundle)
- Pressure (for each of the rods in the bundle separately)
- Circumferential strain
- Max. flow blockage

Table 1
REBEKA multi-rod burst tests [10]

Test number	Bundle size	Heating rate	Coolant flow	Flow direction	HTC	Temperature[3]	Temperature[4]	Pressure	Circumferential strain	Intergrid distribution of bursts	Max. Flow blockage	Remarks	Reference
		K/s			W/m²/K	°C	°C	bar	%	mm	%		
1		7[1]…<1[2]	· Steam · Reflood	Reversed	30…100	685	810	60	28		25	· Inner 3x3 pressurized · Only 2 rods burst · High reflood rate at start of reflood	[11],[12]
2		7[1]	· Steam	Uni-directional	30	870	870	55	54	95	60	· Inner 3x3 pressurized	[13]
3	5x5	7	· Steam · Reflood	Reversed	30…100	808	830	51	51	203	52	· Inner 3x3 pressurized	[14]
4		7[1]…<1[2]	· Steam · Reflood	Reversed	30…100	795	830	53	53	242	55	· Inner 3x3 pressurized · Control rod guide tube in centre	[14][15]
M		0	· Quasi-stagnant steam		<10	754	754	70	70	28	84	· 1 W/cm · All pressurized · 2 rods leaked	[16]
5		7[1]…0[2]		Reversed	30…100	775	800	68	68	242	52	· All pressurized	[17]
6	7x7	7[1]…-4[2]	· Steam · Reflood	Uni-directional	30…100	765	790	62	62	140	60	· 2 rods unpressurized · Instrument tube in the centre	[18]
7		7[1]…-9[2]		Uni-directional	30…100	755	790	57	57	200	66	· All pressurized	[19]

Common test conditions:
Heated length: 3900 mm; decay heat at midpoint: 20 W/cm; axial peaking factor: 1.19; axial power profile: 7 axial steps (5x5 tests), cosine-shaped (7x7 tests); system pressure: 4 bar; coolant flow: ≈2 m/s steam, ≈3 cm/s forced flooding from bottom; Zircaloy-4 claddings: 10.75 mm x 0.72 mm, stress relieved

1) During heat up   2) during reflood in the time period of high plastic deformation before burst
3) Measured nearest to burst at time of burst   4) best-estimate burst temperature

Based on the single rod tests, the burst temperature as a function of the burst pressure and heating rate was determined and a deformation model was derived from the data (shown by Fig. 6.). At the same heating rate, a higher rod internal pressure leads to a lower burst temperature. Furthermore, a significant influence of the

heating rate on the burst temperature is observed, i.e. high heating rates lead to higher burst temperatures than low heating rates. The results of the seven bundle tests are in good agreement with the single-rod test results.
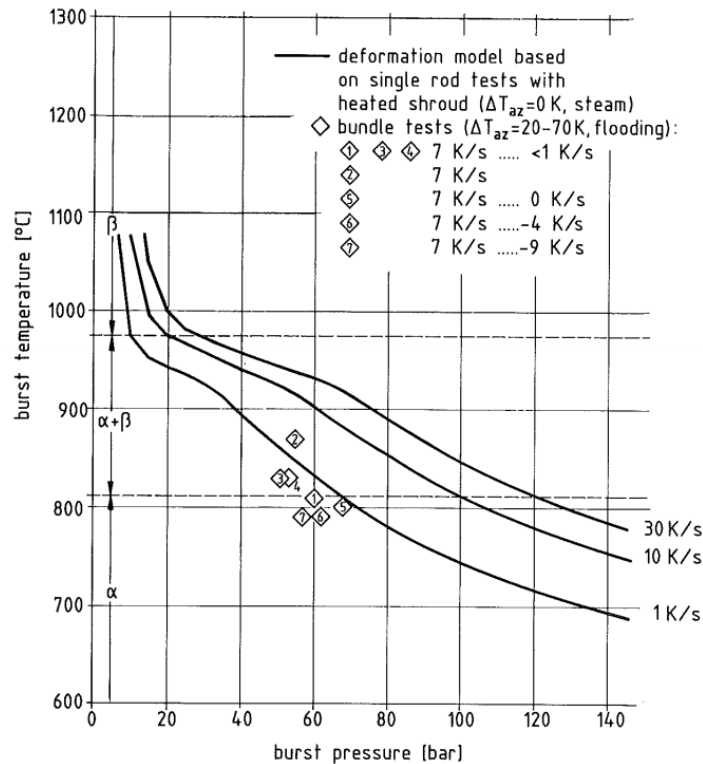
Fig. 6. REBEKA tests burst temperature vs. burst pressure [7].

Fig. 7. shows the circumferential burst strain versus the burst temperature with the heating rate as the parameter. The calculated values represented by curves describe the circumferential burst strains measured in the single-rod tests on the cladding tube circumference at uniform temperature. These idealized conditions were specifically provided by a heated shroud surrounding the fuel rod simulator. The averaged values from the bundle tests entered in the diagram indicate a significant reduction in the circumferential burst strains to values around 50%. This limitation is due to temperature differences on the cladding tube circumference.
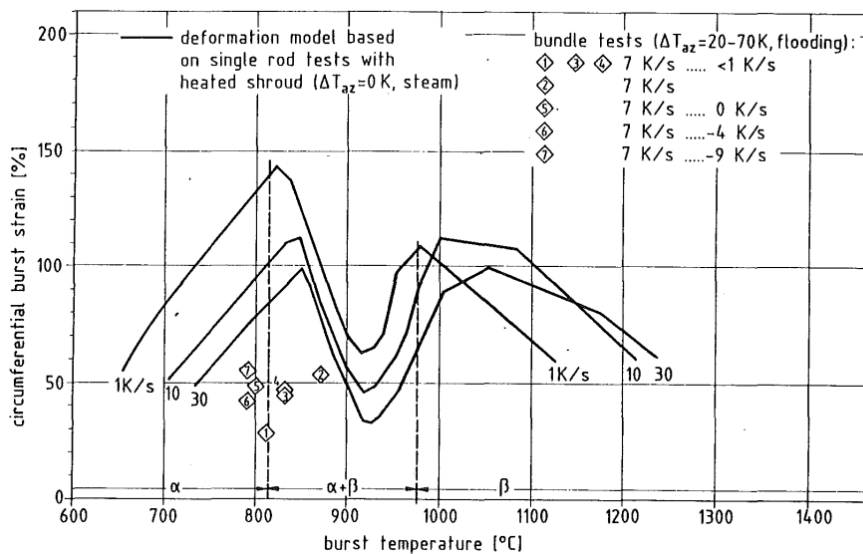
Fig. 7. REBEKA tests burst strain vs. burst temperature [7].

The influence of flow direction on coolant channel blockage was assessed and the maximum coolant flow blockage (under reactor typical conditions) was approx. 70 %. Under such conditions the temperature and pressure transients of the individual rods in the bundle were assessed, see Fig. 8.
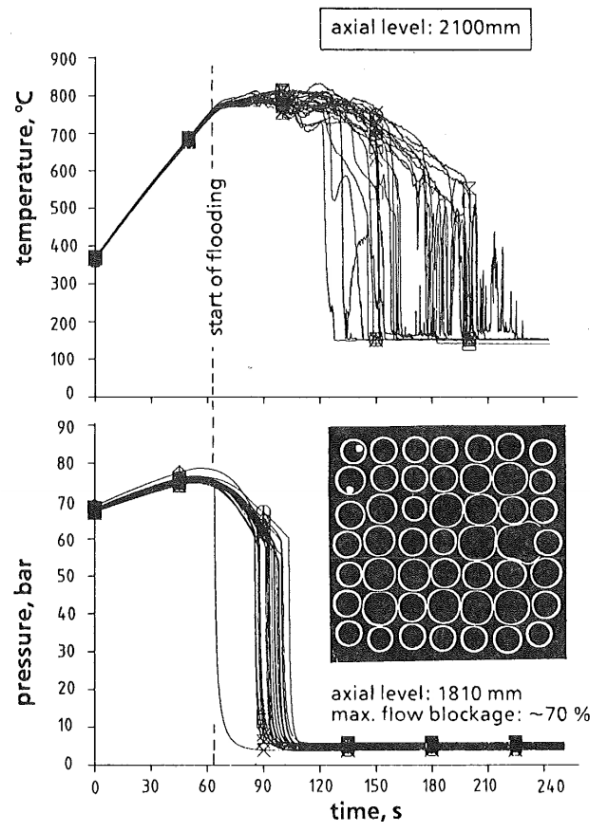
Fig. 8. Temperature and pressure transients of a 70 % blocked rod bundle observed in REBEKA 7 test [7].

The REBEKA tests were the subject of many numerical analyses and benchmarks, e.g. [20]. The REBEKA 6 test was assessed in the framework of ISP-14 [21],[22],[23],[24]. A recent simulation of REBEKA-6 was performed with DRACCAR [25].

3.4 General conclusions

The main results of the REBEKA program can be summarized as follows [7]:
- The number of burst cladding tubes and their circumferential burst strain can be determined with sufficient accuracy if the temperature and pressure developments of the cladding are known.
- The circumferential burst strains of Zircaloy cladding tubes are kept relatively small due to temperature differences on the cladding circumference and the anisotropic behaviour of Zircaloy.
- The cooling effect of the two-phase flow increases the temperature differences on the cladding tube circumference and limits in this way the mean circumferential burst strains to values of about 50%.
- A unidirectional flow through the rod bundle during the refill and reflooding phases causes cooling channel blockage of about 70% at the maximum.
- Burst cladding tubes generate secondary quench fronts, which propagate relatively fast and lead to efficient cooling.

By the experiments, it was shown that in a LOCA of a German PWR, the coolability of the fuel assemblies is guaranteed and that the safety margin is greater than predicted by most of the computer codes.

By the additional temperature-transient single-rod creep burst tests on ZrNb1 cladding tubes of Russian VVER reactors, comparison to the Zircaloy results was possible [9],[26]. The burst temperature and burst strains, respectively as influenced by the burst pressure, burst temperature and heating rate exhibit a similar tendency. In

general, the data of ZrNb1 tend to lower values. Main differences exist in the phase transformation temperatures, which are up to 100 K lower for ZrNb1 compared to Zry4.

3.5 References

All given references are available in open literature. Most of the KfK reports are in German, but contain an English summary.

[7] *F.J. Erbacher, H.J. Neitzel, and K. Wiehr, Cladding deformation and emergency core cooling of a pressurized water reactor in a LOCA. Summary description of the REBEKA program. KfK-4781. 1990.

[8] K. Wiehr, REBEKA-Buendelversuche. Untersuchungen zur Wechselwirkung zwischen aufblaehenden Zircaloyhuellen und einsetzender Kernnotkuehlung. Abschlussbericht. KfK-4407. 1988.

[9] F.J. Erbacher, et al., Temperaturtransiente Kriechberstversuche an Zirconium-Niob1-Hüllrohren. FZKA-5726. 1997.

[10] F. Erbacher and S. Leistikow, A review of Zircaloy fuel cladding behavior in a loss-of-coolant accident. KfK-3973. 1985.

[11] K. Wiehr, et al., KfK-2600, p. 383–400. 1978.

[12] K. Wiehr, et al., KfK-2700, p. 4200-103–4200-120. 1978.

[13] K. Wiehr, et al., KfK-2750, p. 4200-109–4200-144. 1979.

[14] K. Wiehr, et al., KfK-2950, p. 4200-155–4200-183. 1981.

[15] K. Wiehr, F. Erbacher, and H. Neitzel. Influence of a cold control rod guide thimble on the ballooning behaviour of zircaloy claddings in a LOCA. in Proceedings of a CSNI specialist meeting on safety aspects of fuel behaviour in off-normal and accident conditions, Espoo, Finland, 1-4 September 1980. 1981.

[16] K. Wiehr, et al., KfK-3250, p. 4200-90–4200-121. 1982.

[17] U. Harten and K. Wiehr, Datenbericht REBEKA-5. KfK-3842. 1985.

[18] K. Wiehr and U. Harten, Datenbericht REBEKA-6. KfK-3986. 1986.

[19] K. Wiehr and U. Harten, Datenbericht REBEKA-7. KfK-4145. 1987.

[20] H. Karwat, Verhalten eines Brennstabbündels während einer spezifierten Aufheiz- und Flutperiode: Vergleichsbericht. GRS-A-1015. 1984.

[21] H. Karwat, International Standard problem ISP 14: behaviour of a fuel bundle simulator during a specified heatup and flooding period (Rebeka experiment): results of post-test analyses: final comparison report. CSNI85-98. 1985.

[22] G. Sdouz, Austrian contributions to fuel rod failure models shown at the International Standard Problem ISP-14. Oesterreichisches Forschungszentrum Seibersdorf GmbH. 1984.

[23] G. Sdouz, Simple models for the simulation of fuel rod behavior at ISP-14 (International Standard Problem). 1985.

[24] D. Sweet and T. Haste, Further calculations for REBEKA-6 (ISP-14). 1985, UKAEA Atomic Energy.

[25] A. Fargette, Simulation of REBEKA 6 with DRACCAR v2.1. Nuclear Engineering and Design, 2017. 321: p. 244-257.

[26] Database of REBEKA creep burst tests for ZrNb1, data based on FZKA-5726.

*available in the R2CA database

4. AEKI and MTA EK burst tests

4.1 Objectives

Several series of ballooning tests with single rods and bundles were carried out in the KFKI Atomic Energy Research Institute (AEKI) and in its successor Centre for Energy Research (MTA EK) in Hungary. The main objective of the single rod tests was to provide the necessary experimental data for model development in transient fuel behaviour codes. The comparison of Zircaloy-4, E110 and sponge based E110G cladding behaviour was also an aim of the test series. Investigations of cladding tube deformation and flow blockage phenomena in a VVER assembly were the main objectives of the bundle tests.

4.2 Tested materials, test facility

Non-irradiated cladding samples were used. Zircaloy-4, traditional E110 and sponge based E110G alloys were tested. The length of the specimens varied between 50-250 mm in the different series.

Plugged cladding samples were investigated in high temperature furnaces without internal heating of the rods. Most of the tests were carried out under isothermal conditions (see Fig.9). The inner pressure of the test tube was increased until the burst of the sample. The pressurization was performed through small diameter Zr tubes attached to one end of the specimen.

Most of the tests were performed in inert gas (argon) atmosphere, but some of the burst tests were done in steam atmosphere. Pre-oxidation of selected samples was done in high temperature steam for different time periods. Iodine pre-treatment was carried in special argon-filled ampoules containing iodine.

The last tests series were conducted in a special furnace, which had two observation holes for optical measurements. Using this facility, the on-line deformation of cladding samples could be tracked (see Fig.9)
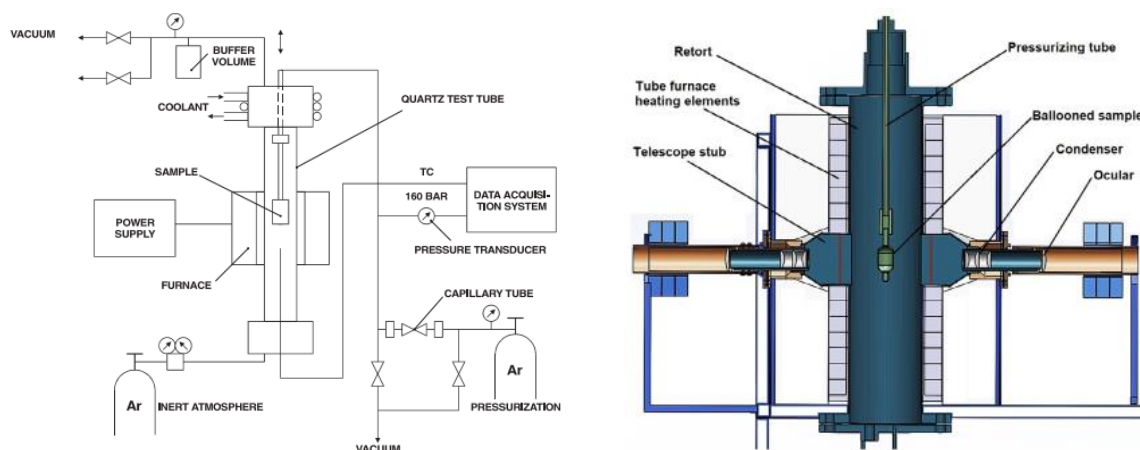
Fig. 9. Scheme of the high temperature furnace used for single rod tests (left) [27] and the furnace with telescopes used in the last test series (right) [32]

Some of the burst tests were combined with secondary hydriding investigations of cladding tubes filled with Al_2O_3 pellets. Those tests started with cladding burst in inert atmosphere and continued with oxidation in steam at high temperature isothermal conditions.

Most of the tests were performed with single rods without any limitation on the ballooning. Some multi-rod tests with VVER hexagonal arrangements including 7 rods were also performed to study the interaction between ballooned rods inside of a bundle.

4.3 Measured parameters, PIE data

The inner pressure of the cladding tubes and the temperature in the furnace were recorded in all tests. In some selected test the temperature of cladding was also measured. Using the telescopes and cameras, the diameter change of the samples could be recorded with high speed, too.

Different post-test examinations were carried out to provide data on the maximum deformation, oxidation scale thicknesses, hydrogen content of the samples. In case of multi-rod tests the blockage rates were also determined.
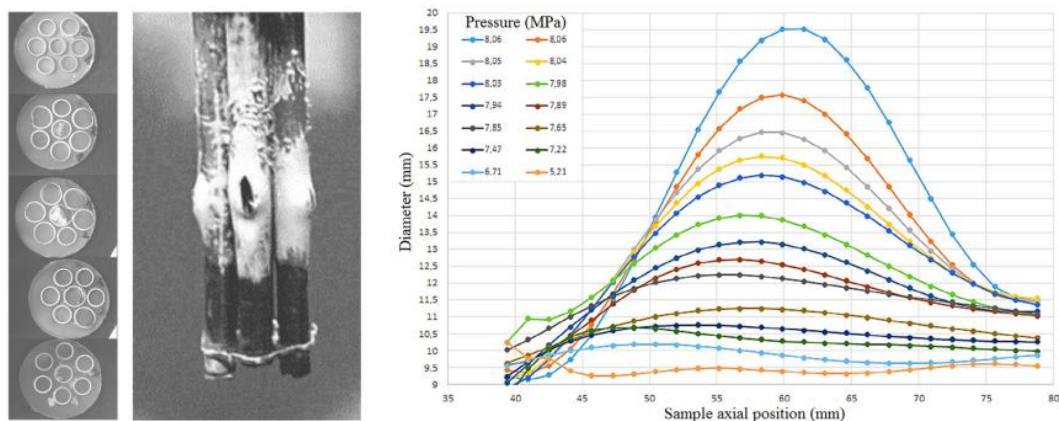
Fig. 10. View and cross section of a 7-rod bundle tested in steam (left)[27] and diameter evaluation of a 85 mm long, E110 sample at 850 °C with pressurization rate 49 kPa/s (right).[31]

4.4 General conclusions

The test series produced significant amount of new data on the ballooning and burst behaviour of E110 claddings.

The pressurization rate played an important role in the burst conditions as faster pressurization considerably increased the burst pressure. On the other hand, no influence of the temperature increase rate was experienced.

The coolant-side oxidation had a significant effect on the mechanical behaviour of the cladding. The strength of E110 increased up to 10- to 20 μm oxide layer thickness but decreased with further oxidation. The evidence of decreasing deformation with an increasing ZrO_2 layer was clearly observed.

The experiments revealed that in the temperature range of 800 to 1000 °C, the mechanical strength of the E110 cladding is lower than that of the Zircaloy-4 since the α-β phase transition temperature is different for the two alloys. Below and above this range, the E110 and Zircaloy-4 claddings burst at the same overpressure.

The comparison of new, sponge based E110G data traditional, electrolytic E110 data indicated that failure of E110G cladding took place at slightly higher pressure than E110.

The iodine treatment did not significantly influence the mechanical behaviour of the fuel rods under accident conditions.

4.5 References

[27] *Zoltán Hózer, Csaba Győri, Márta Horváth, Imre Nagy, László Maróti, Lajos Matus, Péter Windberg, József Frecska: Ballooning Experiments with VVER Cladding, Nuclear Technology, Volume 152 · Number 3 · December 2005 · Pages 273-285

[28] *Erzsébet Perez-Feró, Csaba Győri, Lajos Matus, László Vasáros, Zoltán Hózer, Péter Windberg, László Maróti, Márta Horváth, Imre Nagy, Anna Pintér-Csordás, Tamás Novotny: Experimental database of E110 claddings exposed to accident conditions, Journal of Nuclear Materials 397 (2010) 48–54

[29] *E. Perez-Feró, Z. Hózer, T. Novotny, G. Kracz, M. Horváth, I. Nagy, A. Vimi, A. Pintér-Csordás, Cs. Győri, L. Matus, L. Vasáros, P. Windberg, L. Maróti: Experimental database of E110 claddings under accident conditions, EK-FRL-2011-744-01/04

[30] *Eszter Kozsda-Barsy, Katalin Kulacsy, Zoltan Hozer, Marta Horvath, Zoltan Kis, Boglarka Maroti, Imre Nagy, Richard Nagy, Tamas Novotny, Erzsebet Perez-Fero, Anna Pinter-Csordas, Laszlo Szentmiklosi: Post-test examinations on Zr-1%Nb claddings after ballooning and burst, high-temperature oxidation and secondary hydriding, Journal of Nuclear Materials 508 (2018) 423-433

[31] *Richard Nagy, Márton Király, Tamás Szepesi, Attila Gábor Nagy, Ádám Almási: Optical observation of the ballooning and burst of E110 and E110G cladding tubes, Nuclear Engineering and Design 339 (2018) 194–201

[32] *Richárd Nagy, Márton Király, Tamás Szepesi, Attila G. Nagy and Ádám Almási: Optical measurement of the high temperature ballooning of nuclear fuel claddings, Rev. Sci. Instrum. 89, 125114 (2018)

[33] *Z. Hózer, I. Nagy, A. Vimi, M. Kunstár, P. Szabó, T. Novotny, E. Perez-Feró, M. Horváth, A. Pintér-Csordás: Mechanical testing of ballooned E110 and E110G cladding after high temperature oxidation in steam, Proc. TOPFUEL 2015, 337-343

[34] *Zoltan Hozer, Erzsebet Perez-Feró,Tamas Novotny, Imre Nagy,Marta Horvath, Anna Pinter-Csordas, Andras Vimi, Mihaly Kunstar, and Tamás Kemény:Experimental Comparison of the Behavior of E110 and E110G Claddings at High Temperature," Zirconium in the Nuclear Industry: 17th International Symposium, STP 1543, Robert Comstock and Pierre Barberis, Eds., pp. 932–951 (2015)

[35] *BALLOON (database with 460 files in 28 folders)

*available in the R2CA database

5. JAERI and JAEA burst tests

A large number of integral LOCA tests in single and bundle configurations were performed by JAERI and JAEA since the 1980's. Not all tests will be described here since only a few quantitative burst data could be retrieved from literature.

5.1 Objectives

5.1.1 Multi-rod tests

The multi-rod tests performed at JAERI in the late 70s to early 80s were carried out on bundles of 7x7 simulators of Japanese 15x15 PWR rods. The main objective was to investigate flow channel blockage in a multi-rod configuration [37].

5.1.2 Single rod tests

Later in the 2000's, Integral Thermal Shock (ITS) tests were performed on as-received, pre-hydrided and irradiated cladding tubes of different alloys. Main objective was to study thermomechanical resistance of cladding tubes after a simulated LOCA transient (heating up, ballooning, burst, high temperature oxidation and quench under axial load). Complete burst data cannot be retrieved from papers but at least some data are available from [36] and some incomplete data will be taken from figures (strain versus burst temperature) available in literature for example in [39].

5.2 Tested materials, test facility

5.2.1 Multi-rod tests

These simulators had a heated length of 0.9 m (W-Re wire heaters inside alumina pellets), were internally pressurized in the range 20-70 bar and were maintained by two spacers. Different configurations were studied around the 7x7 studied bundles with unheated shroud, outer ring of 32 unpressurized heaters or unheated shroud backed by a ring of 32 guard heaters. More details can be found in [36].

5.2.2 Single rod tests

The ITS test facility scheme is given on Fig. 11. The main components are an Instron-type tensile testing machine, a quartz reaction tube, an infrared furnace with four tungsten–halogen lamps, a steam generator, and a water supply system for reflooding [39]. Cladding tubes (190 mm long for irradiated and 580 mm long for non-irradiated) with alumina pellets are heated-up under steam at 3 to 10 °C/s up to a high-temperature oxidation plateau before being quenched by water under axial load imposed by a loading cell. Tubes are pressurized with Ar at about 5 MPa at room temperature and then sealed. Cladding temperature is measured by three thermocouples.
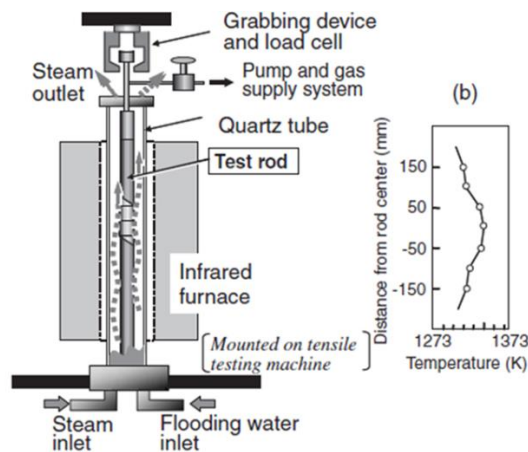
Fig. 11. JAEA LOCA test device from [39].

Various alloys were tested, Zy-4 as received and pre-hydrided and irradiated ones as shown in Table 3.

5.3   Measured parameters, PIE data

5.3.1   Multi-rod tests

Burst characteristics are not available for each rod but only ranges are given for some bundle tests (see Table 2). In some bundle tests, several sites with very high channel blockage (> 91%) were observed.

Table 2
JAERI test matrix of bundle burst tests using W-Re wire heaters and a close fitting unheated shroud from [38].

Bundle N°	Steam Flow Rate (g/cm^{2}xmin)	Heating Rate (°C/s)	Initial Internal Pressure (kg/cm^2)	Maximum Internal Pressure (kg/cm^2)	Burst Temperature (°C)
7805	0.44	6.6 – 8.7 (500 – 860°C)	50	64 – 70	805 - 860
7806	0.40	7.3 – 9.0 (500 – 900°C)	20	26 – 29	870 - 920
7807	0.40	5.9 – 7.2 (430 – 830°C)	70	87 – 93	750 - 790
7808	0.44	5.9 – 7.9 (500 – 890°C)	35	45 - 48	870 - 880

5.3.2   Single-rod tests

On-line measured parameters are cladding temperature at three elevations and axial load. Post-test examinations give maximum circumferential strain, hydrogen axial distribution, oxide and alpha(O) oxide layers (metallographies). Since the main goal of these tests was to study mechanical axial resistance during quenching after high-temperature oxidation, few data linked to burst are reported in the papers. In [39], maximum strain versus burst temperature is given for pre-hydrided (11-1500 wppm) Zy-4 tubes (see Fig. 12.) heated-up at 10°C/s and pressurized at around 5 MPa at room temperature.
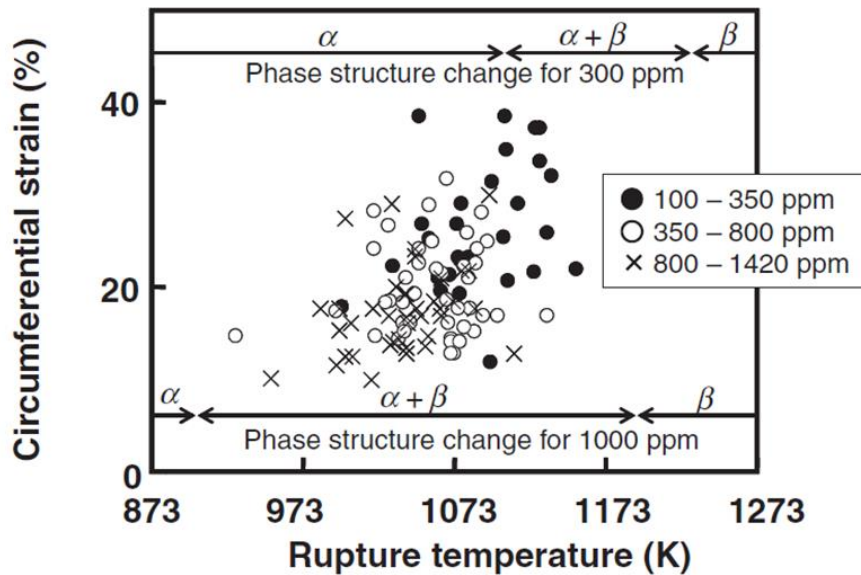
Fig. 12. Circumferential strain (%) versus burst temperature (K) from [39] in single rod tests with Zy-4 pre-hydrided pressurized at around 5 MPa at room temperature.

Table 3
Burst data in JAEA tests on irradiated tests from [36] and [37] . (NA: not available)

Test-ID	Alloy	BU (GWd/tU)	H (wppm)	e-ox ext (um)	dT/dt (°C/s)	T_{burst} (°C)	P_0 (MPa)	Strain (%)
MDA-1R	MDA	76	720	51	3-10	714,85	5	9,9
MDA-2R	MDA	76	838	62	3-10	NA	5	6,1
NDA-1	NDA	69	214	33	3-10	714,85	5	8,9
ZIR-2R	Zirlo	71	496	51	3-10	671,85	5	28
ZIR-3R	Zirlo	77	764	79	3-10	675,85	5	20,6
MFI-1	M5	66	73	6	3-10	779,85	5	20,1
MFI-2	M5	66	69	7	3-10	761,85	5	19,2
ZRT-1	Zy-2	66	297	30	3-10	762,85	5	17,7
ZRT-2	Zy-2	73	182	25	3-10	777,85	5	20,6
A3-1	Zy-4	44	170	20	10	799,85	5	14,1
A1-2	Zy-4	44	210	25	10	750,85	5	27,7
BL-3	Zy-4	39	140	18	10	819,85	5	24,3
BI-3	Zy-4	41	140	18	10	784,85	5	13,6
BI-5	Zy-4	41	120	15	10	754,85	5	8
BL-7	Zy-4	39	120	15	10	803,85	5	7,5

5.4   General conclusions

From tests performed at JAERI and the JAEA detailed above, some conclusions can be drawn taking into account that quantitative data retrieved from literature are limited:

- From bundle tests: the higher the initial pressure is the lower burst temperature is (in the range 2-7 MPa);
- From non-irradiated single-rod tests: the higher the hydrogen content is the lower burst temperature is for Zy-4 pressurized around 5 MPa at room temperature and circumferential strain is lower than 40%;
- From irradiated single-rod tests pressurized at 5 MPa at room temperature: strain is limited (6 to 28%) and burst temperatures are in the range 670-820 °C.

5.5 References

[36] *Nagase, F. and T. Fuketa, Fracture Behavior of Irradiated Zircaloy-4 Cladding under Simulated LOCA Conditions. Journal of Nuclear Science and Technology, 2006. 43(9): p. 1114-1119.

[37] ALSO *update of Nuclear Fuel Behaviour in Loss-of-Coolant Accident (LOCA) Conditions.* NEA, To be published.

[38] Grandjean, C., A State-Of-The-Art Review Of Past Programs Devoted To Fuel Behavior Under Loca Conditions Part One. Clad Swelling and Rupture. Assembly Flow Blockage.SEMCA-2005-313. 2005.

[39] Nagase, F. and T. Fuketa, *Behavior of Pre-Hydrided Zircaloy-4 Cladding under Simulated LOCA Conditions.* Journal of nuclear science and technology, 2005. **42**(2): p. 209-218.

*available in the R2CA database

6. UK burst tests

6.1 Objective

Several single-rod and multi-rod burst test were performed in UK during the 1970s and 1980s. One test series was performed in the PROPAT rig at UKAEA Springfields Nuclear Laboratories. In these tests, it was the objective to study the deformation of nuclear-grade Zircaloy-4 tubes under conditions, similar to occur during a LOCA. In the first part of the tests, the rod behaviour was studied under mainly radiative heat transfer conditions [40][41], in the second part mainly convective cooling conditions were applied (heat transfer coefficient of approximately 80 W/m^2·K) [42]. Further tests were performed with the same test rig under conditions similar to the TMI-2 accident conditions [43].

Similar single-rod burst tests were performed at Berkeley Nuclear Laboratories [44][45]. As the available description of these tests is very limited, they are not further discussed in the current report.

Tests with irradiated fuel rods were performed at the UKAEA Windscale Nuclear Laboratories [46]. 450 mm lengths cut from commercial PWR fuel rods were internally pressurised and subjected to temperature transients to simulate LOCA conditions. The primary purpose of this work was to examine the mechanical stability of the fuel column when the cladding has bulged away from it under internal pressurisation and to evaluate the extent of fuel fragmentation and re-location that occurs. However, data on the ductility of cladding which has experienced actual reactor service have also been produced.

Multi-rod tests were performed at the FOURSQUARE test rig at Springfields Nuclear Laboratories in which a 4x4 array contained in a shroud was heated to 750°C and 850°C in steam to investigate creep deformation of Zircaloy cladding in postulated PWR loss-of-coolant accidents, which may lead to rod-to-rod mechanical interactions [47]. One main objective of this test was to study mechanical interactions of balloons to assist code development [45].

6.2 Tested materials, test facility

The further description in this chapter is focused on the PROPAT test facility and the tests with mainly convective cooling [42]. The geometry of the Zircaloy-4 specimens was 9.5 mm outer diameter, 0.57 mm wall thickness and 450 mm length [42]. The tubes were filled with alumina pellets and directly resistance-heated. The specimens were heated with heating rates of 10 K/s to temperatures between 630 and 915°C and then hold at constant control temperature until rupture. Internal test pressures (at the beginning of the transients) were in the range 0.69 to 11.0 MPa. Radiative heat loss was minimized by surrounding the specimen with a cylindrical reflecting copper shroud. The specified heat transfer coefficient was obtained by adjusting the steam flow in the experiment [42].

According to the available open literature, mainly Zircaloy-4 tubes have been tested. Stainless steel tubes (i.e. Type 304) have also been investigated, as stated in the CSNI SOAR report [45], but no original publication with detailed data is available.

6.3 Measured parameters, PIE data

The following data was measured during the tests [42]:
- Cladding temperatures (by thermocouples attached to the top, middle, and bottom of the specimen)
- Steam inlet and outlet temperatures
- Internal tube pressure

- Shroud temperatures
- Power input

The time to rupture was measured and after the tests, the axial distribution of strain was determined in the cladding specimens. Fig. 13. shows results from the tests with mainly convective cooling [42] and compares them to tests with mainly radiative cooling performed earlier in the same test rig [40][41]. The maximum circumferential strains in both types of tests at the same temperature were comparable, that is 50 to 100 percent in the α-phase region.
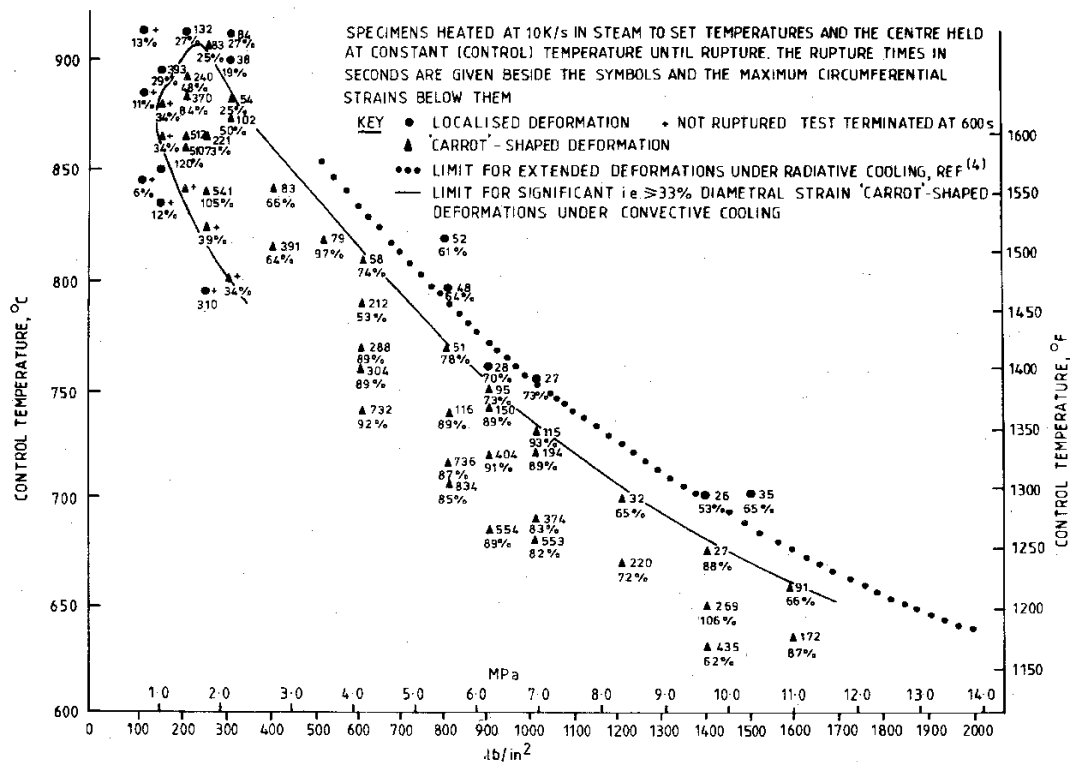
Fig. 13. Results of rupture testing of Zircaloy-4 PWR cladding with mainly convective cooling and comparison to results from tests with mainly radiative cooling [42]

6.4   General conclusions

The described single-rod experiments have certain limitations (e.g. due to direct resistance heating of the cladding, no real interaction with adjacent rods could be studied). In both experiments (with mainly radiative and with mainly convective cooling), axially extended deformation was found. Thus, it was demonstrated, that in a certain range of possible conditions predicted for LOCAs there is a potential for the occurrence of axially extended deformation, which may has a negative impact in the cooling of the rods. It was shown that compared to radiative cooling, convective cooling leads to a top-skewed distribution of the axial strain. The progressively increasing strain in the top part of the specimen was associated with the decrease in cooling as the steam temperature increases along the flow path.

Regarding the multi-rod experiments, the available data from these tests is rather limited [47].

6.5   References

[40] E.D. Hindle, Zircaloy fuel clad ballooning tests at 900-1070 K in steam. UKAEA Report ND-R-6(S). 1977
[41] E.D. Hindle, Zircaloy fuel clad ballooning tests at 900-1070K in steam. Further results at 890-1150K. UKAEA report ND-R-6(S) 1st supplement. 1977

[42] E.D. Hindle and C.A. Mann, An experimental study of the deformation of zircaloy PWR fuel rod cladding under mainly convective cooling, in Conference Proceedings: Zirconium in the Nuclear Industry. 1982, ASTM International.

[43] E.D. Hindle, C.A. Mann, and A.E. Reynolds, Simulation of Zircaloy cladding deformation under accident conditions derived from analysis of data from Three Mile Island-2, in CSNI Specialist Meeting on Safety Aspects of Fuel Behaviour in Off-Normal and Accident Conditions. 1980: Espoo, Finland. p. 155-157.

[44] T. Healey, B.D. Clay, and R.B. Duffey, Analysis of the axial ballooning behaviour of directly heated Zircaloy tubes. CEGB RD/B/N4145. 1977.

[45] P.D. Parsons, E.D. Hindle, and C.A. Mann, PWR Fuel Behaviour in Design Basis Accident Conditions - The Deformation, Oxidation and Embrittlement of PWR Fuel Cladding. A State-of-the-Art Report by the Task Group on Fuel Behviour of CSNI Principal Working Group No 2. CSNI Report 129. 1986, OECD NEA.

[46] A. Garlick and P. Hindmarch, Cladding elongation and fuel stack mechanical stability during internal pressurization tests on irradiated PWR fuel. UKAEA Report ND-R-628(W). 1983

[47] E.D. Hindle, T.J. Haste, and W.R. Harrison, Laboratory simulation of rod-to-rod mechanical interactions during postulated loss-of-coolant accidents in a PWR involving cladding oxidation, in Conference Proceedings: Materials for Nuclear Reactor Core applications. 1987.

[48] *Nuclear Fuel Behaviour in Loss-of-Coolant Accident (LOCA) Conditions, NEA No. 6846, 2009, NEA.

*available in the R2CA database

7. MRBT (ORNL) burst tests

7.1 Objectives

The main objective of the MRBT (Multi-Rod Burst Tests) tests in the late 1970's was to investigate the influence of the bundle size and the thermal & mechanical boundary conditions on the burst strain and flow blockage under thermal heat transfer conditions that did favour large deformations. Single tests were also performed in the MRBT program [49][50][51] [54].

7.2 Tested materials, test facility

7.2.1 Single rod tests (ORNL-79)

The Zy-4 test rods, with 915 mm heated length, were internally electrically heated (external diameter 10.92 mm, wall thickness 0.635 mm). The internal electric heater has a spiral Kanthal heating element wound on a MgO core and isolated from its stainless steel sheath by boron nitride. The gas annulus between heater and clad is filled with helium at a desired pressure value, this pressure being not controlled during the test transient. The nominal gap value was 0.23 mm in cold conditions. The test rod is placed inside a cylindrical shroud that can be heated or not and the gas atmosphere is steam or argon.

7.2.2 Bundle tests

Six MRBT tests have been carried out on rod bundles of different sizes:
- 4x4 for tests B1, B2 and B3;
- 6x6 for the test B4;
- 8x8 for tests B5 and B6.

In test B1, with heated shroud, the temperature was ramped at ~ 30 K/s from 350°C until the burst of rods, which occurred within 850-880°C interval. Burst strains range between 32 and 59% [49] .

Test B2 was run under conditions very close to those of B1 test, but without shroud heating. The burst strains are similar to those in B1: 34 to 58% [49].

In test B3, with heated shroud, the temperature ramp rate is lower (9.5 K/s) and the initial rod internal pressure was increased so as to cause rupture at about 760°C. All rods in B3 failed below 780°C, in the α-phase region, with burst strains in the range 42-77%; six rods had strains greater than the maximum of either B1 (59%) or B2 (58%) [49].

In test B4, carried out on a 6x6 rod array, a dysfunction has occurred that led to an early stop of the test at a low level of strain on the rods.

The B5 and B6 tests have been carried out on a 8x8 rod array surrounded by an unheated shroud. Test B5 has been conducted under conditions very close to B3: 9.8 K/s temperature ramp, same steam mass velocity. Rods burst occurred around 775°C. In test B6, the concluding test of the ORNL MRBT program, the conditions were chosen so as to obtain rod bursting around 930°C i.e. 3.5 K/s temperature ramp and filling pressures around 30 bars, in the $\alpha+\beta$ phase domain, in order to ascertain the typically smaller strain level observed in single rod tests under similar conditions. The B6 results showed burst strains ranging from 22 to 56% with a 30% average.

7.3 Measured parameters, PIE data

During tests cladding temperatures at various elevations (sheeted thermocouples welded inside the cladding) were recorded as well and internal pressure (fast response transducer). After the test, strain measurements were made after bundle epoxy casting and cut every 10 to 20 mm. In open literature only single-rod tests and data from B1, B2, B3 and B6 tests were found (illustrated on Fig. 14. and Fig. 15.). From these figures we can conclude that:

- The highest the pressure burst is the lower the burst temperature is;
- Low heating rates seems to lead to higher maximum burst strains;
- At 29.5°C/s with a differential pressure around 70 bars, bundle tests lead to higher maximum strain (comparison of B1 results with single rod tests ORNL-79).
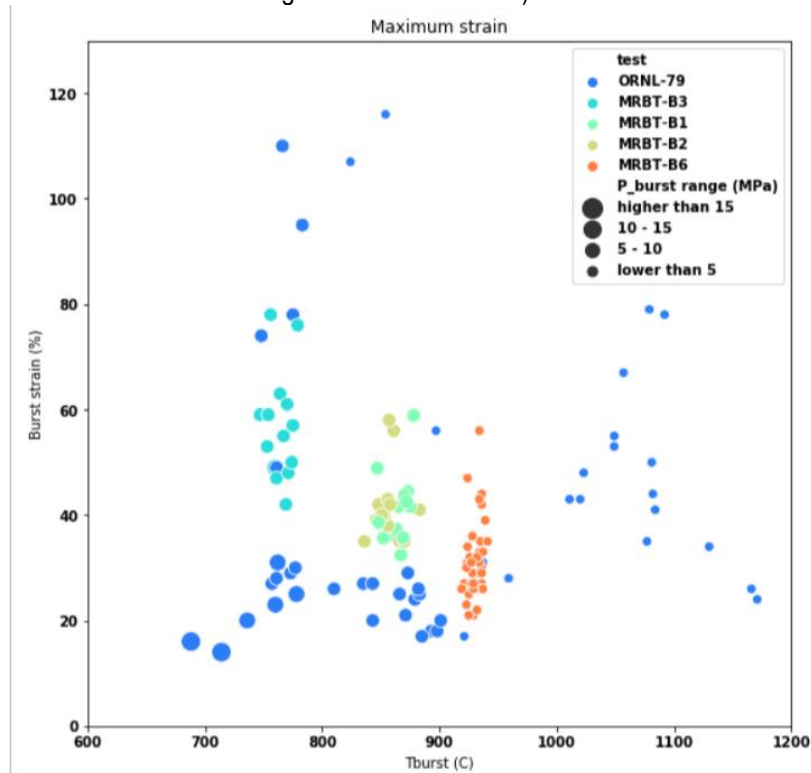
Fig. 14. Circumferential strain (%) versus burst temperature (°C) for single (ORNL-79) and bundle tests B1, B2, B3 and B6 in the MRBT program. Marker size depends on burst pressure.
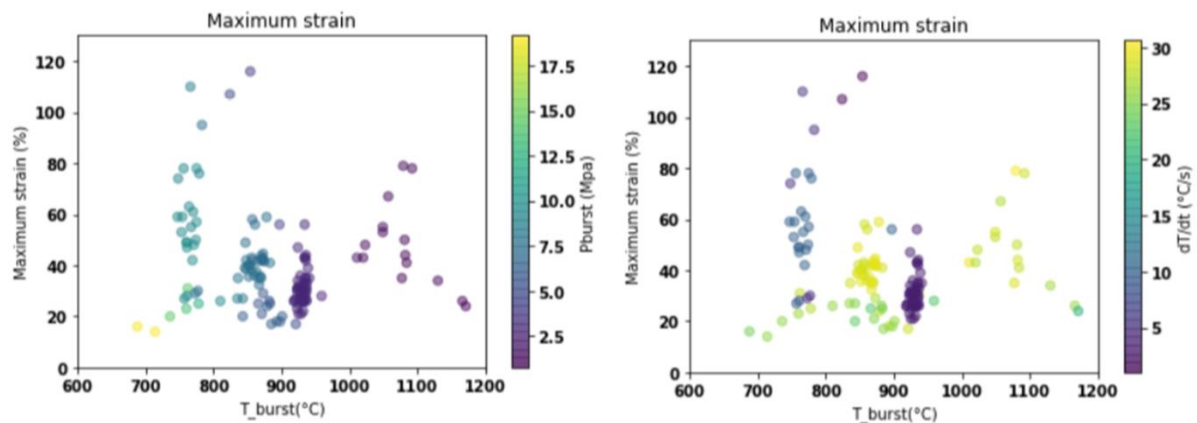
Fig. 15. Circumferential strain (%) versus burst temperature (°C) for MRBT burst tests. Left: colour map depends on burst pressure (MPA), right: color map depends on heating rate (°C/s).

7.4 General conclusions

Conclusions are taken from references [49] and [51] "The main results, as provided by the comparison of the B3 and B5 data, indicate that in a large array the straining of inner rods lead to mechanical interactions between neighbour rods that, although of limited impact on burst temperature and elongation, will modify significantly the spatial development of deformation until rupture. Notably, the trapping of bulging rods has appeared to cause the deformation to extend axially, resulting in a larger volume expansion and a greater axial extent of blocked regions. This also results in a deviation from the rupture temperature/pressure curve deduced from single-rod heated-shroud-tests data. Thus the authors concluded that the flow area restriction in large arrays may be underestimated by tests results on small unconstrained arrays and that at least two rows of deforming "guard" rods are necessary around the central deforming array to properly simulate representative conditions which would be present in reactor fuel assembly."

7.5 References

[49] Grandjean, C., A State-Of-The-Art Review Of Past Programs Devoted To Fuel Behavior Under Loca Conditions, Part One. Clad Swelling And Rupture Assembly Flow Blockage, SEMCA-2005-313.

[50] Massih, A.R. and L.O. Jernkvist, Assessment of data and criteria for cladding burst in loss-of-coolant accidents, 2015:46. 2015.

[51] *Nuclear Fuel Behaviour in Loss-of-Coolant Accident (LOCA) Conditions, NEA No. 6846, 2009, NEA.

[52] Chapman, R.H., A.W. Longest, and C.J. L., Experiment Data Report for Multirod Burst Test (MRBT) Bundle B-6, NUREG/CR-3460,1984.

[53] Chapman, R.H., Multi Rod Burst Test Program Progress Report for July-December 1977, NUREG/CR-0103, 1977.

[54] *Powers, D.A. and R.O. Meyer, Cladding Swelling and Rupture Models for LOCA Analysis, in NUREG-0630,1980, U.S. NRC.

*available in the R2CA database

8. Russian burst tests

8.1 Objectives

The main objective of the Russian burst tests summarised in this chapter was the measurements of parameters characterising the mechanical behaviour of Zr-1%Nb cladding under ballooning conditions. The high temperature rupture of the cladding due to ballooning is the specific feature of testing VVER fuel rods under IGR conditions. It was important to obtain the data base to try to describe this process by computer codes. It should be mentioned that of the two considered codes only FRAP-T6 code allowed to predict mechanical behaviour of the cladding under ballooning conditions. That is why the program of special tests has been developed with consideration of FRAP-T6 code requirements to the respective data base. Still, the motivation targeted at better understanding of the ballooning key phenomena was also evidently present.

8.2 Tested materials, test facility

Burst tests of pressurized specimens are the classical type of tests to study ballooning phenomena. The special setup developed for this test series (left) and a typical burst test scenario (right) are shown in Fig. 16.
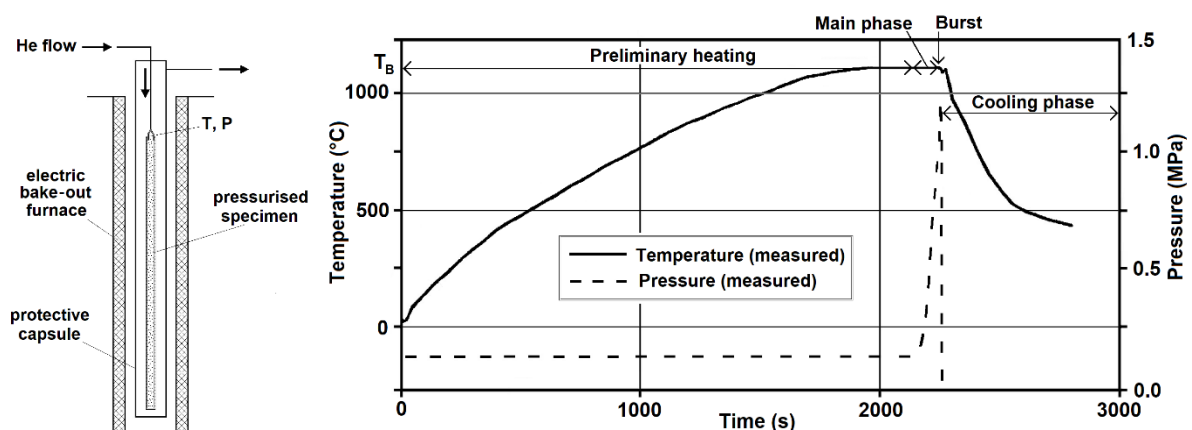
Fig. 16. Principle part of the experimental setup (left) and time history of the temperature and pressure for one of the burst tests (right) [55]

Each specimen 150 mm long was fabricated of the VVER tube, or irradiated VVER cladding. A special cap was placed in the bottom part of the specimen. The top part of the specimen was connected to the source of helium supply by the set of special technological elements. The whole assembly was located inside the protective capsule, which in its turn was put into electrical bake-out furnace. The history of temperature (T) and pressure (P) in the top part of the specimen was registered in the process of testing. Besides, the original structure of the furnace was designed to ensure video filming of the specimen surface during testing, and thus to obtain time history of the cladding hoop strain and burst.

Preliminary heating stage of the scenario called for the step by step temperature increase of the specimen up to the specified T_B value under slightly excessive helium pressure inside the specimen. Non-uniformity of the temperature distribution along the specimen height and radius was not more than ±4°C. Then helium pressure inside the specimen was increased according to the specified value of the pressure increase rate up to the burst of specimen. After that the cooling phase took place.

Two types of specimens were tested: specimens fabricated of unirradiated VVER tubes and specimens fabricated of the cladding of commercial VVER fuel element #153 of the fuel assembly #4108 irradiated at Unit 5 of NV NPP. The parameters of the burst tests and the samples are summarised in the Table 4.

Table 4
Summary of the burst experiments and the unirradiated samples (left) and the irradiated samples (right)

Parameter	Value	Parameter	Value
temperature	800 - 1200 °C	outer diameter	9.068 – 9.096 mm
pressure increase rate	0.01 - 1.0 MPa/s	cladding thickness	0.69 ± 0.015 mm
specimen length	150 ± 1 mm	burn-up	47.2 – 48.0 MWd/kgU
outer diameter	9.136 - 9.149 mm	ZrO_2 thickness (outer)	3 – 5 μm
inner diameter	7.712 - 7.735 mm	ZrO_2 thickness (inner)	< 1 μm
cladding thickness	0.697 ± 0.015 mm	H conc. in the cladding	0.051 – 0.057 %(w)

The respective characteristics for irradiated specimens were obtained with the help of profilometry, Eddy-current testing and γ-scanning of the fuel element.

8.3   Measured parameters, PIE data

The program of testing of unirradiated specimens called for measurement of the following parameters:
-   pressure of the burst versus temperature and pressure increase rate;
-   axial radius of the curvature of the cladding burst area versus temperature and pressure increase rate;
-   circumferential elongation of the cladding burst area versus temperature and pressure increase rate.

The program for irradiated specimens was the same but for the fact that no study of the influence of the pressure increase rate was planned.

The results confirm that mechanical behaviour of unirradiated and irradiated specimens is identical under high temperatures. In the temperature range of 700 – 900 K the burst pressure decreases practically 6 times, but this dependence becomes much weaker as the temperature continues to grow. The obtained data indicate that cladding elongation decreases abruptly along with the α+β→β phase transition. Beside that, the tests indicate that beginning with 1000 °C elongation of Zr-1%Nb starts to increase along with the increase of the cladding temperature. Moreover, influence of pressurization rate on burst parameters was studied. Obtained results are presented in Fig. 17.
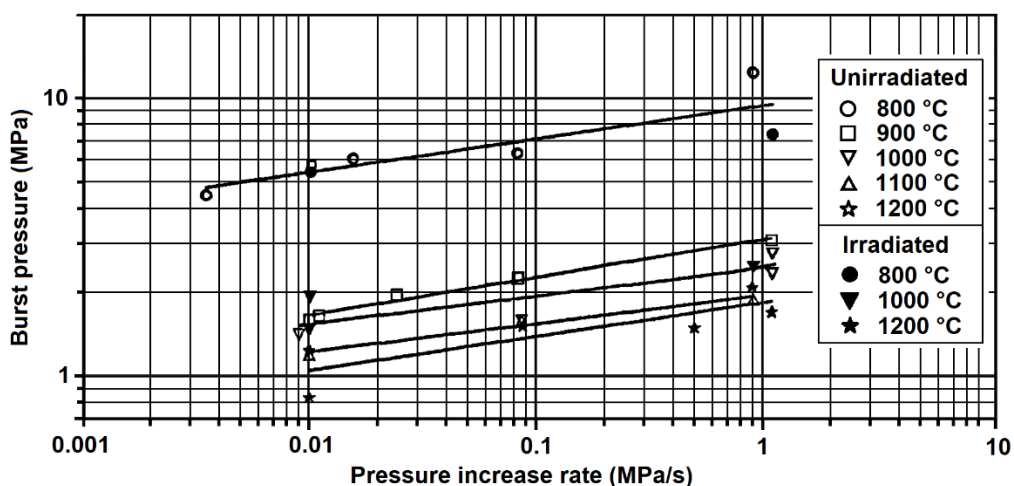
Fig. 17. Burst pressure vs. pressure increase rate at different temperatures for unirradiated and irradiated Zr-1%Nb cladding [55]

After burst tests all the tested specimens were subjected to post-test examination to define specific ballooning parameters. The first stage of the work included making photographs of each specimen in different projections. Metallographic cross-sections were produced and their photographs made over the second stage of the post-test

examinations, so that to get the view of the specimen in the centre and at the boundary of the cladding rupture area. The third stage of examinations called for computer processing of the whole set of photographs according to the following issues:
- determination of the middle line profile for each cross-section of the cladding;
- measurement of the cladding thickness;
- measurement of the ballooning axial radius;
- measurement of the circumferential radius of the curvature;
- measurement of the peak circumferential elongation.

Data base to characterise burst tests is presented in Appendix K of the report [56]. It includes the parameters of unirradiated and irradiated specimens before tests; photographs of specimens after-tests and photographs of cross-sections of the specimens; and tables with measured results.

8.4   General conclusions

From reactor safety point of view, the high temperature rupture of the cladding due to ballooning in the design basis accidents is important. The mechanical behaviour of unirradiated and irradiated Zr-1%Nb claddings under ballooning conditions were investigated during the Russian burst tests. In the experiments the specimens were heated up to the specified temperature under lower pressure, and then the inner pressure was increased. The experiments were also important to obtain the data base to try to describe this process by computer codes.

Based on the result of the tests it can be concluded, that abrupt decrease of the burst pressure can be observed in the region of α-β phase transformation of the alloy. A slight dependence of burst pressure versus temperature can be noted for β-phase of Zr-1%Nb alloy. The mechanical behaviour of unirradiated and irradiated specimens is identical under high temperature conditions. Reduction of circumferential elongation is observed in the area of α+β→β transition in the whole range of pressurization rates. Detailed experimental results are available in the Appendix K of the report [56].

8.5   References

[55] * L. Yegorova: Data base on the behaviour of high burn-up fuel rods with Zr-1%Nb cladding and UO_2 fuel (VVER type) under reactivity accident conditions - Volume 2. Description of test procedures and analytical methods, NUREG/I-0156, IPSN 99/08-2, 1999

[56] *L. Yegorova: Data base on the behaviour of high burn-up fuel rods with Zr-1%Nb cladding and UO_2 fuel (VVER type) under reactivity accident conditions - Volume 3. Test and calculation results, NUREG/I-0156, IPSN 99/08-2, 1999

*available in the R2CA database

9. ANL burst tests

9.1 Objectives

Argonne National Laboratory (ANL) performed a number of integral LOCA tests ten years ago in order to study ballooning, burst, high temperature oxidation and post-quench ductility. More details can be found in references [57] to [60].

9.2 Tested materials, test facility

Westinghouse 17×17 low-Sn Zirlo (external diameter 9.5 mm, 570 µm thick) as-received and pre-hydrided (200-600 wppm) were tested. As-received Zy-2 (external diameter 11.18 mm, 710 µm thick) and irradiated Zy-2 (BU 54-57 GWd/t, 70 wppm) were also tested. The LOCA high-temperature apparatus was designed to perform both LOCA integral tests using long (≈300 mm) pressurized fuelled cladding samples and oxidation-quench tests using short (25 mm) defueled cladding samples. An out-of-cell unit was used for thermal-benchmarking purposes and for generating data for as-fabricated and pre-hydrided alloys. Two in-cell units have also been developed. The radiant-heating furnace has four vertical bulbs, a reflecting inner surface, and a 250-mm-high uniform heating zone. LOCA integral tests were conducted with 300-mm-long samples initially under high internal pressure. Typical thermal transients in steam or argon environments are illustrated on Fig. 18.
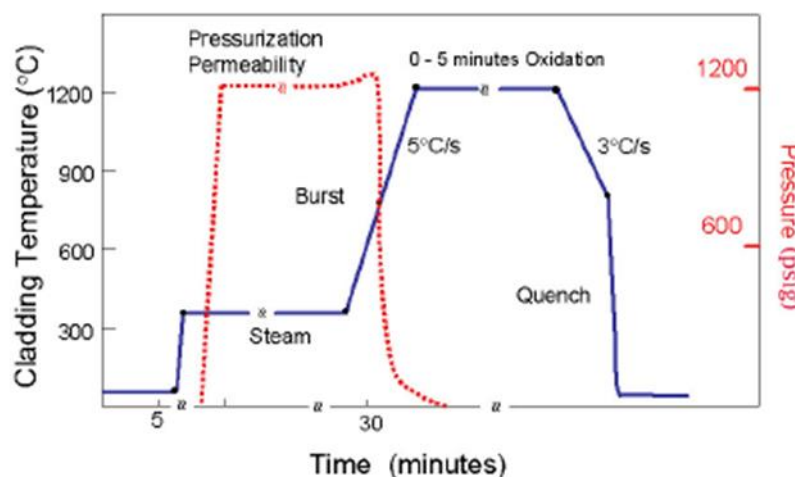
Fig. 18. Temperature and pressure histories for full LOCA integral test sequence, including quench from 800°C to 100°C [57].

9.3 Measured parameters, PIE data

Cladding temperature is recorded during transient and post-mortem strain is evaluated from circumference measurements (increase in cladding mid-wall circumference normalized to the initial mid-wall circumference) or estimated from diameters measurements, the uncertainty on strain is ± 10%. Initial pressure at 300°C and burst temperature were measured. The evaluation of burst temperature is given within ± 30°C. Burst data for as-received and pre hydrided Zirlo are given in Table 5 and plotted on Fig. 19. Data for Zy-2 samples are given in Table 6.

Table 5
Burst test data for as-received and pre hydrided ZIRLO cladding tubes in steam performed at ANL

Test-ID	H0 (wppm)	P_0 (MPa)	T_{burst} (°C)	Strain (%)	Test-ID	H0 (wppm)	P_0 (MPa)	T_{burst} (°C)	Strain (%)
6	11	8,3	750	42	25	11	8,3	757	42
7	11	5,5	810	22	26	11	8,3	765	34
8	11	4,1	845	22	27	11	8,3	760	43
9	11	2,8	875	33	29	11	8,3	746	49
10	11	11,0	715	70	30	11	8,3	746	42
11	11	9,7	750	40	32	11	8,3	748	49
12	11	6,9	805	33	36	11	8,3	750	53
13	11	8,3	741	42	37	11	8,3	755	46
14	11	8,3	735	48	43	11	8,3	738	50
15	11	8,3	755	52	39	660	4,1	742	57
16	11	8,3	734	35	40	390	8,3	690	47
17	11	8,3	750	45	41	220	8,3	730	56
18	11	8,3	748	43	42	520	8,3	682	71
19	11	4,1	840	25	44	700	8,3	673	56
21	11	4,1	850	28	45	220	8,3	737	68
22	11	4,1	837	23					
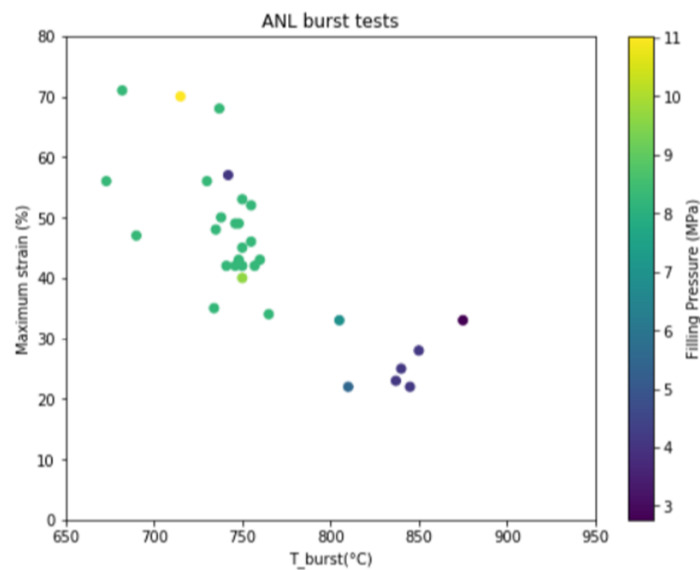
Fig. 19. Maximum strain (%) versus burst temperature in ANL LOCA burst tests (as-received and pre hydride Zirlo).

Table 6
Burst test data for as-received and irradiated BWR Zy-2 cladding tubes performed at ANL

Test-ID	H0 (wppm)	P_{max} (MPa)	P_{burst} (MPa)	T_{burst} (°C)	Strain (%)	Atmosphere
OCL5	11	8,96	8,3	733	44	Ar
OCL8	11	8,62	7,7	766	60	Ar
OCL22	11	8,887	6,9	747	54	Steam
OCL17	11	9,1	9,1	750	49	Steam
OCL11	11	8,61	7,9	753	43	Steam
OCL13	11	9,09	6,4	766	43	Steam
ICL1	70	8,96	8,6	755	38	Ar
ICL2	70	8,887	8,0	750	39	Steam
ICL3	70	9	8,6	730	43	Steam

9.4   General conclusions

From these set of burst tests at 5°C/s on Zirlo (as-received and 200-600 wppm pre hydride) and Zy-2 as-received and irradiated tubes, we can conclude:

- The higher the initial pressure is the lower burst temperature is (in the range 2,8-11 MPa);
- Pre-hydrided samples, pressurized at 8.3 MPa, burst at lower temperatures and show slightly higher maximum burst strain than as received-samples;
- Ductility at high temperature seems to have a local minimum around 820°C;
- Irradiated and as-received Zy-2 tested samples have similar burst behaviour in terms of pressure, temperature and strain.

9.5   References

[57] *Billone, M., et al., Cladding Embrittlement During Postulated Loss-of-Coolant Accidents, NUREG 6967, 2008, U.S.-NRC

[58] *Billone, M.C., et al., Cladding Behavior during Postulated Loss-of-Coolant Accidents, NUREG/CR-7219, 2016.

[59] Yan, Y., et al., Update of LOCA-integral and post-LOCA-bend test results for fresh ZIRLO cladding. Argonne National Laboratory letter report to U.S. Nuclear Regulatory Commission, ML111380437., 2010

[60] Massih, A.R. and L.O. Jernkvist, Assessment of data and criteria for cladding burst in loss-of-coolant accidents, 2015:46. 2015

*available in the R2CA database

10. EDF burst tests

10.1 Objectives

The main aim of the PhD from R. Thieurmel (EDF) was to study quench resistance of ballooned/burst cladding tubes after high temperature oxidation under steam and axial load. The manuscript is available on-line (in French). Some of the results are available in paper [62].

10.2 Tested materials, test facility

The test device is similar to the one used in Studsvik tests (SCIP III and NRC tests) or some ANL tests. The heat-up is performed in steam environment in an infrared furnace (four lamps). During test the temperature is controlled by a thermocouple attached by a wire to the cladding 50 mm above cladding mid-height. Internal pressure is measured by a manometer during the test.
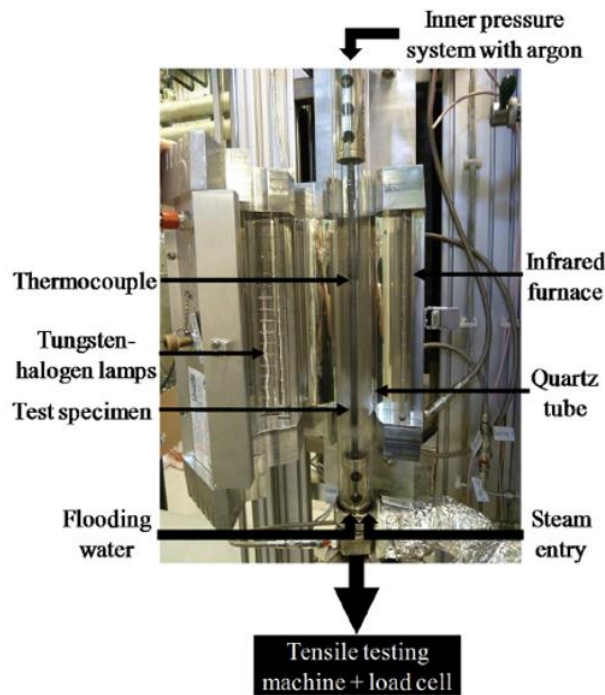
Fig. 20. Semi-integral LOCA test device from [62].

300 mm long as-received or pre-hydrided to 600 wppm Zy-4 cladding tubes (external diameter 9.5 mm, 570 µm thick) were pressurized to about 6 MPa at room temperature. More than 80 semi-integral LOCA tests were performed.

10.3 Measured parameters, PIE data

During transient, cladding temperature and internal pressure are measured. Post-mortem, external circumference at burst is measured, which is then used to calculate strain (external circumference increase/initial external circumference). Strain versus burst temperature is plotted on Fig. 21.
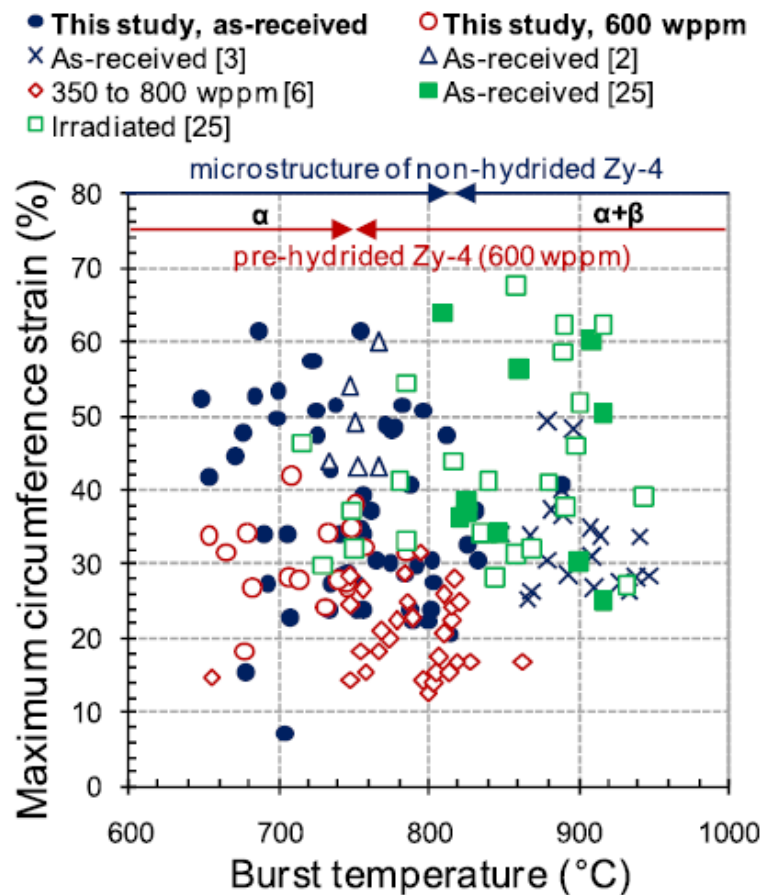
Fig. 21. Maximum strain (%) versus burst temperature in EDF burst tests (as-received and 600 Hwppm Zy-4).

10.4 General conclusions

From EDF burst tests results on as-received and 600 wppm Zy-4 pressurized around 60 bars we can conclude that:

- Burst temperature is slightly lower for pre-hydrided samples (mean 714 °C) than for as-received ones (mean 753 °C);
- Maximum circumferential strain is smaller than ~60% and slightly smaller for pre-hydrided samples (mean 30%) than for as received ones (mean 37%).

10.5 References

[61] *Thieurmel, R., Identification des conditions de rupture fragile des gainages combustibles en alliage de zirconium oxydés sous vapeur d'eau à haute température et trempés sous charge axiale., in Paris Sciences et Lettres, 2018

[62] Thieurmel, R., et al., Contribution to the understanding of brittle fracture conditions of zirconium alloy fuel cladding tubes during LOCA transient. Journal of Nuclear Materials, 2019. 527.

*available in the R2CA database

11. PBF LOCA tests

11.1 Objectives

The power burst facility (PBF) at Idaho National Engineering Laboratory (INEL, now INL) was a water-cooled and moderated tank type research reactor used for various reactor transient tests. One of the test series performed was the PBF-LOC tests to obtain data for analytical model verification and for the development and the assessment of fuel behaviour computer codes used to predict the response of a pressurized light water reactor (PWR) during a hypothetical break in the cold-leg inlet or hot-leg outlet, and to determine the behaviour of fuel rods when exposed to a wide variety of loss-of-coolant (LOCA) conditions. The test programme was designed to investigate the two major parameters determining cladding circumferential strain during ballooning, i.e. cladding temperature and differential pressure, using both unirradiated and irradiated rods.
The mostly published and cited tests of the PBF-LOC series are the LOC-11, LOC-3, LOC-5 and the LOC-6.

11.2 Tested materials, test facility

In each PBF LOCA test, there were four separated 15×15 type PWR test rods with a 0.9 m active length, each contained in a separate unheated shroud. Two of the rods were internally pressurised to values representative of high burn-up rods. The plenum volume was scaled in proportion to the active length compared to the that of a full length rod. The target peak cladding temperatures were attained by varying the rod power history and time of critical heat flux. Each test with four single rods consisted of a pre-blow-down power calibration and decay heat build-up, blow-down (depressurisation of the coolant) and test termination by rapid quenching. During depressurisation, the normally sub-cooled water surrounding each test rod flashed to steam as the coolant was released through the cold leg and the cladding temperature increased.
Test LOC-11 consisted of four, separately shrouded, fresh fuel rods of PWR design, with initial plenum pressure as a variable. Maximum cladding temperatures of up to 800 °C (corresponding to high ductility α-phase Zircaloy) were sought during Test LOC-11. The fuel rods were exposed to a series of three blowdowns from different power and coolant conditions. The second PBF-LOCA test (LOC-3) was conducted as planned with peak cladding temperatures of about 920 °C. Test LOC-5, the third in the PBF LOCA series, was to achieve cladding deformation and ballooning at temperatures in the range of 970 to 1080 °C. For these temperatures, a maximum in ductility of the β-phase cladding is approached, and significant cladding ballooning is expected before rupture.
The cladding temperatures shown in Fig. 22 corresponds to the region where maximum ductility occurs in α-phase Zircaloy, the strain-rate-dependent ductility trough in the transition region from α to β-phase, and the region of maximum ductility in the β-phase under oxidising conditions.
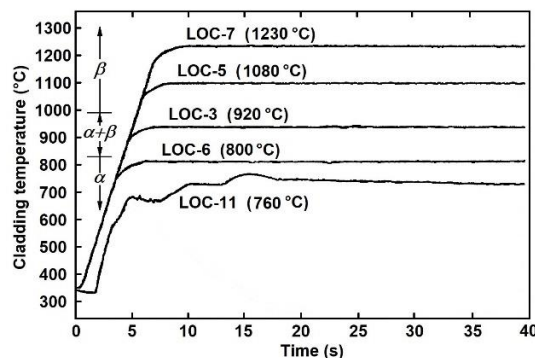
Fig. 22. The cladding temperature in some PBF-LOC experiments

Test LOC-6 was conducted with four rods of PWR 15 x 15 design with the exception of fuel stack length (89 cm) and enrichment (12.5 w% ^{235}U). Each rod was surrounded by an individual flow shroud. The rods were subjected

to the same thermal-hydraulic conditions. The test transient started from a steady-state regime under water at nominal condition: 320 °C, 15.2 MPa, 45 kW/m linear heat rate. After isolation of the test section from the PBF circuit, a valve opening led to blowdown representative of a cold leg break large LOCA. The axial profile of the nuclear power has been flattened to simulate the mid height of a PWR. During the test the power was monitored in order to reach and maintain the target temperature of the test. The heating rate of the different rods in the test varied between the rods, depending on initial stored energy and the fuel/clad heat transfer. After having maintained the plateau temperature for a sufficient duration so as to reach rod rupture, the test is terminated by quenching.

11.3 Measured parameters, PIE data

Out of the thirteen rods tested in the LOC series, nine ballooned and ruptured, two did not burst and two failed to achieve the planned transient owing to malfunction of the equipment. The thermal and mechanical behaviour data for the eleven rods which were satisfactorily tested are given in Table 7.

Table 7
Summary of cladding deformation data from tests LOC-3, LOC-5 and LOC-6

Test	Rod number	Initial pressure (MPa)	Burn-up (MWd/kgU)	Max. circumferential elongation (%)	Axial extent of deformation >5% (m)
LOC-3	1	2.45	0	29	0.20 – 0.60
	2	2.38	15.96	40	0.50 – 0.60
	3	4.92	0	20	0.15 – 0.60
	4	4.75	16.62	41.6	0.10 – 0.65
	6	2.41	17.66	35	0.13 – 0.65
LOC-5	7A	4.83	0	19	0.10 – 0.60
	7B	4.83	0	48	0.10 – 0.60
	9	2.41	0	<1	-
LOC-6	10	2.41	10.80	13.6	0.25 – 0.56
	11	4.74	0	31	0.25 – 0.43
	12	4.83	10.80	74	0.22 – 0.52

The cladding strain was generally concentrated within the axial zone of uniform temperature, i.e. between 0.2 and 0.5 m from the bottom of the fuel stack and failure generally occurred between 0.2 and 0.4 m. The circumferential strain at the burst elevation and over the axial zone of uniform temperature was greater in the rods previously irradiated in Saxton PWR than in the unirradiated rods for both tests which burst in the high α region and the α+β
region (Fig. 23).
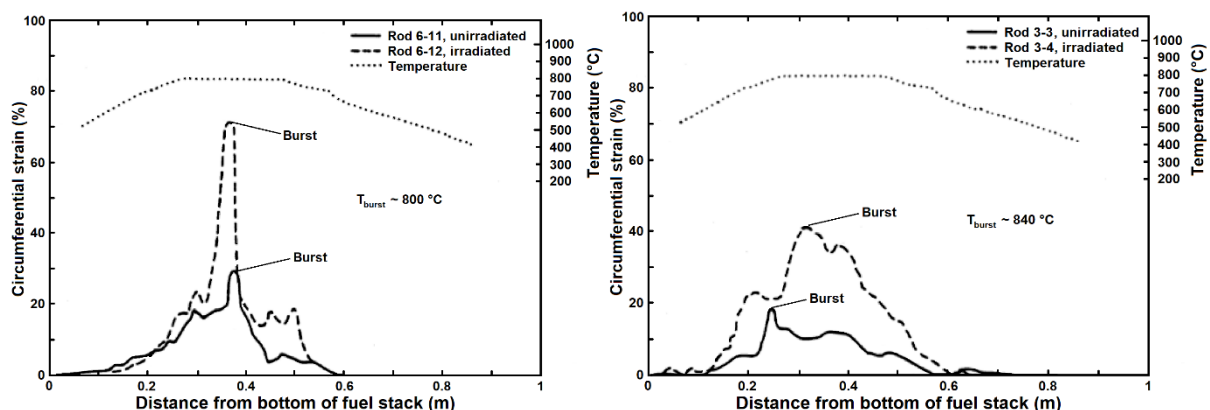
Fig. 23. Comparisons of the axial profiles of cladding circumferential strain in the high pressure fresh and irradiated rods: rods 11 & 12, burst in the α-phase (left) and rods 3 & 4, burst in the α+β transition (right)

.

Fuel relocation and dispersal were also observed after the experiments. The experimental studies reported that (1) no axial relocation of fuel occurs until the cladding hoop strain exceeds a value of 8%; (2) after the cladding hoop strain exceeds 8%, the fuel pellets crumble, and (3) as the cladding continues to strain, axial fuel relocation occurs so that the fuel void fraction in the balloon region remains equal to the void fraction at the time of fuel pellet crumbling.

11.4 General conclusions

From reactor safety point of view, the deformation and the burst of fuel cladding in the design basis accidents are important. The effects of initial rod internal pre-pressurization and prior irradiation were investigated during the PBF-LOC experiments, and the effect of rod pre-pressurization was found to be significant. However, for burnups of about 17 MWd/kgU, prior irradiation increased cladding circumferential strains at failure. The wall thinning was primarily concentrated in the burst region of the cladding of the unirradiated rods, whereas in the case of the previously irradiated rods the wall thinning was more uniformly distributed around the circumference. Axial fuel relocation during some PBF LOCA transients has been evidenced and the reports also noted the observation of fuel dispersal.

11.5 References

[63] *H. J. Zeile: Overview of the PBF test results, EG&G, The Fourth NSRR Technical Review Meeting, 1980, Tokai-mura

[64] *Nuclear Fuel Behaviour in Loss-of-coolant Accident (LOCA) Conditions, State-of-the-art Report, OECD 2009 NEA No. 6846

[65] Report on Fuel Fragmentation, Relocation and Dispersal, OECD Report, NEA/CSNI/R(2016)16

[66] Broughton, T.M., Vinjamuri, K., Hagrman, D.L., Golden, D.W., MacDonald, P.E.: PBF LOCA test LOC-6 fuel-behaviour report, NUREG/CR-3184, 1983

[67] J. M. Broughton, R. E. Mason, R. K. McCardell, P. E. MacDonald: PBF LOCA Test Series, Tests LOC-3 and LOC-5 Fuel Behaviour Report, NUREG/CR-2073/XAB, 1981

[68] Nuclear Fuel Behaviour in Loss-of-coolant Accident (LOCA) Conditions, State-of-the-art Report, OECD 2018 (in publication process)

*available in the R2CA database

12. FR-2 tests

"A series of in-reactor experiments using PWR-type single rods (active fuel length 50 cm, enrichment 4.7%) both unirradiated and irradiated (2 500-3 5000 MWd/t) and simulating the second heat-up phase of a cold leg break has been carried out in the DK loop of the FR-2 reactor at Kernforschungszentrum Karlsruhe (KfK) West Germany" [69].

12.1 Objectives

"A total of 47 single rod tests were performed in the FR2 reactor at KfK[20], aiming at providing a database of results to be compared with the REBEKA single rod tests, in view to evaluate the possible influence of a reactor environment on the behaviour of a fuel rod with fresh and irradiated fuel under LOCA transient conditions" [70].

12.2 Tested materials, test facility

Single tests were performed on Zy-4 fuelled tubes (0 → 35 GWd/tU) and some tests were performed with electrical simulators.

Table 8
Test matrix of the FR2 in-pile tests on fuel rod behaviour.

Test Type	Test Series	Number of Irradiated Rods	Number of Tests	Target Burnup (GWd/tU)	Range of Internal Pressure at Steady State Temperature (bar)
Calibration, Scoping	A	-	5	-	25 – 100
Unirradiated Rods (main parameter: internal pressure)	B	-	9	0	55 – 90
Irradiated Rods (main parameter: burnup)	C E F G1 G2/G3	6 6 6 6 6	5 5 5 5 5	2.5 8 20 35 35	25 – 110 25 – 120 45 – 85 50 – 90 60 – 125
Electrically-Heated Fuel Rod Simulators (main parameter: internal pressure)	BSS	-	8	-	20 - 110

The tests were performed in the DK loop of the FR2-reactor which could provide the desired thermal hydraulic conditions for the tests. The test rod was enclosed in a thin cylindrical unheated shroud with narrow spacing between them. The experimental sequence that aimed to reproduce the quasi-adiabatic phase of a large break LOCA transient typically consisted of:

- An initial steady-state under steam at 573 K, 6 MPa;
- The blowdown phase with stopping of the steam flow that led to a temperature rise at 12 K/s on average with neutronic power maintained around 40 W/cm;
- Near 1200 K, the reactor scram leading to the temperature turnover and followed in a given number of tests by a steam quench near 1000 K activated by the re-opening of the steam inlet flow valve.

12.3 Measured parameters, PIE data

During the tests, several cladding temperatures were measured by thermocouples. Internal rod pressure was also measured on-line. Post-test, maximum circumferential strain was measured (cf Fig. 24.).
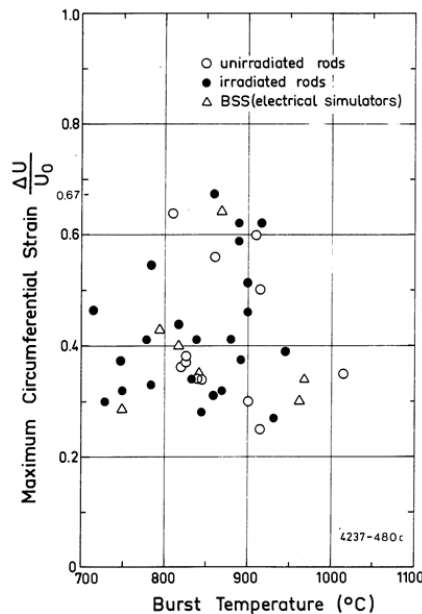
Fig. 24. FR2 - maximum circumferential strain versus burst temperature.

12.4 General conclusions

From single rods performed in the FR2-reactor one can conclude:
- For internal pressures from 2.5 to 12.5 MPa, burst temperatures are in the range 700-1000 °C;
- Maximum circumferential strain is smaller than 67% (due to the small heater inner diameter);
- The results of the FR2 tests do not reveal any appreciable differences between the behaviour of irradiated rods, fresh rods and even of electric simulators.

Table 9
Single-rod tests in FR2, burst data (data set IV from [71])

Rod No	Burnup (MWd/kgU)	T˙ (K/s)	p0 (MPa)	pB (MPa)	pmax (MPa)	TB (K)	Eθ,max (%)	tB (s)
A1.1	0	7.0	5.2	5.0	5.4	1083	64	79
A2.1	0	19.0	9.4	8.8	10.0	1093	36	20
A2.2	0	12.1	6.7	5.8	7.5	1133	56	38
A2.3	0	13.0	2.6	2.5	2.7	1288	35	55
B1.1	0	17.5	5.6	5.2	5.9	1173	29	40
B1.2	0	8.7	5.0	4.5	5.5	1188	26	72
B1.3	0	12.5	6.6	6.1	7.1	1118	34	37
B1.5	0	9.2	5.2	4.5	5.8	1183	60	72
B1.6	0	8.2	8.5	8.0	9.0	1098	38	56
B1.7	0	11.5	6.6	6.1	7.1	1113	34	41
B3.1	0	10.0	8.5	7.9	9.1	1098	37	46
B3.2	0	12.1	5.6	5.0	6.1	1188	50	55

C1	2.5	14.0	5.1	5.6	5.6	1173	51	47
C2	2.5	12.6	3.2	3.4	3.4	1218	39	58
C3	2.5	13.2	10.5	11.2	11.2	1022	37	32
C4	2.5	12.1	7.3	8.1	8.1	1088	44	41
C5	2.5	9.3	2.4	2.5	2.5	1189	62	78
E1	8	12.5	2.5	2.6	2.6	1183	30	59
E2	8	11.7	12.1	12.9	12.9	981	46	29
E3	8	11.2	5.3	5.6	5.6	1133	31	47
E4	8	11.6	7.9	8.6	8.6	1054	55	35
E5	8	11.5	2.3	2.6	2.6	1129	67	63
F1	20	10.6	6.4	7.2	7.2	1163	59	43
F2	20	8.7	5.8	6.2	6.2	1166	38	57
F3	20	10.1	4.4	4.6	4.6	1205	27	57
F4	20	11.1	7.8	8.4	8.4	1108	34	37
F5	20	10.1	6.6	7.2	7.2	1153	41	49
G1.2	35	6.9†	7.2	7.5	7.5	1003	30	55
G1.3	35	9.0	4.6	5.1	5.1	1163	62	70
G1.4	35	6.1	8.7	9.1	9.1	1058	33	58
G1.5	35	12.0	5.6	6.0	6.0	1053	41	60
G2.1	35	13.6	3.7	…	…	1142	32	38
G2.2	35	13.0	7.1	7.5	7.5	1119	28	31
G3.1	35	12.3	3.3	…	…	1173	46	55
G3.2	35	15.4	6.5	7.4	7.4	1111	41	33
G3.3	35	9.8	12.0	12.8	12.8	1023	32	29
BSS12*	…	12.2	6.3	7.2	7.2	1115	35	47
BSS22*	…	12.9	5.1	5.9	5.9	1135	64	54
BSS23*	…	12.0	8.8	9.5	9.5	1088	40	37
BSS24*	…	12.6	2.6	2.6	2.6	1231	30	51
BSS25*	…	12.3	11.2	12.0	12.0	1020	29	31
BSS26*	…	12.1	9.9	10.9	10.9	1068	42	34
BSS28*	…	12.6	2.1	2.2	2.2	1240	34	61

* electrical simulators

12.5 References

[69] *Nuclear Fuel Behaviour in Loss-of-Coolant Accident (LOCA) Conditions, NEA No. 6846, 2009, NEA
[70] Grandjean, C., A State-Of-The-Art Review Of Past Programs Devoted To Fuel Behavior Under Loca Conditions, Part One. Clad Swelling and Rupture Assembly Flow Blockage, SEMCA-2005-313.
[71] Massih, A.R. and L.O. Jernkvist, Assessment of data and criteria for cladding burst in loss-of-coolant accidents, 2015:46. 2015.
*available in the R2CA database

13. PHEBUS-LOCA tests

Detailed descriptions of the LOCA tests in the PHEBUS reactor (France) are available in references [72] and [73].

13.1 Objective

The experimental program PHEBUS-LOCA has been conducted from 1980 to 1984, with the following objectives:

- To assess the phenomenology of fuel rod behaviour under LOCA conservative conditions, including rod burst and a subsequent temperature plateau for clad oxidation up to the acceptance limit, before a final representative quenching (cf.Fig. 25.);
- To assess the adequacy of safety criteria with respect to the coolability of fuel rods and the clad embrittlement, so as to allow an assessment of safety margins;
- To provide an experimental data base for the validation of computer codes.
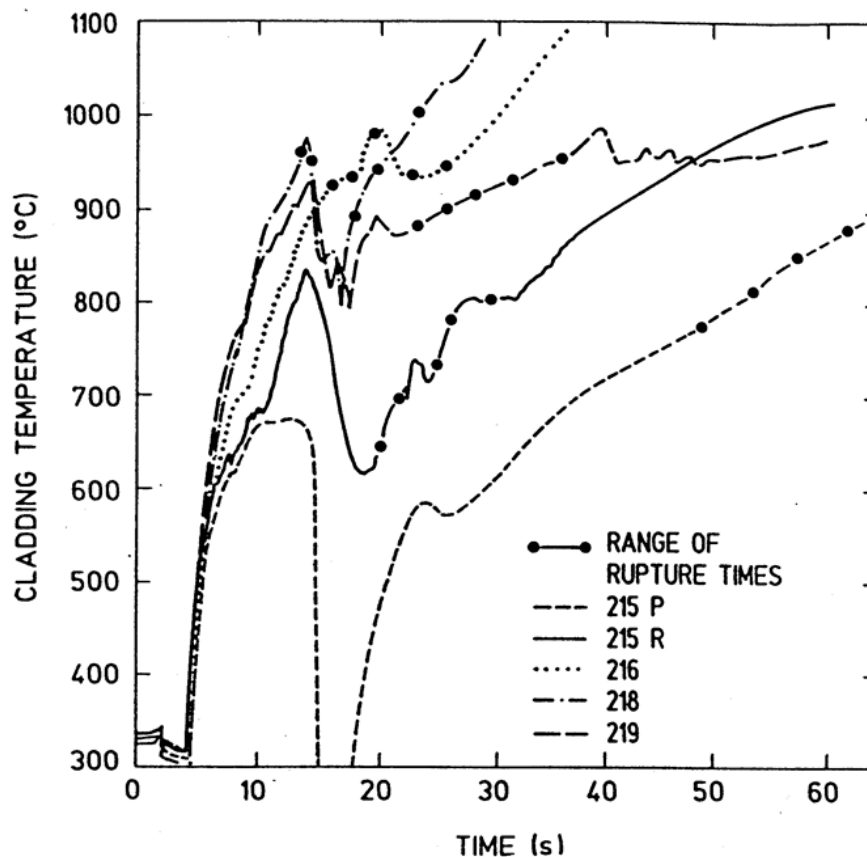
Fig. 25. PHEBUS LOCA temperature transients.

13.2 Tested materials, test facility

It has included 3 single rod tests and 22 tests with 25-rods bundles. Among these bundle tests, only 7 were performed with pressurized rods, the remaining tests with all unpressurized rods having been used mostly to study the thermal-hydraulic behaviour from blowdown to reflood so as to adjust the conditions and procedure for the tests with pressurized rods.

Tested bundles were made of 25 rods of fresh UO_2 fuel of PWR type on a 5x5 pattern, maintained by 4 Inconel spacer grids. The fuel pins are 1 m long (0.8 m active length) and can be internally pressurized. The test device

is thus included in a loop inserted in the PHEBUS driver core that provides the neutronic flux for the nuclear heating of the test rods.

Only five tests: 215P, 215R, 216, 218 (ISP 19) and 219 have provided reliable information relative to thermomechanics (cf.
Table 10). Moreover, due to lack of instrumentation, a minimum set of data like (burst temperature, pressure and strain) could not be retrieved for each rod.

Table 10
Main burst data from LOCA PHEBUS tests from [72].

Test number (rod pressure)	Rod group	Burst time (s)	Burst temperature (°C)	Orientation of ruptures	Burst strain			T at first peak (°C)
					Range (%)	Mean (%)	Std. Dev (%)	
215-P (40 bar)	central outer	50 – 66 65 – 150	840 ? – 830	center center	20 – 54 15 – 38	38 26.6	13 6	No
215-R (40 bar)	central outer	20 – 25 25 – 30	800 – 860 760– 830	center hot pins	20 – 50 15 – 35	38 29.6	9 5.5	800 – 860 760– 830
216 (40 bar)	central outer	14.6 – 17 18.5 – 26.4	920 – 1000 800 – 860	center center	20 – 30 16 – 31	– 23.6	– 5	930–1000 760 – 830
218 (40 bar)	central outer	11.5 – 13 15 – 26	900 – 1000 820 – 900	center center	14 – 27 15 – 38	20 26	5 6	930 – 980 860– 930
219 (40 bar)	central outer	21 – 34 33 – 36	850 – 950 820 – 880	center ?	19 – 46 14 – 27	28 20	9 4	910 – 950 850– 910

13.3 Measured parameters, PIE data

The instrumentation of the test consisted mainly in the measurement of:
- Flow rates of coolant in the hot and cold legs (through measurement of volumetric flow, temperature, pressure and void fraction), and in the injection lines;
- Temperatures at the fuel centreline, in the gas plenum, on the claddings and the shroud;
- The rod internal pressure (only for rods);
- The nuclear power in the bundle, by using fission chambers.

13.4 General conclusions

From
Table 10, inner and outer rods exhibit a distinct overall behavior, which is reflected by the small standard deviation on the rupture strain for each group of rods. For inner rods, the ruptures occurred in the α-phase domain for tests 215-P and 215-R and in the mixed $\alpha+\beta$ phase domain for tests 216, 218 and 219. The rupture strain was thus significantly higher in tests 215-P and 215-R than in the other tests. For the outer rods, lower burst strain was generally observed with respect to that of the inner rods. This result was mainly attributed to the effect of azimuthal temperature difference, larger on outer rods owing to the influence of cold outer structures, particularly in tests 215-P and 215-R where these temperature differences were more pronounced. Unfortunately, PHEBUS LOCA tests data may not be usable in R2CA work package 3 because of the lack of data.

13.5 References

[72] Grandjean, C., A State-Of-The-Art Review Of Past Programs Devoted To Fuel Behavior Under Loca Conditions, Part One. Clad Swelling and Rupture Assembly Flow Blockage, SEMCA-2005-313.

[73] *Nuclear Fuel Behaviour in Loss-of-Coolant Accident (LOCA) Conditions, NEA No. 6846, 2009, NEA
*available in the R2CA database

14. Halden LOCA tests

14.1 Objectives

OECD Halden Reactor Project (HRP) conducted a LOCA test series in a boiling heavy-water reactor (HBWR) situated in Halden, Norway, from year 2003 onwards. The LOCA test series was named IFA-650 ("IFA" stands for Instumented Fuel Assembly). First two tests were commissioning tests with fresh fuel [74], and more than ten tests were done with refabricated fuel rodlets irradiated in various power reactors.

The motivation for the Halden LOCA tests came from the need to verify that the currently utilized fuels in power reactors meet the safety requirements [75]. Namely, the preceding tests had mostly been done with fresh fuel, and the end-of-life fuel burnup had constantly been increasing. Fuel designs and cladding materials had also evolved. Objectives of the test series included to study fuel fragmentation, relocation of the fragments inside the deformed cladding, and dispersal of fragments from the burst opening. These objectives were further emphasised when test 650.4 showed significant fuel fragmentation and relocation. Cladding inner surface secondary hydriding after the burst and the release of volatile fission products from the failed fuel were also studied [75].

14.2 Tested materials, test facility

Halden test rig configuration is shown in Figure 26. Fuel rod was located in the centre of the rig, surrounded annularly by the coolant, cylindrical electrical heater and another layer of coolant. Heat generation consisted of external electrical heating and fuel internal fission heat production [76]. The electrical heat simulated the heat from surrounding rods while the nuclear heat took the role of decay heat in LOCA. Prior to a LOCA test, reactor was operated at steady-state power to reach the desired power level in the test segment. After the hold time at maximum temperature, electrical heating was shut down and the reactor was scrammed. No quench was applied and the tests were terminated about 5 minutes after the blowdown [76].
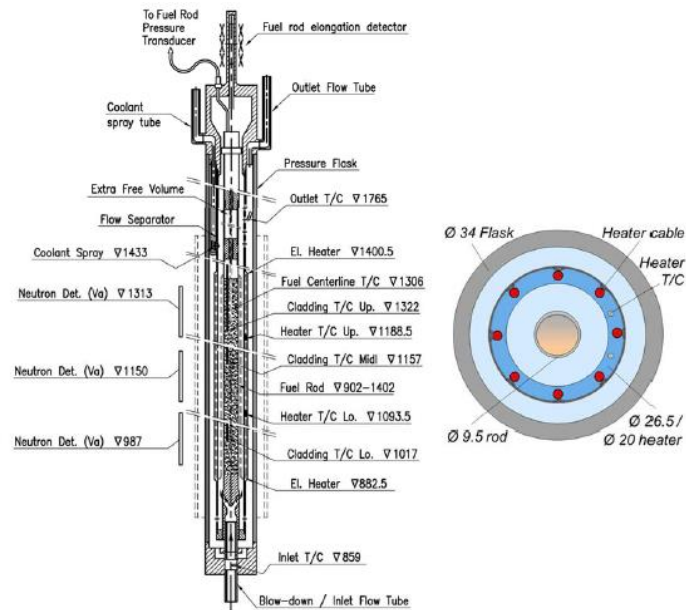
Figure 26: Test rig from the side and above [77].

The refabricated test rodlets were backfilled with argon-helium mixture or pure helium. The segment lengths were approximately 50 cm. Test materials including the respective reactor types are shown in Table 11.The tested PWR cladding materials were Zircaloy-4 and M5 (latter in 650.15). Burnup in test 650.3 - 650.15 varied from 44.3 to 92.3 MWd/kgU. All the BWR rodlets were from 10 × 10 assemblies, and PWR assembly dimensions were either 16 × 16 or 17 × 17..

Table 11
Halden IFA-650 LOCA test series.

Test number	Fuel type	Notes
IFA-650.1		commissioning test with fresh fuel
IFA-650.2		commissioning test with fresh fuel
IFA-650.3	PWR 16 × 16	failed thermocouple welding
IFA-650.4	PWR 16 × 16	92.3 MWd/kg, ballooning and burst at 790°C, considerable fuel fragmentation, relocation and dispersal
IFA-650.5	PWR 16 × 16	restricted gas flow, ballooning and fuel ejection
IFA-650.6	VVER	
IFA-650.7	BWR	
IFA-650.8		fresh fuel, for checking the system
IFA-650.9	PWR 16 × 16	considerable ballooning, fragmentation and relocation (650.4 sibling material)
IFA-650.10	PWR 17 × 17	moderate ballooning, fragmentation and dispersal
IFA-650.11	VVER	small ballooning and some fragmentation
IFA-650.12	BWR	
IFA-650.13	BWR	
IFA-650.14	BWR	
IFA-650.15	PWR	
IFA-650.16		not much publicly available information is available at the moment

Tests 650.9, 650.10 and 650.11 have been used in recent IAEA coordinated research project Fuel Modelling in Accident Conditions (FUMAC) [77]. Previously, tests IFA-650.3, 650.4 and 650.5 were simulated in a modelling benchmark organized within the NEA Working Group on Fuel Safety (WGFS) [78]. Another modelling effort worth mentioning related to the topics of R2CA project is the analysis of tests 650.2-650.7 while performing LOCA cladding burst criterion assessment for a fuel performance code [79].

14.3 Measured parameters, PIE data

The on-line instrumentation in Halden LOCA tests consisted of cladding and heater surface thermocouples (TCC and TCH, respectively, see Figure 27), rig inlet and outlet thermocouples, cladding extensometer, fuel rod pressure sensor, and neutron flux detectors. Post-test examinations included visual inspection, gammascan, neutron radiography, and in some cases axial profilometry, cladding metallography, fuel ceramography, and evaluation of fuel fragment size distribution [76]. Some test results are found in [75][76][79]. Additional advanced post-test examinations, such as hydrogen analysis and hardness measurements, were also conducted in some cases [80].
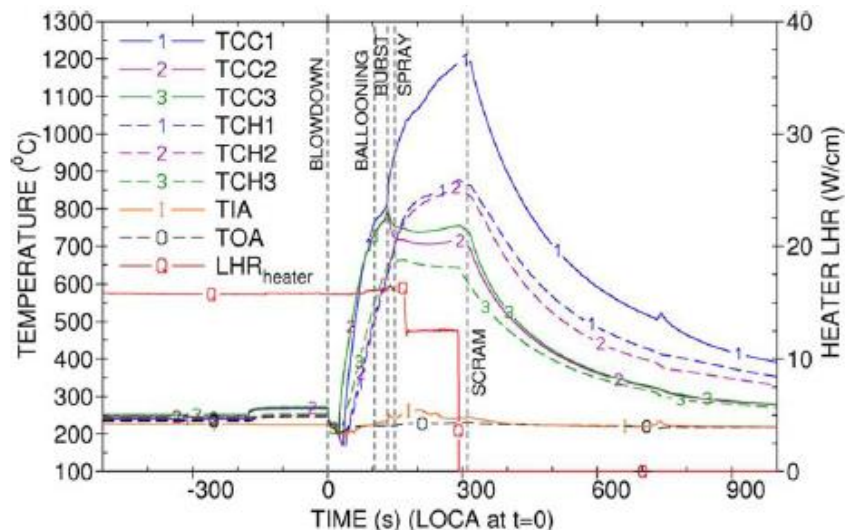
Figure 27: Cladding (TCC) and heater (TCH) temperature evolutions and heater linear heat rate in IFA-650.9 [77].

14.4 General conclusions

With very high burnup tests, significant fuel fragmentation, relocation and dispersal was observed. However, no unique parameter could be found that could explain the fragmentation behaviour [75]. Tests with burnups higher than 72 MWd/kgU showed increased fragmentation. Preserving the contact between the fuel and cladding could suppress fragmentation. Only mild fuel relocation was found with the exception of the very high burnup cases. [69]

Further detailed discussion on the Halden LOCA test results are found in [75][76][81].

14.5 References

[74] *Kolstad, E., 2003. Halden LOCA test series trial runs - IFA-650.1. Presentation at review meeting, Argonne, July 2003. www.nrc.gov/docs/ML0320/ML032060159.pdf (accessed: 25 Feb. 2020)

[75] *OECD/NEA, 2016. Report on fuel fragmentation, relocation, dispersal. NEA/CSNI/R(2016)16

[76] OECD/NEA, 2019. Updated LOCA state-of-the-art report, November 2019 draft version

[77] *IAEA, 2019. Fuel modelling in accident conditions (FUMAC). Final report of a coordinated research project. IAEA-TECDOC-1889. www-pub.iaea.org/MTCD/Publications/PDF/TE-1889web.pdf (accessed: 25 Feb. 2020), and Annex II: Country reports from participants. www.iaea.org/publications/13604/fuel-modelling-in-accident-conditions-fumac?supplementary=67882 (accessed: 25 Feb. 2020)

[78] *OECD/NEA, 2010. Benchmark Calculations on Halden IFA-650 LOCA Test Results. NEA/CSNI/R(2010)6

[79] *Massih, A. R., Jernkvist, L.-O., 2015. Assessment of data and criteria for cladding burst in loss-of-coolant accidents. Report prepared for the Swedish Radiation Safety Authority SSM. Report number: 2015:46, ISSN: 2000-0456
www.stralsakerhetsmyndigheten.se/contentassets/2a78bc357d954d21987ef87ec6527453/201546-assessment-of-data-and-criteria-for-cladding-burst-in-loss-of-coolant-accidents (accessed: 25 Feb. 2020)

[80] *Oberländer, B.C., Espeland, M., Jenssen, H.K., 2008. LOCA testing of high burnup PWR fuel in the HBWR. Additional PIE on the cladding of the segment 650-5. IFE/KR/E-2008/004 www.nrc.gov/docs/ML0817/ML081750715.pdf (accessed: 25 Feb. 2020)

[81] *OECD/NEA, 2010. Safety Significance of the Halden IFA-650 LOCA Test Results. NEA/CSNI/R(2010)5

*available in the R2CA database

15. ACRR (SNL) tests

15.1 Objectives

At the Annular Core Research Reactor (ACRR) different tests on nuclear fuel were performed in the 1980s and early 1990s. In particular,

- two ACRR-ST (source term) erperiments,
- four ACRR-DF (damaged fuel) experiments,
- two ACRR-MP (melt progression) experiments, and
- two ACRR-DC (dry capsule) experiments.

The objective of the **ACRR-ST** experiments was to obtain time-resolved data on the release of fission products from irradiated fuels under severe accident conditions. The release behaviour was observed under highly reducing conditions. The major difference in the two runs of the experiment was the pressure, 0.16 MPa (ST-1) and 1.9 MPa (ST-2) respectively.

The objective of the **ACRR-DF** experiments was to obtain phenomenological information on core degradation and melt progression. DF-1 and DF-2 experiments addressed the effects of initial clad oxidation state on subsequent severe damage progression. DF-3 observed the effects of a Cd-In-Ag control rod on the damage process. In DF-4, a BWR control blade structure in a larger rod bundle is included in order to determine the effects of B4C and stainless-steel control blade materials on the melt and damage progression.

The **ACRR-MP** tests were designed to complement the DF tests by investigating "late phase" melt progression and analysing the behaviour of a degraded core after the postulated formation of a metallic blockage upon which a debris bed rested. Both tests, the MP-1 and MP-2, had three active regions of the experimental packages: the stub, crust, and debris regions. The differed mainly in the dimensions and the material composition of the test setup.

The **ACRR-DC** experiments had some similarities to the MP tests. They were designed to characterize heat transfer in dry high temperature fuel debris geometry and to investigate the melting dynamics. The DC-2 test additionally investigated the effect of metal content on these processes.

15.2 Tested materials, test facility

The Annular Core Research Reactor (ACRR) at Sandia National Laboratories (SNL) is an epithermal pool-type research reactor licensed up to a thermal power of 2.4 MW. The reactor is used for short duration power runs, pulses and tailored transients and is equipped with a dry central irradiation cavity capable of driving experiments with fissionable material.

For the **ST** tests a small fuel bundle consisting of four of four irradiated fuel pins having a high burnup and four fresh fuel pins (5% enrichment) were used. The irradiated fuel pins used were cut from two research reactor fuel rods and had a maximum burnup of approximately 47000 MWd/mtU.

The **DF** test bundles consisted of half metre long, Zircaloy-4 clad fresh fresh UO_2 fuel rods (9 or 14 depending on the test). An enrichment of 10% U^{235} was used. The array was surrounded by an insulating shroud within a stainless steel pressure vessel. For DF-3, a stainless steel clad Ag-In-Cd control rod (DF-3) was used. The BWR control blade for DF-4 consisted of B_4C-filled stainless steel tubes encased in stainless steel sheath. A cross section of the DF-4 bundle is shown in Figure 28.

The test configurations used in the **MP** tests were 25 – 30 cm high, with different dimensions of the stub, crust and debris regions. The fuel debris bed was situated above an intact fuel rod array of 32 fresh fuel rods. The materials used in the MP-1 test were UO_2, Zr and ZrO_2. In addition, Sn, Ag, In, Fe, Cr, Ni and Mo were used in the MP-2 test. The test sections were insulated so temperatures sufficient for partial material melting were reached.

For the **DC** experiments, fuel debris bed consisting of powdered and granular UO_2 fuel material was contained within ThO_2-lined tungsten crucible. The debris was actively cooled on the top and bottom.
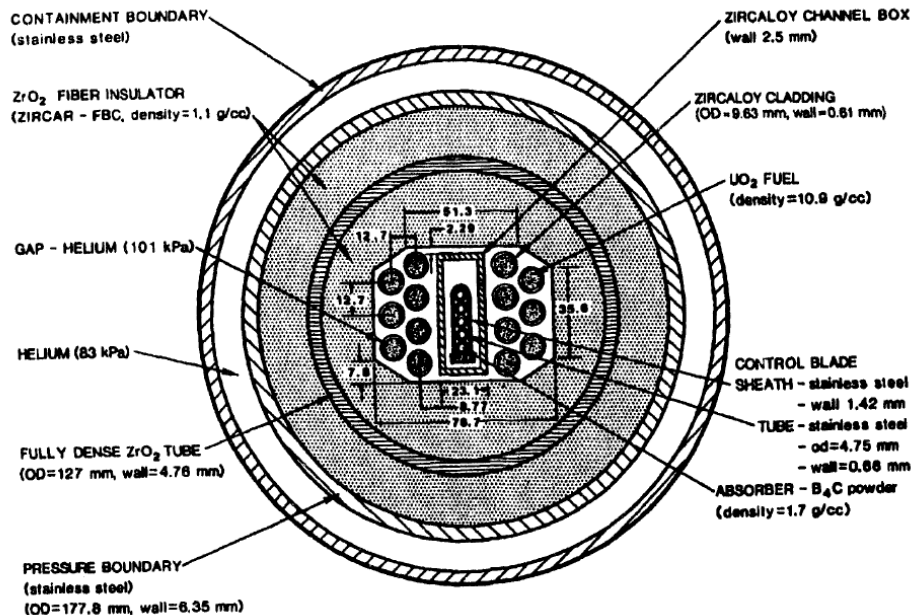
Figure 28: Radial Cross Section of DF-4 Test Bundle.

15.3 Measured parameters, PIE data

In the **ST** experiments fission product release rates from degrading fuel was measured. Release rate data were measured for Cs, I, Te, Ba, Sr, Eu, and U. The release rates were higher than predicted by existing codes for Ba, Sr, Eu, and U. Important information was obtained for fuel damage

Behavior, such as fuel foaming and swelling that occurred as the cladding became molten and penetrated the cracks in the fuel pellets. This may have enhanced fission product release, especially in the high pressure test.

The conditions observed in the **DF** test included fuel heat-up in flowing steam, clad heating by oxidation with steam, hydrogen generation from metal oxidation, fuel pellet attack by molten cladding material, metallic melt relocation and blockage formation, and the nature of the degradation of the fuel rod geometry. Fuel temperatures were measured with thermocouples and an end-on view of the damage process was provided by a video recording system. The DF tests had some unplanned features which complicated post-test analysis. E.g. DF-1 experienced condensation of steam within the test section, which later revaporized, causing uncertainties in the knowledge of the steam flow rate for the test.

The **MP** tests provided were also fully instrumented with thermocouples in both experiments. Information on ceramic melt formation and flow through porous fuel debris, on material interactions between ceramic fuel melt and adjacent metallic crusts, and on the migration of the ceramic melt into the intact fuel rod region was gathered. The Post-Irradiation Examination task included package stabilization, x-ray analysis, sectioning, metallography, optical macroscopy, and electron microscopy.

In the **DC** tests thermal records of the heating profiles were recorded and metallurgical examinations performed.

15.4 General conclusions

In the OECD/NEA "In-Vessel Core Degradation Code Validation Matrix" from the year 2000, four of the ACRR tests are rated as category 1 tests, which describes tests best qualified for code validation in their field. These are ACRR ST-1, ACRR DF-4, and ACRR MP-1&2.

15.5 References

[82] *OECD/NEA, "In-Vessel Core Degradation Code Validation Matrix Update 1996-1999", Organisation for Economic Co-Operation and Development, NEA/CSNI/R(2000)21, 2001.
[83] Tautges, T., "MELCOR 1.8.2 Assessment: The MP-1 and MP-2 Late Phase Melt Progression Experiments", SAND94-0133, 1994.
[84] Allen, M.D. et al., "ACRR Fission Product Release Tests: ST-1 and ST-2", SAND--88-0597C, 1988.
[85] Tautges, T., "MELCOR 1.8.2 Assessment: The DF-4 BWR Damaged Fuel Experiment", SAND93—1377, 1993.
[86] *Gasser, R.D. et al., "Late-Phase Melt Progression Experiment: MP-2. Results and Analysis", US NRC, NUREG/CR-6167, 1997.
*available in the R2CA database

16. NRU MT-4 test

16.1 Objectives

A series of multi-rod tests simulating LOCA transients were carried out by PNNL in the NRU reactor at Chalk River (Canada) with the objective to study the thermohydraulic (TH test series) and thermomechanical behavior (MT test series) within a bundle of 32 PWR full-length rods. Various reports are available [87][88][89][90][91] but quantitative and detailed burst data are only available for the MT-4 test. General tests description and main conclusions are taken from [91] and [50].

16.2 Tested materials, test facility

The test assembly consisted of a 6x6 array with the 4 corner rods removed, the 20 non-pressurized outer rods making a guard ring for the 12 inner pressurized rods. The test bundle was surrounded by a stainless steel shroud to protect the loop pressure tube. The fuel length of the test rods (3.66 m) was greater than the NRU core height (2.74 m), with the bottom and top ends of these rods thus being out of the neutron flux. The Zy-4 test rods (external diameter 9.63 mm, thickness 0.61 mm) were fueled with fresh UO_2 pellets but were preconditioned prior to the LOCA transients by power cycling to full power which caused the fuel pellets to fracture. For each test various transients were performed. Several thermocouples allowed measuring clad temperatures (inside), fuel centerline temperature and each rod was equipped by pressure transducers. All pressures mentioned in the text are given at room temperature.

The first materials experiment (MT-1) was performed with 11 rods pressurized to 3.21 MPa. Six of the rods ruptured and all pressurized test rods expanded significantly. The average peak burst strain was 43% (maximum higher than 60%), the average burst temperature was 872 °C (cf. Fig. 29). The second materials experiment (MT-2) was performed with 12 rods pressurized to 3.21 MPa. Eight of the rods ruptured and all pressurized test rods expanded significantly. The average peak burst strain was 43% (maximum higher than 70%) and the average burst temperature was 887 °C (cf. Fig. 29.). The third second materials experiment (MT-3) was performed with 12 rods pressurized to 3.8 MPa. All pressurized test rods burst and expanded significantly during the transient (3 °C/s). The average peak burst strain was 46% (maximum higher than 90%) and the average burst temperature was 797 °C (cf. Fig. 29.). In the MT-4 test, the 12 rods were pressurized to 4.62 MPa. All rods burst at an average temperature of 821 °C. The average peak burst strain was 72% (maximum higher than 96%). Complete burst data are available for this test and are given in Table 12.
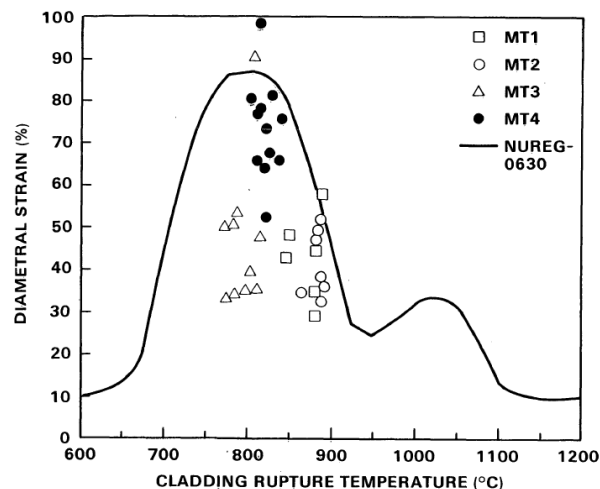
Fig. 29. MT bundle tests diametral strains versus burst temperature (°C).

MT-5 was finally not performed (proposed to NRC with irradiated fuel) and two other tests MT-6A and MT-6B were performed. The last test MT-6B indicated that small notches in the stainless steel shroud that surrounded other MT test bundles are probably responsible for much greater local cladding strain. However, these last two tests were not mentioned in the summary report from PNNL, the validity of these tests may not be insufficient [50].

Table 12
Burst data for MT-4 test.

Rod-ID	ΔP_{burst} (MPa)	T_{burst} (°C)	Strain (%)
2C	5,58	841	76,2
2D	6,13	826	67,6
3B	6,23	819	64,6
3C	6,03	821	53
3D	6,3	837	59,4
3E	6,48	822	73,7
4B	6,37	804	68,4
4C	6,06	815	99,2
4D	5,79	815	78,5
4E	6,06	828	81,5
5C	5,82	813	66
5D	6,1	813	77,3

16.3 General conclusions

Although MT tests were bundle tests, very high burst strains were observed. Complete burst data are only available for MT-4 test and unfortunately only partial burst data could be retrieved for test MT-1 to MT-3.

16.4 References

[87] *Russcher, G.E., et al., LOCA Simulation in the NRU Reactor, Materials Test - 1, NUREG/CR-2152, 1981.

[88] *Barner, J., et al., Materials Test-2 LOCA Simulation in the NRU Reactor, NUREG/CR-2509. 1982.

[89] Mohr, C.L., et al., LOCA Simulation in the National Research Universal Reactor Program. Data Report for the Third Materials Experiment (MT-3), NUREG/CR-2528, 1983.

[90] Wilson, C.L., et al., LOCA Simulation in NRU Program, Data Report for the Fourth Materials Experiment (MT-4), 1983.

[91] Wilson, C.L., et al., Large-Break LOCA, In-Reactor Fuel Bundle Materials Test MT-6A, PNNL-8829, 1993.

[92] Grandjean, C., A State-Of-The-Art Review of Past Programs Devoted to Fuel Behavior Under LOCA Conditions, Part One. Clad Swelling and Rupture Assembly Flow Blockage, SEMCA-2005-313.

*available in the R2CA database

17. LOFT LP-FP tests

17.1 Objectives

The Fission Product (FP) Release experiments LOFT LP-FP-1 and LOFT LP-FP-2 were performed at the Loss-of-Fluid Test facility (LOFT) at the Idaho National Engineering Laboratory (INEL) in the framework of the OECD LOFT project. These experiments were the last two experiments conducted in the LOFT before its decommissioning.

In the LP-FP-1 experiment, conditions of a large-break LOCA of a PWR with delayed ECCS are investigated. The ECCS was specified in a way to be representative of the German PWR ECCS in nominal (best estimate) conditions for combined upper plenum and cold leg injection [93]. During the experiment, fuel rod failure was expected to lead to the release of fission products. The rise of fuel temperature should be safely terminated by ECCS injection before any fission products held in the fuel pellet matrix could be released. Major objectives of the experiment were the measurement of the retention of the noble gases and iodine within the primary cooling system (PCS) and their release to the blowdown header and the suppression tank, and the washout of fission products for up to 12 hours after system recovery [93].

In the LP-FP-2 experiment, the early phase of a V-sequence LOCA scenario of a PWR was investigated that resulted into severe core damage [94]. The specific V-sequence LOCA scenario was a simulated pipe break in the Low Pressure Injection System (LPIS) line, attached to the hot leg of the LOFT broken loop piping. However, the intact loop cold leg (ILCL) break line served as the primary blowdown pathway prior to fission product release for fast reduction of the primary system pressure and consequently to maximize the decay heat for core heat-up. The primary core temperature objective for LP-FP-2 was to obtain peak-cladding temperatures in the central part of the core above 2100 K for at least 3 minutes while maintaining peripheral bundle fuel rods below 1390 K. A major objective of the LP-FP-2 experiment was to provide on-line and post-experiment data concerning airborne and deposited fission products and aerosol concentrations [94].

17.2 Tested materials, test facility

The LOFT test facility was designed to represent the major components and system response of a commercial PWR. The test facility was a scaled-down simulator of a full-size PWR (volume scaling factor 50) with a nuclear core with reduced length (1.67 m). The facility consisted of five major subsystems: reactor vessel, intact loop (representing three loops of a Westinghouse 4-loop PWR), the broken loop (representing the fourth loop) and blow-down suppression system, used to collect the discharged fluid from the PCS, and the ECCS [93].
Significant modifications of the LOFT facility were applied for the preparation of the two FP release experiments in order to limit the occurrence of fuel rod damage to the centre of the core, while in the periphery of the core, the rise of fuel rod cladding temperature is limited to avoid damage of those rods.

For LP-FP-1, the centre fuel assembly of the core was replaced by a special designed 15x15-centre fuel module (CFM) with a thin Zircaloy shroud, which enclosed the inner 11x11 fuel rod array where 24 of the fuel rods were enriched to 6-wt%. Twenty-two of the centre fuel rods were also pressurized (2.41 MPa) [93]. The first attempt of experiment LP-FP-1 was performed on December 12th, 1984. However, the experiment was aborted because of a malfunction of a position indicator. The experiment was then repeated successfully on December 19th, 1984 [93].

For the LP-FP-2 experiment, the specially designed CFM with an 11x11 rod array consisted of 11 control rods, 100 pressurized fuel rods (2.41 MPa) and 10 instrumented guide tubes (Fig. 30). The fuel rods were separated from the outer fuel assemblies by a 0.025-m-thick, Zircaloy-clad, zirconium-oxide insulated thermal shroud. This design enabled the CFM fuel rods to heat up to temperatures above 2100 K, while maintaining low-enough peripheral bundle rod temperatures (below 1390 K). It also ensured that fission products released during the

experiment flowed only into the upper plenum of the test facility and facilitated removal of the damaged core from the reactor vessel, decontamination and recovery of the fuel [94]. The experiment was conducted on July 9th, 1985.

Materials applied in CFM of LOFT LP-FP-2 [94]:

- Fuel: UO_2 with 9.74 wt% U-235, irradiated during the preconditioning and pre-transient phase of the experiment to a burn-up of 448 MWd/tU
- Fuel cladding: Zircaloy-4,
- Control rod cladding: 204 stainless steel
- Absorber: 80 wt% Ag, 15 wt% In, 5 wt% Cd
- Guide tubes: Zircaloy-4
- Spacers: Inconel 718
- Shroud material: Zircaloy-4
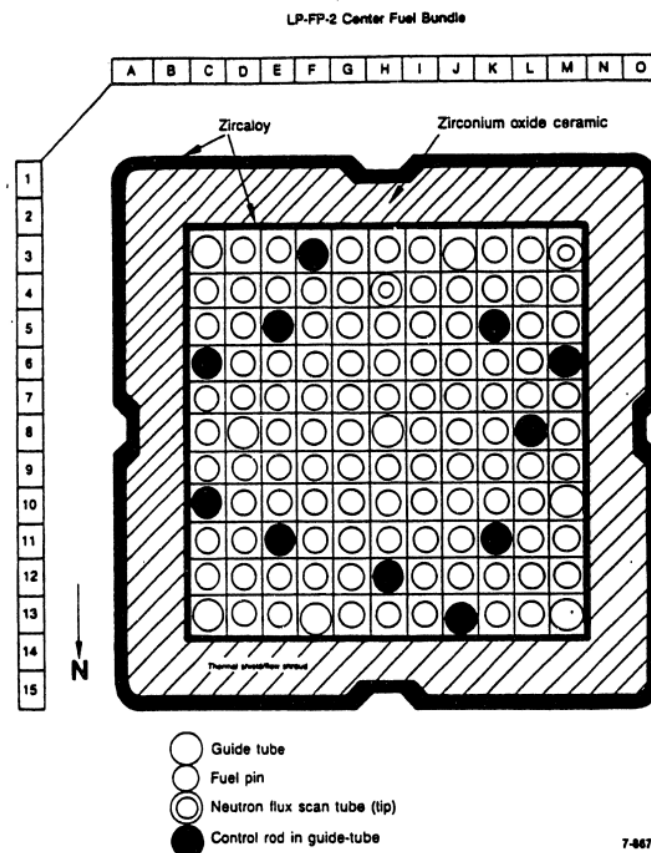
Fig. 30. Centre fuel module design of experiment LOFT LP-FP-2 [94].

17.3 Measured parameters, PIE data

In the following, the focus is set to experiment LOFT LP-FP-2. The following data was collected during the experiment [94]:

- Surface temperatures on 79 fuel rods in several elevations, temperatures of guide tubes, upper and lower tie plates, and structural components
- Neutron flux
- Liquid level
- pressure and differential pressures
- coolant density, flow rates.

The fission product measurement system consisted of four gamma spectrometers and one gross gamma detector, a deposition sampling system and steam/aerosol sampling lines [94].

Fig. 31 shows selected temperatures measured by several thermocouples in different elevations, including the TC-5IO8-27 fuel centreline thermocouple where the highest temperature before reflood was observed (2313 K). The activity of several isotopes was measured for example at the LPIS line, as shown by Fig. 32.
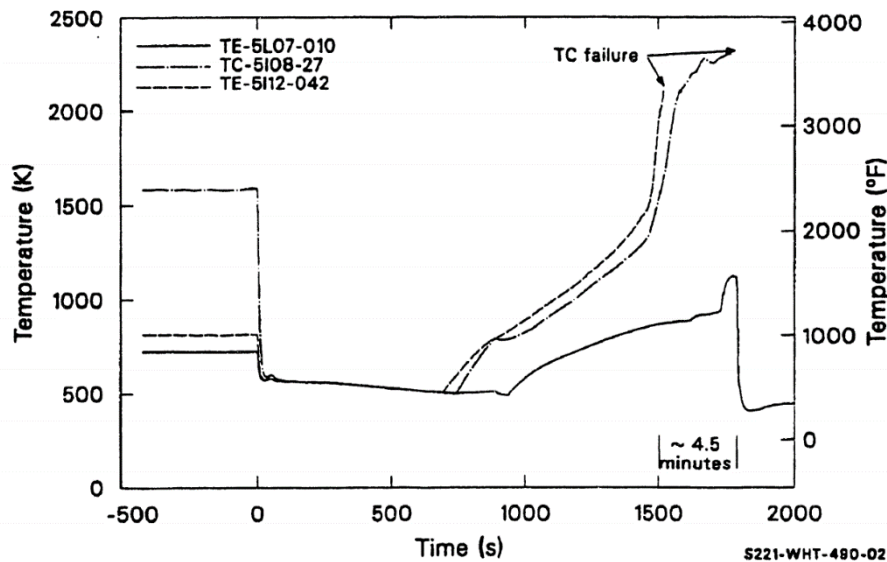
Fig. 31. LOFT LP-FP-2 experiment. Temperatures measured by thermocouples in the CFM at 0.25-, 0.68-, and 1.07-m elevations [94].
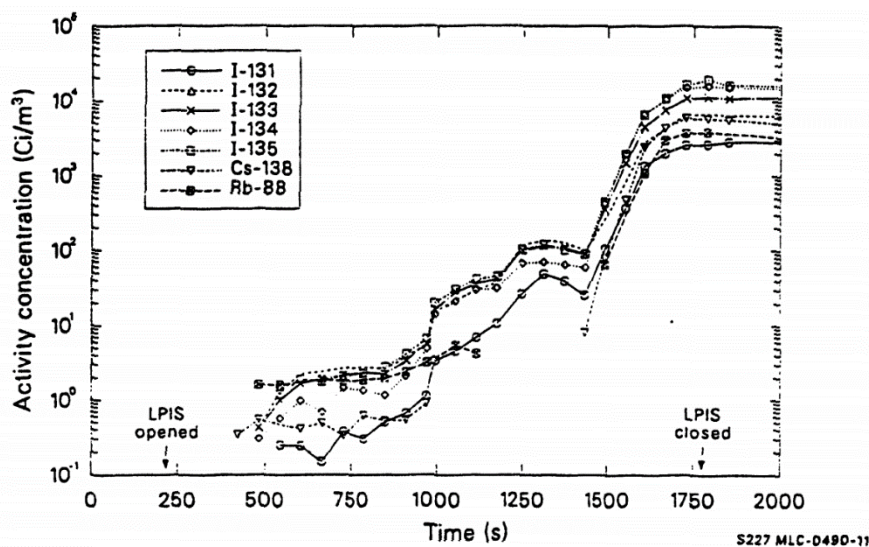
Fig. 32. LOFT LP-FP-2 experiment. Activity concentration measured at the G5 gamma spectrometer located in the LPIS line [94].

A comprehensive post-irradiation examination of the fuel bundle was performed. This included the assessment of:

- the final distribution of fuel and control rod materials (including phenomena such as fragmentation, liquefaction melting, relocation, freezing and blockage formation),
- specification of the post-test metallurgical and chemical form of materials,
- the estimation of maximum temperatures achieved during the transient,
- assessment of oxidation and hydrogen generation,

-    and the quantification of fission product distribution in both fuelled and nonfueled materials.

17.4 General conclusions

General conclusions from the LOFT LP-FP-1 experiment [93]:
The core thermal behaviour during the first FP release experiment was quite different from the behaviour observed in previous large-break LOCA experiments. In LP-FP-1, the reactor was scrammed intentionally one second before the break opening, and consequently the almost immediate temperature rises seen in other LB-LOCA experiments could not be observed. Furthermore, several unexpected early quenches prevented an early cladding temperature rise, and the actual core heat-up started very late in the transient (approx. at 80 s). Due to inhomogeneous temperature distribution, only eight of the 22 pre-pressurized fuel rods ruptured. Despite these and other limitations (such as low burnup of the fuel), the LP-FP-1 experiment contributed significantly to the knowledge base of fission product release during loss-of-coolant accidents.

General conclusions for LOFT LP-FP-2 experiment [94]:
The LP-FP-2 experiment provided information on the release, transport and deposition of fission products and aerosols during a V-sequence large-break LOCA accident that resulted in severe core damage. The measurements, observations and post-test analyses indicated that most of the CFM damage occurred during the reflood phase of the experiment. The highest temperatures (> 3120 K) were also reached during reflood phase and were caused by rapid metal-water reaction. The stratification of material in LP-FP-2 was similar to that observed in TMI-2. Approximately 15 % of the fuel and 63 % of the Zircaloy cladding and liner were liquefied-Large amount of the absorber material (70 %) was released to the fuel bundle. During reflood, material is relocated upwards to the upper end box. Most of the hydrogen and major release of fission products occurred during reflood.

17.5 References

A compilation of the available data and detailed reports are available upon request from the OECD NEA database.
For LOFT FP-LP-1: http://www.oecd-nea.org/tools/abstract/detail/csni0012/
For LOFT FP-LP-2: http://www.oecd-nea.org/tools/abstract/detail/csni0013/

[93] *J. Fell and S.M. Modro, *An account of the OECD LOFT Project*. OECD LOFT-T-3907. EG and G Idaho, 1990.
[94] E.W. Coryell, *Summary of important results and SCDAP/RELAP5 analysis for OECD LOFT experiment LP-FP-2*. NUREG/CR-6160. Nuclear Regulatory Commission. 1994
*available in the R2CA database

18. FLASH tests (Grenoble, Siloe)

Detailed descriptions of the FLASH LOCA tests in the Siloé reactor (France) are available in references [95], [96], [97], [98] and [99].

18.1 Objective

The FLASH experiments realized in the early 80ies were designed to obtain information on the behaviour of a PWR fuel rod and fission products release during a LOCA type accident scenario, in order to assess safety margins taken in the power plant safety evaluation reports and to qualify the dedicated safety codes and verify their predictions regarding:
- The cladding strains and cladding rupture (time and conditions such as temperature, differential pressure).
- The UO_2 pellets fragmentation.
- The noble gases and volatile fission products release.
- The burn-up effect on the fuel rod behaviour and fission products release during a LOCA accidental sequence (FLASH 05 test)

The FLASH program was co-sponsored by the Institut de Protection et de Sûreté Nucléaire (IPSN), the Electricité de France (EDF) and Central Electricity Generating Board (CEGB), and carried out in the SILOE reactor of the Centre d'Etudes Nucléaires (CEN) Grenoble, France. .

18.2 Tested materials, test facility

The FLASH tests were performed on a pre-conditioned fresh fuel rod (FLASH-1 to FLASH-4) and a 50.3 Gwd.t^{-1} irradiated fuel rod (FLASH-5). The PWR 17x17 type test rod with an active length of 30 cm was centered in an unheated shroud tube and cooled under a thermo-siphon regime within a finger-shaped irradiation device located on the reactor periphery, with this last particularity having induced large azimuthal temperature heterogeneities.

The SILOE pool reactor is equipped with a specific pressurized water loop (13 MPa) which allows irradiation of a short fuel rod under operating conditions as close as possible of nominal power reactors values, and then followed by a LOCA sequence with or without hot re-flooding, which calculated conditions in a power plant are namely: a peak clad temperature equal to 1270°C, a heat-up rate ranging from 0.3 to 30°C.s^{-1} and a residual fission heat maintained at 80 KW.m^{-1} during re-flooding.

The following parameters are controlled in this loop: fission power, internal pressure and major thermo-hydraulic conditions before and during the sequence. An accelerometer has also been inserted in the bottom part of the rig in order to detect the cladding rupture.

The experimental fuel rodlets were 30 cm long, refabricated with 17X17 array PWR characteristics and contained 27 UO_2 pellets each. They were plugged at both ends and had a large plenum filled with helium at an internal pressure calculated to obtain a proper clad deformation during the test sequence, ranging from 2.5 to 4 MPa. They were instrumented with external cladding thermocouples and internal pressure transducers (FLASH 03 and 04 only). After completion of the standard Non Destructive Examination (NDE), the pre-irradiation necessary to recreate equilibrium amounts of the short-lives isotopes measured during the test were performed at a linear heat power rate of:
- 35 kW.m^{-1} during 4-5 days for the fresh fuel (FLASH 01 to 04), leading the samples to a final burn-up ranging from 1.65 to 3.32 GWd.t^{-1},
- 18 kW.m^{-1} during 3 weeks for the 50.3 Gwd.t^{-1} irradiated fuel segment used in FLASH 05, which added 0.58 Gwd.t^{-1} to its burn-up.

The fuel rodlet and irradiation device schemes are shown in Fig. 33. Experimental fuel rod and irradiation device in FLASH experiments
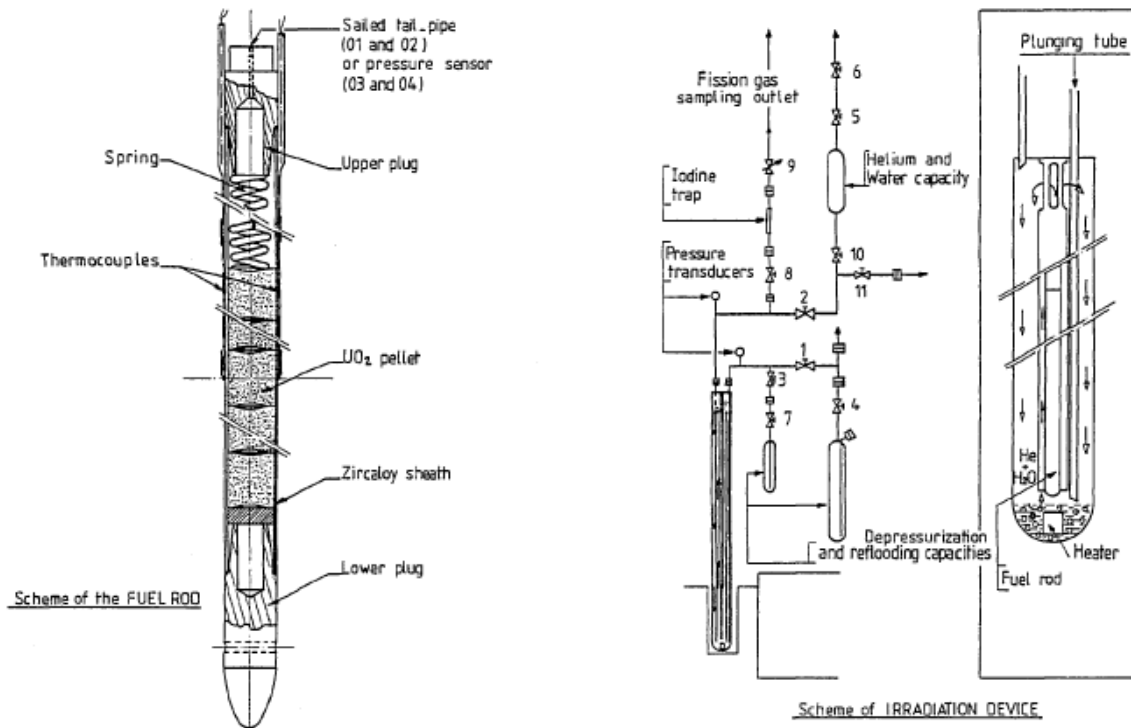
Fig. 33. Experimental fuel rod and irradiation device in FLASH experiments
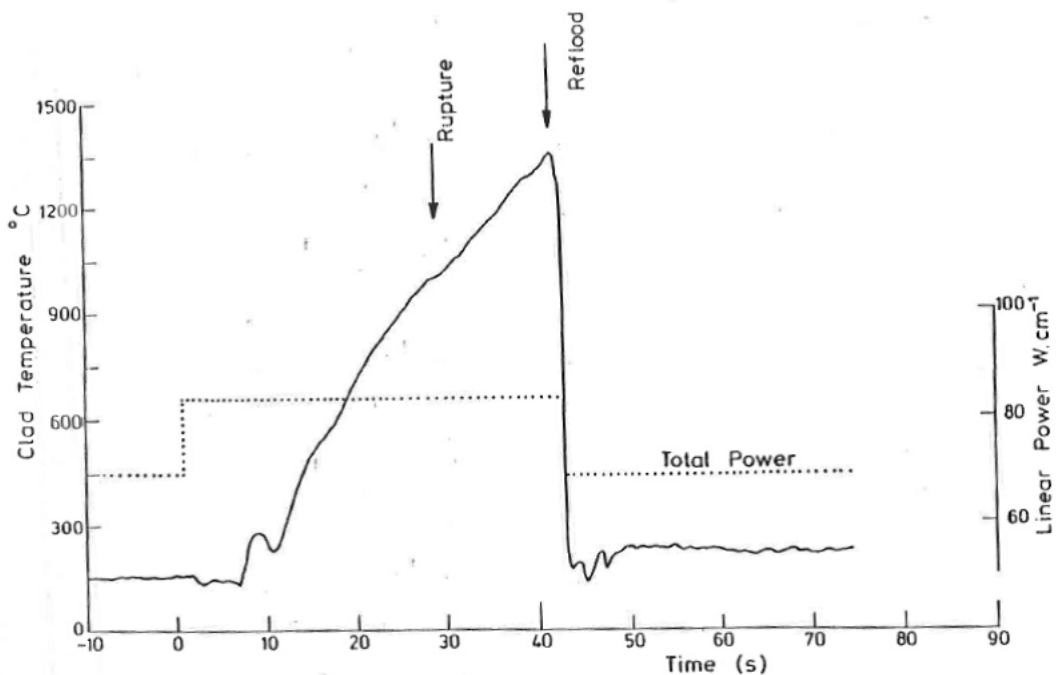
Fig. 34. Clad temperature and linear power rate during the FLASH 05 test

The simulations of a LOCA sequence were conducted after pre-irradiation in the SILOE reactor then in-pile γ-scannings of the samples, to establish the initial FP inventory and to benchmark the neutron physics computations: this benchmark was necessary because Pu contributes to 75% of the power generated in the SILOE reactor. At the end of the pile's second cycle (performed at 17.2 kW.m^{-1}) and according to the experimental procedure for the FLASH tests, the irradiation device was slightly retreated from the core to reduce

the power to 7.2 kW.m^{-1}, while a valve was opened to depressurize the loop from 12.4 to 0.5 MPa. The total or partial coolant expelling lasted 4 to 8 s. The temperature of the uncovered and uncooled fuel rod increased at a heating rate depending on the residual fission power and atmosphere composition and conditions (adiabatic or gas thermosiphon): for instance, 28 K.s-1 for FLASH 05 as shown in Fig. 34. After the cladding burst occurred, the heating was maintained up to a fixed maximum cladding temperature triggering the cooling sequence, either by immediate reactor scram plus cold water reflooding (FLASH 01 to 03) or by hot re-flooding: water at 1.2 MPa under irradiation at 7.2 kW.m^{-1} for 10 to 12 min before reactor scram (FLASH 04 and 05).

After the scenario was completed, the loop was transferred to the in-pile gamma spectrometry bench in order to analyse the FPs deposits on its components, while the gases released in the loop (mostly the helium used as a carrier gas) and the samples from the re-flooding water were stored and analysed in the laboratory associated to the reactor. The fuel rod was then sent to the hot cell for PIE.

18.3 Measured parameters, PIE data

- Cladding temperatures were recorded, but no pressure sensors were available in FLASH experiments. Very few data are available for FLASH tests. The main experimental measuring results are summed up in Table 13. No fission products (I, Cs) deposits have been detected on the surfaces around the fuel rods burst in spite of a LOCA type cladding rupture.
- The particles size distribution due to UO_2 fragmentation observed in the PIE is identical to that obtained during normal operating conditions.
- The oxide thickness measurements performed on tests with steam environment show an external Zircaloy cladding oxidation in agreement with the Cathcart oxidation kinetic law, while internal oxidation is limited around the clad rupture.
- Neither fuel relocation in the ballooning region occurred, nor any change in the fuel filling density was observed.

Table 13
Main FLASH experiments measuring results [98], [99]

Test	FLASH 01	FLASH 02	FLASH 03	FLASH 04	FLASH 05
Clad rupture time (s) and temperature (°C)	Not detected	n. d.	34.5 – 930	32.9 – 940	30 - 995
Max. peak cladding T (°C)	1100	1120	1270	1270	1345
% ^{85}Kr inventory in gap	~0.24[a]	~0.24 [a]	~0.24 [a]	~0.24 [a]	0.41[b]
% ^{85}Kr inventory released	n. d.	0.3	0.2	0.2	4.6
% invent. stable gases rel.	-	-	-	-	6.12[c]
% inventory ^{131}I and ^{137}Cs released	-	-	-	-	^{131}I 0.31 - ^{137}Cs 0.62
[a]*estimated* [b]*gas measure by rod puncturing after PWR irradiation -* [c]*0.12 in reflooding water*					

In the FLASH 05 test, the clad temperature raised up to 1350 °C in 34 s after the rodlet de-flooding, and its burst occurred away from the plane of maximum flux, with limited cladding strain. The total volatile fission product and fission gas releases were high compared to the previous tests. In addition, a significant damage of the fuel was observed with major fracturing of the fuel rod central part. It was explained by an oxidation of the fuel matrix during the final step of the test sequence (reflooding): the rodlet with its large gap was held for 12 mn at moderate power, under low-pressure steam.

18.4 General conclusions

In spite of the fact that the FLASH 01 to 04 tests were performed under experimental conditions that can be considered as severe regarding the calculated power plant LOCA conditions, the fission gas release remained

low corresponding to the fuel-to-clad gap inventory prior to the accidental sequence. The burn-up effects on which the FLASH 05 test focused resulted in much more important fuel damage, and corresponding fission gas release slightly superior to the gap inventory and low volatile fission product releases.

In FLASH-1 test (28 K/s) burst occurred at 995 °C. In the tests FLASH-3 and 4 with similar temperature ramps (∼ 30 K/s) clad burst occurred at 930 and 940 °C respectively. Finally, in FLASH-1 and 2, an untimely scram led to much lower temperature ramps (∼ 1 to 2 K/s), resulting in axially extended strain with a slight opening in the clad.

18.5 References

[95] Grandjean, C., A State-Of-The-Art Review Of Past Programs Devoted To Fuel Behavior Under Loca Conditions, Part One. Clad Swelling and Rupture Assembly Flow Blockage, SEMCA-2005-313

[96] Raynaud, P.A., Fuel Fragmentation, Relocation, and Dispersal During the Loss-of-Coolant Accident, in NUREG-2121,2012, U.S. NRC.

[97] Nuclear Fuel Behaviour in Loss-of-Coolant Accident (LOCA) Conditions, NEA No. 6846, 2009, NEA

[98] *M. Bruet, J.C. Janvier: FLASH Experiments in SILOE reactor - Fuel rod behaviour during LOCA tests – 4th specialist's meeting on water reactor fuel safety in off-normal and accident conditions – Roskilde, Denmark – May 16, 1983

[99] M. Bruet, C. Lemaignan, J. Harbottle, F. Montagnon, G. Lhiaubet: High burn-up fuel behavior during a LOCA type accident : the FLASH 5 experiment, IAEA Technical Committee Meeting on Accident Conditíons in LWRs, Cadarache, France, 16-20 March 1992

*available in the R2CA database

19. GASPARD tests

19.1 Objectives

The GASPARD experimental program was conducted from years 2000 to 2002 at the Commissariat à l'Energie Atomique (CEA), in partnership with EDF, in order to identify and to quantify the basic mechanisms which promote the Fission Gases Release (FGR) from high burn-up PWR UO_2 fuels but also to improve the models predicting the behaviour of various fuels – namely MOX fuels, during simulated LOCA and RIA conditions. The internationally available literature regards the high burn-up UO_2 results of this program.

19.2 Tested materials, test facility

The experimental samples used in the GASPARD program, each constituted by some fuel pellets with their open cladding, were cut out from UO_2 or MOX rods coming from standard PWR. The UO_2 father rods (initial enrichment 4.5% ^{235}U) were irradiated during four and six normal operating cycles in EDF power reactors and their respective characteristics were:
- burn-up 48.5 GWd/tU, fractional fission gas release ~2% rod inventory (estimated).
- burn-up 71.8 GWd/tU, fractional fission gas release 5.8% rod inventory (measured by a pin puncturing test after base irradiation), established High Burnup Structure thickness 0.2 mm.
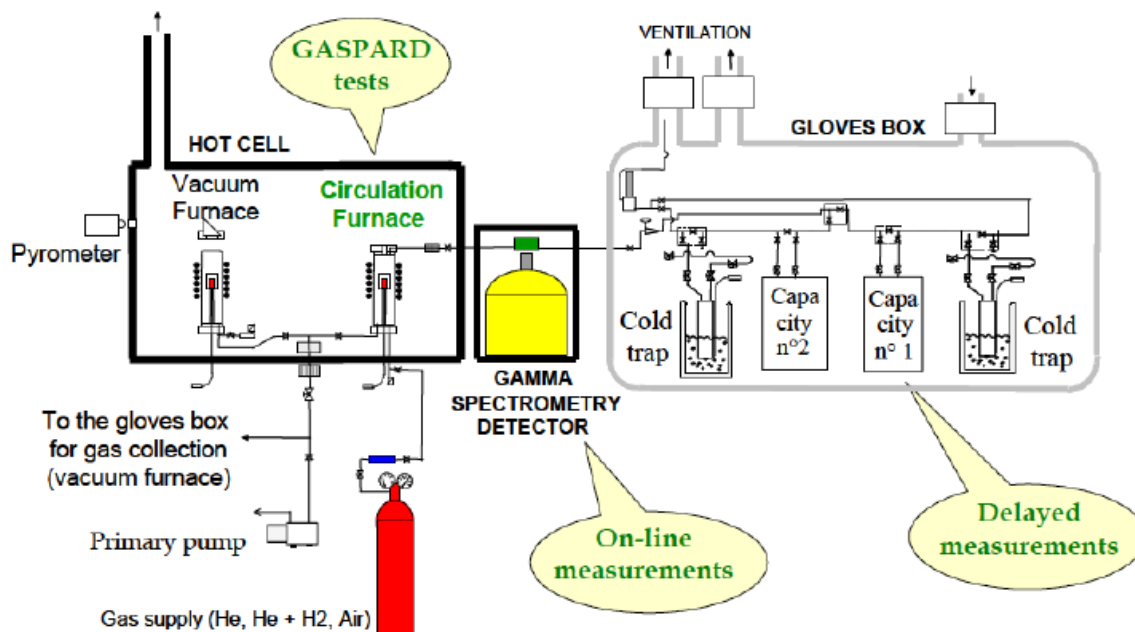
Fig. 35. GASPARD experimental device

The 6 cycle samples were re-irradiated in the OSIRIS Material Test Reactor (Saclay, France) at a linear power rate close to 9 W/cm during 8 days, in order to recreate short and intermediate half-life FPs. Prior to the thermal sequence completed in the GASPARD device (Fig. 35), the initial state and isotope inventories of the sample were determined by gamma spectrometry measurements coupled to a calculation code of the FP concentration based on the manufacturing data of the sample and its power history in PWR. These evaluations were completed, in some cases, by direct experimental determinations of the pellets inter and intra-granular gas distribution with the ADAGIO technique. These tests using the GASPARD furnace and online gamma spectrometer to monitor the ^{85}Kr and ^{133}Xe release consisted in:

- UO$_2$ oxidation into U$_3$O$_8$ at 380°C under air flow, occurring preferentially along the grain boundaries, and releasing the corresponding gas - the potential intra-granular gas contribution being determined by ^{133}Xe release.
- Increase of the temperature in order to extract all the gas of the sample.

The thermal sequence consisted in annealing the sample in the HF induction furnace located in a hot cell, (Fig. 35) from 300°C (thermalization of the loop and initial conditions of PWR operation) up to a temperature ranging from 1000°C to 1200°C to cover the prototypical LOCA temperature range, with temperature increase rates equal to 0.2, 10 or 20°C/s. Upper temperature was maintained for 10 or 15 minutes or immediately decreased. The initial (clad burst) and final step (reflooding) of the LOCA sequence were not reproduced in the GASPARD experiments. Only the fission gases releases were measured: on-line gamma spectrometry provided data on their i release rates kinetics, and the cumulative gas release at the end of each test were obtained by gamma spectrometry (plus sometimes gas chromatography coupled to mass spectrometry (GC-MS) measurement of the isotopes trapped in the gloves box (Fig. 35).

19.3 Measured parameters, PIE data

The FGR final releases for the 4 and 6 cycles UO$_2$ samples are synthetized in
Table 14 below, and the 85Kr release kinetics is shown on Fig. 36. for the 6 cycle sample. In parallel, the ADAGIO experimental determination of the inter and intra-granular gas distribution showed that respectively 8% and 23% of their gas inventory is located at the fuel grain boundaries of the 4 cycle and 6 cycle samples.

Table 14
FGR final releases for the 4 and 6 cycles UO$_2$ samples in the GASPARD tests

Test	T increase rate (°C/s)	Tfuel max (°C) - during (mn)	Remarks	FGR % i.i.		
				[85]Kr, 4 cycles	[85]Kr, 6 cycles	[133]Xe, 6 cycles
A-0	0.2	1200 - 15	id as VERCORS RT7	8.8	15.3	2.1
A-1	10	1200 - 10		5.4	-	-
A-2	20	1200 - 10	"ref" LOCA	5.2	11.6	1.7
A-2bis	20	1200 - 0	No upper step	3.3	11.1	0.9
A-3	20	1000 - 10	Considered realistic	3.3	11.7	0.9
A-4	0.2	1000 - 10		-	6.2	0.6
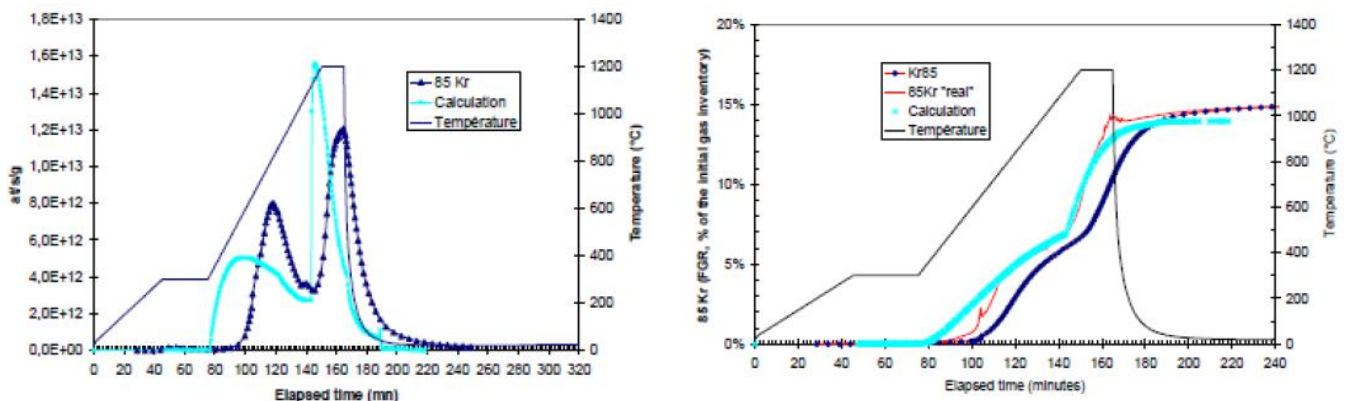
Fig. 36. [85]Kr release kinetics and cumulative release for A0, 6 cycles in GASPARD tests (slow T increase: 12 °C/mn)

Post Test Examination (PTE) were carried out to investigate the FP distribution evolution and microstructure changes in the samples matrixes, especially in terms of cracks distribution, pellet embrittlement and gas bubbles distribution, using the following techniques: longitudinal or radial metallography, SEM, fractography (example on Fig. 37). Similar examinations were conducted on reference samples (re-irradiated or not, but without annealing).
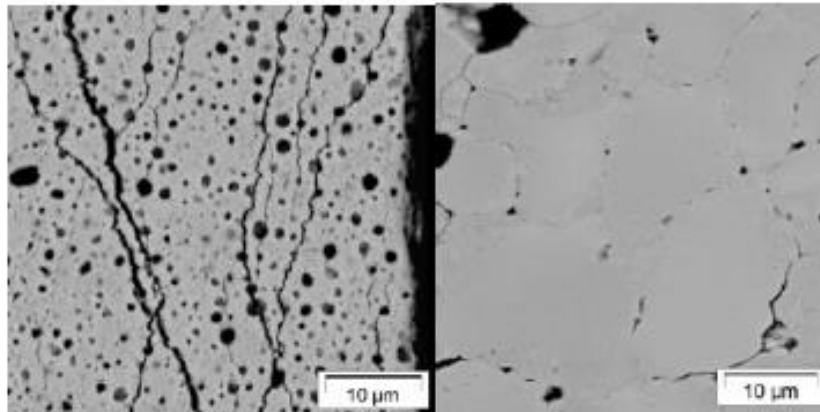
Fig. 37. SEM details of the HBS rim area (left) and at 0.75R (right) of the 6 cycles UO_2 fuel after the GASPARD A-2 test. Gas precipitation form very small bubbles at the grain boundaries, which are found in great numbers in the RIM zone, as well as a high density of cracks

19.4 General conclusions

The GASPARD experiments lead to the following conclusions:
- The release of fission gas from the fuel is mainly due to intergranular bubbles and is driven principally by two mechanisms: (i) the bubbles interconnection (diffusion of atoms and vacancies at high temperature), and (ii) the fracture of grain boundaries which leads to the burst release of gases present in over-pressurized bubbles.
- However, the contribution to global FGR from intra-granular gases (obtained from the ^{133}Xe signal) ranges from 0.6% to 2.1% i.i., depending on the final temperature of the test.
- Besides, for 4 cycles UO_2 fuels, a large majority of their inter-granular gas inventory (estimated at ~8% of the total inventory by ADAGIO technique) is released even for short tests.
- As far as the 6 cycles UO_2 fuel is concerned, it seems that whatever the final temperature, a maximum of 50% of the initial intergranular gas is released during the test (i.e. intergranular FGR ranging from 10% to13%) since ADAGIO yields to ~22% of intergranular gas.

19.5 References

[100]   *Y. Pontillon, M.P. Ferroud-Plattet, D. Parrat, S. Ravel, G. Ducros, C. Struzik, I. Aubrun, G. Eminet, J. Lamontagne, J. Noirot, A. Harrer, Experimental and theoretical investigation of fission gas release from UO_2 up to 70GWd/t under simulated LOCA type conditions: The GASPARD program. Orlando international meeting on LWR Fuel Performance, 2004

[101]   * Y. Pontillon, L. Desgranges, A. Poulesquen, ADAGIO technique: from UO_2 fuels to MOX fuels, Journal of Nuclear Materials 385 (2009) 137-141

*available in the R2CA database

20. VERCORS tests

20.1 Objectives

VERCORS is an analytical experimental program focusing on the release of fission products (FP) and actinides from an irradiated fuel rod, under conditions representative of those encountered during a severe PWR accident. Following on from the HEVA program, 17 tests – financed jointly by EDF and IRSN – were conducted by the CEA on its Grenoble site over a 14-year period (1989–2002), in accordance with three test series:

- Six tests (VERCORS 1–VERCORS 6) were carried out between 1989 and 1994 on UO_2 fuel, at temperatures close to its relocation (1860 – 2350°C).
- Two different test series – VERCORS HT (three tests) and RT (eight tests) –were alternately performed between 1996 and 2002 at higher temperatures (2260 – 2350°C) p to the fuel sample collapse. These tests focused on UO_2 and MOX fuels with a variety of initial configurations (intact or debris beds).

    The experimental results of this programme were used to:

- Define the envelope values for released fraction under SA conditions within the scope of assessing reference source terms for all French PWRs.
- Validate the semi-empirical rmechanistic models regarding FP release and transport while qualifying the simulation codes by integrating these models.

20.2 Tested materials, test facility

The VERCORS experiments were carried out in a facility built in a specific high-activity cell at the Laboratory for Active Materials (LAMA), which evolving over time, with the installation of increasingly complex instrumentation required to either extend the database on the transportation of FP (HT loop), or focusing on the contrary on release objectives in association with actinides (RT loop). Fig. 38 and Fig. 39 below present the experimental loop used in the RT and HT tests, while Table 16 and Table 16 summarize the sample characteristics and experimental conditions for all the VERCORS tests.
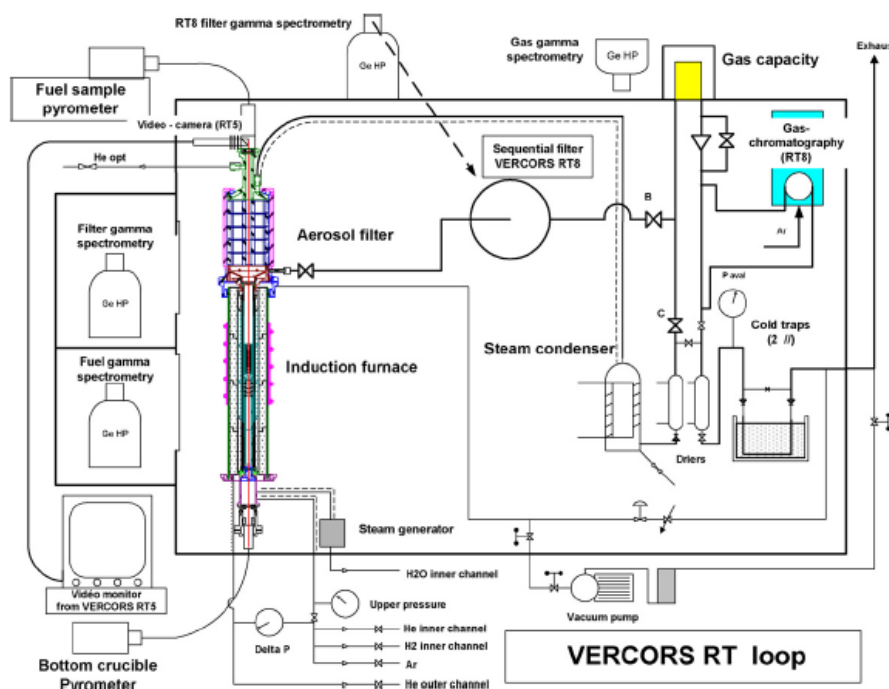
Fig. 38. Experimental loop for VERCORS RT 1 - 8
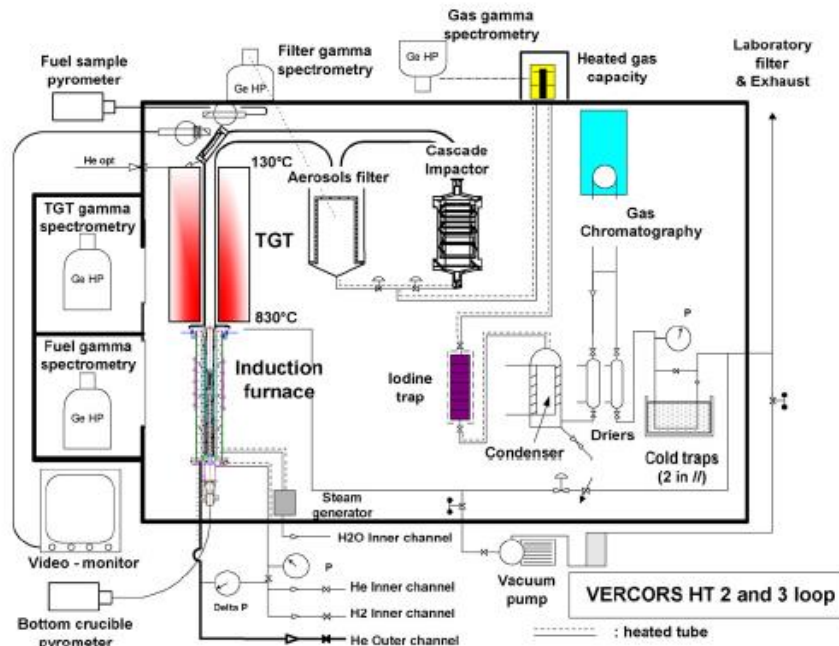
Fig. 39. Experimental loop for VERCORS HT

All the annealing test sequences comprised a clad oxidation phase at 1500°C. In some tests (VERCORS 2, 4, 5, RT7, RT8) were also included temperature steps at 800°C, 1000°C and 1300°C, to provide information on FP release in LOCA conditions.

Table 15
VERCORS and VERCORS RT sample characteristics and test grids

Test	VERCORS 1	VERCORS 2[a]	VERCORS 3	VERCORS 4[b]	VERCORS 5[c]	VERCORS 6
Date of test	11-1989	06-1990	04-1992	06-1993	11-1993	06-1994
Fuel	UO_2	UO_2	UO_2	UO_2	UO_2	UO_2
PWR irradiation	Fessenheim	Bugey	Bugey	Bugey	Bugey	Gravelines
Fuel burn-up (GWd/t)	42.9	38.3	38.3	38.3	38.3	60
Re-irradiation	Siloe	Siloe	Siloe	Siloe	Siloe	Siloe
Test conditions						
Max fuel temperature (K)	2130	2150	2570	2570	2570	2620
Atmosphere (end of test)	Mixed H_2O+H_2	Mixed H_2O+H_2	Mixed H_2O+H_2	Hydrogen	Steam	Mixed H_2O+H_2
Last plateau duration (min)	17	13	15	30	30	30
Steam flow rate (g/min)	0.15	1.5	1.5	1.5–0	1.5	1.5
Hydrogen flow rate (g/min)	0.003	0.027	0.03	0.012	0	0.03

[a] Test with intermediate temperature plateaus at 800°C, 1000°C,1200°C, 1500°C for 32 min, 12 min, 37 min and 30 min.
[b] Test under hydrogen, but with oxidizing intermediate plateau under mixed H_2O+H_2 at 1300°C for 60 min.
[c] Test under pure steam, but with intermediate temperature plateaus at 800°C, 1000°C, 1300°C for 30 min, 30 min and 70 min.

Test	VERCORS RT1	VERCORS RT2	VERCORS RT4	VERCORS RT3[a]	VERCORS RT7[a,b]	VERCORS RT6	VERCORS RT8
Date of test	03-1998	04-1998	06-1999	11-1999	04-2000	09-2002	11-2002
Fuel	UO_2	MOX (AUC)	Debris UO_2/ZrO_2	Debris UO_2	MOX (AUC)	UO_2	UO_2
PWR irradiation	Gravelines	Gravelines	Gravelines	BR3	Saint Laurent B1	Gravelines	Gravelines
Fuel burn-up (GWd/t)	47.3	45.6	37.6	39	43.0	71.8	70
Re-irradiation	No	No	No	Yes (partly)	Yes	Yes	Yes
Test conditions							
Max fuel temperature (°C)	2300	2170	2250	2700	2620	2200	2380
Atmosphere (end of test)	Mixed H_2O+H_2	Mixed H_2O+H_2	Mixed "oxidising"	Mixed "reducing"	Hydrogen	Mixed H_2O+H_2	He + 10% air
Last plateau duration (min)	[c]	[c]	[c]	[c]	[c]	[c]	[c]
Steam flow rate (g/min)	1.5	1.5	0.876	0.075	1.5–0	1.5	
Hydrogen flow rate (g/min)	0.027	0.027	0.024	0.075	0.012	0.027	
Airflow rate (g/min)							0.048

[a] Detailed analysis of the programme led to re-evaluation of the maximum temperatures attained in the course of the different tests, for RT7 and RT3 a significant drop of around 200–300°C.
[b] Test with intermediate temperature plateaus at 1200°C for 15 min under mixed atmosphere (H_2O+H_2) to simulate LOCA conditions.
[c] Succession of plateaux of 10 min every 100°C from 2000°C until "relocation" was obtained (after specific plateau for total cladding oxidation in H_2O+H_2 at 1500°C for 60 min).

Table 16
VERCORS HT sample characteristics and test grids

Test	VERCORS HT1[a]	VERCORS HT3	VERCORS HT2
Date of test	06-1996	06-2001	04-2002
Fuel	UO$_2$	UO$_2$	UO$_2$
PWR irradiation	Gravelines	Gravelines	Gravelines
Fuel burn-up (GWd/t)	49.4	49.3	47.7
Re-irradiation	Yes	Yes	Yes
Test conditions			
Max fuel temperature (°C)	2630	2410	2150
Atmosphere (end of test)	Hydrogen	Hydrogen	Steam
Last plateau duration (min)	7	b	b
Steam flow rate (g/min)	1.5–0	1.5–0	1.5
Hydrogen flow rate (g/min)	0.012	0.012	0
Injection Ag, In, Cd, B	No	Yes	Yes

[a] Test under hydrogen with intermediary plateau for total cladding oxidation in H$_2$O+H$_2$ for 60 min. [b] Succession of plateaus of 10 min every 100 °C from 2000 °C until fuel relocation was obtained (after specific plateau for total cladding oxidation in H$_2$O+H$_2$ at 1500 °C for 60 min).

Except for the RT3 and RT4 tests (debris beds configurations, the fuel samples were composed of a PWR section (irradiated in one of EDF's power plants) containing three pellets in their original cladding, and sealed at each end (without any specific leak tightness) by half a fresh pellet of depleted UO$_2$, blocked against the fissile column and maintained by crimping.

20.3 Measured parameters, PIE data

In addition to the on-line monitoring of the loop pressure, temperatures and flow rates, the FPs release kinetics were measured by several complementary gamma spectrometry stations aimed at the fuel sample plus the other loop components. The initial FP inventory was established by scanning the sample before the experiment. The effects of physical parameters such as the fuel burn-up on the measured FPs release kinetics (namely: noble gases, I, Cs, Te, Sb, Mo, Ba, Ru, La, Eu, Zr, Nb) were highlighted by comparing experimental results (Fig. 40). The temperature steps performed below 1500°C in a few tests, and the cladding oxidation phase at 1500°C in all of those performed in rod geometry, can provide release data at typical LOCA temperatures. At 1200°C, release rates higher than the fuel-to-gap FG inventory indicate partial inter-granular FP release. When partial intra-granular release is found, it can come only from HBS zones or highly oxidized matrixes. However, the gases and volatile FPs release kinetics curves in the VERCORS tests showed:

-   Important uncertainties on release measured below 1300°C.
-   Strong influence of the temperature e step duration on releases below 1300°C.
-   Steep release increase over short temperature differences above 1300°C.
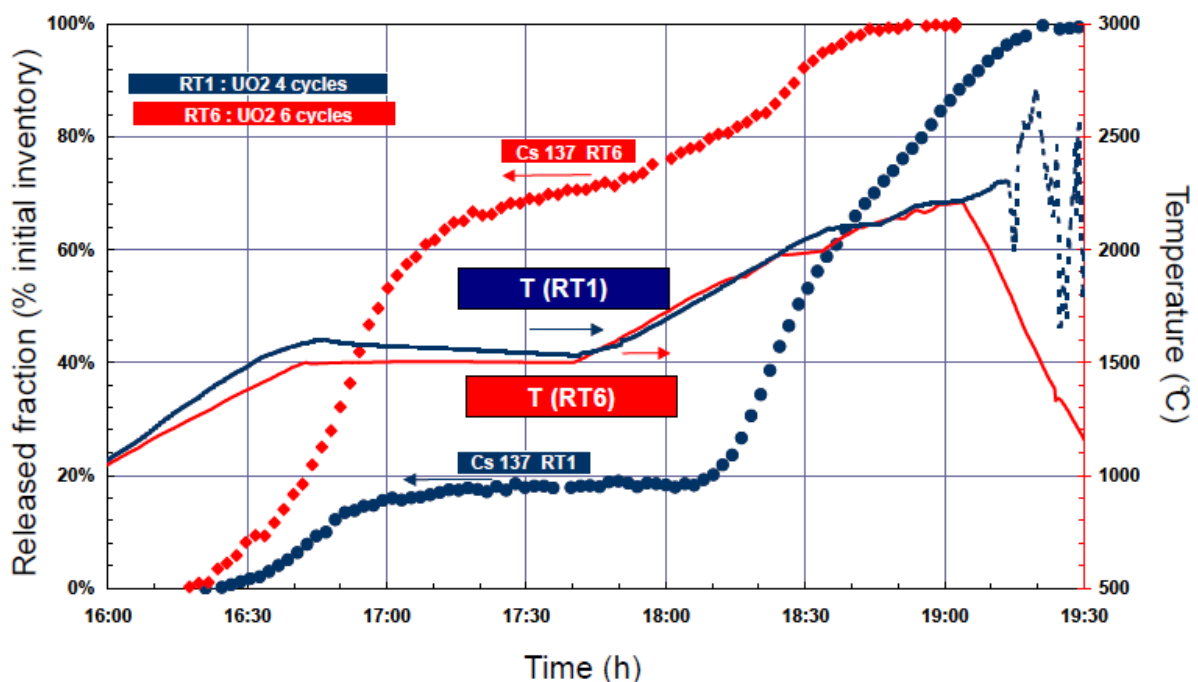
Fig. 40. Comparison of 137Cs release kinetics at middle (RT1) and high (RT6) UO$_2$ burn-up

Finally, post-test characterisation of the fuel state and micro-structural changes were carried out by means of post-test X-ray of the fuel (useful for intact geometries like in the VERCORS 1–6 series), ceramograph (VERCORS 1-6, RT1–RT4 and HT1 tests). In addition, SEM/EDS on aerosol deposits and on melted fuel were also performed.

20.4 General conclusions

The VERCORS program made it possible to precisely quantify fission products and actinides releases in all the situations explored, as well as to identify similar behavioural patterns between some of these fission products, thus allowing to classify them schematically into four groups with decreasing volatility: (1) volatile FPs (Xe, Kr, I, Cs, Te, Sb, Rb, Ag, Cd), practically totally released at temperatures around 2350°C; (2) semi-volatile FPs (Mo, Ba, Rh, Pd, Tc), with releases reaching 50–100% i.i. and very sensitive to the fuel matrix oxygen potential, and with marked redeposits nearby the emission point; (3) low volatile FPs (Sr, Y, Nb, Ru, La, Ce, Eu) with average releases of around 3–10% i.i. capable of reaching 20–40% i.i. for some elements – especially Ru - and under particular conditions (e.e. oxygen potential, high temperature and burn-up); (4) non-volatile FPs (Zr, Nd and Pr), for which no release could be measured by gamma spectrometry for the conditions of the VERCORS test grids. Actinides can be subdivided in two categories: U and Np with releases of up to 10% i. i. and behaviour similar to that of the low volatile FP, and the Pu group with releases less than 1% i. i.

Also, the cross-sectional analysis of the various VERCORS experimental sequences allowed to highlight the main physical parameters that affect these different elements release kinetics and rates: temperature (main parameter until loss of the sample rod geometry), fuel nature (UO_2 or MOX) and burn-up, matrix oxygen potential, interactions with the cladding and/or structural elements, and fuel state (transition from a ''rod'' geometry to a ''debris bed'' geometry and/or molten pool).

20.5 References

[102]   *Yves Pontillon∗, Gérard Ducros, P.P. Malgouyres, Behaviour of fission products under severe PWR accident conditions VERCORS experimental program - Part 1: General description of the program. Nuclear Engineering and Design 240 (2010), 1843 - 1852

[103]   *Ducros, P.P. Malgouyres, M. Kissane, D. Boulaud, M. Durin, Fission Product release under severe accidental conditions; general presentation of the program and synthesis of VERCORS 1 to 6 results. Nuclear Engineering and Design 208 (2001), 191–203

[104]   *Ducros, Y. Pontillon, P.P. Malgouyres, Synthesis of the VERCORS experimental programme: Separate-effect experiments on Fission Product release, in support of the PHEBUS-FP programme. Annals of Nuclear Energy 61 (2013) 75-87

*available in the R2CA database

21. VERDON tests

21.1 Objectives

An international co-operative research programme, called the ''International Source Term Program (ISTP)'', was launched in the 2000ies in order to reduce remaining uncertainties concerning the source term assessment under LWR severe accident conditions. In the research field of FP release from high burn-up UO_2 and MOX fuels, five VERDON tests were performed in the VERDON laboratory at the CEA Cadarache Centre between September 2011 and November 2015. The internationally available literature regards the tests VERDON-1 to VERDON-4.

21.2 Tested materials, test facility

The VERDON tests were conducted in an entirely new laboratory at the CEA Cadarache Centre in the LECA-STAR facility.The VERDON laboratory is constituted of:
- a glove-box for analyzing and storing the fission and carrier gases,
- two high activity cells: C4 for the pre/ post-test operations and C5 dedicated to the accidental sequence carrying out and to on-line measurements, both thermal-hydraulics and gamma spectrometry (Fig. 41).
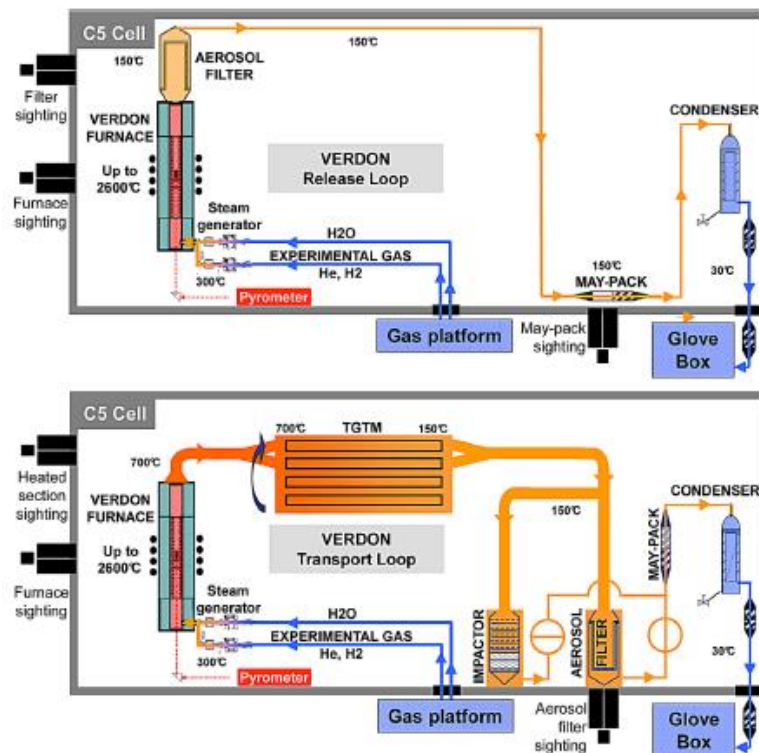
Fig. 41. VERDON C5 cell: release and transport circuit

The sample father rods characteristics and experimental conditions for all the VERDON tests are summarized on Table 17. The same father rod was used for test 1 and 5 (UO_2 72 and 68 GWd/thm) and for test 2, 3, 4 (MOX 56 GWd/thm). The samples consisted in two irradiated pellets in their original cladding and two half-pellets of depleted (and un-irradiated) uranium oxide placed at each end of the sample and held there by crimping the cladding so it would not be fully sealed.The five thermal sequences comprised a clad oxidation phase at 1500°C, plus a step at ~1200°C, respectively during 10 and 15 min in tests VERDON-3 and 4. Tests VERDON-1, 3 and 4 are focused on studying FP release from high burn-up UO_2 and MOX fuels. Tests 2 and 5 are dedicated to

assessing air ingress scenarios – the latter one with boric acid injection; for both of them, the facility was equipped with a specific loop including of thermal gradient tubes exposed at different phases of the sequence, dedicated to FP release and transport. Test 2 addressed two issues: Ru release under mixed steam-air conditions following lower head failure and transport/re-volatilization of Ru and volatile FPs in the primary circuit.

Table 17
VERDON sample characteristics and test conditions

Test	VERDON 1	VERDON 2	VERDON 3	VERDON 4	VERDON 5
Date	09/11	06/12	04/13	10/14	11/15
Fuel	UO₂ Gravelines	MOX Chinon	MOX Chinon	MOX Chinon	UO₂ Gravelines
BU GWj/thm	72	55,6	55,6	55,6	68
Reirradiat°	oui	oui	oui	oui	oui
Test Conditions					
T fuel max (K)	2670 -> 2875	2373	2570	2600 -> 2800	2270
Tmax during (mn)	18	70	10	13,5	60
Atmosphere	Neutral, oxidizing, reducing	Oxidizing (air ingress scenario)	Oxidizing	Reducing	Oxidizing (air ingress scenario)
Atmosphere end test	He/H₂O + H₂	H₂O/air	Steam	Hydrogene	H₂O/HBO₄ then H₂O
Steam flow rate g/mn	1,5 - 0,018 - 0	1,5 - 0,16	1,5 - 0,15	1,5 - 0	1,5 – 2,25 – 0,16
H₂ flow rate g/mn	0,027 - 0,02 - 0	0	0,027 - 0	0,024	0
Air flow rate g/mn	0	0,25	0	0	0,25

21.3 Measured parameters, PIE data

The pre-test sample characterizations, on-line measurements gamma spectrometry for FP releases and PIE were based on the same techniques than those applied to the VERCORS experiments (20.3).
The VERDON-1 test demonstrated the good behaviour of the loop at very high temperatures, and clearly highlighted the burn-up effect on the gases and volatile FPs release rate below 1500°C (Fig. 42). The fuel sample did not lose its integrity during this test, due to reducing final atmospheric conditions.
According to the released fractions measured by the online gamma station and thanks to the information obtained through pre- and post-test gamma scanning, the FP general classification, in relation to their released fractions and specific behaviour, remains similar to the one established with the data from the VERCORS program. The comparison between the VERDON-1 test and the VERCORS RT6 (performed on the same fuel type and in the same conditions during the first part of the thermal sequence) also proved a satisfactory continuity between VERCORS and VERDON databases.
The VERDON-2 test showed a rather unexpected low release of ruthenium from the MOX sample, and no re-volatilization from the thermal gradient tubes TGT). On the contrary, a significant re-volatilization of iodine was observed when switching to mixed steam-air conditions, as well as a low, but measurable amount of gaseous iodine transported downstream of the TGTs.
In the VERDON-3 and VERDON-4 complementary tests focused on MOX fuel and FP releases at temperatures higher than >2300 °C under oxidising and reducing atmospheres, pre and post-test qualitative and quantitative characterisations of the VERDON-3 and 4 samples highlighted the impact of the atmosphere on FP speciation:

- Enhanced migration of the metallic precipitates, only composed of Ru, Tc and Rh, in oxidising conditions. No more Mo and Pd could be found in the sample after the VERDON-3 test, which confirms Mo high release rates in such conditions (Pd release depending only on high temperatures).
- Melting and coalescence of metallic precipitates (composed of Mo, Ru, Tc and Rh) in reducing conditions during the VERDON-4 test, which a mobility most probably enhanced by a higher final temperature than in VERDON-3, and the melting of the UyZr1-yO2±x phase.
- The effect of the atmosphere on the behaviour of Ba proved difficult to assess, significant releases occurring in both tests.
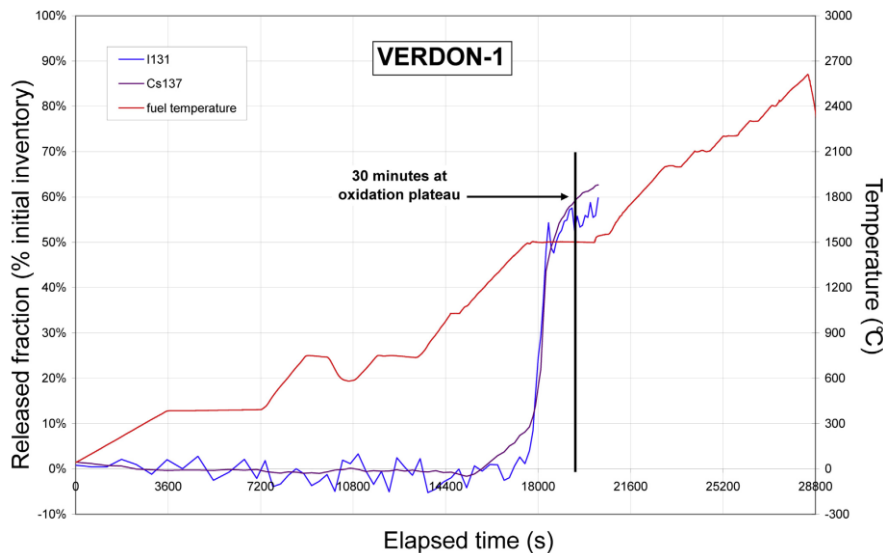
Fig. 42. Volatile FPs release in test VERDON-1

At temperatures close to LOCA conditions, the HBS zone is identified as main source of FG release. The « burst » release by grain boundaries cracking is likely due to over-pressurisation of pores. FP release measurements below 1300°C in the VERDON-4 test show good consistency with the GASPARD results on MOX fuels.

21.4 General conclusions

The VERDON program confirmed and extended the conclusions and data obtained from the VERCORS program, especially concerning high burn-up UO$_2$ fuels, MOX fuels, air-ingress major accident scenario. Its results highlighted the high burn-up influence on the fission gases and volatile FPs release kinetics, and atmospheric effects on Mo and Ba releases. However, a major difference comparing to all the other VERCORS tests on standard UO$_2$ fuel is observed here: it concerns the very fast release kinetics for volatile and semi-volatile FPs during the oxidizing phase. The influence of several key parameters and their impact on release kinetics could be identified in the VERDON tests. From a general point of view, the release rate increases with the burn-up, in oxidizing condition, and with MOX compared to UO$_2$ fuels.

21.5 References

[105]   *Y. Pontillon, E. Geiger 1, C. Le Gall*, S. Bernard, A. Gallais-During, P.P. Malgouyres, E. Hanus, G. Ducros, Fission products and nuclear fuel behaviour under severe accident conditions part 1: Main lessons learnt from the first VERDON test. Journal of Nuclear Materials 495 (2017) 363-384

[106]   *A. Gallais-During, S. Bernard, B. Gleizes, Y. Pontillon, J. Bonnin, P.-P. Malgouyres, S. Morin, E. Hanus, G. Ducros, Overview of the VERDON-ISTP Program and main insights from the VERDON-2 air ingress test. Annals of Nuclear Energy 101 (2017) 109–117

[107]   *C. Le Gall & al., Fission product speciation in the VERDON-3 and VERDON-4 MOX fuels samples. Journal of Nuclear Materials 530 (2020) 151948

*available in the R2CA database

22. Studsvik LOCA tests

22.1 Objectives

It is important to quantify the extent of fragmentation in LOCA as the fuel ejection into the primary circuit from the rupture opening is dependent, e.g., on the fragment sizes and the amount of fragmentation. Out-of-reactor LOCA testing in Studsvik hotcell laboratory was started with tests for the United States Nuclear Reculatory Commission, U.S.NRC, to study fuel fragmentation, relocation and dispersal during LOCA [95]. The device was designed to perform similar kind of LOCA tests done previously at the Argonne National Laboratory [96]. Integral testing in Studsvik is done with refabricated single fuel rodlets by using external heating, i.e., no nuclear heating is applied. In the U.S.NRC's experimental campaign, six LOCA tests on high burnup rods irradiated in commercial reactors were done. Based on the first test device, Studsvik constructed a second device within the OECD/NEA Studsvik Cladding Integrity Project (SCIP) III that was ongoing between 2014-2019. LOCA testing with the existing devices are planned to continue in SCIP IV (2019-2024) [97]. In addition to LOCA testing, the mechanism of fuel fragmentation is extensively studied in SCIP by means of advanced pre- and post-test examinations studying the fuel microstructure. Furnace heating tests with short samples complement integral LOCA testing.

Fuel fragmentation in LOCA has been linked to the existence of a burnup threshold, and this issue has previously been studied for instance in the Halden reactor project, and was addressed in SCIP III. Furthermore in SCIP III, the effects of temperature and cladding strain on fragmentation were studied. Rodlet internal pressure and free volume were varied to see the effect of these parameters. The impact of axial load on rodlet post-LOCA axial durability was studied, enabled by the new LOCA test device.

22.2 Tested materials, test facility

The initial state of the PWR test materials for the six U.S.NRC's LOCA tests are shown in Table 18. In these tests, the cladding material was ZIRLO™, manufactured by Westinghouse. In SCIP III, more than twenty LOCA tests have been done using fuel material irradiated in power reactors [98]. In SCIP III, the fuel material was standard UO_2, whereas in SCIP IV, various other fuel types are proposed to be studied, such as large grain fuel, additive fuel, MOX, and gadolinia fuel [97]. Data from the SCIP III tests has not been made public, and a NEA non-confidential report on SCIP III results is under preparation (situation in summer 2020). Some simulation results of selected five SCIP III tests have been made available from the SCIP III modelling workshop [98]. U.S.NRC's LOCA tests with identifiers 192 and 198 have been used in recent IAEA coordinated research project Fuel Modelling in Accident Conditions (FUMAC) [99].

Table 18
Test rodlet initial state in U.S.NRC Studsvik LOCA tests [95].

Test	Adjacent hydrogen (weight-ppm)	Average oxide (μm)	Rod average burnup (MWd/kgU)	Rod internal pressure at 300°C (MPa)
189	176	20	68.2	11
191	187, 271	20-30	69.3	11
192	176, 288	25-30	68.2	8.2
193	187	20	69.3	8.2
196	149	20	55.2	8.2
198	225	20	55.2	8.2

The test segment is heated up to maximum 1200 °C by infrared radiation in a clamshell furnace in a flowing steam, air or argon environment [97, 99]. The heating rate is controlled and typically 5 °C/s [97]. Ballooning and rupture is expected at 650-800 °C [97]. The test segment is pressurized with helium or argon. Depending on the desired test sequence, it is possible to have a holdtime at maximum temperature; in U.S.NRC's tests, temperatures were held at 1200 °C for either 0, 5, 25, or 85 seconds to vary the oxidation levels [95]. Cooldown rate from the maximum temperature is also controlled and can be for instance 3 °C/s as reported in [99]. It can be chosen whether to perform quench or not, as well as the timing of quenching. If quenching with room temperature water is applied, typical cladding temperature at that time is 700-800 °C [97].

Schematic drawings of the integral LOCA test devices are shown in Fig. 43.The axial length of the heated section is longer in the new device, 40 cm [97] vs. 26.7 cm [100], and that enables flatter axial temperature gradient [101]. Some of the other improved features between the designs are elaborated in [101]. Cladding axial temperature profiles of the infrared furnace at different temperatures and steam flow rates have been determined during the commissioning tests of the device [97]. The axial temperature profile at 1200 °C and with 150 ml/h flow is given in [97], in Fig. 19 of the report:

$$T = -4.909 \cdot 10^{-12} X^6 + 2.944 \cdot 10^{-10} X^5 + 1.573 \cdot 10^{-7} X^4 - 7.609 \cdot 10^{-6} X^3 - 3.849 \cdot 10^{-3} X^2 + 8.204 \cdot 10^{-2} X + T_{\text{ax.max}}, \qquad (1)$$

where T [°C] is the cladding outer surface axial temperature, X [mm] is the axial position relative to the rodlet centre (i.e., in the axial centre location X=0), and $T_{\text{ax.max}}$ is the cladding maximum temperature.

In the LOCA setup, the total plenum volume consists of various components: upper and lower pressure lines, rod upper plenum, and adapters [100]. Most of the out-of-furnace gas volume remain near room temperature during the tests as majority of the total free gas volume is located outside the heated region [99].
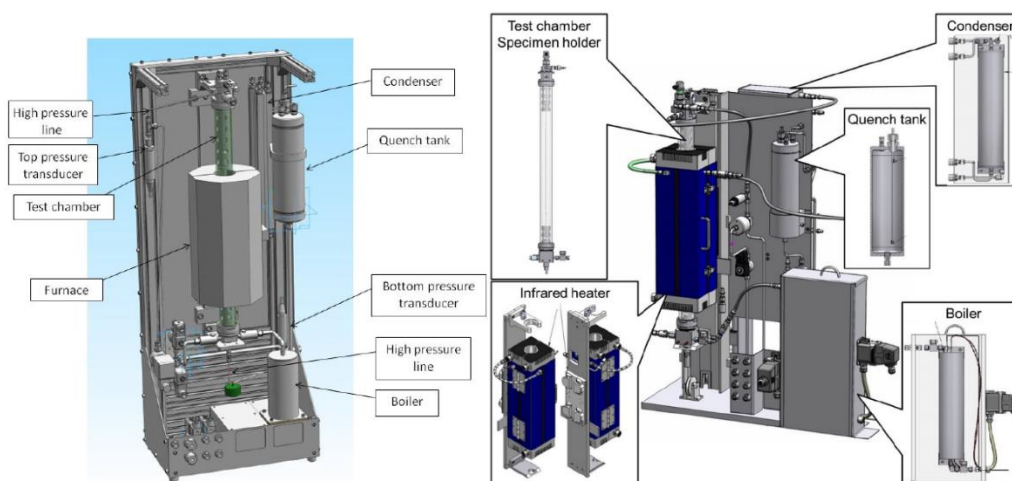
Fig. 43. Studsvik LOCA test device, old version on the left [95] and the new version on the right [97].

In addition to the integral LOCA devices, there is possibility to perform scoping LOCA tests with the heating furnace located in hotcell. Fine fragmentation burnup threshold and temperature dependency were studied by heating tests in SCIP III, typically up to 1000 °C [97]. The furnace is of resistive type, it is not pressurized and the tests are done in air atmosphere. The sample constraint is removed by cutting an axial slit through the cladding. Fast heating rates (10 °C/s) are possible by preheating the furnace before inserting the sample. However, it is reported that the achieved temperature ramp profile is not similar than expected during LOCA [97].

22.3 Measured parameters, PIE data

In integral LOCA tests, temperature evolution of the test segment is measured with a thermocouple attached with a clamp about 5 cm above the axial mid position [97]. The rodlet inner pressure is measured on-line with a pressure transducer, and axial displacement on-line with Linear Variable Differential Transformer (LVDT).

After the test, possible measurements include gamma scanning (data on fuel fragmentation and relocation), profilometry (strain profile), metallography, fuel loss quantification, fragment size distribution, and further mechanical testing such as 4-point bending test [97]. The cladding hydrogen content may be quantified by, e.g., Hot Vacuum Extraction (HVE), and the cladding oxidation from the metallographic examination. It is also possible to determine the fission gas release (FGR) that has occurred during the transient.

Advanced microscopy may include Electron Probe MicroAnalysis (EPMA) and Laser Ablation combined with Inductively Coupled Plasma Mass Spectrometry (LA-ICP-MS). The degree of subgrain formation during LOCA can be determined with Scanning Electron Microscopy Electron BackScatter Diffraction (SEM-EBSD). LA-ICP-MS may be used for instance to study the fission gas content in the fuel [97].

In furnace heating tests, temperature evolution of the test segment is measured with a thermocouple. Heating tests are usually recorder with video and audio.

Transient test results available from the U.S.NRC's Studsvik LOCA tests are show in Table 2. In-cell measurements included maximum circumferential strain, rupture dimensions, length of the circumferential strain greater than 10%, and wire probe that was inserted inside the rodlet to measure the voided cladding length below and above the rupture centre. From Fig. 44 (left hand side) it is seen that no fuel loss occurred during transient in fuel rodlets with lower burnup (tests 196 and 198). Fragment sizes of fuel found outside the rodlets were measured for five tests, shown in Fig. 44 (right hand side). Tests 191-193 with higher burnup showed fine fragmentation, and the portion of fragments larger than 4 mm was small or zero. Tests 196 and 198 with lower burnup did not show fine fragmentation.

Table 19
Transient test results of U.S.NRC Studsvik LOCA tests [95].

	Test	Peak Cladding Temperature (°C)	Rupture Temp (°C)	Rupture Pressure (bar)	Time (s) to 50% of rupture P for top/bottom gauges	CP-ECR (%)	Quench
Transient	189	950	700	109	35 / 7	0	No
	191	1185	680	104	21 / 10	13	Yes
	192	1185	700	81	13 / 15	11	Yes
	193	1185	728	81	45 / 8	17	Yes
	196	950	686	81	5 / 2	0	No
	198	1185	693	81	3 / 2	15	Yes
	Test	Max Strain (%)	Length >10% Strain (mm)	Wire Probe Measurement (mm) (Top/Bottom)		Rupture Dimensions (mm) (Width/Length)	
In-cell Measurements	189	48	105	82 / 66		10.5 / 23.9	
	191	50	70	70 / 55		17.5 / 21.6	
	192	56	85	85 / 73		9 / 22.7	
	193	50	100	113 / 91		13.8 / 17.8	
	196	25	95	90 / 66		0.2 / 1.5	
	198	25	115	55 / 76		1.6 / 11	
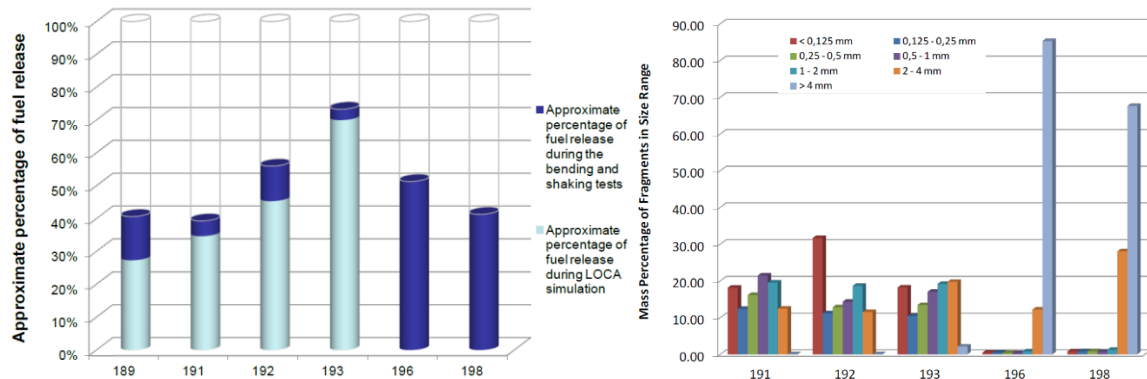
Fig. 44. Approximate fuel loss in U.S.NRC's Studsvik LOCA tests (on the left), and fragment size distribution of fuel found outside of rod (on the right) [95].

22.4 General conclusions

In six integral LOCA tests made for the U.S.NRC, significant fuel fragmentation, relocation and dispersal occurred in rods with higher burnup (tests 189-193) while no dispersal was seen in samples with lower burnup (tests 196 and 198), and the fragment sizes in the latter tests were larger.

In SCIP III, fine fragmentation burnup threshold was determined to be 60-65 MWd/kgU [97]. However, high burnup was not the only factor resulting in fine fragmentation; in some cases 75 MWd/kgU fuel had less fine fragmentation than 65 MWd/kgU fuel, i.e., a simple burnup threshold could not be found [97]. Various factors could contribute to fine fragmentation, such as the local power history leading to pre-test fuel microstructure susceptible to fine fragmentation, repartitioning of fission gases, or fuel subgrain formation. Instead, no clear correlation between end-of-life power and fine fragmentation could be found [97].

The importance of depressurisation shock resulting from rod burst on fuel fragmentation was shown by comparing tests on burst and non-burst rods on similar material [97]. Fuel dispersal was shown to depend on the degree of fragmentation and the burst opening size [97].

22.5 References

[95] *Flanagan, M., Askeljung, P., Puranen, A., 2013. Post-test examination results from integral, high-burnup, fueled LOCA tests at Studsvik Nuclear Laboratory. NUREG-2160, United States Nuclear Regulatory Commission. www.nrc.gov/docs/ML1324/ML13240A256.pdf (accessed: 25 Feb. 2020)

[96] *Helin, M., Flygare, J., 2012. NRC LOCA Tests at Studsvik. Studsvik report STUDSVIK/N-11/130 www.nrc.gov/docs/ML1221/ML12215A431.pdf (accessed: 25 Feb. 2020)

[97] *Zwicky, H.-U., 2018. SCIP IV – Technical Description. STUDSVIK/N-18/027, STUDSVIK-SCIP IV-220 www.studsvik.com/contentassets/e6724b7f468c4660aead7070fc424737/scip-iv-technical-description-public.pdf (accessed: 25 Feb. 2020)

[98] *Karlsson, J., Beccau, P., Magnusson, P. (1); Janzon, C., Struzik, C., Dostal, M., Porter, I., Jernkvist, L.-O., Grandi, G., Jönsson, C., Zheng, W., Taurines, T., Marchand, O., Shuo, X., Zwicky, H.-U., Belon, S., 2018. Modelling out-of-pile LOCA tests on high burnup fuel rods. Results of the fourth SCIP modelling workshop. In proceedings of: TopFuel 2018, 30 Sept. – 4 Oct. 2018, Prague, Czech Republic

[99] *IAEA, 2019. Fuel modelling in accident conditions (FUMAC). Final report of a coordinated research project. IAEA-TECDOC-1889. www-pub.iaea.org/MTCD/Publications/PDF/TE-1889web.pdf (accessed: 25 Feb. 2020)

[100] *Jernkvist, L.-O., 2016. Computational assessment of LOCA simulation tests on high burnup fuel rods in Halden and Studsvik. Report prepared for the Swedish Radiation Safety Authority SSM. Report number: 2017:12 ISSN: 2000-0456

www.stralsakerhetsmyndigheten.se/contentassets/42ba1bfabc51481b8669db9cc580c673/201712-computational-assessment-of-loca-simulation-tests-on-high-burnup-fuel-rods-in-halden-and-studsvik (accessed: 25 Feb. 2020)

[101]   *Minghetti, D., Snis, N., Magnusson, P., 2015. Loss Of Coolant Accident experiments at Studsvik's Hot Cell Laboratory. In proceedings of: HOTLAB conference 2015, Leuven, Belgium, 27 Sep. - 1 Oct. 2015

*available in the R2CA database

23. CORA tests

23.1 Objectives

The CORA out-of-pile facility at Kernforschungszentrum Karlsruhe (KfK, later FZKA, nowadays KIT) was designed to investigate the behaviour of LWR fuel assemblies under severe fuel damage accident conditions. As part of the Severe Fuel Damage Program by the German Nuclear Safety project (Projekt Nukleare Sicherheit PNS), in total 21 test were performed between 1986 and 1993, with different configurations (PWR, BWR and VVER).

Hofmann et. al [108] summarized the main objectives of the test program as follows:

- Study of oxidation behaviour and of the critical temperature at which the temperature escalation starts as a result of the exothermal Zircaloy-steam reaction;
- Investigation of embrittled fuel rods fragmentation, particularly during cool-down and water quenching, and characterization of the resulting debris;
- Investigation of the onset of liquid-phase formation due to chemical interactions of bundle components such as fuel rods, absorber materials, spacer grids, and stainless steel structural materials with each other;
- Determination of the influence of liquid phases and molten components on bundle damage progression;
- Assessment of extent of UO2 and ZrO2 dissolution by molten Zircaloy or α-Zr(O);
- Study of relocation and solidification behaviour of liquid materials and the formation of blockages;
- Investigation of coolability of damaged fuel assemblies and of the quenching process;
- Quantification of generated hydrogen;
- Establishment of a database for code validation and assessment.

23.2 Tested materials, test facility

The CORA test facility is shown by Fig. 45. The fuel rod test bundle was approximately 2 m long and consisted of up to 57 rods (25 rods were used in the standard PWR bundle). Several configurations were assessed, as shown by Fig. 46. A detailed description of the facility is given e.g. in [109],[110].
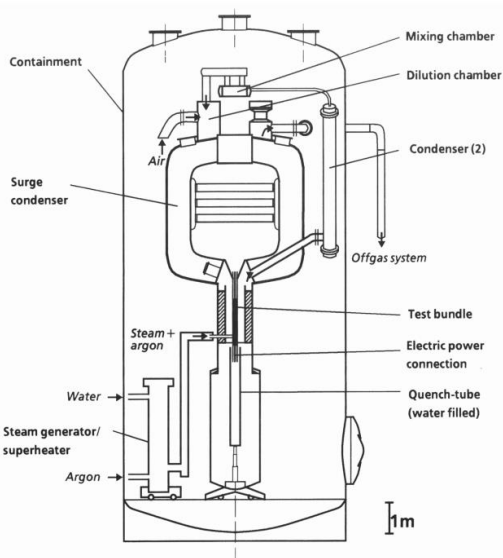
Fig. 45. Main components of the CORA test facility [108]
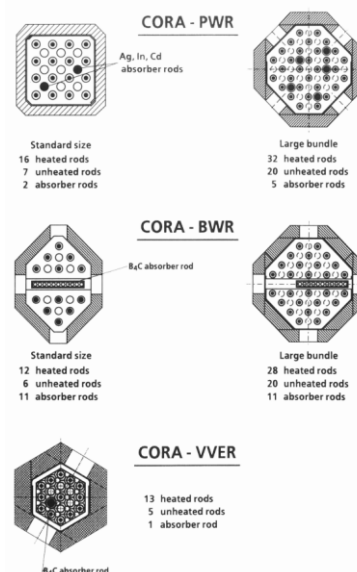
Fig. 46. Different bundle arrangements applied in the CORA experiments (PWR, BWR and VVER configuration) [108]

Table 20 gives an overview of all 21 tests and its main characteristics and references to reports with test description and documentation of test results, results of the post-test examination and selected numerical analyses of the experiments. The primary parameters of the test series were [109]: fuel rod heat-up rate, maximum cladding temperature, coolant flow rate, system pressure, fuel rod internal pressure and cool-down rate (including quench). The table also includes additional tests, which were performed in the framework of the PNS program, but within the predecessor NIELS test facility (single rod tests and bundle tests with smaller 3x3 bundle).

Table 20
CORA test matrix and references to reports with test description, results, post-test examination (PTE) and numerical analyses (Num.)

Test number	Max. Cladding Temp. (K)	Type	Absorber material	Other test conditions	Date of Test	References		
						Test/ Results	PTE	Numerical analyses
ESSI (1-11)		PWR	---	Single rod tests	1981/82	[111][112]	[113]	
ESBU-1	≈ 2520	PWR	---	Zircaloy cladding/shroud 2 K/s heat-up rate	1983	[114]	[115]	
ESBU-2a	≈ 2450	PWR	---	Zircaloy cladding/shroud 0.5 K/s heat-up rate	1984	[116]	[117]	
B	≈ 2500	---	---	Al_2O_3 pellets	03.09.86	[110]	[110][118]	
C	≈ 2500	---	---	Al_2O_3 pellets	02.02.87	[119]	[118]	
2	≈ 2300	PWR	---	UO_2 reference, INCONEL spacer	06.08.87	[119][120]	[121]	[122]
3	≈ 2700	PWR	---	UO_2 reference, high temperature	03.12.87	[121]	[121]	
5	≈ 2300	PWR	Ag-In-Cd	PWR absorber	26.02.88	[123]	[124]	[122][125]
7	< 2300	PWR	Ag-In-Cd	57-rod bundle, slow cooling	22.02.90	[126]	[124]	[122]
9	≈ 2300	PWR	Ag-In-Cd	10 bar system pressure	09.11.89	[124]	[124]	[122][127]
10	≈ 2300	PWR	Ag-In-Cd	Cold lower end, 2 g/s steam flow rate	16.07.92	[128]		
12	≈ 2300	PWR	Ag-In-Cd	Quenching	09.06.88	[123][129]	[124]	[130]
13	≈ 2500	PWR	Ag-In-Cd	OECD/ISP-31; quench initiation at higher temperature	15.11.90	[131]	[131][132]	[133][134] [135][136]
15	≈ 2300	PWR	Ag-In-Cd	Rods with internal pressure	02.03.89	[124]	[124]	[137][138]
16	≈ 2300	BWR	B_4C	BWR absorber	24.11.88	[139]	[140][141]	[142][143]
17	≈ 2300	BWR	B_4C	Quenching	29.06.89	[139]	[141]	[142][144][146]
18	< 2300	BWR	B_4C	59-rod bundle. Slow cooling	21.06.90	[147]	[141][147]	[143][148][149]
28	≈ 2300	BWR	B_4C	Pre-oxidised	25.02.92	[150]	[150]	[143][146][151]
29	≈ 2300	PWR	Ag-In-Cd	Pre-oxidised	11.04.91	[152]	[152]	
30	≈ 2300	PWR	Ag-In-Cd	Slow initial heat-up (0.2 K/s)	30.10.90	[153]	[153]	
31	≈ 2300	BWR	B_4C	Slow initial heat-up	25.07.91	[154]	[154]	

				(0.3 K/s)				
33	≈ 2300	BWR	B$_4$C	Dry core conditions, no extra steam input	01.10.92	[155]	[155]	[143][144]
W1	≈ 2300	VVER	---	VVER test	18.02.93	[156]	[156]	[157]
W2	≈ 2300	VVER	B$_4$C	VVER test with absorber, OECD/ISP-36	21.04.94	[158]	[159]	[160]

Further references with special aspects of the test program, investigation of selected phenomena, or comparison of different tests:

- Chemical interactions of reactor core Materials Up to high temperatures: [161]
- Zircaloy Oxidation and Cladding deformation in PWR-specific CORA experiments: [162]
- Impact of absorber materials: [163]
- Comparison of quench experiments CORA-12, CORA-13 and CORA-17: [129]

The CORA program was accompanied by a large number of separate effect test which are summarized in [164]

23.3 Measured parameters, PIE data

The following data was measured [109], [110]:

- electric power supply of each heated rod,
- gas and steam input, gas outflow (relative gas concentration was measured by mass spectrometer)
- gas temperature and temperature in unheated and heated rods by thermocouples
- surface temperature of bundle (by two-colour pyrometer)
- axial and radial temperature distribution in the insulation shield (32 thermocouples)
- visual inspection of the bundle behaviour by 10 endoscopes/cameras

After each test, a comprehensive post-test examination was performed: with visual inspection, photographic documentation, and collecting of fragments. The test bundles were encapsulated in epoxy resin and afterwards cut into slices. The slices were studied by optical microscopy, scanning electron microscopy (SEM), energy dispersive X-ray spectrometry (EDX), and wave length dispersive measurements (WDX) [121] to study the microstructure of the bundles. Details of integral post-test examination methods applied in the CORA tests are given in [165].

23.4 General conclusions

General conclusions from the test program were drawn by Hofmann et. al [108]. The CORA experiments and the accompanying single-effect tests have contributed substantially to the understanding of material behaviour in reactor accidents. However, most of the tests were made under conditions of severe melting of the core. For the current R2CA project where LOCA under design basis and design extended conditions will be investigated, the most important conclusions from the CORA experiments have to be drawn from the early phase of the experiments with localized core damage. Therefore, the following conclusions from [108] are supposed to play a significant role for analyses to be performed in the R2CA project:

- It is significant that temperature escalation due to the zirconium-steam reaction starts in the upper, i.e. hotter, half of the bundle. With adiabatic conditions (as in the CORA test section), the escalation occurred at relatively low temperatures of approximately 1400 K and propagates from there downwards and upwards. The maximum heat-up rates and maximum temperatures measured are ~20 K/s and 2300 K, respectively.
- After attaining the melting point of Zircaloy cladding, the melt flows over large distances, starting from locations where the ZrO$_2$ oxide layer on the external cladding tube surface might be penetrated because of chemical and/or mechanical effects (ZrO$_2$ failure criteria).
- The cladding integrity can be destroyed, however, far below the melting point of Zircaloy by eutectic interaction with the stainless steel or INCONEL grid spacer, or absorber materials (the Ag-ln-Cd alloy or B$_4$C), which results in larger quantities of liquid phases at temperatures as low as 1550 K.

- It was found that control rod materials might separate from fuel rod materials by relocation processes in the liquid state at temperatures as low as 1550 K. Therefore, reflood water must be sufficiently borated to avoid recriticality and power generation during early phase core degradation, which means prior to the disintegration of the core into a rubble bed.
- The hydrogen generation depends on Zircaloy and steam availability and on the heat-up rate, extent of Zircaloy preoxidation, (maximum) bundle temperature, and cool-down conditions (slow cool-down or quenching).
- In the case of preoxidized fuel element components or smaller heat-up rates, less melt formation and hence relocation is observed.
- Reflood (water quenching) of a damaged core can fragment oxidation-embrittled Zircaloy cladding, fracture solidified once-molten materials (blockages), and induce locally a renewed temperature rise and strong additional hydrogen generation.
- For BWR core material behaviour in severe reactor accidents, the accident progression depends on the selected material combination (B4C/Zircaloy or B4C/stainless steel). B4C/Zircaloy would result in a greater flexibility for accident management measures because meltdown would be delayed in time and shifted to higher temperatures (from 1550 K for B4C/steel to 2030 K for B4C/Zircaloy).
- Despite some specific features, the material behaviour of the VVER-1000 bundle is comparable to that observed in the PWR and BWR tests of Western design.

23.5 References

[108]   P. Hofmann, et al., Chemical-physical behavior of light water reactor core components tested under severe reactor accident conditions in the CORA facility. Nuclear Technology, 1997. 118(3): p. 200-224.
[109]   S. Hagen and K. Hain, KfK-3677. 1986
[110]   S. Hagen, W. Hering, and K. Vogel, CORA scoping test B. Test results report. KfK-4171. 1988
[111]   S. Hagen, et al., ESSI-1,2,3 test results report. KfK-3507. 1983.
[112]   S. Hagen, et al., ESSI-4 to ESSI-11 test results report. KfK-3557. 1985
[113]   S. Hagen, et al., Post test investigation of the single rod tests ESSI 1-11. KfK-3768. 1987.
[114]   S. Hagen, et al., ESBU-1 test results report. KfK-3508. 1983.
[115]   S. Hagen, et al., Post test investigation of the bundle test ESBU-1. KfK-3769. 1986.
[116]   S. Hagen, et al., ESBU-2A test results report. KfK-3509. 1984.
[117]   S. Hagen, et al., Post test investigations of bundle test ESBU-2A. KfK-3789. 1986.
[118]   P. Hofmann, et al., Metallographische Nachuntersuchung CORA-B/CORA-C. KfK-4450, p. 36-40. 1988.
[119]   S. Hagen, et al., Tests CORA-C and CORA-2. KfK-4404. 1988.
[120]   S. Hagen, et al., Versuch CORA-C und Versuch CORA-2. KfK-4450, p. 1-34. 1988.
[121]   S. Hagen, et al., Posttest results of CORA-2 and CORA-3. KfK-4378. 1990.
[122]   K. Trambauer, et al., GRS-A-1689. 1990.
[123]   S. Hagen, et al., Versuche CORA-5 und CORA-12 zum Einfluss von AgInCd-Absorbern auf das Schadensverhalten. KfK-4550, p. 1-27. 1989.
[124]   L. Sepold, et al., Behavior of AgInCd absorber material in Zry/UO$_2$ fuel rod simulator bundles tested at high temperatures in the CORA facility. FZKA-7448. 2009
[125]   T. Steinrötter and H. Unger, Nachrechnung CORA-5 mit ATHLET-CD 1.1D/0.2E. RUB-E-202. 1998.
[126]   S. Hagen, et al., Large bundle PWR test CORA-7: test results. FZKA-6030. 1998.
[127]   J. Paulus and U. Brockmeier, Post-test calculation of CORA-9 with RELAP5/SCDAP. RUB-E-23. 1992.
[128]   S. Hagen, et al., Cold lower end test CORA-10: test results. FZKA-5572. 1997.
[129]   S. Hagen, et al., Comparison of quench experiments CORA-12, CORA-13, CORA-17. FZKA-5679. 1996.

[130]   A. Sharon, et al., Benchmarks of severe fuel damage tests using a stand-alone version of heatup from MAAP-DOE, Task 3. 6. 8. 1990, Fauske and Associates, Inc., Burr Ridge, IL (USA).

[131]   S. Hagen, et al., Results of CORA-13 (OECD international standard problem 31). KfK-5054. 1993.

[132]   J. Burbach, Ergebnisse von REM-Mikrobereichsanalysen CORA-13. KfK-5162. 1993.

[133]   M. Firnhaber, et al., ISP-31 OECD/NEA/CSNI International Standard Problem n. 31. Cora-13 experiment on severe fuel damage. Comparison report. GRS-106. 1993.

[134]   A. Shwetsov, J. Paulus, and U. Brockmeier, Nachrechnung CORA-13 mit ICARE2-V2. RUB-E-68. 1994.

[135]   J. Bestele, K. Trambauer, and J.-D. Schubert, Posttest calculations of bundle quench test CORA-13 with ATHLET-CD. Nuclear technology 117(1): p. 109-123. 1997.

[136]   K. Müller et al., Ergebnisse und Analysen zum ISP 31: CORA-13 Experiment. IKE2-102. 1993

[137]   J. Stuckert, et al., IAEA FUMAC Benchmark On KIT Bundle Test CORA-15. Trans. TopFuel, 2018.

[138]   J. Stuckert, et al., Post-test analyses of the CORA-15 bundle test with the system codes ATHLET-CD and SOCRAT. Nuclear Engineering and Design 342: p. 320-335. 2019.

[139]   S. Hagen, et al., Versuche CORA-16 und CORA-17. KfK-4700 p. 1-27. 1990.

[140]   J. Burbach, REM/EDX-Mikrobereichsanalysen CORA-16. KfK-5282. 1994.

[141]   L. Sepold, et al., Behavior of BWR-type Fuel Elements with B4C/Steel Absorber Tested under Severe Fuel Damage Conditions in the CORA Facility. FZKA-7447. 2009

[142]   V. Di Marcello, U. Imke, and V. Sanchez, Validation and application of the system code ATHLET-CD for BWR severe accident analyses. Nuclear Engineering and Design 307: p. 284-298. 2016.

[143]   T. Okawa, A three-dimensional approach for simulating BWR core melt progression - A validation against CORA-BWR experimental series. Annals of Nuclear Energy 132: p. 512-525. 2019.

[144]   T. Steinrötter, N. Pohl, and H. Unger, Nachrechnungen CORA-17 und CORA-33 mit ATHLET-CD 1.2B/1.0A. RUB-E-259. 2000.

[145]   A. Prestigiacomo, et al., Molten Core Relocation Analysis of CORA-17 and CORA-18 for the SAMPSON/MCRA Validation, in NURETH-16. 2015.

[146]   M. Hoffmann, F. Gremme, M.K. Koch, Simulation CORA-17 und CORA-28 mit Athlet-CD. LEE-75. 2013.

[147]   S. Hagen, et al., Large bundle BWR test CORA-18: test results. FZKA-6031. 1998.

[148]   A. Costa, Validation of the SAMPSON/MCRA code against the CORA-18 experiment. 2015.

[149]   A. Costa, et al., Validation of the SAMPSON/MCRA CODE against CORA-18, ICONE23, 2015.

[150]   S. Hagen, et al., Pre-oxidised BWR test CORA-28: test results. FZKA-5571. 1997.

[151]   T. Hollands, et al., Nachrechnung CORA-28 mit ATHLET-CD 2.1 A, LEE-54. 2007.

[152]   S. Hagen, et al., Pre-oxidised PWR test CORA-29: test results. FZKA-5928. 1997.

[153]   S. Hagen, et al., Slow heat-up PWR test CORA-30: test results. FZKA-5929. 1997.

[154]   S. Hagen, et al., BWR slow heatup test CORA-31: test results. KfK-5383. 1995.

[155]   S. Hagen, et al., Dry core BWR test CORA-33: test results. KfK-5261. 1995.

[156]   S. Hagen, et al., Test results of experiment CORA-W1. KfK-5212. 1994.

[157]   J. Paulus, Th. Steinrötter, Nachrechnungen CORA-W1 und CORA-W2 mit ATHLET/CD, RELAP5/SCDAP, MELCOR und ICARE2. RUB-E-128. 1995

[158]   S. Hagen, et al., Results of experiment CORA-W2. KfK-5363. 1994.

[159]   L. Sepold, Posttest examination of the VVER-1000 fuel rod bundle CORA-W2. FZKA-5570. 1995.

[160]   M. Firnhaber, et al., OECD/NEA-CSNI International Standard Problem ISP36. "CORA-W2 Experiment on Severe Fuel Damage for a Russian Type PWR". GRS-120. 1996.

[161]   P. Hofmann, et al., Chemical Interactions of Reactor Core Materials Up to Very High Temperatures. KfK-4485. 1989

[162]   Zircaloy Oxidation and Cladding Deformation in PWR-Specific CORA Experiments. KfK-4827. 1991

[163]   S. Hagen, et al., Impact of absorber rod material on bundle degradation seen in CORA experiments. FZKA-5680. 1996.

[164]   *W. Hering, P. Hofmann, Material Interactions during Severe LWR Accidents. Summary of Separate-Effects Test Results. KfK-5125. 1994

[165]   W. Hering, W., Integrale Nachuntersuchung von CORA-Bündeln, KfK-Primärbericht 12.07.01P13A. 1989

*available in the R2CA database

Titles of the references have been shortened.

KfK: Report by Kernforschungszentrum Karlsruhe;

FZKA: Report by Forschungszentrum Karlsruhe;

GRS: Report by Gesellschaft für Anlagen- und Reaktorsicherheit (GRS);

IKE: Report by University of Stuttgart, Institut für Kernenergetik und Energiesysteme;

RUB/LEE: Reports by University of Bochum, Institut für Energietechnik.

24. QUENCH-LOCA integral tests

24.1 Objectives

The QUENCH-LOCA test series aims at investigating the behaviour of the PWR fuel rod cladding in case of the LOCA event, for representative DBA conditions ([166]-[173]). Temperature levels and time scenarios are chosen based on a LBLOCA in German PWR. The key parameters are the cladding temperature and oxidation level.

The test matrix includes six tests (
Table 21) with different cladding materials, from Zircaloy-4 to advanced alloys (M5® and ZIRLO™) specific for high-BU fuels; the last two tests are devoted to the effect of hydrogen pre-loading on the advanced alloys.

Table 21
The QUENCH-LOCA test matrix

Test	Simulated conditions
QUENCH-L0	Commissioning test, as-received Zircaloy-4 cladding, different initial fuel rod internal pressure
QUENCH-L1	Reference case, as-received Zircaloy-4 cladding, Ta heaters
QUENCH-L2	As-received M5 cladding, W small-diameter heaters
QUENCH-L3	As-received ZIRLO cladding, W small-diameter heaters
QUENCH-L4	M5 cladding with 100 wppm hydrogen preloading, W small-diameter heaters
QUENCH-L5	ZIRLO cladding with 300 wppm hydrogen preloading, W small-diameter heaters

The main objectives of the QUENCH-LOCA test bundle were:
- the investigation of ballooning, bursting, embrittlement and hydrogen uptake phenomena within the fuel cladding;
- the verification of the safety margins, especially for the German nuclear reactor cases, for high-BU fuels.

24.2 Tested materials, test facility

The QUENCH test section (Fig. 47) is constituted by a vertical cylindrical Zr 702 shroud, surrounded by proper heat insulation and two concentric tubes, forming a cooling jacket, with argon in the gap: the shroud can hence be considered in adiabatic conditions. The 21 simulating fuel rods are housed inside the Zr shroud, with four smaller corner rods used for instrumentation and to avoid high coolant flow regions. Each fuel rod is composed by a central heating rod, a zirconium oxide annular pellet and the cladding, whose material differs for each test. The complete rod (cladding inclusive) has a 10.75 mm diameter, while the cladding is 0.725 mm-thick. The heating rod is made of tantalum (test L1) or tungsten (all other tests), and its diameter is either 6 mm (tests L0 and L1) or 4.6 mm (tests from L2 to L5). At the beginning of the test, each rod is pre-pressurized at 55 bar (except for commissioning test, when different pressures are used) with krypton.

The bundle cooling is carried out through a mixture of argon and steam flowing upward inside the shroud, from its bottom; the off-gases outflowing from the top of the test bundle are continuously analysed through mass spectrometry. After the slow cool-down phase, the quenching starts, with liquid water at 293 K, flooding the bundle from the bottom (Fig. 47).

During the system setup, the bundle is slowly brought to a temperature between 800 and 850 K, in thermal equilibrium with the steam-argon mixture flowing inside the shroud (2 g/s steam + 6 g/s Ar) at 3 bar (constant system pressure during the whole test). After the rods are pressurized to the fixed level, the test starts, increasing steadily at the maximum rate the electric power up to about 60 kW; during this time the rods bursting is observed. Then the power is reduced to 3.5 kW, which is considered as the decay heat level. At the same time, the steam flow through the bundle is raised from 2 to 20 g/s, while keeping the Ar flow constant. The

experiments continue with the interruption of the steam supply and the quenching with water from the bottom of the bundle. The experiment ends after the bundle is completely filled with water.
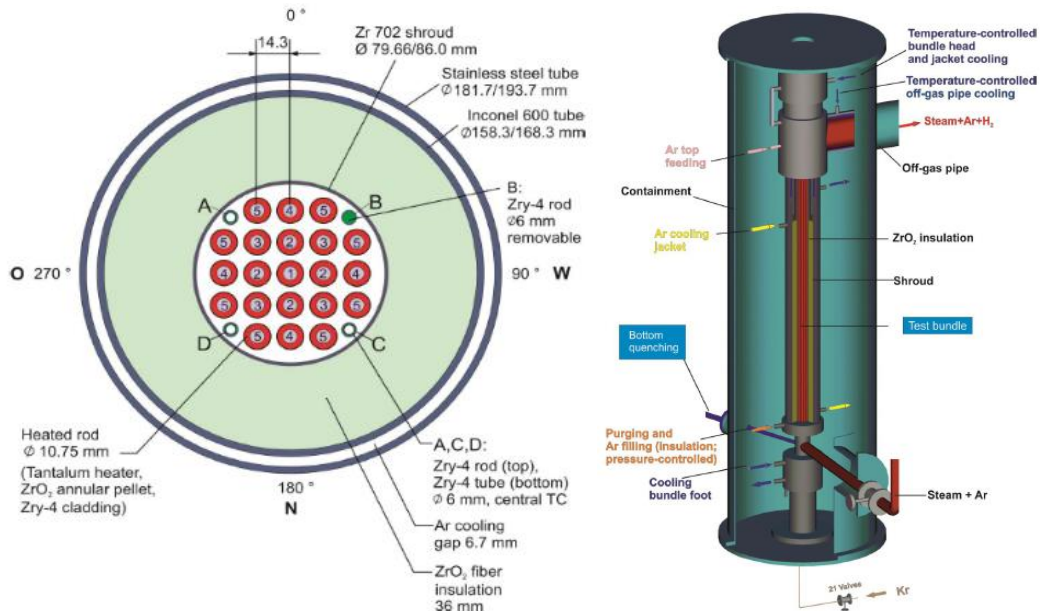
Fig. 47. (left) QUENCH-LOCA test section [167]
(right) QUENCH facility [167]

24.3 Measured parameters, PIE data

Five rods are equipped with more than 50 thermocouples at 17 different elevations (of which 10 within the heated region), attached on the cladding. The temperature is measured also on the shroud external wall, at the inner tube wall of the cooling jacket and on three corner rods.
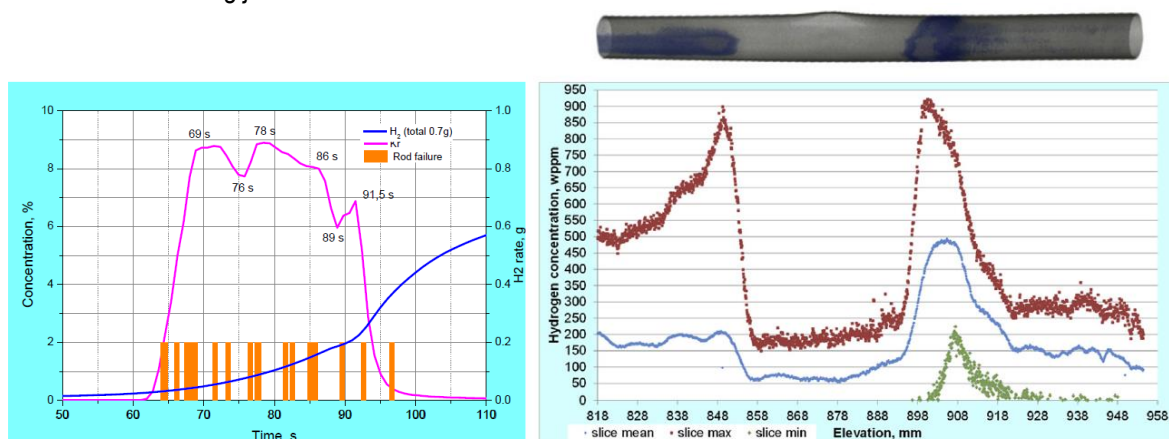
Fig. 48. (left) Outlet gas mass spectrometry in QUENCH-L1 experiment [167],
(right) hydrogen concentration in rod #1 of QUENCH-L2 bundle [173].

Outlet gas temperature and pressure (absolute and differential) are measured throughout the experiment. Steam, hydrogen and krypton content are also measured in the outlet gas through mass spectrometry (Fig. 48), and their mass is calculated based on the mass flow rate of the inlet argon, which is measured and regulated.

Detailed post-test examination of the experimental bundles is carried out in order to collect information on the clad diameter and burst position. Eddy current technique is used to investigate the oxidation degree of the rods cladding. Neutron radiography and X-ray diffractometry are employed to estimate the amount of absorbed

hydrogen into the structures, also including the secondary hydriding. Tensile tests are performed to determine the residual strength and ductility of the samples.

24.4 General conclusions

The QUENCH-LOCA provides experimental data for a number of LOCA-relevant phenomena, which can be used for validation of advanced system codes. The results show that coolability is always kept (even if coplanar ballooning is assumed), with a blockage ratio lower than 35%. In general, the observed peak cladding temperature is about 1350 K, and is reached at 950 mm elevation. Unsymmetrical ballooning has been observed, a phenomenon significantly affected by circumferential temperature gradient caused mostly by the non-coaxial positioning of pellets. The average burst temperature ranges from 1117±30 K for ZIRLO cladding to 1138±34 K for M5 ones. Larger burst size and strain are observed for Zircaloy cladding. Tensile tests at room temperature showed fracture at the hydrogen bands for several inner rods with maximum hydrogen concentrations at the fracture positions about 1500 wppm and more. During quenching, following the high-temperature test stages and starting at about 750 K no fragmentation of the claddings was observed: the residual strength and ductility were sufficient to prevent this.

24.5 References

[166]   *J. Stuckert, M. Große, C. Rössger, M. Steinbrück, M. Walter: Results of the commissioning bundle test QUENCH-L0 performed under LOCA conditions, QUENCH-LOCA-Report Nr. 1, SR-7571, Karsruhe, July 2018, https://doi.org/10.5445/IR/1000083018

[167]   *J. Stuckert, M. Große, C. Rössger, M. Steinbrück, M. Walter: Results of the reference bundle test QUENCH-L1 with Zircaloy-4 claddings performed under LOCA conditions, QUENCH-LOCA-Report Nr. 2, SR-7671, Karsruhe, July 2018, https://doi.org/10.5445/IR/1000083067

[168]   *J. Stuckert, M. Große, C. Rössger, M. Steinbrück, M. Walter: Results of the LOCA bundle test QUENCH-L2 with M5 claddings, QUENCH-LOCA-Report Nr. 3, SR-7677, Karsruhe, July 2018, https://doi.org/10.5445/IR/1000083069

[169]   *J. Stuckert, M. Große, C. Rössger, M. Steinbrück, M. Walter: Results of the LOCA bundle test QUENCH-L3 with optimised ZIRLO claddings, QUENCH-LOCA-Report Nr. 4, SR-7737, Karsruhe, July 2018, https://doi.org/10.5445/IR/1000083087

[170]   *J. Stuckert, M. Große, A. Pshenichnikov, C. Rössger, M. Steinbrück, M. Walter: Results of the LOCA bundle test QUENCH-L4 with pre-hydrogenated M5 claddings, QUENCH-LOCA-Report Nr. 5, SR-7712, Karsruhe, July 2018, https://doi.org/10.5445/IR/1000083094

[171]   *J. Stuckert, M. Große, C. Rössger, M. Steinbrück, M. Walter: Results of the LOCA bundle test QUENCH-L5 with pre-hydrogenated optimised ZIRLO cladding, QUENCH-LOCA-Report Nr. 6, SR-7738, Karsruhe, July 2018, https://doi.org/10.5445/IR/1000083098

[172]   J. Stuckert, M. Große, C. Rössger, M. Klimenkov, M. Steinbrück, M. Walter: QUENCH-LOCA program at KIT on secondary hydriding and results of the commissioning bundle test QUENCH-L0, Nuclear Engineering and Design 255, (2013) 185-201, https://doi.org/10.1016/j.nucengdes.2012.10.024

[173]   J. Stuckert, M. Große, M. Steinbrück, M. Walter, A. Wensauer, Results of the QUENCH-LOCA experimental program at KIT, Journal of Nuclear Materials 534, (2020), https://doi.org/10.1016/j.jnucmat.2020.152143

*available in the R2CA database

25. CODEX-LOCA integral tests

25.1 Objectives

The CODEX-LOCA test series was carried out in order to investigate the LOCA related phenomena for VVER type fuel. The test matrix included five tests with design basis accident conditions and scenarios with limited availability of ECCS. The experimental parameters covered the typical loss-of-coolant accidents for normal reactor operation, shutdown and wet storage in the spent fuel pool.

Table 22
The CODEX LOCA test matrix [174]

Test	Simulated conditions
CODEX-LOCA-200	200% large break LOCA with conservative conditions
CODEX-LOCA-E4	Shutdown LOCA with limited availability of emergency cooling water
CODEX-LOCA-200B	200% large break LOCA
CODEX-LOCA-SFP1	Spent fuel pool LOCA with steam starvation and with limited availability of emergency cooling water
CODEX-LOCA-SFP2	Spent fuel pool LOCA with unlimited steam and with limited availability of emergency cooling water

There were two main objectives in the CODEX-LOCA test series:
- Examination of cladding burst in scenarios close to design basis cases.
- Investigation of cladding oxidation and hydrogen uptake in high temperature steam and their consequences on the embrittlement of Zr alloys.

25.2 Tested materials, test facility

The accident conditions were simulated with seven electrically heated fuel rods in the CODEX (COre Degradation EXperiment) facility. In the LOCA test series the bundle included both traditional and sponge based, non-irradiated E110 type cladding tubes. The seven fuel rods were fixed by original VVER spacer grid in hexagonal geometry. The fuel rods could be pressurised, they were filled with alumina pellets and their lengths was 600 mm. The diameter and thickness of the cladding tubes were 9.1 mm and 0.69 mm respectively. The tungsten heater wires were placed into two holes in the ceramic pellets and electrical connections were needed only at the bottom of the rods. The tops of the cladding tubes were closed by welded Zr plugs. The test bundle was covered by a hexagonal Zr2.5%Nb shroud, insulation materials and a stainless steel tube

The CODEX-LOCA integral tests were started with heat-up to 600 °C and then stabilisation of temperatures at 600 °C in argon atmosphere. The further heat-up in steam atmosphere was performed by using appropriate high powers for the electrical heaters to follow the requested temperature history foe each simulated scenario. After the predetermined oxidation time at high temperature the bundle was cooled-down by water quench from the bottom of the bundle. The fuel rods were individually pressurised to different pressure values.

Detailed post-test examination of the experimental bundles was carried out in order to collect information on the degradation process and on the final state of the rods. Four-point bending type mechanical tests were carried out with the cladding tubes. prompt gamma-ray neutron activation imaging driven by neutron radiography and hot extraction methods were applied to characterize the axial hydrogen profile. Eddy current technique and laser profilometry were used to investigate the deformation of ballooned rods. The microstructure of the claddings was examined by metallography.

25.3 Measured parameters, PIE data

The measurement system recorded system and rod internal pressures, flowrates, values of input power, coolant inlet and outlet temperatures, water levels and rod temperatures. Several high temperature thermocouples were built into the fuel rods, shroud and insulation layers at different elevations. The temperature measurement uncertainty was ±0.4% for temperature values up to 1000 °C, while the pressure measurement uncertainty was ±1% for pressure values between 0 and 100 bar.
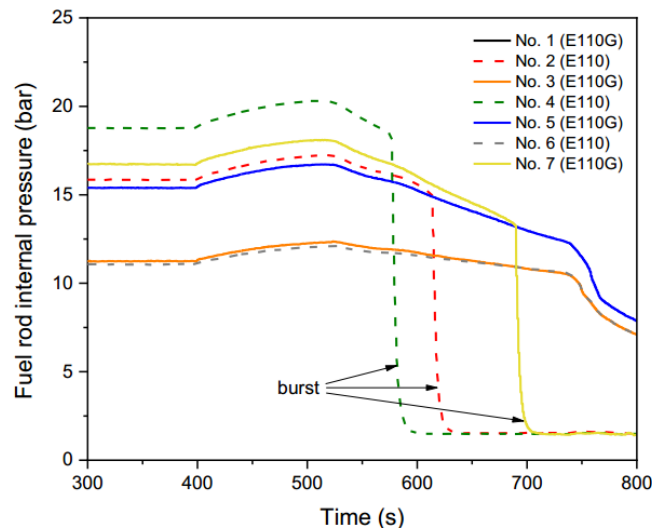
Fig. 49. Fuel rod internal pressure histories in the CODEX-LOCA-200 experiment [175]

Profilometry examinations pointed out that large deformations may take place even in those rods under high internal pressure, which did not burst during the high temperature experiment.

The hydrogen content in ballooned region showed the typical two peaks distribution only in case of long oxidation times. In several cladding tubes with short oxidation times only one peak was observed.

According to the four point bending tests the fuel rods after high temperature LOCA test still had significant load bearing capability and ductility in design basis accident scenarios.

25.4 General conclusions

From reactor safety point of view the burst of cladding in the design basis accidents was a key question. The two related experiments (CODEX-LOCA-200 and CODEX-LOCA-200B) showed that ballooning took place only in those fuel rods, in which the internal pressure exceeded 13 bars. Since in the reference case the high temperature rod had lower internal pressure it could be concluded for the VVER-440 reactor type the burst of fuel rods in the LOCA event has low probability

25.5 References

[174]   *Z. Hózer, I. Nagy, N. Vér, R. Farkas, M. Horváth, Z. Kis: Simulation of Loss-of-Coolant Accidents in
             the CODEX integral test facility, TopFuel, 2018, Prague, Paper A0133
[175]   *Z. Hózer, I. Nagy, R. Farkas, N. Vér, M. Horváth, T. Novotny, E. Perez-Feró, M. Király, Z. Kis, B. Maróti, L. Szentmiklósi, P. Holecz, Gy. Auguszt, Gy. Gémes: Experimental simulation of the behaviour of E110 claddings under accident conditions using electrically heated bundles, 19th Int. Symp. on Zirconium in the Nuclear Industry, May 20-23, 2019 Manchester, UK
[176]   *CODEX-LOCA-200.dat (database file)

[177]   *CODEX-LOCA-200-Power.dat (database file)
[178]   *CODEX-LOCA-200B.dat (database file)
[179]   *CODEX-LOCA-200B-stac150W.dat (database file)
[180]   *CODEX-LOCA-200B-stac300W.dat (database file)
[181]   *CODEX-LOCA-E4.dat (database file)
[182]   *CODEX-LOCA-E4-TCD.dat (database file)
[183]   *CODEX-LOCA-SFP1.dat (database file)
[184]   *CODEX-LOCA-SFP2.dat (database file)
*available in the R2CA database

26. PARAMETR tests

26.1 Objectives

The aims of the tests on the electrically heated PARAMETR facility and post-test examination of the bundles were the followings:

- investigation of the temperature-force loading parameters, corresponding to different thermal hydraulic LB-LOCA scenarios, influence on the assemblies damage characteristics;
- research of deformation behaviour of the fuel rod simulator claddings gathered in an assembly and their depressurization parameters (temperature, pressure, deformations and coordinates of places of rupture);
- definition of the FA cross section blockage and cladding balloonings distribution along the assembly height.

Verification of the codes used to design VVER-type reactors was an important goal of the integral experiments. The results of the experiments presented are used for verification of the RAPTA-5 code.

26.2 Tested materials, test facility

The PARAMETR test facility was designed to investigate fuel rod behaviour under LOCA and non-LOCA conditions. Power release in experimental fuel rod is simulated by electrode (tungsten or tantalum), which is fixed at the center of fuel pellet (UO_2).The axial power profile is simulated by a variable cross-section of electrode. The galvanic separation between fuel and heater is realized in experimental fuel rod. This allows to exclude contact of heater element with fuel rod cladding and to maintain the construction operability up to cladding temperature of 1800 °C. In the experimental series 19-rod, 37-rod bundles and single rods were tested

The fuel assembly is placed in a hexagonal Zr1%Nb shroud with thermal insulation of porous ZrO_2. In the 37-element assembly the central simulator and 12 simulators of the second row are passive, while 6 simulators of the first row and 18 of the fourth are electro-heated by means of the central tungsten electrode.

The systems of coolant delivery provide the steam, superheated, heated argon (different combinations are available) supply to the test section with specified flow rate. There are systems of quenching from top and from bottom, which provide the water delivery with controlled flow rate. The facility is equipped with systems of discrete and continuous control of gas mixture composition at the outlet. The gas supply systems allow setting the internal pressure in fuel rod up to 10 MPa, the pressure in test section up to 16 MPa. The pressure can vary during the test according to a given algorithm.

The rods have active length of 300 mm, 600 mm and 1275 mm for tests simulating in following transients: non-LOCA, the first stage of LOCA, the second stage of LOCA, respectively. The cladding materials included traditional and sponge based E110 and E635 zirconium alloys. The test matrix is given in Table 23.

Table 23
Experiments on the PARAMETR test facility

№	Year	Alloy	Number of fuel rods	Accident stage	Coolant (flow rate, g/s)	Heating rate, K/s	Tmax, °C	Holding time, s	Reflood (flow rate, g/s)
1	1999	E110	19	II	Steam (4)	1,5-2,0	1100	30	-
2	1999	E635	19	II	Steam (4)	1,0-1,5	1200	400	-
3	1999	E110	19	II	Steam (4)	0,2-0,3	900	180	Bottom (50)
4	2000	E110	37	II	Steam (8)	0,4-0,5	1200	100	Bottom (30)
5	2000	E635	37	II	Steam (6)	1,5-2,2	900	90	Bottom (30)
6	2001	E635	37	II	Steam (6)	1,4-1,8	900	90	Bottom (80)
7	2001	E110	37	II	Steam (6)	3,0-4,0	850	100	Bottom (80)

8	2002	E110	37	II	Steam (6)	1,5-3,5	1010	150	Bottom (50)
9	2002	E635	37	II	Steam (6)	2,5-3,5	1100	100	Bottom (50)
10	2003	E635	37	II	Steam (8)	1,5-2,5	1040	100	Bottom (80)
11	2003	E110	1 (all 6)	I	Argon	80-100	850-950	8-9	Bottom (60)
12	2003	E110	37	II	Steam (8)	1,5-2,5	950	100	Bottom (80)
13	2004	E110	37	II	Steam (8)	2,0-3,0	1020	40	Bottom (30)
14	2004	E110	1 (all 6)	I	Argon	80-90	950	1-4	Bottom (160)
15	2004	E110*	37	II	Steam (8)	2,5-4,0	950	90	Bottom (30)
16	2005	E110[1]	19	II	Steam (4)	2,0-2,5	1080	120	Bottom (75)
17	2005	E110	19	II	Steam (4)	2,4-2,7	1230	80	Bottom (75)
18	2005	E110	1 (all 4)	I	Argon	80-90	800–1200	5	Top (40)
19	2005	E110	1 (all 2)	I, II	Steam (0,06)	80 / 2,0-3,0	800-900 / 950-1000	5	Top (40)
20	2006	E110[1,2]	19	II	Steam (4)	2,0-2,7	1100	100	Bottom (100)
21	2006	E110[1,2]	1 (all 9)	I	Argon	80-90	860–1060	5	Top (40)
22	2006	E635M[1]	19	II	Steam (4)	2,0-2,2	1070	70	Bottom (102)
23	2007	E110[1]	19	II	Steam (4)	2,5	1000	70	Bottom (130)
24	2007	E110[1,3]	1 (all 7)	I	Argon	50-120	800-1000	5	Top (80)
25	2008	E110[1,3]	25	II	Steam (4)	4	1100	200	Bottom (80)
26	2008	E110[1,3]	25	II	Steam (4)	4	1100	150	Bottom (80)

* – thermal treatment by the temperature regime of the 1st stage [190]
[1] – sponge base
[2] – ∅9.1×7.93 mm
[3] – ∅9.5×8.33 mm

26.3 Measured parameters, PIE data

The data acquisition and recording system has 576 measuring channels. During test the following parameters are controlled:
- temperatures of the fuel rod claddings, spacer grids, shrouds (120 thermocouples);
- internal pressure in fuel rods;
- pressure and temperature of coolant at test section inlet and outlet.

Depending on the experiment conditions (mainly it is heating rate) the temperature measurements are carried out by the thermocouples with covers, which are clamped to cladding surface at a given elevation, or the thermocouples without covers, with electrodes directly welded to the cladding.

After the experiments the FAs are dismantled and the claddings cross-section perimeters are measured.
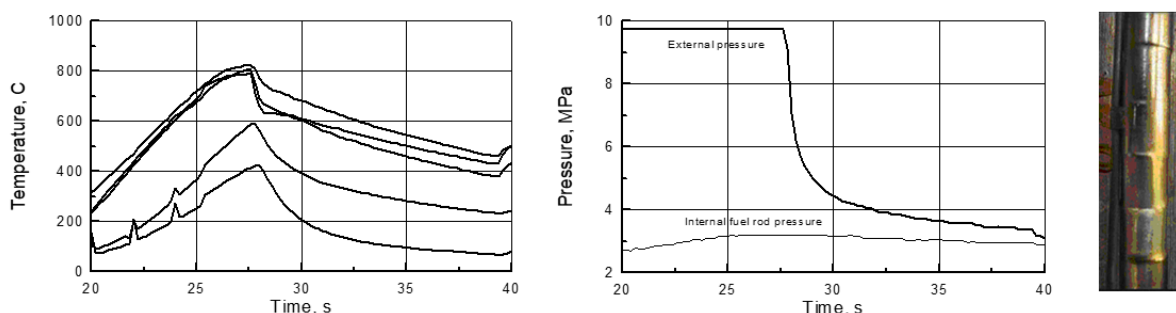
Fig. 50.Temperature (left) and pressure (center) histories leading to cladding collapse(right) [189]
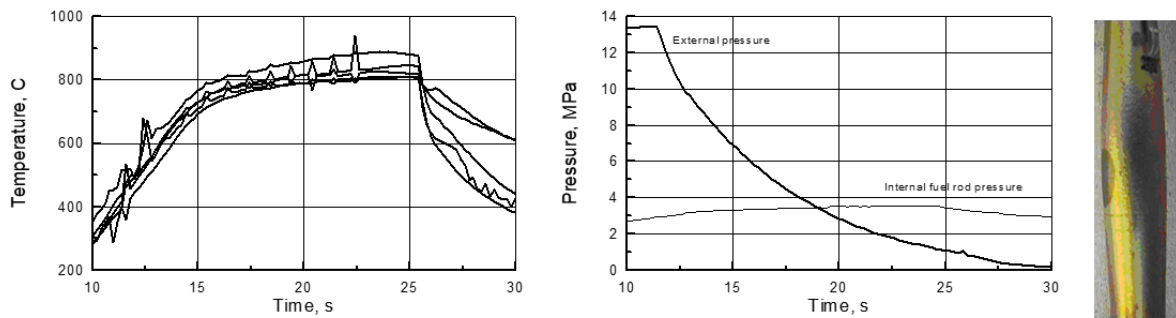
Fig. 51.Temperature (left) and pressure (center) histories leading to cladding burst (right) [189]

26.4 General conclusions

The testing of experimental fuel rod assemblies with Ze1%Nb-alloy claddings has been made for representative group of heat-stressed fuel rods of reactor VVER-1000 type on electrically heated PARAMETR facility under LOCA simulating conditions.

Cladding rupture of fuel rods took place at heating-up stage within the temperature interval 800-900 °C. Cladding collapse (negative deformation) due to high external pressure was also demonstrated. There were identified the basic cladding deformation and rupture parameters: temperature, pressure, axial distribution of hoop strain, and azimuthal distributions of radial deformation in rupture section. The cross section blockage in the assembly under testing was below 38%.

26.5 References

[185]   *Nuclear Fuel Behaviour in Loss-of-coolant Accident (LOCA) Conditions, State-of-the-art Report, OECD 2009 NEA No. 6846
[186]   *Fuel behaviour under transient and LOCA conditions, Proceedings of a Technical Committee meeting held in Halden, Norway, 10–14 September 2001, IAEA-TECDOC-1320, Part 1
[187]   *Fuel behaviour under transient and LOCA conditions, Proceedings of a Technical Committee meeting held in Halden, Norway, 10–14 September 2001, IAEA-TECDOC-1320, Part 2
[188]   *Salatov, A.V., Fedotov, P.V., Afanasyev, P.G., Deniskin, V.P, Konstantinov, V.S, Nalivaev, V.I., Parshin, N. Ja., Popov, E.B., Fedik I.I., Semishkin V.P, Shumsky, A.M., "Modeling of behaviour of 37 fuel rod assembly with Zr1%Nb-alloy simulators cladding under loss-of-coolant accident conditions on PARAMETR-M facility", Proceedings of the Fifth International Conference: WWER Fuel Performance, Modelling and Experimental Support, 29 September - 3 October 2003, Albena, Bulgaria
[189]   *Fedotov, P.V., Nechaeva, O.A., Novikov, V.V., Salatov, A.V., Alekseev A.V, Goryachev, A.V., Kiseleva, I.V, Kuzmin, I.V., Shulimov V.N., Konstantinov, V.S, Nalivaev, V.I., Gukov, V.M, Donnikov, V.E., Latunin, V.I., "Studies of VVER fuel rods behaviour under LOCA condition, current status", Ad-hoc LOCA meeting. NEA Headquarters, Le Seine Saint-Germain, France, 27th - 28th June 2006
[190]   Nuclear Fuel Behaviour in Loss-of-coolant Accident (LOCA) Conditions, State-of-the-art Report, OECD 2018 (in publication process)
*available in the R2CA database

27. Halden FGR tests

27.1 Objectives

The objective of Halden FGR experiments was to study fission gas release in commercial fuels, to assess the data demonstrating the effect of different factors on the amount of fission gas release from UO2 fuel and determining the thermal FGR threshold, which may limit fuel operational power with burn-up increase [191], [192], [193].

27.2 Tested materials, test facility

Halden Reactor Project (HBWR) is a natural-circulation boiling water reactor cooled with heavy water. HBWR contains special water circulation loops to pressure flasks mounted inside the reactor, into which instrumented test rigs are mounted. These loops employ equipment such as electric heaters and coolers, pressurizers, and purifiers (Fig. 52). The Halden reactor has 11 such loops. Test rigs consist of fuel or material samples attached to equipment [194]. Fission gas release (FGR) tests were one type of long-term fuel tests that had been carried out at HBWR [195].
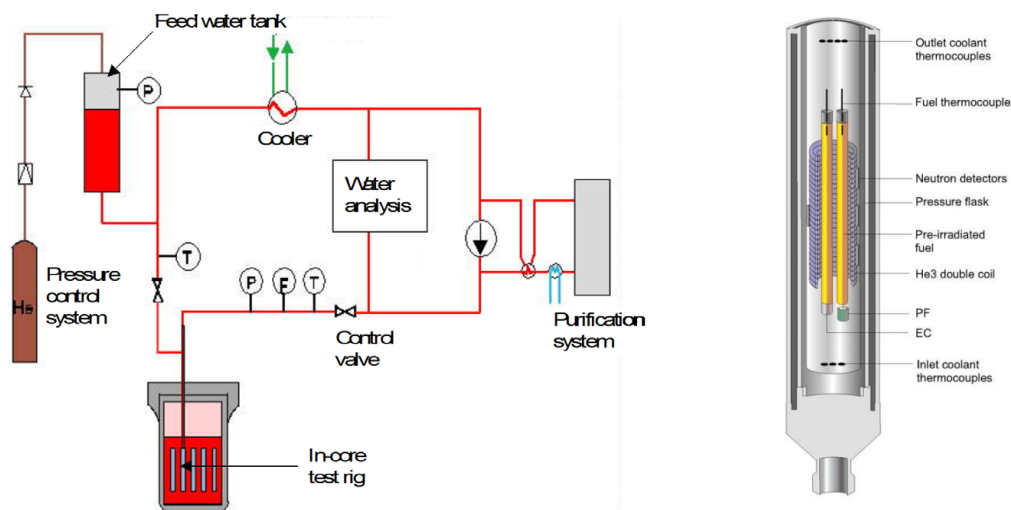
Fig. 52. Loop systems in the Halden reactor (left) [195] and Test rig for determination of FGR threshold (right) [193]

The most common rig for FGR tests contains refabricated rods pre-irradiated in a commercial NPP. The rods are instrumented with a pressure transducer or a cladding elongation detector in one end and with fuel thermocouples in other end. The rod instrumentation allows FGR to be detected at the moment, and at the fuel center temperature, at which it occurs. The rig is designed and produced with He-3 coil surrounding the test channel in order to control the power of the test fuel assembly independent of the reactor power.

The test was usually performed with a step-wise increase in fuel temperature, with steps of around 50 °C held for 12-24 hours to allow the fission gases to be thermally activated and released if the thermal threshold is exceeded [193].

In addition, power / fuel temperature reductions were usually performed at the end of each hold period in order to ensure that all gas released during the preceding power/temperature period, but trapped due to tight fuel-clad contact or within fuel cracks, actually reached the pressure detector that was positioned in the fuel rod plenum.

27.3 Measured parameters, PIE data

The typical results of the in-pile measurements during the test are shown in Fig. 53. Data obtained in Halden for higher burnups show that the temperature of fission gas release onset exhibits a decreasing trend, as also shown in Fig. 53 [193].
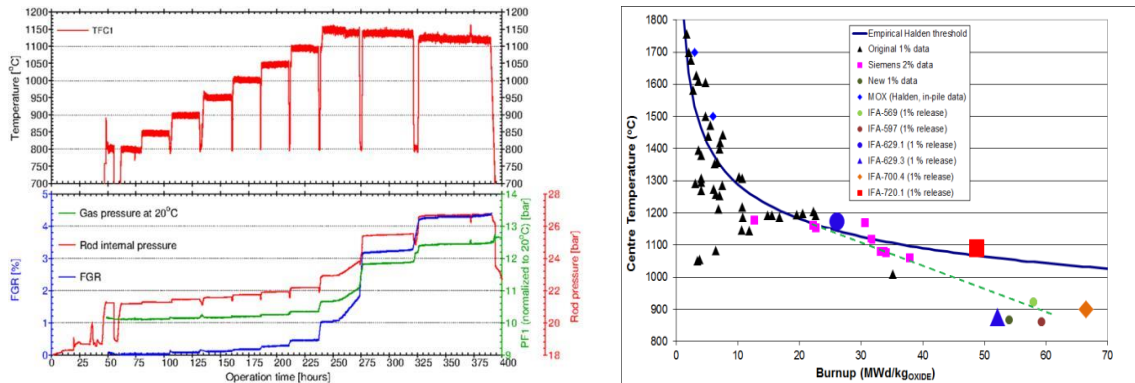
Fig. 53. Typical in-pile measurements for FGR threshold determination (left) [193] and thermal FGR Vitanza threshold vs fuel burnup (right) [193]

The potential for fission gas release increases with increasing burnup, and it is therefore attempted to produce fuel with good retention properties. One such attempt was fuel with increased grain size, and several comparative experiments had been conducted in the Halden Reactor to test this effect. The example shown in Fig. 54 demonstrates that an increased grain size may in fact be effective in minimising fission gas release. From the evaluation of this and several similar comparative tests, one of them with a final burnup of 85 MWd/kgUO2, it appears that large grains are most effective at modest powers and a release fraction of ≤ 10% [196].
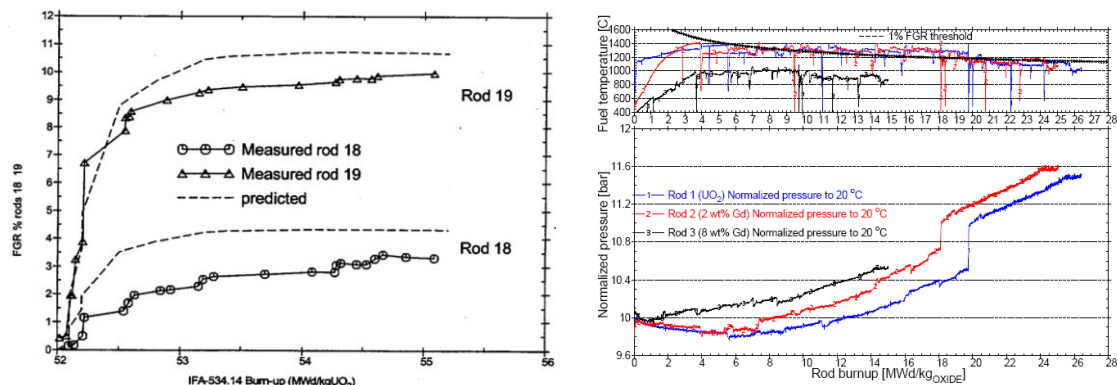
Fig. 54. The effect of grain size during power ramping at ~52 MWd/kgUO$_2$ (left) [196] and testing thermo-mechanical and FGR behaviour of different fuels with Gd-additive [195]

27.4 General conclusions

It should be noted that the thermal FGR threshold may be dependent on fuel type (UO2 or MOX, Gd-doped) but independent of fuel design (PWR, BWR and VVER).

The so-called Vitanza threshold and the trend obtained with additional data represent a valuable knowledge base when it comes to controlling experiments in such a way that fission gas release is avoided or provoked.

Analysis of experiments where FGR from different grain size material is compared shows that particularly at high power, FGR may be affected by grain growth of the smaller grain material, thus influencing the conclusions regarding the benefits or otherwise of advanced fuels.

27.5 References

[191]   *SECY-99-290. William D. Travers. NRC plants to participate in the OECD Halden reactor project during 2000-2002. https://www.nrc.gov/docs/ML0036/ML003675460.pdf.

[192]   *Seminar Proceedings Cadarache, France 26-29 September 2000. Fission Gas Behaviour In Water Reactor Fuels. Nuclear Energy Agency Organisation For Economic Co-Operation And Development. https://www.oecd-nea.org/science/pubs/2002/3053-fission-gas-behaviour.pdf.

[193]   *Boris Volkov, Wolfgang Wiesenack, M. McGrath, T. Tverberg. Halden Fuel and Material Experiments Beyond Operational and Safety Limits. Proceedings of WRFPM 2014 : 2014 Water Reactor Fuel Performance Meeting, Top Fuel, LWR Fuel Performance Meeting, 14 - 17 September 2014, Sendai, Japan. https://pdfs.semanticscholar.org/eb77/384bc9a249ac0aff500acae9da32de1e860a.pdf.

[194]   Halden research reactor: 54 years young. https://www.neimagazine.com/features/featurehalden-research-reactor-4175370/.

[195]   *IFE and OECD Halden Reactor Project - Experimental Capabilities. https://gain.inl.gov/SiteAssets/Fuel%20Safety%20Presentations/19%20McGrath%20-%20Halden%20Reactor%20Project.pdf.

[196]   *Yvonne Broy, Wolfgang Wiesenack, Lise A. Moen. The OECD Halden reactor project - international research on safety and reliability of nuclear power generation. https://inis.iaea.org/collection/NCLCollectionStore/_Public/33/011/33011198.pdf.

*available in the R2CA database

28. FIRST-Nuclides leaching tests

28.1 Objective

A common experimental program was set up by a group of laboratories, in the framework of the FP7 Collaborative Project FIRST-Nuclides (Fast/Instant Release of Safety Relevant Radionuclides from Spent Nuclear Fuel) in 2012-2014. The experimental investigations included the gas release, rim and grain boundary diffusion processes, and leach tests, for quantification of the fast release of activation and fission products into the aqueous phase.

28.2 Tested materials, test facility

The leach tests were performed with well characterized spent nuclear fuel samples by Karlsruhe Institute of Technology (KIT) Germany, Joint Research Centre (the formerly called Institute for Transuranium Elements , ITU), Paul Scherrer Institut (PSI) Switzerland, Studiecentrum voor Kernenergie - Centre d'Etude de l 'energie Nucleaire (SCK·CEN) Belgium, Fundacio Centre Tecnologic de Manresa (CTM) Spain, and Studsvik Nuclear AB (STUDSVIK) Sweden. The leach tests were performed with fuels from pressurized water reactors or Boiling Water Reactors (BWR) with average rod burn-ups ranging from 42 to 63 GWd/tHM. The leach tests were complemented by analysis of release rates of relevant radioisotopes from damaged and leaking VVER fuel elements which were irradiated in the Hungarian nuclear power plant.

Leaching tests were done with samples from various UO_2 fuels and one type of MOX fuel, irradiated either in PWR's or BWR's. The fuel samples for the leach tests were prepared as follows:
- Fuel segments with their cladding were cut from the fuel rods.
- The cladding of segments was opened and separated from the fuel fragments but leached together with them.
- mm size fuel fragments were separated and leached without cladding.
- Small size (10 to 90 μm) fuel powder was leached without cladding.

The prepared fuel samples were immersed in a leachant, consisting of 19 mM NaCl and 1 mM $NaHCO_3$. Studsvik used a slightly different composition (10 mM NaCl and 2 mM $NaHCO_3$). Most of the tests was performed in oxidizing (aerobic) conditions. Test typical durations was 1 year.

28.3 Measured parameters, PIE data

The leachates were analysed for a number of radionuclides, depending on the techniques available in the participating laboratories. All laboratories provided measurements for caesium and most of them also for iodine. Several laboratories measured additional elements/radioisotopes, such as ^{14}C, Se, Sr, Tc, Pd, Sn, Mo, and Rb.

28.4 General conclusions

The FIRST-Nuclides project has extended the experimental database on the fast release by leach tests with BWR and PWR spent nuclear fuels. The fast release of iodine and caesium is comprised mainly in the range below the FGR (for I) or below 0.6 FGR (for Cs), in agreement with theoretical considerations. The contribution of oxidative fuel matrix dissolution as measured by the U concentrations in the leachates was relatively small. The existence of a continuous fission gas release mechanism and parallel iodine release mechanism during the leaching was demonstrated. The caesium and iodine release in the leaching experiments could be qualitatively correlated to the exposed surface areas. Closure of the fuel-cladding gap slows down the release.
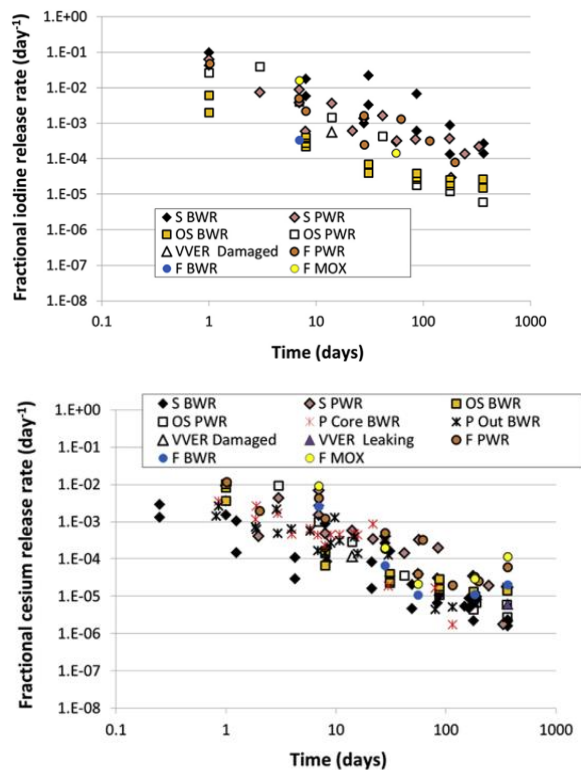
Fig. 55. Fractional release rates of iodine (left) and caesium (right) for leach tests of FIRST-Nuclides project as a function of time (S: clad fuel Segment, OS: Opened Segment, F:Fragment, data for the damaged and leaking VVER fuel are also included)

28.5 References

[197]   *K. Lemmens, E. Gonzalez-Robles, B. Kienzler, E. Curti, D. Serrano-Purroy, R. Sureda, A. Martínez-Torrents, O. Roth, E. Slonszki, T. Mennecart, I. Günther-Leopold, Z. Hózer: Instant release of fission products in leaching experiments with high burnup nuclear fuels in the framework of the Euratom project FIRST- Nuclides, Journal of Nuclear Materials 484 (2017) 307e323

[198]   *Final Workshop Proceedings of the Collaborative Project „Fast / Instant Release of Safety Relevant Radionuclides from Spent Nuclear Fuel", Karlsruhe 01 - 02 September 2014, KIT Scientific Reports 7716

[199]   * V. Metz et al.:Characterisation of spent nuclear fuel samples to be used in FIRST-Nuclides – relevance of samples for the Safety Case, Deliverable No: 1.1 (2013)

[200]   * V. Metz et al.: Characterisation of spent nuclear fuel samples and description of methodologies and tools to be applied in FIRST-Nuclides, Deliverable No: 1.2 (2013)

*available in the R2CA database

29. MTA EK H uptake tests

29.1 Objective

The objective of the test series was the creation of experimental data for computer codes to simulate H uptake inside of a defective fuel rod in a nuclear reactor under normal operational conditions.

29.2 Tested materials, test facility

The experimental set-up used for hydrogenation of Zr claddings is a high temperature three-zone tube furnace attached to a vacuum system. Half of a long, on one end sealed quartz tube was heated by a three zone tube furnace at constant temperature, while the other half was joined to a vacuum pump with a calibrated volume inlet system. The pressure of the gas system was controlled with a Vacuubrand type DVR 5 pressure gauge.

In the first series traditional and sponge based E110 samples were charged at different temperatures close to reactor operation. In the second series Zircaloy.4 cladding will be also investigated and the temperature ranges will be extended.
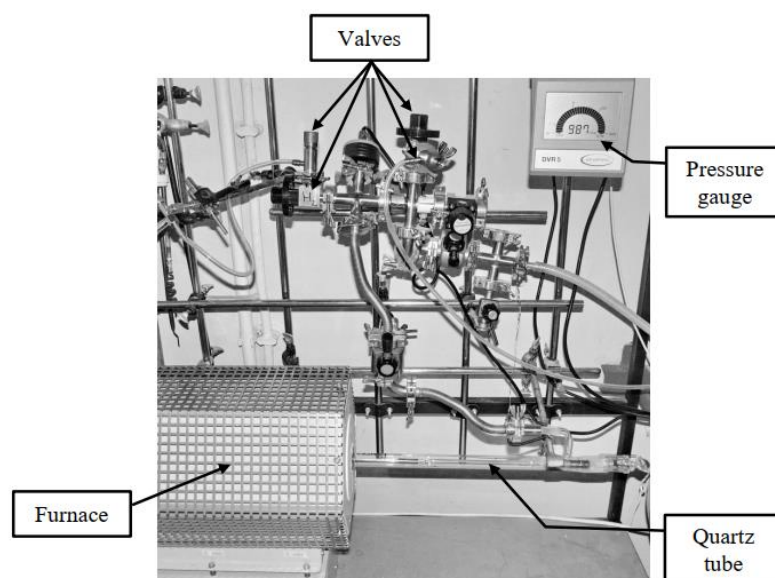
Fig. 56. View the facility used for H charging Zr samples [201]

29.3 Measured parameters, PIE data

Before the absorption, the mass of the samples was measured and the initial pressure of hydrogen was calculated. The samples on the sample holder were placed in the cold part of the furnace. The system was uploaded with high purity hydrogen and it was completed with high purity argon gas, and then the sample was inserted into the hot furnace with a strong magnet.

The pressure was monitored online with PC. At the end of the H-uptake (it was evaluated on the basis of the pressure change) the sample was pulled to the cold part of the quartz tube by magnet.

The hydrogen concentrations of the specimens were determined from the changes in the hydrogen pressure and from the mass gained after the hydrogenation without the destruction of the samples. The verification of the absorbed hydrogen content measurement was carried out by hot extraction method and with scanning electron microscope (SEM) as well.
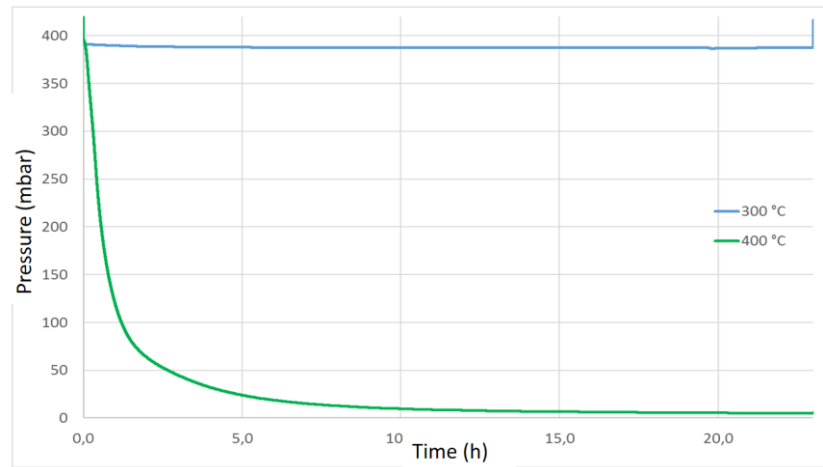
Fig. 57. Change of pressure in the H charging facility at 300 °C and 400 °C [201]

29.4 General conclusions

The provided data (pressure histories at different temperatures and measurement of H content of the specimens) facilitates the development of H uptake models. The data showed acceleration of H uptake above 300 °C.

29.5 References

[201]   *Novotny T., Perez-Feró E., Horváth L.: Hydrogenation and high temperature oxidation of zirconium claddings, Proceedings of the 11th International conference on WWER fuel performance, modelling and experimental support. 2015., Varna, pp. 364-369

*available in the R2CA database

30. DEFECT tests with defective fuel rods

30.1 Objective

The release of fission products from irradiated UO_2 into the fuel-clad gap of a sound rod has been studied extensively, both theoretically and experimentally. By contrast very little is known about the behaviour within a defective rod, where the pressure of water or steam in the gap may modify the processes of release from the fuel, through the defect, to the coolant.

A series of loop experiments have been performed on short fuel rods by CEA in France with the aim of measuring and interpreting the release rate of fission gases and iodine under a range of experimental conditions of linear power, defect type, gap dimensions etc. The results from these experiments, which cover steady state and transient power operation on new and pre-irradiated fuel, provide invaluable data for modelling the escape of fission products from defective fuel rods. In a commercial reactor, such modelling is important for assessing the occurrence and characteristics of defective fuel from analysis of coolant activity. Knowledge of the presence of defective fuel can eliminate the need for premature shut down of the reactor and also minimizes outage time, thus improving the safety and economics of power generation.

The experiments were all performed in the Siloe reactor in one of two water loops called Bouffon and Jet Pompe.

30.2 Tested materials, test facility

The Bouffon loop consists of two vertical tubes connected at both ends to form a continuous circuit for pressurized water. The experimental fuel rod is situated in the bottom of one tube below a heater which provides an up current of water and hence by thermosyphoning, a flow of cooling water over the experimental fuel rod.

The Jet Pompe loop comprises two co-axial vertical tubes. The experimental fuel rod is situated in the inner tube and coolant flow over it is provided by a steam injector pump at the bottom of the same tube. The steam at 400 °C and 35 bars is obtained from a steam generator installed elsewhere in the rig.

Table 24
Conditions of both loops of the SILOE facility [202]

Parameters	Bouffon boiling flow	Jet Pompe pressurized water
Channel diameter (mm)	29.5	38
Fuel rod length (мм)	350	500
Number of rods	1	1 or 4
Max length of fuel rods (mm)	400	1200
Max surface power (W/cm^2)	233	165
Circuit volume (l)	4.2	3.7
Flow rate (m^3/hr)	0.3	1.1
Clean up rate (l/hr)	2.6	34
Rod inlet temperature (^{0}C)	150	280
Rod outlet temperature (^{0}C)	150	up to saturation temperature
Pressure (bar)	130	130

The CEA Defect Fuel experiments are CYFON 1, CYFON 2, EDITH 1, EDITH 2, EDITH 5, CRUSIFON 1BIS, CRUSIFON 1 and CRUSIFON 5.

The CYFON experimental series investigated the release of fission products from failed fuel rods during variable power/load following. In the EDITH series period of power variations was increased in order to approach the steady state release. The CRUSIFON series investigated the behaviour of fuel rods which were initially intact but artificially defected during irradiation in Siloe.

The geometry of the fuel rods complies with the 17 x 17 design specification with small modifications to the fuel-to-cladding gap.

Table 25
.DEFECT-FUEL Experimental Matrix [203]

Experiment	Loop	Objective	LHR KW/m	Type of rupture	Burn-up MWd/kgU	SILOE cycles
CYFON 01	Bouffon	FP release Rupture during load following	40-30	Hole at level of plenum	2.6	2
CYFON 02	Bouffon	FP release Rupture during load following	40-12	Hole at level of plenum	4.0	2
EDITH 01	Bouffon	FP source term Steady power Pre-defected	20-40	Simulated manufacturing defect at level Of plenum	4-5.4	3
EDITH 02	Jet Pompe	FP source term Steady power Pre-defected rod	10-30	Simulated manufacturing defect at level of plenum	<2.0	3
EDITH 05	Jet Pompe	FP source term Steady power pre-defected rod	10-30	Very thin crack at level of fuel PCI type defect	<5.0	2
CRUSIFON 1bis	Bouffon	FP source term Steady power Defected during operation	40	Mechanically induced, fine crack at level of fuel	~5.0	4
CRUSIFON 2bis	Bouffon	FP source term Steady power Defected during operation	38	Mechanically induced large defect at level of fuel	1.0	1
CRUSOFON 5	Bouffon	FP source term Steady power Defected during operation	23	Multiple defects induced by PCI at level of fuel	20-27	7

30.3 Measured parameters, PIE data

Evaluation of the fission products concentrations has been performed during the irradiation. PIE have also been performed on each sample to focus on the failed part of the sample.

30.4 General conclusions

The thermalhydraulic conditions in the fuel gap have to be considered and analysed: at intermediate powers (15-17 kW/m): a transition between liquid-filled and steam-filled gap can occur, leading to an unstable thermalhydraulic regime and very high release rates. This critical regime is less important for small defects as the input or output of water is then a slow process. For a slight increase in linear power, corresponding to a shift from liquid gap to steam gap, the release rate is drastically reduced. In the case of a power cycling regime, the fission products may be washed by the water and lead to activity release peaks during power increase or decrease, depending on the cycling levels with respect to the critical regime [205].

On the basis of experiments EDITH and CRUSIFON, dedicated to FGR from a defective fuel rod, a release rate for the analysis of power plants contamination was recommended in [204].

30.5 References

Most of the DEFECT reports are in French and they are available in the IFPE database, which can not be shared with all partners involved in the project.

[202]   Likhanskii V.V et al. Verification of the RTOP-CA code against the OECD/NEA/IAEA IFPE database on activity release from defective fuel rods.
[203]   IFPE Database. http://www.nea.fr/abs/html/nea-1615.html
[204]   Seveon, H., Leuthrot, C, Stora, J.P., Chenebault, P., Hari.Op, R., Release of Fission Products by Defective Pressurized Hater Reactor Fuel - international Conference in Thermal Reactor Safety, Karlsruhe (September 10-13, 1984)
[205]   International Working Group On Water Reactor Fuel Performance And Technology, Fuel Rod Internal Chemistry And Fission Products Behaviour, IWGFPT/25, 1986

31. DEFEX secondary defect tests

31.1 Objective

A total of 20 tests have been performed in the R2 reactor with the aim to study secondary hydriding of cladding caused by water from a simulated primary defect in test rodlets of 8x8 BWR design. Three kinds of Zircaloy-2 cladding have been compared, namely standard cladding, cladding with unalloyed zirconium liner and so called rifled cladding, which is a proposed remedy.

From 1990 to 1993 seven tests with previously unirradiated fuel were run in two exploratory test series, DEF-I and DEF-2. With the results from these tests the DEFEX Project was conducted in international co-operation between 1993 and 1995, aiming at the study of secondary defect formation as a consequence of primary defects. A total of 11 tests on unirradiated fuel were carried out within the DEFEX program. In these DEF and DEFEX tests, the intrusion of water through the primary defect was simulated by applying an open water reservoir in an extended plenum on top of the rodlet [207], [209].

The objectives of the exploratory two DEF Projects were the demonstration of the experimental technique applied to different types of cladding. In the DEFEX Project the aim was further elaborated to be investigation of phenomena and design parameters relevant to the degradation process in defected fuel. In particular, the collected data should be used for modelling of defect fuel behaviour, thus providing a theoretical and experimental basis for further testing of potential remedies In the DEF and DEFEX tests Zircaloy-2 standard and liner cladding were compared to rifled cladding, the latter being characterized by the polygonal shape of the bore cross-section, which is intended to prevent secondary hydriding by facilitating axial gas communication.

In 1996 two more DEFEX II DEMO tests on irradiated fuel with medium burnup were made with a modified test method in order to better simulate defection of a rod during operation. The water was contained in a closed ampoule in the extended plenum, and the ampoule was made to burst when the test rodlet had been irradiated at full power for a predetermined period of time [208], [209].

These two tests have been performed at the R2 reactor with the aim of demonstrating a technique for simulating a primary defect and the conditions leading to secondary failure of the cladding by hydriding. In the tests, steam was introduced into the rodlets at power. Upon detection of failure of the cladding, the linear heat rate was increased in two steps. These two tests also aimed at accomplishing cracks propagating from hydrided regions in standard Zircaloy-2 cladding. Destructive investigation of the cracks would give information on the mechanism for crack propagation in irradiated cladding [206].

31.2 Tested materials, test facility

For DEF-I, DEF-II and DEFEX, the experiments were made in the R2 test reactor using a special simulation technique for the primary defects. Test rodlets typical of 8x8 BWR fuel with three different types of Zircaloy-2 cladding were investigated in a total of eleven tests. Standard cladding was compared to zirconium liner cladding as well as to rifled cladding, which has been proposed as a remedy against secondary failure by hydriding. Linear Heat Rate, pellet - clad gap and irradiation time were the principal test parameters. The rodlets were previously unirradiated.

For DEFEX II DEMO, the two test rodlets were refabricated from a segment rod, which had obtained a burnup of around 25 MWd/kgU in the Ringhals-1 BWR plant.
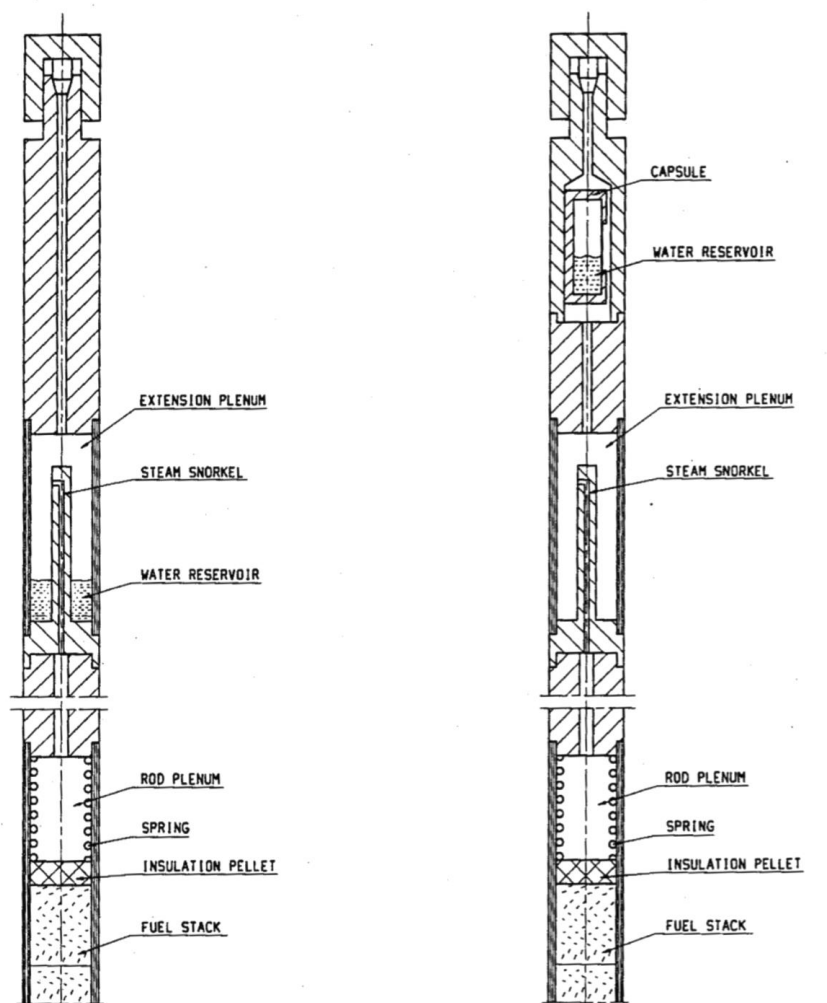
Fig. 58. Experimental test rodlets for simulating defective fuel rod in DEF and DEFEX program (left) and the DEFEX II DEMO (right)

31.3 Measured parameters, PIE data

The non-destructive measurements that were made include on-line elongation measurement, profilometry measurement, eddy current scanning, neutron radiography, gamma scanning, visual inspection and gap squeeze measurement.

Destructive examinations included metallography, fuel grain size measurements, determination of fuel porosity distribution, cladding hydrogen determination by SEM, Electron Probe Micro Analysis in one case, mass spectrometry of residual gas and UO2 oxidation determination by X-ray powder diffraction.

For DEFEX II DEMO, neutron radiography and profilometry before and after irradiation were used in order to determine hydride blisters, defects and dimensional changes. The defects were further examined visually. Gamma scanning showed the distribution of fission products.

31.4 General conclusions

Four of the DEFEX test rodlets, all with 0.15 micron gap but with different types of cladding, failed in conjunction with extensive hydriding at Linear Heat Rates of 40 and 50 kW/m. For three of these rodlets, with standard and rifled cladding, time to failure varied between 76 and 102 hours. The fourth rodlet, with liner cladding, failed after 216 hours. The hydriding degradation process could be followed by studying the elongation curve. It was observed that those rodlets that failed early exhibited a steeper increase after the initial features than those that did not fail. This fact is ascribed to intensive hydriding of the cladding. For the liner rodlet, which remained intact for the longest time, the elongation curve had a similar shape in the beginning, but after two days' irradiation it levelled off. The ensuing elongation is ascribed to the influence of irradiation growth.

The oxidation behavior of the rodlets with liner cladding and those with standard cladding was not very different at the low burnups of the DEFEX Project. However, the liner cladding showed less hydrogen pick-up than the standard cladding.

The two DEFEX II DEMO rodlets were operated at different linear heat ratings: 35 and 40 kW/m, respectively. Rodlet No. 1 failed at the bottom weld. The resulting crack had propagated in a direction which was mainly circumferential. Rodlet No. 2 failed with three axially oriented cracks emanating from local hydride concentrations. SEM examinations of fracture surfaces from both rodlets revealed a brittle fracture with almost no signs of ductile fracture. The cracks were seen to have propagated both radially and axially from the outside of the cladding. All macroscopic features seen in the examined axial crack of rodlet No. 2 have previously been observed in failed power reactor rods with long axial splits. The cracking mechanism of long splits in power reactor rods is therefore believed to have been duplicated in this R2 test.

Rodlet No. 2 yielded two specimens for metallographical examination. A transverse specimen was examined at successively ground and polished cross sections at the crack tip. No significant redistribution of the hydride was seen in the transverse sections. Hydride accumulation was observed at the crack tip of a tangential specimen with a crack. It was observed that crack propagation was accompanied by plastic deformation amounting to a wall thickness reduction of about 9 %.

31.5 References

[206]   Gräslund, C., Lassing, A. (1997). Study of secondary hydriding in BWR test fuel. Proceedings of the European Working Group "Hot Laboratories and Remote Handling". Studvisk Nuclear AB
[207]   Grounes, M., Lysell, G., & Bengtsson, S. (1997). Fuel R&D at Studsvik II. General studies of fuel behaviour including pellet-cladding interaction. *Nuclear Engineering and Design*, *168*(1-3), 151-166.
[208]   *Grounes, M., Gräslund, C., Lysell, G., & Tomani, H. (1997). Fuel R&D at Studsvik III. Studies of special phenomena in fuel behaviour: lift-off and defect fuel degradation. *Nuclear Engineering and Design*, *168*(1-3), 167-176.
[209]   Rudling, P. (2001). *Secondary degradation mechanisms-a theoretical approach to remedial actions* (No. SKI-R--00-32). Swedish Nuclear Power Inspectorate.
*available in the R2CA database

32. Halden IFA-631 secondary degradation test

32.1 Objectives

The IFA-631 test in Halden research reactor, was carried out to study the phenomena involved in secondary degradation of BWR fuel after simulation of a primary failure [210].

32.2 Tested materials, test facility

Four short rodlets were tested with liner claddings consisted of an outer Zircaloy-2 component and an inner ZrSn-liner. The liner was about 10% of the cladding's wall thickness. In two rodlets the inner cladding surface was preoxidized (zirconia layer ~ 2 µm) to create an additional barrier towards hydrogen pick-up after simulation of the primary failure. Solid fuel pellets of two different diameters were used to ensure different pellet-to-cladding gaps [210].

Fuel stack length in the rodlets was 1200 mm. Each rod was instrumented with two fuel center thermocouples (TCs) – in the lower and in the upper end. To insert the TCs two central holes of 2.2 mm diameter were drilled to a depth of 100 mm (TC position) in the fuel column from each rod end. The as-fabricated rodlets were filled with 30%Ar + 70%He gas mixture to a pressure of 2.9 bar at 20 °C. With the chosen composition a thermal conductivity of the fill-gas was distinctly higher than that of steam and markedly lower than that of hydrogen. The main features of the four test rodlets are presented in table below.

Table 26
The main parameters of the IFA-631 test rodlets, [210], [213]

Parameter/Rodlet	631-1	631-2	631-3	631-4
Cladding outer diameter, mm	9.62	9.62	9.62	9.62
Cladding inner diameter, mm	8.36	8.36	8.36	8.36
Pellet outer diameter, mm	8.19	8.25	8.19	8.25
Radial pellet-to-cladding gap (µm)	85	55	85	55
Preoxidized inner cladding surface	no	no	yes	yes
Rod power at time of 'failure'	27 kW/m	27 kW/m	27 kW/m	27 kW/m
Labeling of TCs in the lower/upper part of fuel stack	TC1/TC5	TC2/TC6	TC3/TC7	TC4/TC8

To simulate the primary failure the test rods were equipped with a special water-ingress device (WID) connected to the upper end plug. After opening a valve in the device the water passed through a 110 mm long tube with an outer diameter of 1 mm and a wall thickness of 0.2 mm before entering the rod. The IFA-631 test was performed in the Halden reactor loop under BWR conditions (286 °C, 70 atm, normal BWR water chemistry). The axial power profile during irradiation was asymmetric with the maximum in the lower part of the rodlets. The bottom-skewed power profiles are typical for a considerable part of the operating cycle in commercial BWRs. Prior to opening of the WID valves the test rodlets were irradiated under steady-state conditions for 144 days, reaching an average burnup of 5.3 MWd/kgUO$_2$. After simulation of the primary failure the valves remained open for additional 118 days of irradiation [212]. The final fuel burnup was close to 9 MWd/kgUO$_2$. The PIE metallography revealed massive cladding hydriding of sunburst type and crack initiation in the lower part of all four rods. The rod 631-4 had a through-wall circumferential crack approximately 70 mm above the bottom end of the fuel stack.

32.3 Measured parameters, PIE data

The data from the in-pile measurements clearly show the evolution of so called oxygen- or steam starvation immediately after the simulation of the primary failures. The upper part of the rods (close to the simulated primary failure) is dominated by steam, while the lower part of the rods is characterized by a gas mixture with a very high hydrogen partial pressure. The upper parts of the rods were filled with steam from the point in time where the primary failure was simulated until the end of the in-pile experiment. The environment in the lower end of the fuel rods changed within a few days after simulating the primary failure showing that steam after a certain period reached all parts of the fuel rods [211].

The post-irradiation examination showed heavily hydrided areas in regions of the cladding near the lower end of the fuel stack in all four rods. In these regions the measured hydrogen concentration was in the range from 400 to above 5500 ppm, while 100-160 ppm of hydrogen was measured in the upper and middle sections of the claddings [211]. It is concluded that the experimental set-up enabled simulation of the conditions that occur following a primary debris failure in the top end of a fuel rod in a commercial reactor. It is further concluded that excessive hydrogen pick-up takes place during the first few days after the occurrence of a primary failure and that a pre-oxidized layer does not function as a barrier towards hydrogen pick-up under exposure in an environment with a very high partial pressure of hydrogen.

The results of data processing are shown in Fig. 59. An additional uncertainty in final results is induced by initial fill-gas in the rodlets – the ArHe mixture. Estimations show that He and Ar should leave the rod in 1-3 days after occurrence of the primary failure. Nevertheless, the additional series of calculations was carried out with assumption that contents of Ar and He in the rodlets remained unchanged. This case leads to higher hydrogen-to-steam ratios inferred from the TC data. As follows from the analysis, the uncertainty in solution of the inverse problem due to the unknown Ar/He content in the rodlets is noticeably lower than that due to error (~10 degrees) in temperature calculations and measurements.

Severe hydriding occurred in all four rodlets. So, the massive hydriding threshold may be conservatively estimated by the minimal hydrogen-to-steam ratio reached in the lower part of the test rods. The actual threshold $\beta = P_H/P_{H2O}$ may be even less than this conservative estimation.
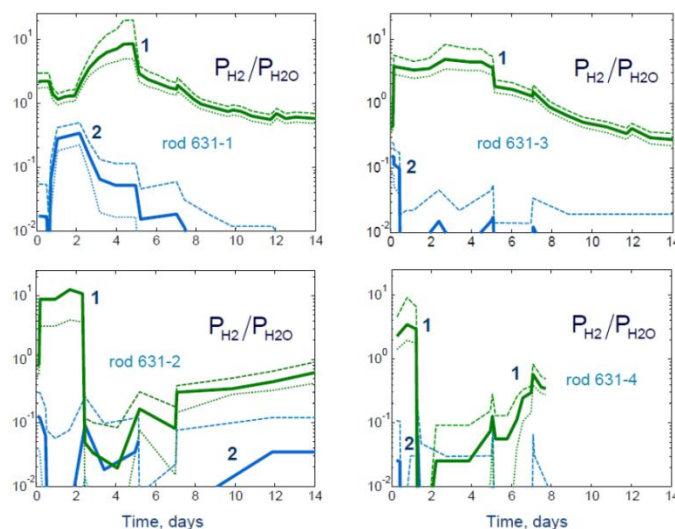
Fig. 59. Evolution of hydrogen-to-steam ratio. Lines in green color (1) are for the lower part of the rodlets with higher heat rate (area of secondary hydriding), lines in blue (2) are for the upper part of the rodlets (the low temperature domain). Dashed lines show the uncertainty boundaries

According to Fig. 59 the threshold β value is bounded from above by a value of ~10. Temperature of the inner cladding surface in the lower part of the IFA-631 test rodlets was about 310 °C. Thus, the critical hydrogen-to-

steam ratio under the in-pile conditions differed from the out-of-pile threshold by more than ~4 orders of magnitude.

32.4 General conclusions

The in-pile secondary fuel failure degradation experiments clearly demonstrated the development of secondary degradation inside an operating fuel rod with a simulated primary failure in its upper part. The experimental set-up was able to track the change in gas composition in the fuel pellet cladding gap following the primary failure and ingress of water/steam and that steam starvation conditions prevailed in the lower part of the operating fuel rods (i.e. a very high partial pressure of hydrogen). Subsequent PIE also demonstrated massive hydriding in the lower parts of the cladding. It was also concluded that a pre-oxidized inner surface of the liner does not act as a very efficient remedy against the development of secondary fuel failures under steam starvation conditions.

32.5 References

[210]   *I.A. Evdokimov, A.A. Sorokin, V.D. Kanukova, V.V. Likhanskii. A mechanistic approach to develop the secondary hydriding criteria. 8th International Conference on WWER fuel performance, modelling and experimental support. Helena Resort (Bulgaria). 28 Sep - 2 Oct 2009. https://www.oecd-nea.org/science/wprs/fuel/Secondary%20hydriding.pdf

[211]   *I. Matsson. Studies of Nuclear Fuel Performance Using On-site Gamma-ray Spectroscopy and In-pile Measurements. Acta Universitatis Upsaliensis. Digital Comprehensive Summaries of Uppsala Dissertations from the Faculty of Science and Technology 191. 103 pp. Uppsala. ISBN 91-554-6582-X. 2006. http://uu.diva-portal.org/smash/get/diva2:168460/FULLTEXT01.pdf

[212]   *W. Liu, W. Lyon, J. Rashid, S. Yagnik. Modeling axial gas transport in defective fuel rods. In TopFuel Reactor Fuel Performance 2012. Transactions. Manchester. UK. September 2–6. 2012. https://www.studsvik.com/SharepointFiles/2012%20TopFuel%20Modelling.pdf

[213]   *J. Wright, T. Tverberg, S. Yagnik, M Limbäck, D. Schrire. Summary of test reactor experiments to simulate secondary fuel degradation and its mitigation. 2017 Water Reactor Fuel Performance Meeting September 10 (Sun) ~ 14 (Thu). 2017 Ramada Plaza Jeju • Jeju Island. Korea. https://docplayer.net/92340531-2017-water-reactor-fuel-performance-meeting-september-10-sun-14-thu-2017-ramada-plaza-jeju-jeju-island-korea.html

*available in the R2CA database

33. OECD BIP

33.1 Objectives

OECD NEA BIP (July 2007 to March 2011)
The original BIP had been created to provide separate effects and modelling studies of iodine behaviour in a nuclear reactor containment building following a severe accident. The scope of this project was aimed at three research areas:
- Iodine deposition onto surfaces (adsorption in water and gas phase on various materials which can be present in NPP containment),
- Organic iodide formation from irradiated surfaces (organic iodine destruction in presence or dose rate), and
- Radioiodine Test Facility experiments.

OECD NEA BIP 2 (April 2011 to September 2014)
The Behaviour of Iodine Project Phase 2 (BIP-2) is a follow-up of the BIP project. The original project was aimed at the epoxy paint mainly, which is a common surface coating within an NPP containment. The technical scope of the BIP 2 project is twofold.
- Firstly, to obtain a more detailed understanding of iodine adsorption as well as desorption on containment surfaces with use of new experiments with well characterized containment paint composition and spectroscopic methods,
- Secondly, to obtain a more detailed understanding of organic iodide formation with use of new experiments with well characterized containment paint composition.

OECD NEA BIP-3 (January 2016 to December 2018)
The Behaviour of Iodine Project Phase 3 (BIP-3) is a follow-up to the BIP Phase 2 (BIP-2) and BIP Projects that provided results from separate effects and modelling studies of iodine behaviour in a nuclear reactor containment building following a severe accident. While painted surfaces are a very important iodine sink within containment, they represent a pathway that converts molecular iodine into organic iodine which is less easily trapped than molecular iodine by conventional iodine filtration methods (charcoal, wet scrubbers) [214].

33.2 Tested materials, test facility

33.2.1 OECD NEA BIP
The materials tested are of various nature. The vast amount of the specimens was equipped with epoxy coating, i.e. Ameron Amerlock, Ripolin or Epigrip. Several tests included materials which may be present in containment as well, including 316Ti stainless steel (samples from ThAI vessel steel), Reflective Metal Insulation (RMI), Nukon™ wool insulation, Gibbsite ($Al(OH)_3$) and Goethite (α-FeO(OH)). The complete overview on available materials and experiments can be found in [214]

33.2.1.1 Iodine adsorption studies
The water phase experiments were conducted in a glass vessel, see c.f. Fig. 60., which was filled with aqueous I-131 traced iodine solution (I_2 or I^-). The solution comprised of boric acid (H_3BO_3) and the desired pH was achieved by addition of LiOH. The specimens in a form of small cylinders were placed inside this vessel and measured periodically. The solution was stirred by a magnetic stirrer.

Fig. 60. A glass vessel used for water adsorption studies [214]

The gas phase experiments studied the iodine adsorption and desorption as a function of iodine concentration in the carrier gas, relative humidity and temperature. The experiments were conducted in the Radioiodine Adsorption Apparatus, which is presented in Fig. 61. below. A typical test consisted of three samples placed in a glass flow cell and exposed to a continuous flow of humidified air containing I131 trace labelled I_2. The adsorption phase was then followed by a purging phase with iodine free air. The cumulated activity was on-line measured on the sample.
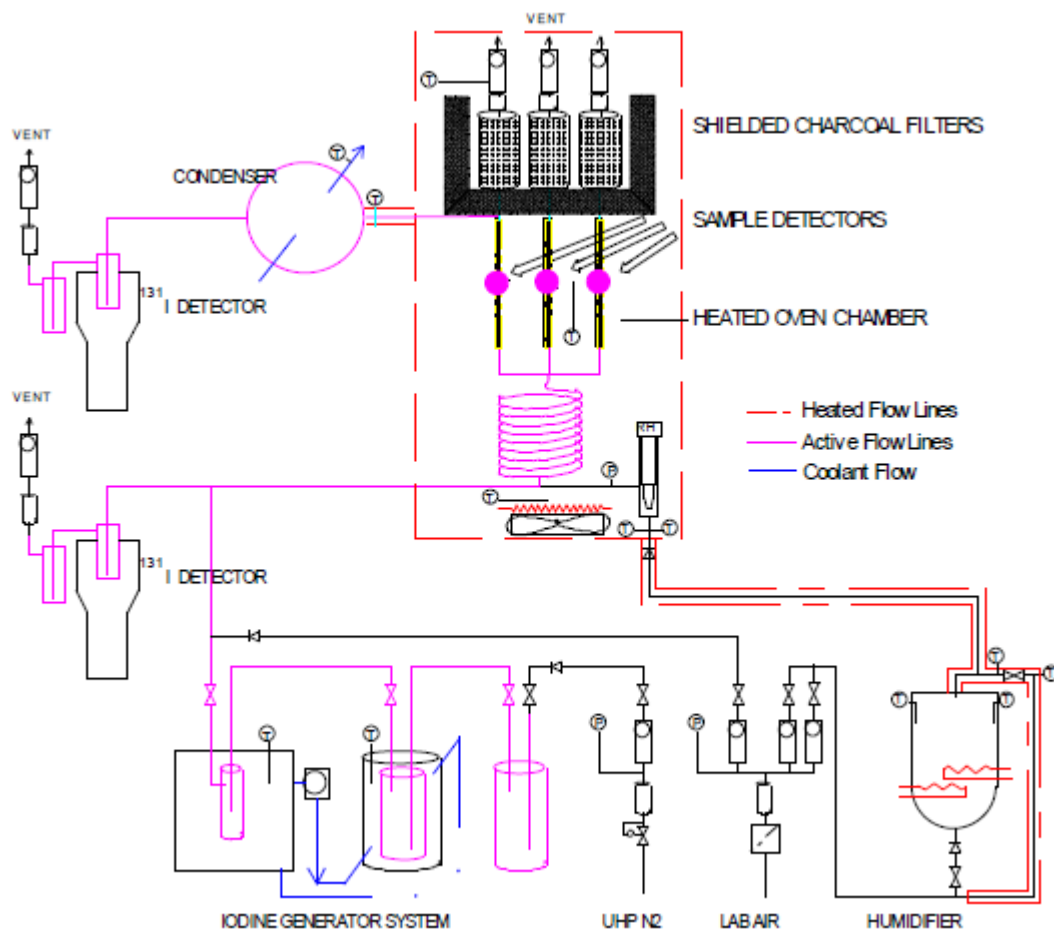
Fig. 61. A schematics of the radioiodine adsorption apparatus (RAA) [214]

33.2.1.2   Organic iodide production tests

The tests were carried in a glass tank containing pre-loaded painted samples. The pre/loading was conducted either in water or gas phase. The vessel was irradiated with Co-60. During the irradiation, the atmosphere composition, i.e. the organic iodide concentration was studied using a gas tight syringe via a gas sampling septum located at the top of the vessel. Some of the tests were conducted without the presence of painted samples. The aim of these experiments was to study the degradation of injected organic iodide in the presence of dose rate. As a part o these tests a lot of iodine adsorption measurements was conducted.

Fig. 62. Vessel for organic iodide studies with samples after irradiation [214]

33.2.1.3   Radiodine Test Facility (RTF)

The RTF is an integral test facility consisting of an instrumented replaceable cylindrical vessel and a variety of gas and water flow loops. The vessel was generally partially filled with water and could be equipped with a radiation source. The vessel itself was made of carbon or stainless steel. The carbon steel vessels were coated with several different types of coatings applied to the inner surface to simulate the surfaces present in containment. The schematic of the RTF facility is given in Fig. 63.

Table 27
List of RTF experiments [214]

Test #	Vessel	Dose rate (kGy/h)	Temperature (°C)	Notes	pH	Duration
P9T1	Stainless steel	0.78	60	pH steps	10 to 5 to 9 in steps	500
P9T2	Epoxy paint	0	60	Initial species was I_3^-	Controlled at 5, then 9	265
P10T2	Epoxy paint	0.61	25	Includes 48 h pre-test with no iodine tracer – organic analysis	Initially 10, then uncontrolled	283
P10T3	Epoxy paint	0.56	90	Includes 26 h pre-test with no iodine tracer –	Initially 10, then uncontrolled	187

Test #	Vessel	Dose rate (kGy/h)	Temperature (°C)	Notes		pH	Duration
				organic analysis. Condensing conditions halfway through test.			
P11T1	Electropolished stainless steel	0.6	25	Slow injection to simulate dissolution	MIBK	Mainly uncontrolled	306
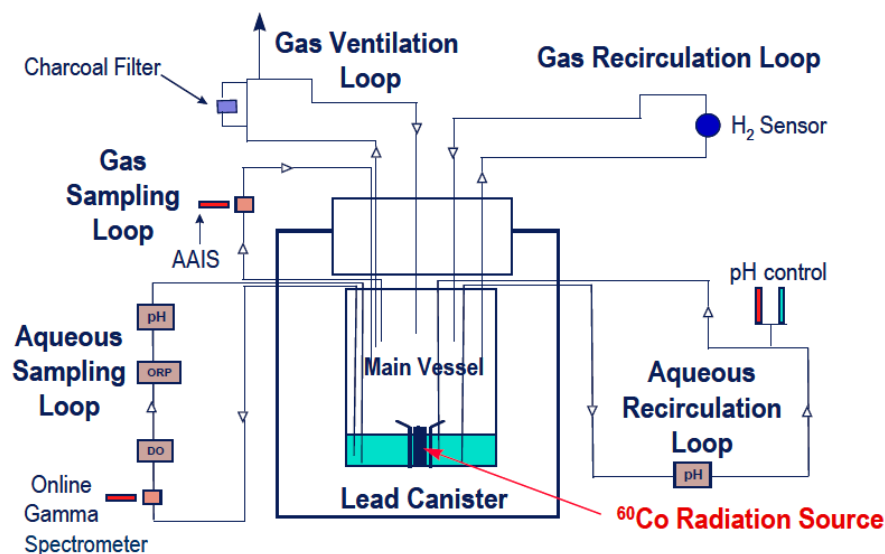
Fig. 63. RTF integral test schematic [214]

33.2.1.4 OECD NEA BIP-2

Following the original BIP project, the BIP-2 extended the iodine adsorption and iodine organic production tests with the use of existing experimental equipment. The materials tested within this project comprised painted coupons, polypropylene, nylon, amine cured epoxy, uncured epoxy monomer.

33.2.1.5 OECD NEA BIP-3

Building on the earlier experiments performed by CNL (Canada), BIP-3 addressed some of the outstanding questions raised during BIP and BIP-2 where the specific technical objectives were:

- to perform experiments to resolve outstanding questions and improve the simulations of BIP and the Source Term Evaluation and Mitigation (STEM) Project results, including by improving the ability to simulate iodine adsorption and desorption on containment surfaces; predicting organic iodine behaviour (formation and degradation) under accident conditions; and investigating the effects of paint ageing on these processes;
- to further investigate the effects of contaminants (nitrous oxides, chlorine and other potential contaminants);
- to share simulation strategies involving all partners in a code comparison exercise.

33.3 Measured parameters, PIE data

Table 28
Measured parameters

Project	Experiment	Measured parameters
BIP	Gas phase adsorption	Iodine mass [g]
	Water phase adsorption	Iodine loading [mol/dm^2]
	Organic iodide production	Iodine loading
		Gas phase organic iodide concentration [mol/l]
		Post-test mass in vessel etc. (I$_2$, LVRI, HVRI, misc.) [g]
	RTF	Gas phase – iodine concentration (I$_2$, LVRI, HVRI) [mol/l]
		Water phase – iodine concentration (I$_2$, RI, IO$_3^-$), pH [-]
BIP2	Gas phase adsorption	Iodine mass [g]
	Water phase adsorption	Iodine loading [mol/dm^2]
	Organic iodide production	Iodine loading
		Gas phase organic iodide concentration [mol/l]
		Post-test mass in vessel etc. (I$_2$, LVRI, HVRI, misc.) [g]
BIP3	-	-

33.4 General conclusions

The BIP projects addressed the main issues concerning the iodine adsorption in water phase and organic iodide production in the gas phase. The gas phase adsorption experiments deal with dry conditions only, i.e. no condensation on coupons. This area should be explored in the future, as it is relevant to LOCA conditions in an NPP containment. The adsorption in gas and water phase contains large database of various materials at different conditions, which can be used in computational code validation. The RTF integral experiment can be used for model development and validation as well.

33.5 References

[214]   * Glowa, G.A.; Moore, C.J: Behaviour of Iodine Project: Final Summary Report. AECL 2011, [available online https://www.oecd-nea.org/nsd/docs/2011/csni-r2011-11.pdf]
[215]   Glowa, G.A.; Moore, C.J.; Boulianne, D.; Mitchell, J.R.: *Behaviour of Iodine Project 2: Final Report.* AECL 2014
[216]   https://www.oecd-nea.org/jointproj/bip.html
[217]   https://www.oecd-nea.org/jointproj/bip-2.html
[218]   https://www.oecd-nea.org/jointproj/bip-3.html
*available in the R2CA database

34. MARVIKEN FSCB

The Marviken FSCB (full scale containment blowdown experiments) were performed at the abandoned Swedish nuclear power plant in Marviken. The Marviken NPP was originally a BHWR power plant with natural circulation. The nuclear section of the power plant was never commissioned.

34.1 Objectives

The full scale experiments were conducted in two series, where the first was aimed at [219]:

- containment response to simulated ruptures in pipe systems connected to the pressure vessel - blowdown
- iodine transport within the containment and containment leakage during and after blowdown
- auxiliary component response to and behaviour under loss of coolant accident conditions within a containment

The second test series were supplementary to the first series, aimed at the pressure oscillations in the containment specifically. The scope of the project was to investigate the influence of following factors [220]:

- Total vent pipe area.
- Submergence depth (varying pool level).
- Pool surface area (reduced by a partition wall).
- Pool mass (varying pool level and pool surface area).
- Vent flow path geometry.
- Pool temperature (due to heating during blowdown).
- Vent mass flow rate.
- Mixture composition in vents (fraction of air).

34.2 Tested materials, test facility

The Marviken Test Facility consists of several main components, namely [222]:

- The pressure vessel with net volume 425 m^3, maximum design pressure 5.75 MPa and maximum design temperature 272°C,
- The discharge pipe consisting of the ball valve and pipe spools which house the test nozzle upstream instrumentation,
- The nozzles and rupture disc assemblies: a set of nozzles of specified lengths and diameters to which the rupture disc assemblies were attached,
- The containment and exhaust pipes consisting of the drywell with net volume 1934 m^3, the wetwell with net volume 2144 m^3, the fuel element transport hall with net volume 303 m^3, the ground level 3.2 m diameter and the upper 0.4 m diameter exhaust pipe.

The schematic of the facility is presented in Fig. 64.
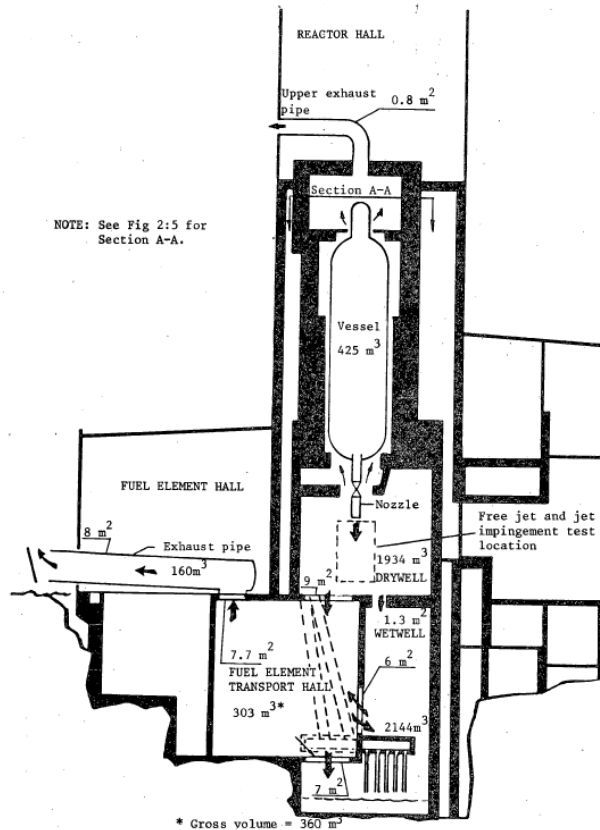
Fig. 64. Marviken test facility [221]

34.3 Measured parameters, PIE data

Table 29
Measured parameters [224]

Measured parameter	Position	Measured parameter	Position
Absolute pressure	pressure vessel containment	Void	Pressure vessel Drywell Wetwell Pool
Differential pressure	Pressure vessel Containment	Acceleration	Wetwell header
Mass flow	Discharge devices Spray cooling system Drain pipe from wetwell to drywell	Wall condensation	Drywell
Water level	Pressure vessel Drywell Wetwell	Local pressure pulsaiton	Wetwell pool
Temperature	Pressure vessel Containment	Average flow rate, water and mixture composition	Blowdown channel

34.4 General conclusions

Even though the experiment is old, it is probably the only full-scale experiment dealing with the LOCA conditions and fission products transport, namely the iodine. The experiment should find its use in the validation procedure. The experimental data is available through the OECD NEA data bank.

34.5 References

[219]   http://www.oecd-nea.org/tools/abstract/detail/csni0078
[220]   http://www.oecd-nea.org/tools/abstract/detail/csni0079
[221]   https://www.oecd-nea.org/tiethysweb/facility/set/92
[222]   *CALVO, A.; SOKOLOWSKI, L.; KOZLOWSKI, T.: International Agreement Report: Assessment of Two-Phase Critical Flow Models Performance in RELAP5 and TRACE Against Marviken Critical Flow Tests. US NRC 2012 [available online https://www.nrc.gov/docs/ML1204/ML12047A136.pdf]
[223]   *Description of the Test Facility.* MXA-1-101; Joint Reactor Safety Experiments in the Marviken Power Station 1974
[224]   *Instrumentation and Equipment and Data Acquisition System.* MXA-1-110; Joint Reactor Safety Experiments in the Marviken Power Station 1974

*available in the R2CA database

35. OECD THAI

Progress in nuclear reactor technology and safety helped in deeper understanding of the phenomena related to the nuclear accident conditions. During the decades many national and international projects filled in the database, but some gaps and uncertainties remained. The THAI project series aims at the distribution of combustible hydrogen and to the behaviour of fission products, the iodine and aerosols.

35.1 Objectives

OECD NEA THAI (January 2007 to December 2009)
THAI provided an experimental database devoted to the spatial distribution of hydrogen in containment, its removal by passive autocatalytic recombiners (PARs) and slow hydrogen combustion processes in accident conditions. Concerning fission products (FPs), the programme focused on iodine and aerosol interaction with PARs and a scoping test on a wash-down of soluble aerosol from walls by condensate film.

OECD NEA THAI-3 (August 2011 to July 2014)
THAI-2 addressed additional experimental and analytical needs regarding hydrogen-related issues: PAR performance under different thermal-hydraulic conditions including the effect of reduced oxygen content in the air on PAR onset and ignition behaviour; one test series focused on investigating hydrogen deflagration during water-spray operation. Experimental investigations related to FPs focused on the interaction of gaseous iodine with tin oxide and silver aerosols and the release of gaseous iodine from a flashing jet.

OECD NEA THAI-3 (1 February 2016 to 31 July 2019)
Remaining open issues related to hydrogen and fission products issues have been investigated in THAI-3 benefiting from the enhanced capabilities of the THAI+ facility. Experiments performed in OECD/NEA THAI-3 project are a follow-on of the previous hydrogen and fission product related investigations conducted in OECD/NEA THAI and OECD/NEA THAI-2 projects and took advantage of former and current national THAI projects, see [225], [228], [229]. Experimental matrix took into account open issues mentioned in the previous OECD/NEA THAI-2 project, the SOAR on Filtered Containment Venting Systems , [232] as well as comments/suggestions made by the different countries and organizations present at the THAI-3 Expert meeting, which took place in Frankfurt on November 17th, 2014.

35.2 Tested materials, test facility

OECD NEA THAI and THAI-2
The THAI containment test facility is mainly composed by a cylindrical steel vessel of 9.2 m height and 3.2 m diameter with a total volume of 60 m^3. The maximum admissible overpressure is 14 bar at 180°C. Thanks to the large size of the vessel a natural convection can be established to study heat and mass transport processes. This can be achieved for a multi compartment geometry as well. The vessel itself is made of AISI 316 TI stainless steel and insulated by a 120 mm thick layer of ROCKWOOL. The vessel wall is double-walled and equipped with a heating/cooling system. The penetrations of the vessel are placed at five different height levels (+2.1 m, +3.5 m, +4.9 m, +6.3 m and +7.7 m). The vessel is further equipped with several supply systems, which include the steam supply system, the gas supply system, the aerosol injection system and the iodine injection system (I-123 traced I$_2$ gas). The original THAI test vessel used within the THAI and THAI 2 project is given in the left part of Fig. 65.

OECD NEA THAI-3
The experimental investigations carried out in the frame of the THAI-3 project were conducted in the original stainless-steel THAI vessel with a 60 m3 volume, enhanced to a linked, two-vessel apparatus named THAI+ with a total enclosed volume of 80 m3.
The following experiment series have been performed:
1. PAR performance in the adverse conditions of counter-current flow;

2. hydrogen combustion and flame propagation in a two-compartment system and looking in particular at the impact of higher flow velocities of the unburned gas on flame acceleration;
3. FP re-entrainment from water pools at elevated temperature;
4. resuspension of FP deposits (aerosol and molecular iodine) due to a highly-energetic event, e.g. hydrogen deflagration.
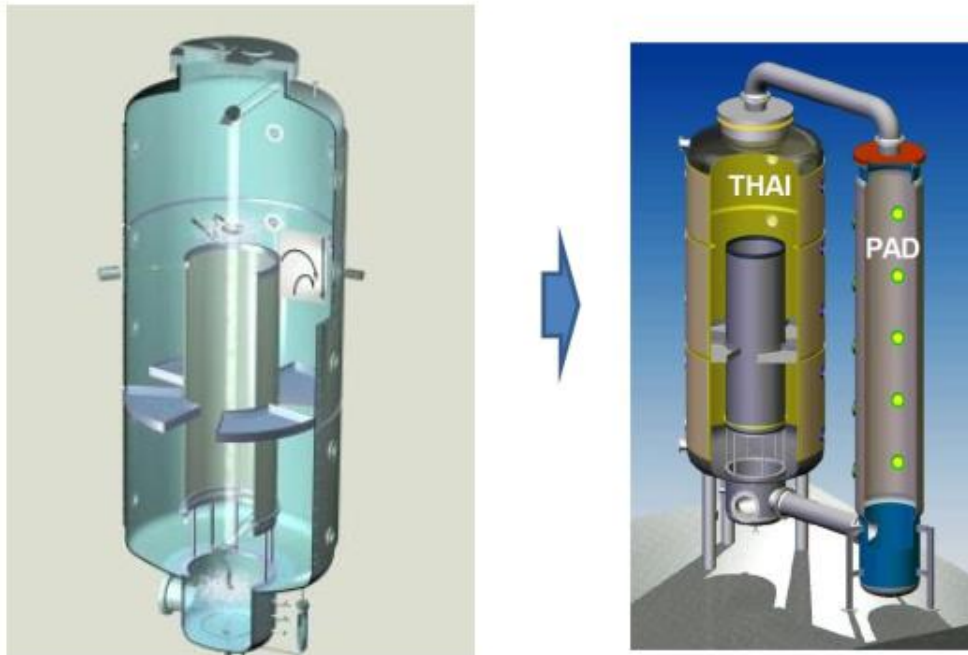
Fig. 65. THAI test facility: original THAI (left) and extended THAI+ (right)

35.3 Measured parameters, PIE data

OECD NEA THAI and THAI-2
The measurement system for both experimental series consists of standard instrumentation (thermal hydraulic and gas composition measurements) and special instrumentation which is dependent on the test design and objectives. The overview on the instrumentation is given in a table below.

Table 30
THAI and THAI-2: General Instrumentation

Type of instrumentation	Measured quantity	Measurement device/approach	Additional information
Standard	Feed mass flow	Rotatometer (float type gauge)	Measured flow compared with the storage bottle pressures and vessel pressure increase He, N_2, O_2
	Gas concentration	15 sampling lines, 2 equipped with oxygen concentration analyzers	Concentration achieved by conductivity measurements
	Temperature	1.5 mm thermocouples placed at each gas sampling line and at other locations in the atmosphere	Additional 200 thermocouples measuring vessel wall -

	Pressure	2 absolute pressure transducers	Initial pressure and pressure increase measurements
		2 high precision manometers	
Additional instrumentation (test specific)	Gas flow velocity	Vane wheels	
	Flow velocity and velocity profile	Laser-Doppler Anemometry (LDA)	He/H_2 jet
	Flow field	Particle image velocimetry (PIV)	
	Flame propagation	Fast sheathed 0.25 mm thermocouples at 13 different elevations	Monitoring of the flame propagation and combustion temperature
	Deflagration pressure	4 fast pressure transducers – strain gauge type	Transient deflagration pressure monitoring
	Aerosol concentration	Aerosol filter stations	
		Laser-light extinction	On-line aerosol concentration measurements
	Size distribution	Cascade impactors	Aerosol particle size
	Iodine concentration	Gas scrubbers	Gaseous iodine only
	Iodine speciation	Maypack filter stations	
	CsI concentration	Electrical conductivity sensors	On-line and off-line
	Gaseous and particular iodine concentration	Surface deposition	Coupons

OECD NEA THAI-3

Conventional instrumentation is provided for pressure, fluid and structure temperature, feed mass flow, water level, and condensate mass measurements. It is supplemented by a 15- channel sampling system for continuous gas (He, H_2) concentration monitoring, and by six new-developed dew point sensors designed to measure relative humidity under near-to-saturation conditions up to 140°C. Furthermore, a spectral photometer (FASP) is available for in-situ measurement of fog droplet size and droplet density in the gas volume.

Large efforts have been made to monitor local and large-scale flows inside the test vessel by field measurements in the bulk as: Laser-Doppler Anemometer for 2-D velocity and turbulence measurements along the vessel radius, 2-D and 3-D Particle Image Velocimetry with laser light sheets up to 1 m². For the measurement of gas concentration, a 40 channel mass spectrometer is available.

Table 31 to
Table 35 provide the details of THAI instrumentation. For iodine distribution measurements, radioactive iodine I-123 is used as a tracer for inactive iodine, and liquid and gas samples are taken at numerous locations. Iodine

concentration in the gaseous phase is determined by gamma-ray evaluation of samples from in-situ gas scrubbers, or from Maypack filters, the latter discriminating molecular, organic, and aerosol-borne iodine.

Table 31
General Instrumentation

Quantity measured		Device, Method	Coding	No.	Range	Accuracy
Pressure in test vessel and piping		Strain-gauge based transducer	PA, PG	5	1 - 4 (10) bar	15 (25) mbar
Temperature of gas, water, structure		Thermocouple	TF, TW	180	0 - 180 °C	0.3 K (2.5 K)
Feed mass flow (steam, air, helium/hydrogen)		Float-type flow meter	FR	8	40; 7; 0.6 g/s	1.6 % of max.
Vessel wall conditionong	$\Delta T_{in/out}$	Resistance thermometer	TR	18	± 10 K	0.15 K (calib.)
	Volume flow	Turbine flow meter	VT	3	0 - 2 l/s	0.4% of max.
	Heat flux	From mass flow and ΔT	JH	3	± 25 kW	0.7 kW
Dewpoint temp., rel. humidity of vessel atm.		Dew point mirror + resistance therm.	TD, MD	6	$\Delta T_{fluid-dewpoint}$ < 30K	0.5 K
Water level in sump and condensate collectors		Float-type level meter	LI	5	0 - 1.2 (0.5) m	2 mm
Mass spectrometer				1	1 ppm – 100%	resol. 1 ppm

Table 32
Flow velocity monitoring

Quantity measured	Device, Method	Coding	No.	Range	Accuracy
Local velocity in test vessel	Vane wheel	VT	5	0.3 - 3 m/s	0.05 m/s
Radial profile in annulus (vertical + circumf.l)	2D/3D Laser-Doppler Anemometry	UL, VL	1	ThAI-typical: ±1 m/s	0.01 m/s
Vertical and radial velocity field in annulus	2D/3D Particle Image Velocimetry	UP,VP	1	ThAI-typical: ±1 m/s	0.01 m/s

Table 33
Hydrogen and PAR Performance Monitoring

Quantity measured		Device, Method	No.	Range	Accuracy
Helium/hydrogen distribution in test vessel		Continuous sampling, heat conductivity	15	0 – 15 vol%	0.15 vol%
Slow H_2 deflagrations	Flame front velocity	Array of thermocouples 0.25 mm OD	45	0 – 100 m/s	
	Combustion pressure	High-dynamic pressure gauge	3	0 – 10 bar	0.1 bar
Passive Autocatalytic Recombiner (PAR) performance	Flow rate	Vane wheel	1	0.3 – 2 m/s	0.05 m/s
	H_2 concentr. $\Delta C_{in/out}$	Continuous sampling, heat conductivity	2	0 – 8 vol%	0.2 vol%
	$\Delta T_{in/out}$	Thermocouple	2	0 – 700 °C	3 K
	Recombination rate	From flow rate and $\Delta C_{in/out}$	1	0 – 200 g/h	3 %

Table 34
Iodine monitoring using I-123 Radiotracer

Quantity measured		Sampling device	No.	Measurement
Iodine in gas phase	Total iodine concentration	In-situ gas scrubber	6	Off-line evaluation of the samples by scintillation counter
	Concentration of iodine species	Maypack filter	2	
Total iodine concentration in condensate		Condensate collector	4	
Total iodine concentration in sump water		Sampling lines at different heights	4	
Total iodine wall deposits, resuspension		Deposition coupon with heating	3	On-line by scintillation counter

Table 35
Aerosol monitoring

Aerosol monitoring

Quantity measured	Device, Method	No.	Measuring range	
Aerosol concentration	In-situ filter sampling	2	2 x 12 samples	0.001 - 10 g/m³
	Condensation Nuclei Counter (CNC)	1	P. size 0.01 – 1 µm	max.1E7 P/cm³
Particle size distribution	Electrostatic Classifier + CNC	1	P. size 0.01 – 1 µm	
	Low Pressure Impactor	2	P. size 0.02 - 10 µm	max. 5 g/m³
	Aerodynamic Particle Sizer	1	P. size 0.5 – 30 µm	max. 500 P/cm³
Light extinction by aerosol or fog	Extinction Photometer	2		
Concentration and mean diameter (aerosols/droplets)	Fast Aerosol Spectral Photometer	1	P. size 0.1 – 10 µm	max. 50 g/m³

35.4 General conclusions

The experimental data obtained from various tests conducted in the ThAI test facility proved the ability in producing high quality and high resolution data on gas mixing and stratification issues and interaction with fission products. The database can be utilized in CFD code validation in the future. An extensive overview on the results can be found in [225] through [228].

An analytical working group with voluntary contribution from participating organisations has been organized in the OECD-NEA THAI-3 project. The activities carried out had been a valuable adjunct to the project with benchmarks on PAR performance [233], hydrogen combustion [234] and analysis of fission-product re-entrainment from a water pool.

35.5 References

[225]   OECD NEA: THAI Project Final Report. OECD NEA 2010
[226]   S. Gupta; G. Poss; M. Freitag; E. Schmidt; M. Colombet; B. von Laufenberg; A. Kühnel; G. Langer;F. Funke; G. Langrock: Aerosol and Iodine Issues, and Hydrogen Mitigation under Accidental Conditions in Watercooled Reactors:Thermal-hydraulics, Hydrogen, Aerosols and Iodine (THAI-2) Project Final Report. OECD NEA 2017
[227]   *S. Gupta, G. Poss, M. Sonnenkalb, OECD/NEA THAI program for containment safety research: main insights and perspectives, EUROSAFE 2016
[228]   *S. Gupta, et al. Main outcomes and lessons learned from THAI passive autocatalytic recombiner experimental research and related model development work, NURETH-17
[229]   http://www.oecd-nea.org/jointproj/thai.html
[230]   http://www.oecd-nea.org/jointproj/thai2.html
[231]   https://www.oecd-nea.org/jointproj/thai3.html
[232]   *D. Jacquemain, et al., OECD/NEA/CSNI Status Report on Filtered Containment Venting, NEA/CSNI/R(2014)7, 2014
[233]   M. Freitag, M. Sonnenkalb, Comparison Report for Blind and Open Simulations of HR-49 Passive autocatalytic recombiner operation under counter current flow conditions (Test ID HR-49), Report No. 150 1516 – CR – HR-49, April 2018
[234]   M. Freitag, M. Sonnenkalb, Comparison Report for Blind and Open Simulations of HD-44 Hydrogen combustion and flame propagation in two-compartment system with initial convective flow (Test ID HD-44), Report No. 150 1516 – CR – HD-44, September 2019

*available in the R2CA database

36. ARTIST

36.1 Objectives

Aerosol Trapping In Steam GeneraTor (ARTIST) was an international collaborative project developed in two stages, between 2003 and 2011. The primary objective of the project was the experimental determination of aerosol retention in the steam generator during a SGTR accident sequence through an eight-phase program. Even though, the program was mainly focused on aerosol retention and severe accident conditions, droplet retention in the separator and dryer sections was also investigated under SGTR Design Basis Accident (DBA) conditions. Analytical model developments complemented the experimental research.

According to the target of R2CA project, gas velocity and droplet retention in separators and dryers are the phases with utmost relevance here.

36.2 Tested materials, test facility

The ARTIST tests were performed at the pressure of 0.2–0.5 MPa upstream of the break with the gas being released into the secondary side at atmospheric pressure. The carrier gas in most of the tests was dry nitrogen.

Several experimental facilities were used in the ARTIST project tests [124]:

- The ARTIST facility at PSI in different configurations (Fig. 66 and Fig. 67)
    - Integral mock-up facility with all the components.
    - The tube bundle without the separator and dryer for the flooded bundle tests.
    - The tube bundle with the separator for the flooded separator tests.

- Separate effect facilities at PSI.
    - Aerosol retention inside the tube upstream of the break (Single tube).
    - Gas velocity and aerosol retention in the break vicinity (Break stage).
    - Aerosol retention in the tube bundle away from the break (Far field).
    - Gas velocity and droplet retention in the separator and dryer.

- The PECA-SGTR facility at CIEMAT.
    - Gas velocity measurements in the break vicinity.
    - Aerosol retention in the break vicinity.
    - The effect of the tube vibration.

- Separate effect test facilities for the thesis work of students.
    - Fragmentation by turbulence in a single tube facility at PSI.
    - High velocity impaction test section at the University of Eastern Finland.
    - Resuspension test section at VTT.
    - Particle depletion in a cavity DIANA at VTT.
    - Hydrodynamic bundle facility TRISTAN at PSI.

Four types of aerosol particles with different AMMDs were used to cover the range of possible shapes of nuclear aerosols: monodisperse, compact, spherical S_iO_2; monodisperse, compact, spherical Latex particles; T_iO_2 agglomerates; and fine droplets of di-2-ethylhexyl sebacate (DEHS) as "sticky aerosol" to investigate the effect of

surface adhesive forces on particle retention. Despite the scientific and technological interest of particle retention during severe accident SGTR sequences, this is of no major significance in R2CA.
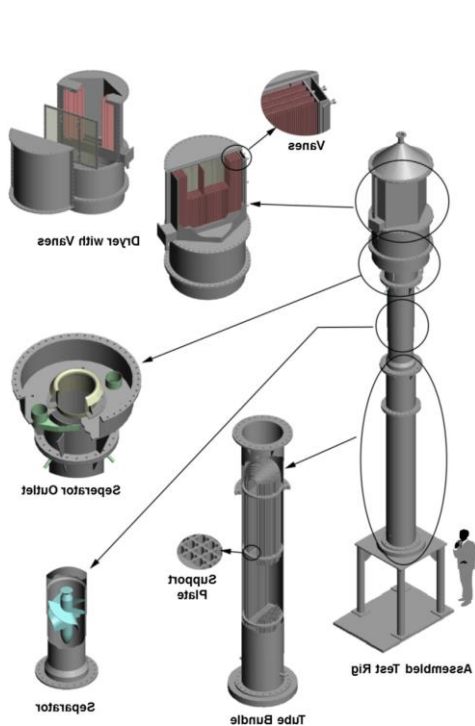
Fig. 66. Schematic view of the different components of the ARTIST facility [235].
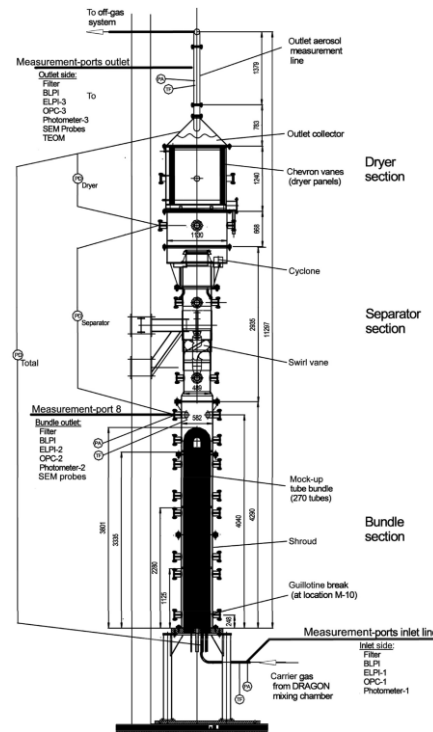
Fig. 67. Schematic of the ARTIST integral mock-up test facility [236]

36.3 Measured parameters, PIE data

Different experiments were performed in the ARTIST projects. A brief description of results concerning particle retention follows.

Aerosol transport inside the faulted tube

The effect of particle size and shape was studied by using both spherical S_iO_2 and agglomerate T_iO_2 particles in three different tube geometries, a straight tube and a U-tube with 2 different curvatures, 83 mm and 384 mm, were used. TiO_2 aerosols size decreased from AMMD = 3.0 μm at the tube inlet to AMMD = 0.8 μm at the outlet due to de-agglomeration of the particles in the test section. Deposition of the particles inside the tube was proved to be very low [235]. The spherical S_iO_2 particles did not disintegrate as TiO_2 ones inside the tube due to their compact structure; on the contrary, the retention inside the tube was very high.

Aerosol retention in the break vicinity

Investigations were performed at CIEMAT (PECA-SGTR) and at PSI (experimentally and by CFD simulations) to determine the flow fields and the gas velocities in the break vicinity, and to measure aerosol retention as well as to simulate the retention using CFD calculations. The experiments were carried out using two different break geometries considered typical of SGTR events: guillotine and a fish-mouth breaks. Based on the flow characteristics at the break exit, empirical data relevant to the SGTR conditions were compiled and used for the

development of one-dimensional models and empirical correlations for aerosol retention. Retention of spherical compact SiO_2 particles was much higher than the retention of T_iO_2 particles; in addition, the tests with SiO_2 particles showed that the bigger the particle size, the higher the retention. The mechanisms that were thought to play a major role in aerosol removal from the gas were inertial impaction and turbulent deposition.

Aerosol deposition in the tube bundle

In these tests was investigated the aerosol deposition in the tube bundle of the secondary side away from the break (far field). The tests showed that aerosol deposition in this region was very small and the inertial effects are not significant in transporting particles in the low gas velocity in the far field region.

Flow field, aerosol and droplet retention in the steam separator and dryer.

The objective of this test was the investigation of the flow fields and the aerosol and droplet retention in the steam separator and dryer.

The aerosol retention was measured as part of the integral mock-up tests including the separator and dryer sections using T_iO_2 and S_iO_2 particles with AMMD = 1.4-3.5 μm [235]] with the average inlet pressure of 1 bar and average temperature of 25 ^{0}C. The results of the aerosol retention in the separator and dryer section showed low retention values: DF=1.1 for the spherical S_iO_2 particles and DF=1.1-1.5 for the agglomerate T_iO_2 particles (Fig. 68). The carrier gas flow rate did not seem to have significant effect on the retention.

The flow fields and droplet retention relevant for primary coolant release during a DBA SGTR conditions were determined in the dedicated separate effect experimental configuration of the separator and dryer sections. Droplet retention was measured using Di-Ethyl-Hexyl-Sebacat (DEHS) droplets of relatively large size with average aerodynamic mass median diameters of 21.5, 30.5 and 51.5 μm. Furthermore, droplet retention in the dryer was determined only for droplet sizes 10–100 μm. The flow fields were determined using laser Doppler anemometry (LDA) and planar particle image velocimetry (PIV) techniques. The results with droplets showed that the retention increased with increasing droplet size and decreasing carrier gas flow rate (Fig. 69). At the lowest gas flow rate of 10 kg/h, the droplets were retained in the separator-dryer section due to gravitational settling, and with increasing flow rate a larger fraction of droplets were transported through the test section. The DF varied from DF = 2 for the smallest droplets of AMMD = 21.5 μm at the highest flow rate of 800 kg/h to DF = 90 for the largest droplets of AMMD = 51.5 μm at the lowest flow rate of 10 kg/h.
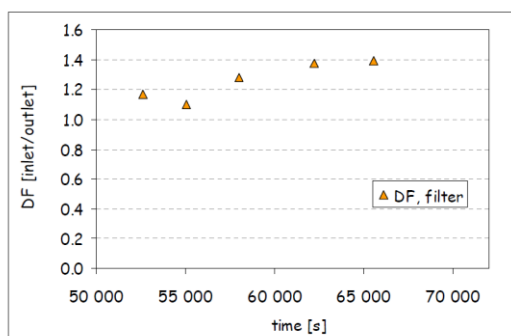
Fig. 68. Decontamination Factor (Test with SiO_2 particles) [235]
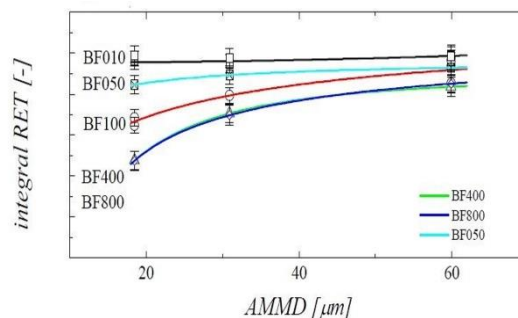
Fig. 69.. Retention in the test section [242]

In these tests, the highest gas flow rates were much lower than the typical steam flow rates during primary coolant release in SGTR conditions when the primary pressure is high at up to 15 MPa.

CFD simulations of the flow fields and aerosol and droplet retention behavior were conducted and their results were compared to experimental data as shown in Fig. 70.
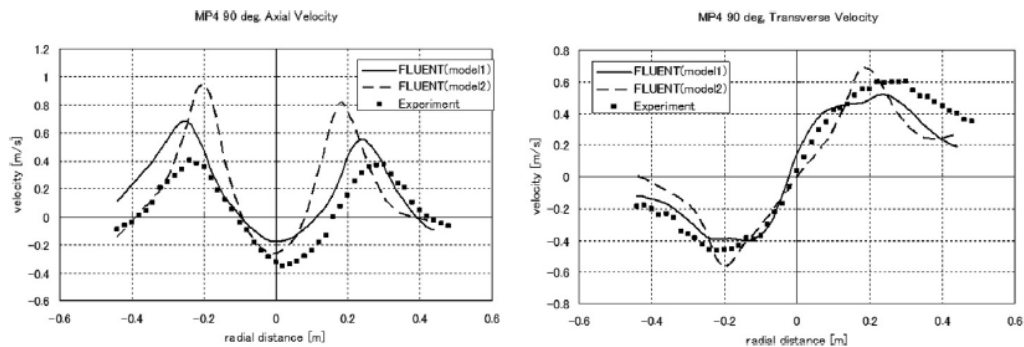
Fig. 70. Comparison of the measured and simulated velocity field at the separator exit [235]

Aerosol retention in the integral mock-up facility.

The tests performed in the scaled-down integral facility at PSI and at the break vicinity showed that aerosol retention depends on the particle type and size. The results of aerosol retention using both SiO_2 and T_iO_2 particles were very close to the retention results in the break stage facility under similar boundary conditions (same break geometry, aerosol type and gas flow rate). This confirmed that the major aerosol deposition would occur in the break vicinity, and that aerosol deposition in the other structures was rather minor.

Aerosol retention in the flooded secondary side.

Considerable retention of aerosols takes place by pool scrubbing and by interactions with the regions of the tubes covered with water. The tests in the flooded secondary side showed that the retention of aerosol particles in the flooded secondary side was significant already with 0.3 m submergence of the tube break and it increased with increasing particle inertia and increasing water level above the tube break. The decontamination factor was about two orders of magnitude higher under flooded conditions than in the dry secondary side. Besides, the results indicated that the presence of tubes enhanced retention.

36.4 General conclusions

The tests and studies conducted in the framework of the ARTIST projects produced significant amount of experimental data and knowledge concerning the aerosol retention in the steam generator during severe accident SGTR sequences. Integral and individual-stage experiments were conducted at various laboratories, mostly PSI.

As a summary, a considerable fraction of the aerosols were observed to be deposited in the steam generator, particularly in the break stage and drastically enhanced in a flooded secondary side.

Most ARTIST tests were performed at pressure ranging from 0.2 to 0.5 MPa upstream of the break and atmospheric pressure at the secondary side (rough room temperature prevailing at both sides) [235]. Droplet retention tests simulating DBA scenarios showed a dependence of retention on the gas flow rate and droplet size. The retention of droplets increased with increasing droplet size and decreasing gas flow rate, indicating that the main retention mechanism was gravitational settling. Nonetheless, it should be born in mind that the highest gas flow rates used in these tests were much lower than the typical steam flow rates encountered during primary coolant release in a SGTR DBA conditions. This factor as well as the thermalhydraulic conditions set in the tests, should be taken into account when using this experimental data for studies of SGTR DBA.

36.5 References

[235]   *Terttaliisa Lind, Salih Guentay, Luis E. Herranz, Detlef Suckow: A summary of the ARTIST: Aerosol retention during SGTR severe accident. Annals of Nuclear Energy 131 (2019) 385-400.

[236]   *A.Dehbi, D.J.Suckow, T.M.Lind, S.Guentay, S.Danner, R.Mukin: Key findings from the ARTIST   project on aerosol retention in a dry Steam Generator: Nuclear Engineering and Technology 48 (2016), 870-880.

[237]   *Guentay, S., Suckow, D., Dehbi, A., Kapulla, R., 2004. ARTIST: introduction and first results. Nuclear Engineering and Design, 231 (2004) 109–120.

[238]   *T. Lind, S. Campbell, L.E. Herranz, M. Kissane, JinHo Song: A summary of fission-product-transport phenomena during SGTR severe accidents. Nuclear Engineering and Design 363 (2020) 110635.

[239]   *Herranz, L.E., Lopez del Prá, C., Dehbi, A.: Major Challenges to modelling aerosol retention near a tube breach during steam generator tube rupture sequences. Nuclear Technology 158 (2007), 83–93.

[240]   *Herranz, L.E., Lopez, C. ARI3SG: aerosol retention in the secondary side of a steam generator. Part I: model essentials, verification and correlation. Nuclear Engineering and Design. 248 (2012) 270–281.

[241]   Herranz, L.E., Velasco, F.J.S., Lopez del Prá, C. Aerosol retention near the tube breach during steam generator tube rupture sequences. Nuclear Technology, 154 (2006)

[242]   R. Kapulla, S. Danner, S. Guentay, Droplet retention and velocity field in a steam generator. Proceedings of the 2008 Annual Meeting of the American Nuclear Society in Anaheim, CA, American Nuclear Society, La Grange Park, IL, (2008)

*available in the R2CA database

37. OECD STEM

The STEM project (Source Term Evaluation and Mitigation) is an international joint project dealing with reduction of known phenomenological uncertainties of two major fission products – ruthenium and iodine. The project period was from July 2011 to September 2015.

37.1 Objectives

The STEM project deals with following issues[244]:

- medium-term iodine releases, with specific attention to the stability of iodine aerosol particles under radiation (decomposition induced by radiation producing gaseous iodine species)**;**
- short-term and medium-term iodine-paint interactions under radiation;
- ruthenium transport chemistry in order to determine the speciation of Ru, in particular the partition between gaseous and condensed forms during its transport through the RCS.

37.2 Tested materials, test facility

The tests were carried in two facilities. The iodine part was conducted in the EPICUR facility, which comprises a 5 litres irradiation tank irradiated by ^{60}Co sources. The test loop is further equipped with a filtration system for ^{131}I for online (quantitative) or offline (qualitative) measurements. The scheme of the setup is presented in Fig. 71.
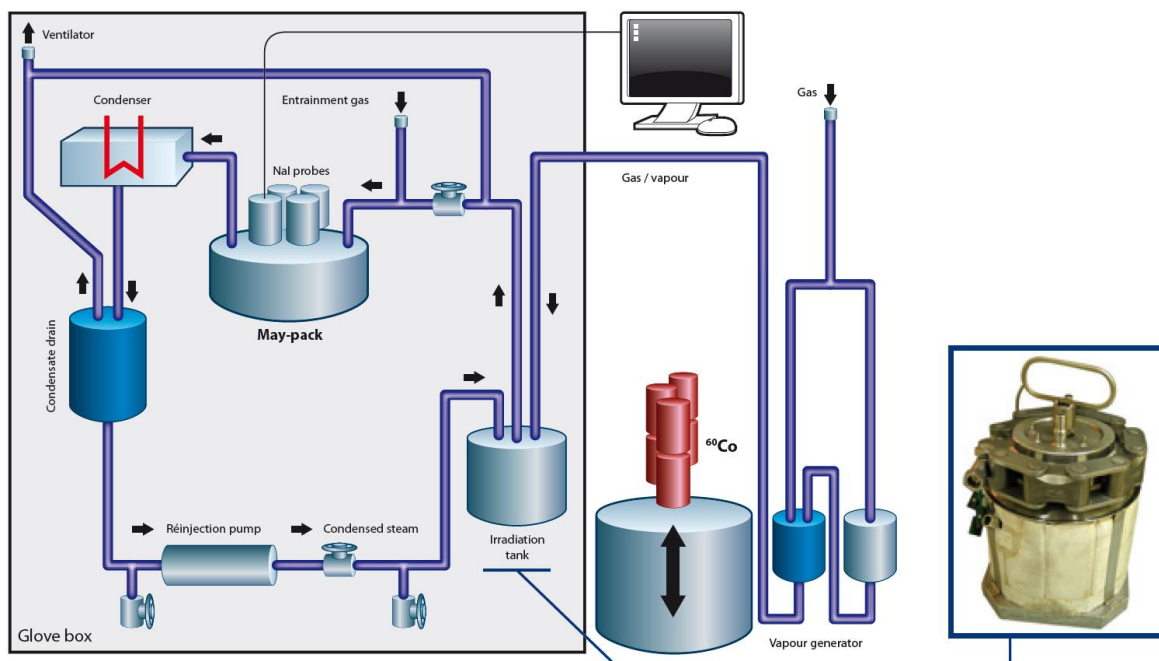
Fig. 71. EPICUR Test Facility

The ruthenium experimental part was carried in the START facility. In total, 22 vaporisation and revaporisation experiments were conducted. The facility which is presented in Fig. 72.
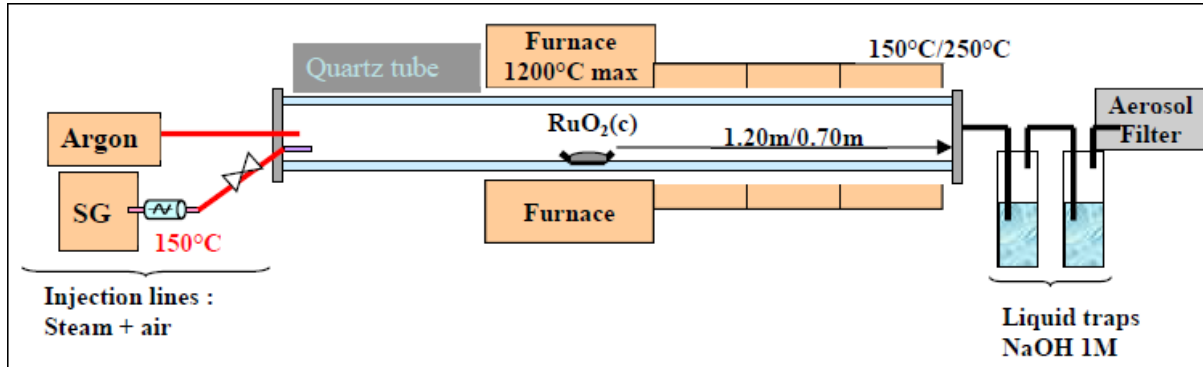
Fig. 72. START Facility

37.3 Measured parameters, PIE data

Table 36
Measured parameters

Experiment	Measured parameters
EPICUR	Iodine loading [mol/dm^2]
	Gas phase organic iodide concentration [mol/l] Post-test mass in vessel etc. (I$_2$, LVRI, HVRI, misc.) [g]
START	Ruthenium partitioning Aerosol, gas and deposited mass

37.4 General conclusions

The STEM project results contributed to better understanding the phenomena concerning the iodine chemistry. This led to an improvement in participants computational tools, e.g. ASTEC. The ruthenium experiments were satisfactory in the same way. A preliminary model of ruthenium transport was implemented in ASTEC. Furthermore, the project revealed areas of interest, which are covered by a follow-up STEM 2.

37.5 References

[243]   http://www.oecd-nea.org/jointproj/stem.html
[244]   *Improving Evaluation of Source Terms for Severe Accidents at Nuclear Installations: Final Report of the Source Term Evaluation and Mitigation Project (STEM)*. OECD NEA, 2020, [available online 26. 5. 2020 http://www.oecd-nea.org/globalsearch/download.php?doc=80285]
[245]   *EPICUR Facility*. IRSN/PSN 2015 [available online 26. 5. 2020 https://www.irsn.fr/EN/Research/Research-organisation/Research-programmes/SOURCE-TERM/EPICUR/Documents/PSN_FICHE_Installation_EPICUR_EN_ver160715.pdf
*available in the R2CA database

38. VVER NPP iodine spiking

38.1 Objectives

Activity concentration measurements were taken at the Paks NPP in order to provide data for the development of iodine spiking model of the RING (Release of Iodine and Noble Gases) code. The RING code was built as a module into the chemical expert system of the NPP and is used for the estimation of the number of defective fuel rods and for the prediction of iodine spike during reactor shutdown.

38.2 Tested materials, test facility

The measurements were performed at different units of Paks NPP. All units are of VVER-440 type. The measurements were carried out only for those cycles, when the presence of defective fuel in the core was confirmed.

38.3 Measured parameters, PIE data

The data collection covered the first days of refuelling period after reactor shutdown. Activity measurements were taken with high frequency in order to have sufficient number of experimental points for the modelling. Beyond the standard NPP measurements some additional actions were taken to collect the data. The shutdown datasets included not only the iodine activity data but other isotopes as well.

The following data were collected and analysed:
• primary circuit pressure,
• boric acid concentration,
• core power,
• core inlet temperatures,
• activity concentrations.
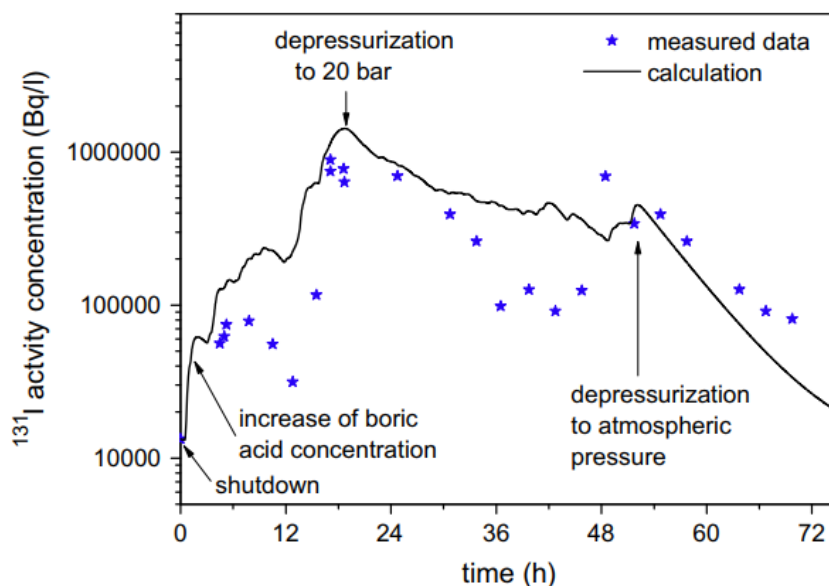
Fig. 73. Measured and calculated ^{131}I activity concentrations following shutdown of a unit VVER-440 unit

38.4 General conclusions

The activity concentrations in the primary coolant significantly increases during reactor shutdown. The iodine spike can reach for two orders of magnitude higher activity concentration compared to steady state 100% power operation with defective fuel rods.

The measured data suggest that:
- power decrease leads to the cooling down of the fuel and results in opening of cracks in the fissile material, which facilitates the release of fission products from the intergranular regions,
- the depressurisation of the primary system creates a driving force for the transfer of isotopes from the fuel into the coolant,
- the injection of boric acid after shutdown can increase the primary activity due to the solution of deposited fission products from the surface of the core components.

38.5 References

[246]   *Hózer Z, Vajda N: Simulation of Iodine Spiking in VVER-440 Reactors, In: Proc. ENS TopFuel 2001, May 27-30, Stockholm (on CD-rom)

[247]   *Z. Hózer: Simulation of leaking fuel rods, Proc. Int. Conf. WWER Fuel Peformance, Modelling and Experimental Support, 2005, pp. 372-380

[248]   *Z. Hózer: Simulation of leaking fuel rods in a VVER reactor, Annals of Nuclear Energy, 70 (2014), 122-129

*available in the R2CA database

39. PWR NPP iodine spiking

39.1 Objectives

The SGTR analysis of NPPs includes assumptions regarding the presence of fission product iodine in the reactor coolant resulting from iodine spikes. To get a better understanding of iodine spiking, reactor trip and associated radiochemistry data were collected from NPPs with PWRs. These data were compared against validation criteria to determine their applicability to an investigation of the magnitude of an iodine spike following a reactor trip.

39.2 Tested materials, test facility

Iodine spiking data resulting from reactor trips were collected from 26 PWRs in the USA between 1972 and 1989. The total number of recorded reactor trips with iodine spiking was 168.

Table 37
PWR plants with iodine spiking data [249]

Arkansas Nuclear One-1	Haddam Neck	Oconee-3
Arkansas Nuclear One-2	McGuire-1	Palisades
Calvert Cliffs-1	McGuire-2	Prairie Island-1
Calvert Cliffs-2	Millstone-2	Prairie Island-2
Catawba-1	Millstone-3	San Onofre-2
Catawba-2	North Anna-1	San Onofre-3
Cook-1	North Anna-2	Surry-1
Cook-2	Oconee-1	Surry-2
Crystal River-3	Oconee-2	
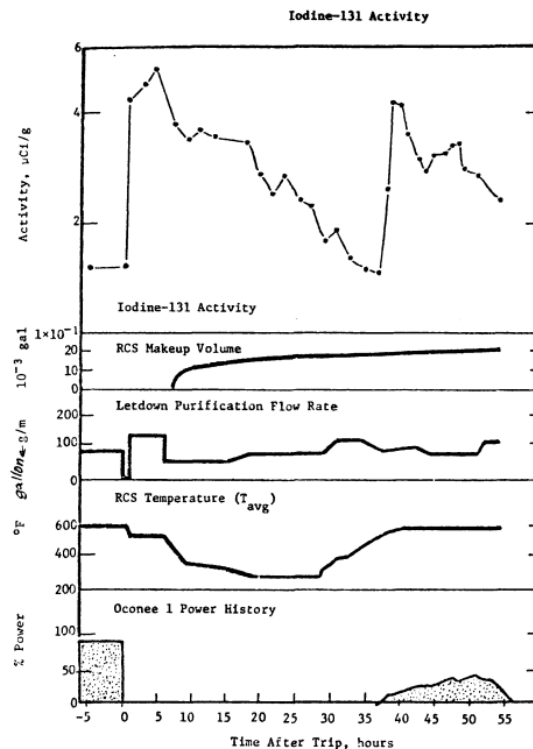
Fig. 74. Measured ^{131}I activity concentrations at PWR unit Oconee-1 [250]

39.3 Measured parameters, PIE data

Five specific criteria were used to ensure that the data could be compared among plants and that the resulting data base would be valid. The criteria were:

- sufficient steady-state power prior to the trip to ensure an adequate buildup of iodine. The specific criterion used was a minimum of 5 days at steady-state power operation, resulting in a minimum of 35% of the steady-state ^{131}I concentration. In nearly all cases, the steady-state power operation lasted several weeks to several months rather than the minimum 5 days.
- knowledge of the steady-state iodine concentration
- availability of at least one posttrip chemistry sample taken 2 to 6 h after trip
- no posttrip RCS perturbation (e.g., recriticality) prior to the RCS sample
- availability of all requisite transient information (purification flow, trip date and time, posttrip sample date and time)

The collected data included the measured steady-state iodine concentration before trip and the maximum measured iodine concentration 2 to 6 h after trip

39.4 General conclusions

The collected data indicated that the iodine release rate assumed in the earlier calculations of an SGTR event could be reduced substantially (e.g., by a factor of 15) and still resulted in a conservative analysis. An alternate formalism was proposed for use in analysis of this accident type wherein an absolute release rate, normalized to plant power, is used, rather than the 500-fold increase in steady-state release rate as was specified by the SRP. The 95/90% (95% confidence, 90th percentile) value of 1.09 Ci/h·MW(electric) ($4.03 \cdot 10^{10}$ Bq/h·MW) was recommended for consideration as iodine release rate specification for an SGTR with coincident iodine spike [249].

39.5 References

[249]   * James P. Adams & Corwin L. Atwood (1991) The Iodine Spike Release Rate during a Steam Generator Tube Rupture, Nuclear Technology, 94:3, 361-371

[250]   * Christensen, H., & Lundqwist, R. (1979). Release of fission products in transients (No. STUDSVIK-E2--79-94). Studsvik Energiteknik AB.

*available in the R2CA database

40. VVER NPP SG collector cover lift-up

40.1 Objectives

The section discusses the incident at Rivne NPP unit 1 (VVER-440/V-213), concerned with the steam generator (SG) primary collector cover lift-up, which happened on January 22, 1982.

The accident was caused by primary-to-secondary reactor coolant leakage as a result of full and partial steam generator header covers lifting. The initiating event was full hot collector cover lifting in one of the sixth steam generators (SG#5) with equivalent diameter 107 mm. Hot collector covers lifting in other three SGs #1, #3 and #4 followed this event. Such accident provides a direct release path for contaminated primary coolant to the environment via the secondary side.

40.2 Tested materials, test facility

At the accident onset, the Unit was in the process of raising power to the nominal with a regulated speed of 2% per minute. All the main equipment and normal operation systems were in operation, the safety systems were on standby according to the plant design. At a power level of 82% (1127.5 MW), the covers of the "hot" collectors of the steam generators #3, #5 and then of the steam generators #1, #4 were lifted, followed by an intensive release of the primary coolant to the SGs.
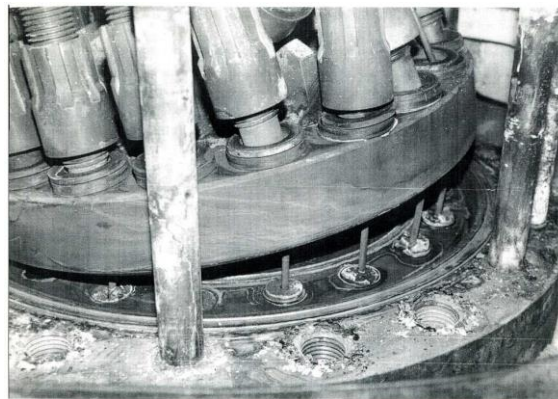
Fig. 75. Destruction studs cover collector SG [254]

40.3 Measured parameters, PIE data

The onset of the accident was identified by a sharp decrease in pressure and pressurizer coolant level. The reactor was stopped by emergency protection (SCRAM) due to a decrease in primary side pressure to 95 kgf/cm^2, but the pressure continued to decrease. By the signal of emergency protection, active safety systems were started automatically and when the primary pressure decreased to 60 kgf/cm^2, the ACC worked. The personnel sequentially tripped both turbines and organized feeding of the primary circuit with high pressure injection pumps. 3 minutes after the start of the accident, the pressure of the primary circuit stabilized at 40 kgf/cm^2, the primary coolant temperature decreased by 50ºC.

At the 13th minute, the operator stopped MCP and closed the main gate valves (MGVs) on loop #5. At the same time, the coolant pressure in the primary circuit remained at the pressure level of the secondary circuit (40 kgf/cm^2), which indicated the leakage of the MGV. At the 30th minute, a rise in the SG-3 water level was noted, after which the MCP was stopped and the MGVs on the third circulation loop were closed.
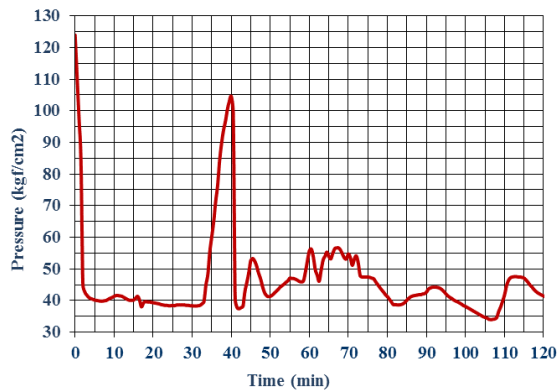
Fig. 76. Reactor pressure
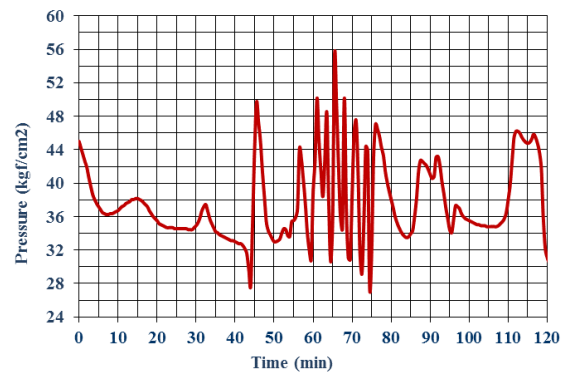
Fig. 77. SG-1 pressure
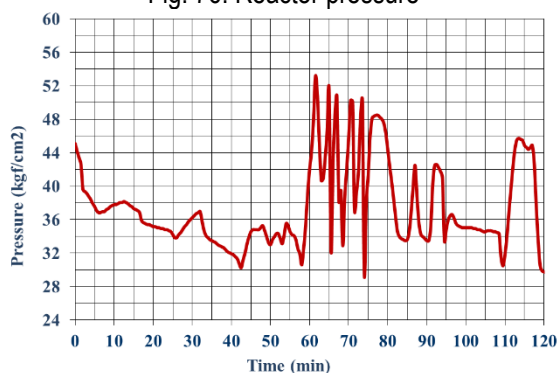
Fig. 78. SG-2 pressure
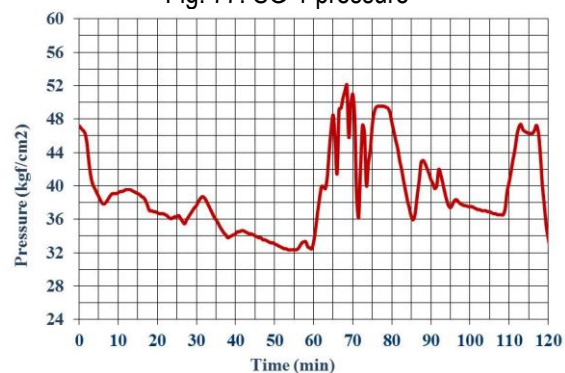
Fig. 79. SG-3 pressure
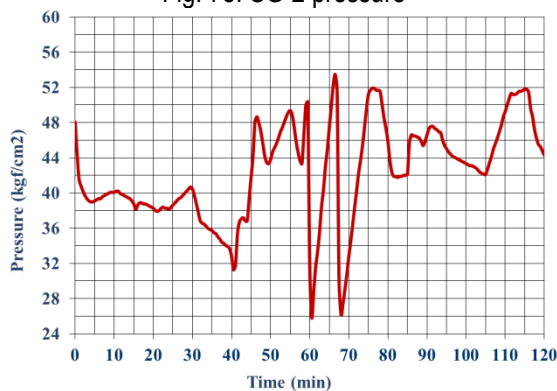
Fig. 80. SG-5 pressure
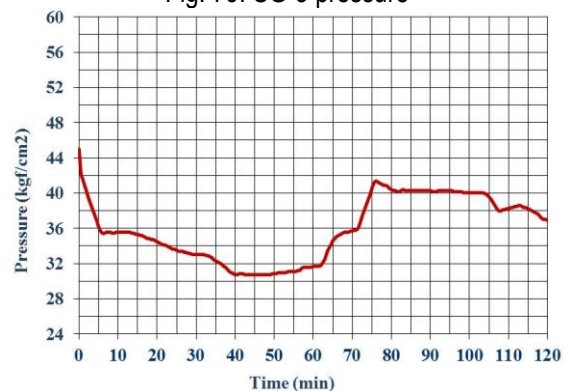
Fig. 81. SG-6 pressure

After the localization of the two circulation loops, the primary pressure reached 105 kgf/cm^2, and then sharply decreased to 40 kgf/cm^2 due to leakage of the hot collector of SG-1. The operator switched off the MCP and closed the MGVs on loop #1, however, the primary pressure and the SG-1 ,3, 5 pressure subsequently changed identically, indicating a significant leakage of the MGVs. At the 50th minute, the MCP was turned off and the MGVs were closed on loop #4. Before that, the cycling operation of the safety valves started at the SG-1 started, and then at the SG-3, 4 and 5.

At the 65th minute, for the undetermined reason, MCP-2 and 6 (on undamaged loops) tripped. The reactor was cooled over the next 27 minutes by the natural circulation of the primary coolant with continued supply of boron water by high pressure injection pumps. Then, MCPs 6 and 2 were sequentially switched on and the Unit was switched to the cool-down according to the standard scheme through the SGs 2 and 6.

Further operator actions were aimed at ensuring the cooling of the reactor in the water-water mode and the transfer of the reactor to the "cold" state. An investigation subsequently undertaken confirmed the facts of the collector covers lift-up at SGs #1, 3, 4, 5, caused by a rupture of the mounting studs of the collector covers.

40.4 General conclusions

According to the Rivne NPP Unit 1 accident data [253], during the accident, 1,100 tons of water flowed from the primary to the secondary side, and then through the systems of the secondary circuit released to the drainage tank, turbine condensers and partially, due to leaks, into the lower elevations of the turbine hall rooms. Approximately 10-20 tons of water and steam were released through the SG SV to the NPP site.

The total radioactivity in the primary coolant before the start of the accident was about 100 Ci. About 17 Ci were released through the SG SV into the atmosphere. Most of the activity was concentrated in the drain tank and turbine condensers. Operator localized the release of activity through the SG SV, as a result, the spread of radioactivity outside the territory of the nuclear power plant and hazardous concentrations in the environment and on the soil were not observed.

The turbine hall pipelines activity level was within the range of 3÷15 µR/s; there was no increase in permissible doses at workplaces. The secondary circuit water was directed for processing. Pipelines and equipment of the secondary circuit required partial decontamination and washing of boric acid.

40.5 References

[251]   *V.I. Borisenko, A.G. Krushinsky, V.P. Mukoid. Standard problem for RELAP5 code validation FOR VVER-440 reactor unit. Problems of nuclear power plants' safety and of Chornobyl. Release 6. 2006 (in Russian). http://www.ispnpp.kiev.ua/wp-content/uploads/2017/2006_06/c41.pdf.

[252]   *Pavlin P. Groudev, Rositsa V. Gencheva, Antoaneta E. Stefanova, Malinka P. Pavlova. RELAP5/MOD3.2 investigation of primary-to-secondary reactor coolant leakage in VVER440. Institute for Nuclear Research and Nuclear Energy, Bulgarian Academy of Sciences, Tzarigradsko Shaussee 72, Sofia 1784, Bulgaria. Received 15 December 2003; accepted 3 January 2004. https://www.academia.edu/18579803/RELAP5_MOD3.2_investigation_of_primary-to-secondary_reactor_coolant_leakage_in_VVER440?auto=download&email_work_card=download-paper.

[253]   http://rb.mchs.gov.ru/mchs/radiation_accidents/m_other_accidents/1982_god/Avarija_na_bloke_1_Rovenskoj_AJES_SSSR_s.

[254]   *E. I. Sharaevskaya. Actual problems of vibroacoustic diagnostics of the first circuit of water-water energetic reactors. Problems of nuclear power plants' safety and of Chornobyl. Release 25. 2015 (in Russian).   http://www.irbis-nbuv.gov.ua/cgi-bin/irbis_nbuv/cgiirbis_64.exe?C21COM=2&I21DBN=UJRN&P21DBN=UJRN&IMAGE_FILE_DOWNLOAD=1&Image_file_name=PDF/Pbaech_2015_25_5.pdf.

*available in the R2CA database

41. VVER NPP non-closure of the pressurizer safety

41.1 Objectives

The Section discusses the incident at Rivne NPP Unit 3 (VVER-1000/V-320), concerned with failure to close (after opening) of the pilot operated relief valve (PORV) of pressurizer during periodic testing, which happened on September 22, 2009 [255], [256].

41.2 Tested materials, test facility

The incident occurred at the 118th day of planned maintenance, the reactor was in "hot shutdown" state. Parameters of the primary coolant: temperature 280 °C, pressure 160 kgf/cm^2. The core was in a subcritical state, the concentration of a liquid neutron absorber (boric acid solution) was 16 g/kg, all control rods were inserted into the core. Equipment of the primary and secondary circuits and the hermetic containment were sealed, all three safety system trains were on duty.

Before starting the Unit, scheduled tests of the pressurizer safety valve with a real increase of pressure were carried out. After primary circuit pressure increasing to 185 kgf/cm^2 PORV opened and the pressure of the primary circuit began to decrease. However, after decrease of the primary pressure to 175 kgf/cm^2 the PORV failed to close.

41.3 Measured parameters, PIE data

Due to the long discharge of steam from the Pressurizer, Bubbler tank parameters (pressure and temperature) began to grow, and at a pressure of 12 kgf/cm^2, the membrane ruptured to protect the Bubbler tank from destruction. From this moment, the coolant began to flow into the Containment. The pressure of the radioactive vapor-air mixture in the Containment reached the set point of 0.3 kgf/cm^2 (excess pressure) and, in accordance with the design algorithm, the containment spray system was launched.

The containment operated in the design mode, therefore the radioactive coolant was localized and did not go beyond the boundaries of Containment to the plant site and the environment. It condensed, cooled, and drained into the Containment sump, with the following injection into the primary circuit with the high-pressure ECCS pumps.
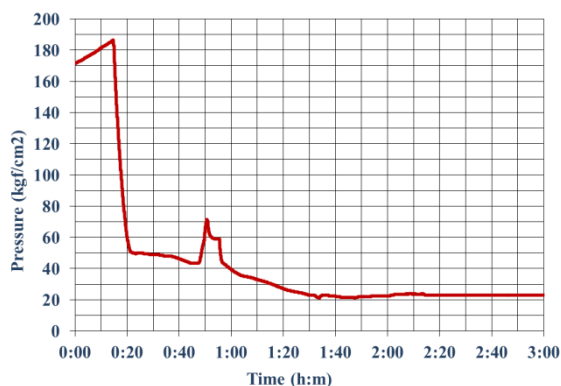
Fig. 82. Reactor pressure
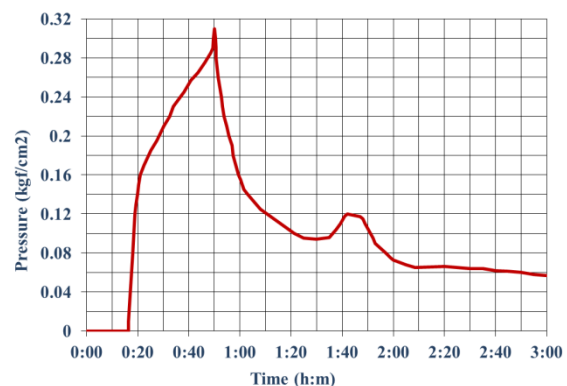
Fig. 83. Containment pressure

Due to the injection of cold borated water into the primary circuit by high-pressure ECCS pumps, the temperature in the primary circuit decreased to 82ºC and the pressure to 35 kgf/cm^2. Next, the NPP personnel continued to fill

the coolant losses with the low pressure ECCS pumps. The pressure in the primary circuit has reduced to atmospheric, and the coolant level was reduced below the PORV elevation, the leakage flow stopped.

41.4 General conclusions

An analysis of the event with the stuck open Pressurizer PORV at the Rivne NPP Unit 3, as well as the results of monitoring and inspections after the indicated event shows: the processes after the failure were in the design mode; the reactor installation was in a safe condition; radiation loads on personnel and the environment were within the established radiation safety standards.

There were no violations of the safe operation limits by the degree of fuel rods depressurization (according to the results of the primary coolant radionuclide composition analysis), specific radioactivity of the iodine isotopes $^{131}I \div ^{135}I$ in the primary coolant remained much smaller than the operational limit (3.7×10^7 Bq/kg) and the safety limit (1.85×10^8 Bq/kg). There was no release of radioactive products beyond the established boundaries. The dose rate of gamma radiation at the NPP site was at the environment level. There was no additional exposure to personnel or public. There were no radioactive contamination of systems, premises and the NPP site, and the territory outside the NPP site.

Gamma radiation dose rate values and the volumetric activity of the Noble gases in the Containment of Rivne NPP Unit 3 did not exceed the boundaries established in the plant TechSpecs (specific volumetric activity of the Noble gases in the containment air shall not exceed 2.6×10^8 Bq/m^3). The maximum value of radionuclide volumetric activity in releases through ventilation chimney was within the regulated range. Gas-aerosol release of radioactive substances did not exceed control and allowable levels of the TechSpecs (activity of Noble gases below 6.7×10^{13} Bq/day and activity of iodines (gas and aerosol phases) below 5.5×10^9 Bq/day).

41.5 References

[255]   State Nuclear Regulatory Inspectorate of Ukraine. Official reports on the results of the investigation of the incident that occurred at the Rivne NPP unit 3 on September 22, 2009. (in Russian) http://www.snrc.gov.ua/nuclear/ru/publish/article/112366.

[256]   *O. O. Klyuchnykov, V. I. Skalozubov, Yu. O. Komarov, M. I. Kolisnichenko, P. I. Kovtanyuк, Yu. O. Pavlov. Analysis of PORV failure to close at Rivne-3 on 22.09.2009. Problems of nuclear power plants' safety and of Chornobyl. Release 15. 2011 (in Russian). http://www.ispnpp.kiev.ua/wp-content/uploads/2017/2011_15/c51.pdf.

[257]   *Yu.Yu.Vorobyov, O.R. Kocharyants. Validation of WWER-1000 Thermal-Hydraulic Model for RELAP5/mod3.2 Computer Code for Evaluation of Reactor Vessel Thermal Shock Conditions. Nuclear and Radiation Safety. 3(51).2011 (in Russian). http://dspace.nbuv.gov.ua/bitstream/handle/123456789/97433/05-Vorobyov.pdf?sequence=1.

*available in the R2CA database

42. OECD-IAEA Paks Fuel Project

42.1 Objectives

The OECD-IAEA Paks Fuel Project aimed to support the understanding of fuel behaviour in accident conditions on the basis of analyses of the Paks-2 event. Numerical simulation of the most relevant aspects of the event and comparison of the calculation results with the available information was carried out between 2006 and 2007. A database was collected to provide input data for the code calculations. The activities covered the following three areas:
• Thermal hydraulic calculations described the cooling conditions possibly established during the incident.
• Simulation of fuel behaviour described the oxidation and degradation mechanisms of fuel assemblies.
• The release of fission products from the failed fuel rods was estimated and compared to available measured data

42.2 Tested materials, test facility

Severe damage of fuel assemblies took place during an incident at Unit 2 of Paks Nuclear Power Plant in Hungary in 2003. The VVER-440 type, irradiated assemblies were being cleaned in a special tank below the water level of the spent fuel storage pool in order to remove crud build up. When the chemical cleaning of assemblies was completed, the fuel rods were being cooled by circulation of spent fuel storage pool water. The later inspection has revealed that due to the special design of the cleaning tank and the characteristic of the fuel assemblies, the cooling of the submersible pump of lower mass flow was insufficient. The coolant was not capable for removing the bulk of the decay heat and this resulted in a complicated natural convection flow in the cleaning tank and the fuel assemblies. The temperature stratification blocked the flow therefore the coolant temperature reached the saturation temperature in the upper part of the cleaning tank. Then the steam-formation pushed the main volume of the coolant out of the cleaning tank vessel due to the disadvantageous design of the instrument. This way, the fuel assemblies were left without cooling for hours and heated up to above 1000 °C which resulted in severe damage and oxidation of the fuel assemblies' structure.

a   b   c   d   e
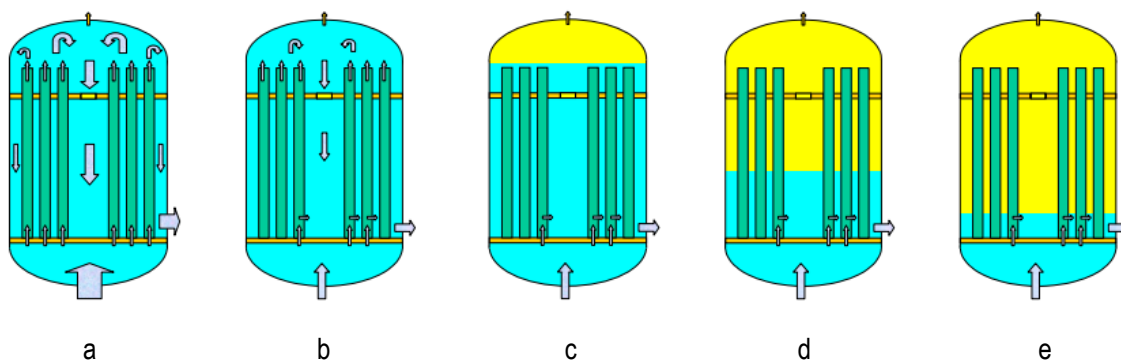
Fig. 84. Flow path of coolant in the cleaning tank during normal cleaning operation (a), at the beginning of intermediate cooling mode (b) and the steps of steam volume formation (c,d,e)

The first sign of fuel failure was the detection of some fission gases released from the cleaning tank. The opening of the cleaning tank was followed by a sudden increase in activity concentrations. The radioactive noble gases escaped from the damaged fuel assemblies were released into the environment through the reactor hall stack. However, the impact on the environment was negligible thanks to the small released quantity.

The visual inspection revealed that all 30 fuel assemblies were severely damaged. The damaged fuel assemblies were removed from the cleaning tank in 2006.

42.3 Measured parameters, PIE data

During the incident a number of technological parameters were recorded:
- temperatures,
- water level measurements and
- cleaning tank outlet flowrates.

The activity measurements covered the
- measured coolant activity concentrations,
- activity release through the chimney,
- the flowrate of water make-up system and
- the released activities.

The activity data included not only the duration of the incident, but the total period of wet storage of damaged fuel until their removal from the service pit

After the incident visual inspection of the fuel assemblies took place, and the results were described in the database.

In addition to the measured parameters, the design characteristics of VVER-440 fuel assemblies were collected (main geometrical data, some mechanical properties, oxidation kinetics of E110 cladding, and integral data of assemblies). The source of these data was mainly the open literature publications of the VVER fuel supplier. Special experimental data on the high temperature behaviour of E110 alloy including oxidation in hydrogen rich steam were provided by the AEKI.

The operational data of damaged fuel assemblies (power histories of fuel assemblies, burnup, fuel rod internal pressure, isotope inventories, decay heat and axial power distribution) were produced by the experts of Paks NPP and AEKI using several computer codes.

42.4 General conclusions

The activity release from damaged fuel rods during the Paks-2 cleaning tank incident was estimated on the basis of coolant activity concentration measurements and chimney activity data. The typical release rate of noble gases, iodine and caesium was 1–3%. During the four year storage period 4-6% of Cm and noble gases was released, while the total release of Pu and Cs isotopes was 3-4%. The dissolution of UO_2 reached 1.8% of the total initial mass.

The produced numerical results improved the understanding of the causes and mechanisms of fuel failures during the Paks-2 incident and provided new information on the behaviour of nuclear fuel under accident conditions.

42.5 References

[258]   *Hózer, A. Aszódi, M. Barnak, I. Boros, M. Fogel, V. Guillard, Cs. Győri, G. Hegyi, G.L. Horváth, I. Nagy, P. Junninen, V. Kobzar, G. Légrádi, A. Molnár, K. Pietarinen, L. Perneczky, Y. Makihara, P. Matejovic, E. Perez-Feró, E. Slonszki, I. Tóth, K. Trambauer, N. Tricot, I. Trosztel, J. Verpoorten, C. Vitanza, A. Voltchek, K.C. Wagner, Y. Zvonarev: Numerical analyses of an ex-core fuel incident: Results of the OECD-IAEA Paks Fuel Project, Nuclear Engineering and Design 240 (2010) 538–549

[259]   *Zoltán Hózer, Emese Szabó, Tamás Pintér, Ilona Baracska Varjú, Tibor Bujtás, Gábor Farkas, Nóra Vajda: Activity release from damaged fuel during the Paks-2 cleaning tank incident in the spent fuel storage pool, Journal of Nuclear Materials 392 (2009) 90–94

[260]   *Emese Slonszki, Zoltan Hózer, Tamas Pintér, Ilona Baracska Varjú: Activity release from the damaged spent VVER-fuel during long-term wet storage, Radiochimica Acta, Volume: 98, Issue: 4, pp: 231 - 236 (2009)

[261]   *Aszódi A, Boros I, Guillard V, Győri Cs, Hegyi Gy, Horváth L G, Hózer Z, Nagy I, Junninen P, Kobzar V, Légrádi G, Molnár A, Pietarinen K, Perneczky L, Makihara Y, Metajovic P, Szabó E, Trambauer K Trosztel I Varpoorten J, Vitanza C, Vogel M, Volchek A, Wagner K C, Zvonarev Y: OECD-IAEA Paks Fuel Project Final Report, NEA/CSNI/R(2008)2, OECD NEA, Paris (2008)

[262]   * Aszódi A, Boros I, Guillard V, Győri Cs, Hegyi Gy, Horváth L G, Hózer Z, Nagy I, Junninen P, Kobzar V, Légrádi G, Molnár A, Pietarinen K, Perneczky L, Makihara Y, Metajovic P, Szabó E, Trambauer K Trosztel I Varpoorten J, Vitanza C, Vogel M, Volchek A, Wagner K C, Zvonarev Y: OECD-IAEA Paks Fuel Project: Final Report, IAEA-TDL-002, IAEA, Bécs (2010)

[263]   * OECD-IAEA Paks Fuel Project, Final Report, Budapest, 2007.

[264]   *OECD-IAEA Paks Fuel Project, Final Report, Appendix A, Description of database, website and output data, Budapest, 2007.

[265]   *OECD-IAEA Paks Fuel Project, Final Report, Appendix B, Detailed description of the results of calculations, Budapest, 2007.

[266]   *PAKS_FUEL_DATABASE (database with 553 files in 82 folders)

*available in the R2CA database

43. PSB-VVER and other thermal-hydraulic loops

43.1 Objectives

As Part of the Project R2.03 of TACIS-97 the development and optimization of AM procedures for VVER100 reactors was envisaged. Therefore, twelve experiments were performed at the integral test facility PSB-VVER to replicate accident progression in the VVER-1000 and

- experimental data with a view to validate thermohydraulic codes for transient analysis of VVER reactors obtained;
- the response of the reference VVER nuclear power plant investigated, as well as
- thermohydraulic phenomena identified and/or verified.

Out of the twelve experiment, five relate to the targets of the R2CA project, four Cold Leg SBLOCAs and one PRISE.

- CL-07-08 - SBLOCA 0.7% with delayed accident management (analogous to BETHSY 9.1b) (Test 4)
- CL-05-03 - Cold Leg SBLOCA 0.5% with failure of HPIS and LPIS and use of normal operation systems for water supply to primary side (Test 8)
- PSh-1.4-05 - 100 mm rupture in the SG hot header with BRU-A stuck open (Test 9)
- CL-0.7-12- Cold Leg SBLOCA 0.7% with failure of HPIS cool-down through secondary circuit, and recovery of one HPIS train in affected loop (Test 11)
- CL-0.7-11 - Cold Leg SBLOCA 0.7% with failure of HPIS and LPIS and use of normal operation systems for water supply to primary circuit (Test 12)

43.2 Tested materials, test facility

The PSB VVER test facility is a four loop, large scale integral installation of the primary circuit of a VVER – 1000/1200. This facility has a volume and power scaling factor of 1:300 regarding the reference unit NPP Balakovo_3. The PSB-VVER test facility includes all main components of the primary- and the secondary system, as well as Emergency Core Cooling Systems. The elevations of the major equipment correspond to the elevations of the prototype reactor.

During the TACIS 2.03/97 project of the European Commission a test matrix was developed at with the purpose of obtaining experimental data for VVER. Another focus of this project was the investigation of accident management procedures on VVER-1000 reactors. This is especially of interest because the "Validation matrix for the assessment of thermal-hydraulic codes for VVER LOCA and transients" of the OECD/NEA does not include any accident management scenarios

Figure 85: PSB-VVER facility

43.3 Measured parameters, PIE data

The documentation of the experiments provides two types of documents

- Test Analysis Reports (TAR), describing experimental research objectives, initial and boundary conditions and the major experimental results, and
- Experimental Data Reports (EDR), also giving a short description of the experiment, but mainly containing plots of the experimental data.

The recorded test data was stored in processed experimental data files (PED), which contain measurements on parameters such as

Absolute Pressure, Differential Pressure, Fluid Temperature, Piping Wall Temperature, SG and FRS cladding Heat Exchange Surface Temperature, Ambient Temperature, Liquid Level, Mass flow rate (single-phase flow), Heat flux, Coolant velocity, Electric heater power, Power supply frequency, and calculated parameters

at different measurement locations in the reactor model. Comments on the measurement uncertainties and the measuring channels which were recorded and used in the experiment are provided in the EDRs.

The core simulator is a bundle of 168 heated FRSs with 28 of them being equipped with 102 thermocouples providing cladding temperature measurements.

43.4 General conclusions

Experimental tests constitute a relevant database for TH system code validation. In the project a number of thermal-hydraulic phenomena were observed in the experiments, which are recorded in the "Verification matrix for thermal hydraulic system codes applied for WWER analysis" by Liesh and Reocreux, and their suitability for code verification assessed. The PSB-VVER capabilities to induce phenomenon and to measure phenomenon were evaluated separately.

In general, the transients in the experimental facility are slower than in a real plant mainly due to heat loss. This is up to 2% of nominal power at PSB. Therefore, heat loss has to be compensated for long duration experiments, as otherwise the core model power would decrease quickly to the heat losses level. Also, feed and bleed in primary and secondary circuits were identified as important elements of accident management, ans were therefore accounted for in the validation for AM.

43.5 References

[267]   A. Del Nevo, "The design of PSB-VVER Experiments Relevant to Accident Management," Journal of Power and Energy Systems, vol. 2, no. 1, pp. 371–385, 2008, doi: 10.1299/jpes.2.371.

[268]   *OECD/NEA, "Validation matrix for the assessment of thermal-hydraulic codes for VVER LOCA and transients. A report by the OECD support group on the VVER thermal-hydraulic code validation matrix," Organisation for Economic Co-Operation and Development, NEA-CSNI-R--2001-4, 2001.

[269]   EREC, "Test Analysis Report: Leak from primary circuit 0.7% with delayed accident management (analogous to BETHSY 9.1b) (Test 4)," 2004.

[270]   EREC, "Test Analysis Report: Cold Leg SBLOCA 0.5% with failure of HPIS and LPIS and use of normal operation systems for water supply to primary side (Test 8)," 2004.

[271]   A. Del Nevo, "Pre-test calculation results by RELAP5Mod3.3 of Test #9 of the experimental matrix to be performed in the PSB-VVER facility in the framework of the TACIS Project - Part A, 2004.

[272]   EREC, "Test Analysis Report: Cold Leg SBLOCA 0.7% with failure of HPIS cool-down through secondary circuit, and recovery of one HPIS train in affected loop (Test 11)," 2004

[273]   EREC, "Data Analysis Report: Cold Leg SBLOCA 0.7% with failure of HPIS and LPIS and use of normal operation systems for Water supply to primary circuit (Test 12)," 2004.

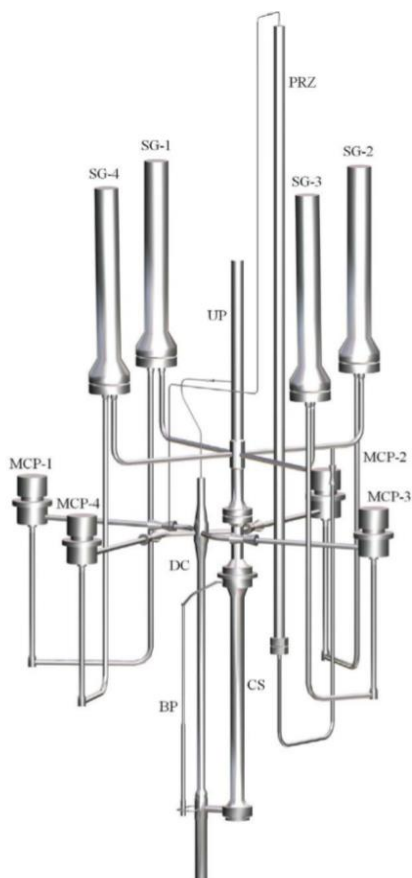[274]   K. Liesh and M. Reocreux, "Verification matrix for thermal hydraulic system codes applied for WWER analysis," Common report IPSN/GRS no.25, 1995.

*available in the R2CA database

Summary and conclusions

The present review of experimental databases covered a large number of tests, which characterizes the phenomena taking place during LOCA and SGTR events in PWRs and VVERs. Among the tests several separate effect tests and integral tests are listed, and some NPP measurements were also included.

- **Fuel failure during LOCA** is well covered by experiments, since many teste series were carried out under different conditions with all important cladding types. Beyond the burst type failure – which took place in more than twenty reviewed test series –, the brittle failure of Zr alloy claddings was observed in some tests. The fuel pellet fragmentation and dispersal was indicated by several tests (PBF, FR-2, ACCR, ANL, FLASH, Halden LOCA, Studsvik LOCA).
- **Fuel failure during SGTR** normally is not expected for intact fuel rods. The related experiments simulate the behaviour of defective fuel rods, which may suffer from secondary defects during the accident. The available experimental data characterise the hydrogen uptake by Zr alloys in the defective fuel rods and its embrittlement effect. The behaviour of water logged fuel under transient loads is not covered by the current database.
- **Activity release from fuel during LOCA** conditions is was simulated in several separate effect tests (VERDON, VERCORS, GASPARD) and also by integral test (ACRR, FLASH, Halden-LOCA, LOFT LP-FP). The available experimental data cover wide range of parameters for different fission products. The Halden FGR tests are also important for this topic, for they may provide part of the gap source term in case of fuel failure.
- **Activity release from fuel during SGTR** conditions is supported by iodine spiking experience at PWR and VVER NPPs and by separate effect tests on leaching fuel pellet samples. The DEFECT and DEFEX test series simulated the behaviour of defective fuel rods in research reactor conditions and provided valuable information on secondary defects and water logged fuel rod phenomena.
- **Activity transport during LOCA** includes several phenomena in the primary circuit and containment, which were investigated in the VERCORS, VERDON, BIP, THAI and STEM projects. The ARTIST project focused on aerosol trapping in steam generators. Some important data can be drawn from the OECD-IAEA Paks fuel project and from NPP event with non-closure of pressurizer safety valve.
- **Activity transport during SGTR** is characterise by complex path configurations, which were studied in the VERCORS, VERDON, BIP, THAI, ARTIST and STEM projects. The BIP, MARVIKEN FSCB and STEM test series simulated fission product transport in the steam generator, too. The primary-to-secondary phenomena were also observed in an NPP event wit steam generator collector cover lift-up.

The project partners indicated that at least 18 test series was already used earlier for code validation purposes and there are intentions to use at least 21 tests series for further validations activities within the R2CA project. The experimental data can be used for the support R2CA tasks in several areas including model development and validation activities:

- burst tests data can be used for the improvement and validation of transient fuel behaviour codes,
- integral LOCA tests allow us to carry out further validation of fuel behaviour codes,
- fission product test data are crucial for the testing of severe accident codes,
- fission product transport experiments provide unique possibilities for severe accident code validation,
- iodine spiking data can be used to develop and improve activity release models which can be applied in SGTR analyses,
- hydrogen uptake data are useful for the simulation of secondary degradation in defective fuel rods,
- the learnings from thermal hydraulic experiments can support the optimisation of accident management strategies.

The common use of data from small scale separate effect test and integral tests provides possibilities for the improved simulation of several phenomena (e.g. cladding burst, oxidation, hydrogen uptake, activity release and transport) under very different conditions. Most of these conditions can be considered typical for LOCA and SGTR event, and some of them cover even wider parameter ranges than that of can take place in these accidents.

The experimental data from 12 test series are included in the present version of the database. Data for other 24 test series are accessible for some of the project partners, but cannot be shared within the project with all partners for different reasons. Some of the experimental data are stored in international databases (e.g. IFPE of OECD NEA, OECD projects, IAEA FUMEX), while some others are stored by the owners of data in private databases. The data of some old test series or experiments carried out ousides of Europe (USA, Russia) are not accessible for the project, but are listed in the database as siginificant contributions to our knowledge on the SGTR and LOCA related phenoemane.

Appendix I. Phenomena matrices

PHENOMENA	fuel failure during LOCA					fuel failure during SGTR				
EXPERIMENTS	cladding oxidation	ballooning and burst	brittle failure after heavy oxidation	water quench	fuel fragmentation and dispersal	secondary defect	brittle failure	hydrogen uptake by Zr	local hydriding of Zr clad	water logged fuel rod
Edgar tests	X	X								
COCAGNE tests		X								
REBEKA tests	X	X								
AEKI/MTA EK burst tests	X	X	X							
JAERI and JAEA burst tests	X	X		X						
UK burst tests	X	X								
MRBT (ORNL) burst tests	X	X								
Russian burst tests	X	X								
ANL burst tests	X	X		X	X					
EDF burst tests	X	X		X						
PBF tests	X	X		X	X					
FR-2 tests	X	X			X					
PHEBUS-LOCA test	X	X		X						
Halden LOCA tests	X	X			X					
ACRR (SNL) tests	X				X					
NRU MT-4 test	X	X		X						
LOFT LP-FP tests	X	X		X	X					
FLASH tests (Grenoble, Siloe)	X	X		X	X					

Studsvik LOCA test	X	X		X	X					
CORA tests	X	X	X	X						
QUENCH-LOCA integral tests	X	X	X	X						
CODEX-LOCA integral tests	X	X	X	X						
PARAMETER tests	X	X		X						
MTA EK H uptake test								X		
DEFECT tests with defective fuel						X				X
DEFEX secondary defect test					X	X	X	X	X	
Halden IFA-631 secondary degradation test					X					
OECD-IAEA Paks Fuel Project	X	X	X	X						

PHENOMENA / EXPERIMENTS	activity release from fuel during LOCA					activity release from fuel during SGTR					
	noble gas release from the fuel rod - steady state	noble gas release from the fuel rod - transient	volatile fission product release from the fuel rod - transient	semi-volatile fission product release from the fuel rod - transient	fission produc release from high burnup structure	noble gas release from the fuel rod - steady state	noble gas release from the fuel rod - transient	volatile fission product release from the fuel rod - transient	semi-volatile fission product release from the fuel rod - transient	leaching of fuel pellets by water	fission produc release from high burnup structure
Halden LOCA tests			X								
ACRR (SNL) tests			X	X	X						
LOFT LP-FP tests		X	X	X							
FLASH tests (Grenoble, Siloe)		X	X								
GASPARD tests		X	X		X						
VERCORS tests		X	X	X	X						
VERDON tests		X	X	X	X						
Halden FGR tests	X				X	X					X
FIRST-Nuclides leaching tests										X	
DEFECT tests with defective fuel						X	X			X	
DEFEX secondary defect test						X	X			X	
VVER NPP iodine spiking									X	X	
PWR NPP iodine spiking									X	X	
OECD-IAEA Paks Fuel Project		X	X	X							

PHENOMENA / EXPERIMENTS	activity transport during LOCA									activity transport during SGTR						
	transport in the primary circuit (from core to break)	deposition in the primary circuit, retention by primary circuit components	tranposrt in the containment	deposition on the containment wall	deposition in the containment sump water	transport to the enironment outside of containment	noble gas transport	volatile fission product (I, Cs) transport	semi-volatile fission product transport	transport in the primary circuit (from core to break)	deposition in the primary circuit, retention by primary circuit components	deposition in the steam generator, retention by steam generator	transport to the enironment outside of containment	noble gas transport	volatile fission product (I, Cs) transport	semi-volatile fission product transport
LOFT LP-FP tests	X	X					X	X	X							
VERCORS tests	X	X					X	X	X							
VERDON tests	X	X					X	X	X							
DEFECT tests with defective fuel														X		
DEFEX secondary defect test														X	X	
BIP			x		X			X				X			X	
MARVIKEN FSCB	X	X	X		X	X		X		X	X	X	X		X	
THAI			X		X			X							X	
ARTIST												X	X			
STEM	X	X	X		X			X	X							
VVER NPP SG collector cover lift-up										X	X	X	X	X	X	X

VVER NPP non-closure of the pressurizer safety valve	X	X	X	X	X	X	X	X	X							
OECD-IAEA Paks Fuel Project							X	X								

Appendix II. Test characterisation matrices

TEST CHARACTERISATION / EXPERIMENTS	type			scale		atmosphere					tested sample						
	separate effect test	integral test	NPP measurement	scaled down	full scale	steam	inert gas	hydrogen	oxidising	reducing	small cladding sample	small pellet sample	single rod	bundle	non-core material	irradiated	non-irradiated
Edgar tests	X			X		X			X		X		X				X
COCAGNE tests	X			X			X		X		X		X	X			X
REBEKA tests	X			X		X	X		X		X		X	X			X
AEKI/MTA EK burst tests	X			X		X	X		X		X		X	X			X
JAERI and JAEA burst tests	X			X		X			X		X		X			X	X
UK burst tests	X			X		X			X		X		X	X		X	X
MRBT (ORNL) burst tests	X			X		X			X		X		X	X			X
Russian burst tests	X			X		X			X		X		X			X	X
ANL burst tests	X			X		X	X		X		X	X	X			X	X
EDF burst tests	X			X		X			X		X		X				X
PBF tests		X		X		X			X					X		X	X
FR-2 tests		X		X		X			X		X	X	X			X	X
PHEBUS-LOCA test		X		X		X			X		X	X		X			X
Halden LOCA tests		X		X		X			X				X			X	X
ACRR (SNL) tests		X		X		X	X	X		X					X	X	X
NRU MT-4 test		X		X		X			X					X			X
LOFT LP-FP tests		X		X		X			X					X		X	
FLASH tests (Grenoble, Siloe)		X		X		X	X		X				X			X	
GASPARD tests	X			X		X	X					X				X	
VERCORS tests	X			X		X	X	X	X	X		X				X	
VERDON tests	X			X		X	X	X	X	X		X				X	
Studsvik LOCA test		X		X		X			X				X			X	
CORA tests	X	X		X		X	X		X				X	X			X

QUENCH-LOCA integral tests		X		X		X	X		X				X			X
CODEX-LOCA integral tests		X		X		X			X				X			X
PARAMETER tests		X		X		X	X		X				X			X
Halden FGR tests	X			X								X		X		
FIRST-Nuclides leaching tests	X			X						X						
MTA EK H uptake test	X			X			X		X	X						
DEFECT tests with defective fuel		X		X		X			X				X		X	
DEFEX secondary defect test		X		X		X							X			
Halden IFA-631 secondary degradation test	X			X		X	X	X					X		X	
BIP	X	X		X				X						X		
MARVIKEN FSCB		X			X											
THAI		X		X										X		
ARTIST	X			X			X							X		
STEM	X													X		
VVER NPP iodine spiking			X		X								X		X	
PWR NPP iodine spiking			X		X								X		X	
VVER NPP SG collector cover lift-up			X		X								X		X	
VVER NPP non-closure of the pressurizer safety valve			X		X								X		X	
OECD-IAEA Paks Fuel Project			X		X	X			X				X		X	
PSB-VVER and other TH loops		X		X		X				X						

TEST CHARAC-TERISATION / EXPERIMENTS	cladding							fuel			heating method					FP release and transport							
	Zircaloy-4	Zircaloy-2	Zirlo	M5	E110	precharged with H	pre-oxidation	UO$_2$	MOX	high burnup	nuclear	electric	internal	furnace	induction	pH	Dose rate	Temperature	transport by natural circulation/gravity	transport by forced flow	transport in gas atmosphere	transport in liquids	interfacial mass transfer
Edgar tests	X			X		X	X					X											
COCAGNE tests	X					X	X					X											
REBEKA tests	X			X								X											
AEKI/MTA EK burst tests	X			X			X					X		X									
JAERI and JAEA burst tests	X		X	X		X	X							X									
UK burst tests	X											X											
MRBT (ORNL) burst tests	X												X										
Russian burst tests				X								X		X									
ANL burst tests		X				X		X						X									
EDF burst tests	X					X								X									
PBF tests	X							X			X												
FR-2 tests	X							X			X												
PHEBUS-LOCA test	X							X			X												
Halden LOCA tests	X	X		X	X			X		X	X	X											
ACRR (SNL) tests	X							X		X	X												
NRU MT-4 test	X							X			X												
LOFT LP-FP tests	X							X			X						X	X			X	X	X
FLASH tests (Grenoble, Siloe)	X							X			X							X					
GASPARD tests	X							X	X	X				X	X			X					

VERCORS tests	X			X				X	X	X				X	X				X					
VERDON tests	X			X				X	X	X				X	X				X					
Studsvik LOCA test		X					X			X				X										
CORA tests	X				X		X	X																
QUENCH-LOCA integral tests	X		X	X		X						X												
CODEX-LOCA integral tests				X								X	X											
PARAMETER tests				X								X	X											
Halden FGR tests								X	X	X	X		X											
FIRST-Nuclides leaching tests								X	X	X														
MTA EK H uptake test	X			X								X		X										
DEFECT tests with defective fuel	X							X			X					X						X		
DEFEX secondary defect test								X			X													
Halden IFA-631 secondary degradation test		X				X		X	X		X													
BIP																		X	X	X				
MARVIKEN FSCB																	X							
THAI																								
ARTIST																								
STEM																	X							
VVER NPP iodine spiking				X				X			X													
VVER NPP iodine spiking	X							X			X													
PWR NPP iodine spiking	X							X			X													
VVER NPP SG collector cover lift-up				X				X			X													
VVER NPP non-closure of the pressurizer safety valve				X				X			X													
OECD-IAEA Paks Fuel Project				X				X			X							X						
PSB-VVER and other TH loops											X													

Appendix III. Data matrices

DATA	Availability of data		On-line data									
EXPERIMENTS	Available for the R2CA project, included into the Appendix of the database report	Accessible for some R2CA partners, but cannot be shared within the project	Temperature history	Pressure history	Fission product release monitoring from fuel	Fission product release monitoring from primary circuit	Fission product release monitoring from steam generator	FPs concentration in containment atmosphere	FPs concetration in containment sump	FPs deposition on surface	pH	dose rate
Edgar tests		X	X	X								
COCAGNE tests		X	X	X								
REBEKA tests	X		X	X								
AEKI/MTA EK burst tests	X		X	X								
JAERI and JAEA burst tests		X										
UK burst tests	X		X	X								
MRBT (ORNL) burst tests		X	X	X								
Russian burst tests	X		X	X								
ANL burst tests		X	X									
EDF burst tests												
PBF tests			X	X								
FR-2 tests		X										
PHEBUS-LOCA test		X	X	X								
Halden LOCA tests		X	X	X								
ACRR (SNL) tests			X	X	X							
NRU MT-4 test	X		X	X								
LOFT LP-FP tests		X	X	X	X	X		X		X		X

FLASH tests (Grenoble, Siloe)		X	X		X								
GASPARD tests		X	X		X								
VERCORS tests		X	X		X								
VERDON tests		X	X		X								
Studsvik LOCA test		X	X	X									
CORA tests	X		X	X									
QUENCH-LOCA integral tests	X		X	X									
CODEX-LOCA integral tests	X		X	X									
PARAMETER tests			X	X									
Halden FGR tests		X	X	X	X								
FIRST-Nuclides leaching tests		X	X		X								
MTA EK H uptake test	X		X	X									
DEFECT tests with defective fuel		X	X	X	X	X							X
DEFEX secondary defect test	X		X	X									
Halden IFA-631 secondary degradation test			X										
BIP		X						X		X			
MARVIKEN FSCB		X						X	X	X			
THAI		X						X	X	X			
ARTIST		X											
STEM		X						X	X	X			
VVER NPP iodine spiking		X	X	X	X								
PWR NPP iodine spiking					X								
VVER NPP SG collector cover lift-up		X	X	X									
VVER NPP non-closure of the pressurizer safety valve		X	X	X									
OECD-IAEA Paks Fuel Project	X				X								
PSB-VVER and other TH loops													

DATA	PIE data								Validation	
EXPERIMENTS	Clad deformation	Clad corrosion state (oxidation, H content)	Fission product inventory in the gap	Cumulative fission product release from fuel rod	Cumulative fission product release from primary circuit	Cumulative fission product release from steam generator	Cumulative fission product release from containment	FPs deposition on surface	The measured datat were used by R2CA partners before the project for code validation purposes	The measured datat will be used by R2CA partners in the project for code validation purposes
Edgar tests	X								IRSN	IRSN
COCAGNE tests	X								IRSN	IRSN
REBEKA tests	X								EK	
AEKI/MTA EK burst tests	X								EK	
JAERI and JAEA burst tests	X									IRSN
UK burst tests	X									
MRBT (ORNL) burst tests	X									IRSN
Russian burst tests	X								EK	
ANL burst tests	X									IRSN
EDF burst tests	X									IRSN
PBF tests	X									
FR-2 tests	X									IRSN
PHEBUS-LOCA test	X								IRSN	IRSN
Halden LOCA tests	X	X							IRSN	IRSN
ACRR (SNL) tests	X	X		X						
NRU MT-4 test	X								IRSN	IRSN
LOFT LP-FP tests	X	X	X	X	X			X	HZDR	
FLASH tests (Grenoble, Siloe)	X		X	X						IRSN

Test										
GASPARD tests			X	X						IRSN
VERCORS tests			X	X				X	IRSN	IRSN
VERDON tests			X	X	X			X	IRSN	IRSN
Studsvik LOCA test	X	X	X	X						
CORA tests	X	X								
QUENCH-LOCA integral tests	X	X								
CODEX-LOCA integral tests	X								EK	
PARAMETER tests	X									
Halden FGR tests				X					EK	
FIRST-Nuclides leaching tests				X					EK	
MTA EK H uptake test		X							EK	EK
DEFECT tests with defective fuel	X	X								IRSN
DEFEX secondary defect test	X	X		X						
Halden IFA-631 secondary degradation test	X	X								
BIP								X	UJV	UJV
MARVIKEN FSCB								X		UJV
THAI								X		UJV
ARTIST									CIEMAT	
STEM								X		UJV
VVER NPP iodine spiking									EK	EK
VVER NPP SG collector cover lift-up						X				
VVER NPP non-closure of the pressurizer safety valve					X		X			
OECD-IAEA Paks Fuel Project				X			X		VTT, EK	
PSB-VVER and other TH loops										